THE UNIVERSITY OF MICHIGAN

INDUSTRY PROGRAM OF THE COLLEGE OF ENGINEERING

TRANSIENT RESPONSE STUDY OF GAS FLOWING THROUGH IRRIGATED PACKING

Francesco De Maria

A dissertation submitted in partial fulfillment
of the requirements for the degree of
Doctor of Philosophy in the
University of Michigan
1958

May, 1958

IP-293

ensm

UMR6514

Doctoral Committee:

Professor Robert R. White, Chairman
Professor Julius T. Banchero
Assistant Professor Kenneth F. Gordon
Professor Victor L. Streeter
Assistant Professor Charles M. Thatcher

ACKNOWLEDGEMENTS

Appreciation is hereby expressed to all those persons who offered their valuable time and availed me of their experience and advice to the preparation of this work.

I wish to express my gratitude to all the members of my Doctoral Committee for their friendly advice, expert guidance and encouragement given; and above all, to my Chairman, Professor Robert R. White, for his experienced advice, for his patient, constructive criticism of the manuscript and his untiring moral support which enabled me to complete this research.

Moreover, I am grateful to Mr. Gordon Colpitts for the exchange of ideas and frequent discussions of various phases of this work; to Messrs. John D. Janicek and Muhammad T. Tayyabkhan for their friendly advice and interest; to the secretaries and shop members of the Chemical and Metallurgical Engineering Department who did their best to make my task a pleasant one.

Lastly, I am indebted to the Visking Corporation and Hercules Powder Company who made this work possible with financial assistance through fellowship grants; the U. S. Stoneware Company who made available the ceramic packings; and to Mr. Patrick Cummiskey of the Friden Calculating Machine Company who provided the use of a desk calculator for the extensive computations required.

TABLE OF CONTENTS

TABLE OF CONTENTS (Cont'd)

TABLE OF CONTENTS (Cont'd)

LIST OF TABLES

LIST OF TABLES CONT'D

LIST OF FIGURES

LIST OF FIGURES CONT'D

LIST OF FIGURES CONT'D

LIST OF FIGURES CONT'D

CHAPTER I

INTRODUCTION

Chemical engineering is concerned with complex and interconnected physical structures (systems) within which a number of physical and chemical changes (processes) take place either simultaneously or consecutively, often at competing rates and with intricate interactions.

If an accurate formulation of these systems is attempted in terms of the microscopic events taking place therein, the problem in many cases defies mathematical formulation. Moreover, research tools and methods designed to probe the "fine structure" of interrelated phenomena such as those taking place in process equipment have not yet been developed.

As a result, the engineer must often resort to the study of a system of process equipment as a whole. This is accomplished by simulation of large commercial scale units by smaller experimental systems. Inlet streams and experimental conditions are set to a predetermined value and once the experimental equipment has reached "steady state", the properties of the outlet stream are measured and recorded. Empirical correlations of overall performance in terms of the independent variables investigated are the end result. Such correlations are very useful in determining optimum operating conditions and for a limited amount of scaleup.

Recently "unsteady state" experimental methods have gained increased attention in chemical engineering research, mainly because statistical information concerning the "time-distribution" of the response can be readily obtained. Such information has significance in that it permits the characterization of the succession of events

occurring in a system in terms of physical models (or which is the same in terms of probability laws). It may also provide a more adequate similarity criterion in the scaleup of equipment (i.e., two systems of different size in which the statistical distribution of a certain succession of events is the same, ought to be considered similar to one another).

Unsteady state experiments are based on the measurements of the response of a system to a known disturbance in experimental conditions. Work of this type has already been reported for relatively simple systems of chemical engineering, such as on single phase flow in pipes and packed beds /13/, /17/, /18/, /23/, /47/ reactors /9/, /15/, /27/, /28/, /55/, /64/, and heat exchangers /8/.

An unsteady state investigation of packed gas-liquid absorption equipment appeared to be both useful and interesting for the following reasons:

1. Simplified equipment such as wetted wall columns and disc absorption columns yield data which is not easily applicable to predictions on the performance of packed absorbers /11/. Mass transfer data as obtained from experimental columns operated at steady state conditions appears to be in wide disagreement /51/. These difficulties are apparently due to the fact that very little is known about the flow of layers of liquid and gas over discontinuous surfaces and the fundamental concepts of hydrodynamics are not sufficient in furnishing valid similarity criteria. It is possible that statistical information on the "distribution of residence-times" of the gas and liquid stream flowing through the column

may provide a valid similarity criterion and thereby provide a more satisfactory parameter for the correlation of absorption equipment performance.

2. As the knowledge of absorption processes becomes more complete, a greater and greater number of these processes appear to involve chemical reactions between components of the gas and liquid phase in addition to physical absorption /51/. For such processes, data on distribution of residence-times of both phases as function of their volumetric rates of flow and column geometry are of direct use in design calculations.
3. Unsteady state experimental techniques applied to gas-liquid flow systems present unusual problems concerning the introduction of a predetermined disturbance in one of the entering phases and the separation of the effluent phases for rapid analysis. The existing theory on the analysis of unsteady state measurements /13/, /38/, is not general enough to make possible the analysis of more complex equipment and conditions of flow other than uniform. Once the reliability and generality of unsteady state measurements could be demonstrated, such a technique would certainly find increased application in chemical engineering research.

For the foregoing reasons, we elected to study a typical gas-liquid packed absorber (a column packed with Raschig rings) under unsteady state conditions.

The problem was limited to the study of the gas phase response to a sudden disturbance in tracer concentration in the inlet stream. Complicating effects such as absorption or chemical reaction between the liquid and gas streams were eliminated. The method of introduction of the transitory disturbance permitted the measurement of the total volume of the column occupied by the gas. Such gas holdup data, for a packed absorption column, not previously available in the literature was one of the specific objectives of this work.

The theory of unsteady state experimentation has been reorganized and presented stressing the interpretation of transient response in terms of its statistical significance. Various models proposed for the correlation of mixing data in packed beds have been presented and discussed in the theory. The concept of a packed bed as a series of perfectly mixed stages was generalized in order to adequately formulate the complications presented by the experimental equipment required to handle a gas and a liquid phase.

The experimental equipment involved the development of a continuous gas analyzer based on an alpha particle ionization chamber already used for the analysis of gas mixtures /16/ and as a leak detector. Analyzers capable of furnishing a continuous output signal of this type are strongly recommended for unsteady state work since they allow direct and automatic computations on the output signal to furnish the desired characteristics of the response.

The reported data consists primarily of gas porosities and Peclet numbers, a dimensionless mixing parameter calculated from the recorded response of the gas stream, as function of gas and liquid flow rates and packing sizes. A discussion of these data is given.

It is recommended that a study of the behavior of the liquid phase be made in a manner analogous to the one followed here for the gas. It is hoped that such a course of action may lead to a more complete picture of the mechanics of heterogeneous flow in packed beds.

CHAPTER II

LITERATURE SURVEY ON GAS-LIQUID PACKED COLUMNS

Packed columns are widely used for the contacting of two fluid phases to effect mass transfer and/or chemical reaction between them. A packed column consists of a vertical shell, constructed of metal, ceramics or glass filled with packing materials such as Raschig rings or other regular or irregular shapes made out of a wide variety of materials.

Two types of columns find use in chemical engineering operations; one in which the gas and liquid flow countercurrently to each other, the other in which both phases flow down the column concurrently. The first type finds applications in most separations in which the absorption of a gaseous component by the liquid or the stripping of a liquid component by the gas is desired. In this case, the countercurrent operation is advantageous in obtaining the maximum possible driving force between the two contacting streams, the packing producing a large surface of contact between the two phases. The second type is generally used in hydrogenation and hydrodesulfurization of heavy petroleum feed stocks and in other catalytic conversion processes. Here, in general, the packing is the catalyst for the reaction. The concurrent flow technique is used to favor greater capacity rather than greater driving force between the flowing phases.

When the two fluid phases are flowing through a porous medium such as a packed tower, the liquid normally wets the solid and flows over it, thus changing the volume of the voids available to the gas flow in absence of liquid. We shall, from now on, refer to the fraction

of the total tower volume occupied by gas, as porosity and the fractional volume occupied by the liquid as holdup.

The extent of our knowledge on the nature of such flow is limited to pressure drop and liquid holdup measurements for countercurrent operation which we shall presently review.

The pressure drop in packed columns increases with an increase in gas rate, liquid rate, or both. The pressure drop for a constant liquid flow rate is proportional to the mass flow rate of the gas raised to a power between 1.8 and 2 until a critical flow velocity is reached where the curve increases in slope /51/. This point is called "flooding point". Another less clearly defined change in slope is sometimes detected before the flooding point is reached. This is called loading point. In recent times, however, a more generally accepted belief is that loading and flooding phenomena develop gradually and not suddenly at a definite flow point. In general, it has been found difficult to obtain correlations of the pressure drop from consideration of the proportions of the voids occupied by the two fluids. Therefore, most of the reported data /44/, /57/, /50/, /60/ is given as function of gas and liquid superficial flow rates for various packing independently of the actual flow conditions in the column.

The total quantity of liquid present in an absorption column at any time during operation has been called liquid holdup. In general, this quantity has been arbitrarily defined to consist of a static and a dynamic or operating holdup. The first is the amount of liquid in the packing which does not drain when the flow to the column is stopped. The latter represents the liquid flowing through the packing and which drains when the flow is interrupted. The total holdup has been found

to increase with liquid flow rates. Below the flooding gas velocity, holdup was found almost independent of gas rate until, as the flooding was approached, the holdup increased exponentially /58/, /19/, /34/, /54/.

Holdup information has been used to shed some light on the flow mechanics of the column. Theoretical discussions of flooding in packed equipment and generalized correlations of limiting velocities with fluid properties and packing dimensions are given by Elgin and Weiss /19/, Sherwood, Shipley and Holloway /52/, and Lobo, Friend, Hashmall and Zenz /43/. In all cases, fluid velocities based on the empty cross section of the column, the superficial area and the void fraction based on the dry packing were the correlation parameters.

Recently, the pressure drop for coke packing was correlated in terms of the true gas velocity by Gardner /26/, this being the first effort to relate quantitatively holdup and pressure drop.

No data of this nature are available for concurrent flow except for a recent study on mixing and flow distribution on the two phases flowing concurrently over glass spheres and porous pellets published by Lapidus /40/ while the present work was in progress.

The performance of packed absorption towers is also dependent on the extent of interfacial area available for the transfer of mass between the two phases. The effective value of the wetted area is, in general, less than the geometrical surface of the packing and there are reasons to believe that it changes with the hydrodynamic conditions in the column.

Wetted surface area has been determined either directly in

various ingenious ways /45/, /29/, or by using gas film controlled absorption data which is amenable to analysis resulting in indirect estimates of effective wetted surface areas /22/, /51/, /53/. These data are in agreement only in that for the operating range below the loading zone, gas rates had no effect on wetted area but extent of wetted area was liquid rate dependent. F. R. Whitt /62/, in a recent review on this subject points out that the directly determined wetted surface values for 3/8" and 1/2" Raschig rings appear to be considerably higher than the indirectly estimated effective values for the same size rings and liquid rates. For a given liquid rate, the effective wetted surface per unit volume is surprisingly similar for Raschig rings from 1/2" to 2" in diameter in spite of a 114/29 or approximately fourfold range of total available surface. The prevalent uncertainty on the actual value of this quantity is believed to be partly responsible for the wide scatter of mass transfer data /51/.

Recent work on correlation of mass transfer data /25/, /20/, /46/, /5/ , has shown that gas porosity is also an important correlation parameter. No direct measurements of gas porosities in countercurrent packed towers have been available to date.

CHAPTER III

THEORY

Experiments in which unsteady state response of a system is to be studied involve the use of an input signal and measurement of the output as function of time.

For process systems one is more or less restricted to use as a signal some alteration of the intensive property of the fluid being processed. Of these, the most readily measurable properties are temperature and concentration. If the disturbance is introduced in a transitory manner, we obtain the so-called transient response of the system. The signal can also be introduced in a cyclic manner and in this case the system response is called frequency response.

Transient Response

An early application of transient response in chemical engineering research is reported by F. C. Fowler and G. G. Brown /23/ in a study of the successive flow of fluids through pipes. Gilliland and co-workers used it in a pioneering study of fluidization /27/, /28/. Later, transient response found increased application in the study of fluidized reactors /15/, /55/, heat exchangers /8/, packed beds /18/, and stirred pot reactors /9/, /64/. Danckwerts /13/ gives a detailed discussion of this technique as a tool for equipment and process studies.

We shall restrict our attention to the case of a flow system in which the signal is generated by changes in concentration of a given component of the fluid stream designated as the tracer.

There are two methods of introduction of the concentration signal which lead to a simple mathematical representation. These are:

1. Injection in the inlet stream of a quantity of tracer virtually instantaneously or within a period of time very short compared to the average residence-time. Such an input is designated mathematically as "impulse function" or "delta function".
2. Introduction of a discontinuity in the concentration of the tracer in the inlet stream by displacing the fluid flowing through the equipment with a fluid of different tracer concentration. If the transition from the leading fluid to the follow-up fluid takes place sharply, the input may be represented mathematically by a "step function".

Impulse Input, Distribution of Residence-Times Function

We consider a flow system having a total volume V and through which the volumetric rate of flow is v. If the quantity Q of tracer is injected instantaneously at the inlet, a continuous analysis of the effluent fluid will yield a plot of tracer concentration versus time as shown in Figure 1.

No matter what the shape of the concentration-time plot the material balance for the tracer:

$$\int_0^\infty v c \, dt = Q \tag{1}$$

must hold. Here t is the time measured from the introduction of the impulse signal and c is the tracer concentration.

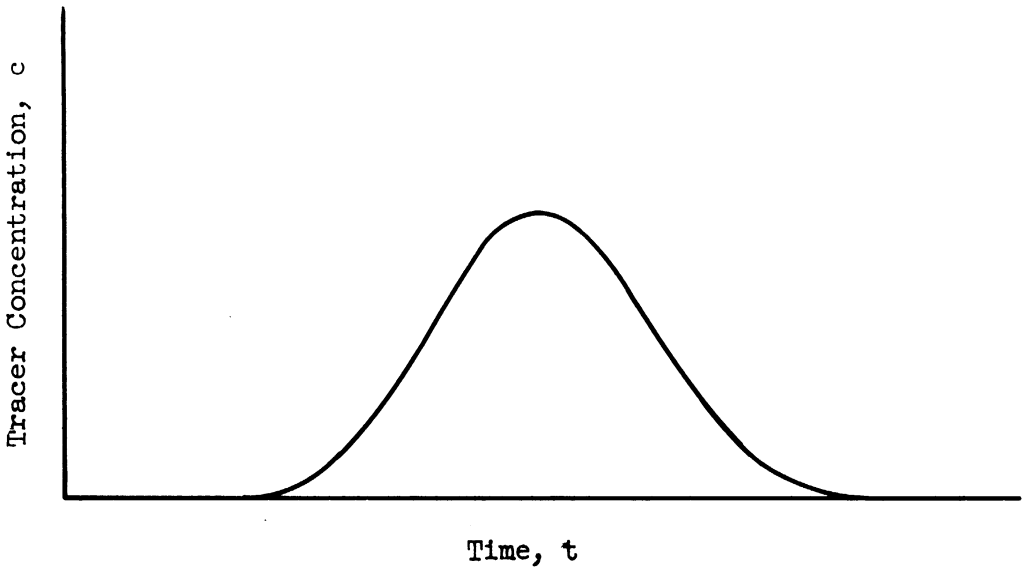

Figure 1

Response To A Tracer Impulse

By transposing Q in equation (1) the material balance can also be written in the form:

$$\int_0^\infty \frac{vc}{Q}\,dt = 1 \qquad (2)$$

Equation (2) suggests that the quotient $\frac{vcdt}{Q}$ may be regarded as that fraction of the tracer injected at the inlet at time t=0 over an infinitesimal amount of time which has emerged in the effluent in the interval of time t and t+dt. The sum of all such fractions over all times must of course be equal to unity.

We realize then, that if one could tag each molecule which is introduced in the system at any time t over a very small interval of time dt the same relationship would exist between all the tagged mole-

cules at the outlet so that quite independently from the injection of an impulse of tracer all the molecules flowing through the system obey a "probability" law governing their time of residence in the system.

The pulse experiment offers a convenient method to measure such a probability so that with the quantity $\frac{vc}{Q}$ we may associate the function $E(t)^*$ such that:

$$\int_0^\infty E(t)\,dt = 1 \qquad (3)$$

E(t) may thus be defined as the fraction of the entering feed, flowing in the effluent per unit time, which has been in the reactor between times t and t+dt. We shall designate E(t) as the distribution of residence-time function or simply time distribution.

The Average Residence-Time, Moments of the Distribution of Residence-Times

A plot of E(t) versus t as shown in Figure 2 gives a graphical representation of the mass fraction of those elements of fluid which enter the system at the same moment and which are flowing out per unit of time as a function of the time spent in the system.

The time spent on the average by the fluid flowing through the system may be readily found by the well-known method of calculating the average of a continuous function.

$$\vartheta = \frac{\int_0^\infty tE(t)\,dt}{\int_0^\infty E(t)\,dt} \qquad (4)$$

* In probability theory E(t) is called a probability frequency function /10/. Equation (3) gives a basic property of the frequency function.

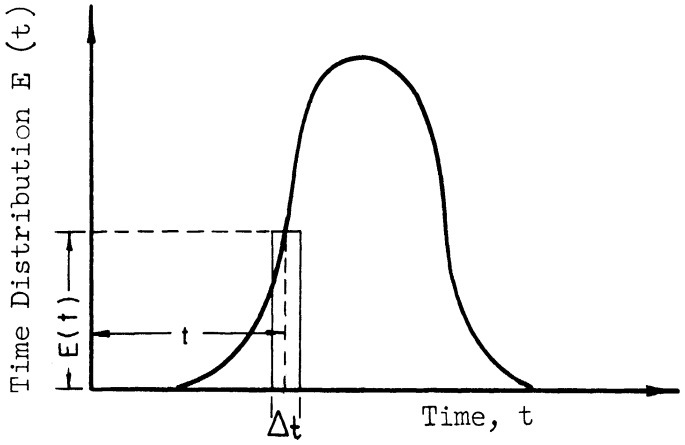

Figure 2

Distribution of Residence-Times Plot

θ is the average or mean residence-time and is a useful quantity to characterize the system, since no matter what the flow conditions are:

$$\vartheta = \frac{\epsilon V}{v} \tag{5}$$

where ϵ is the fraction of the total volume occupied by the fluid. Thus, if the average residence-time θ and the volumetric flow rate of the fluid v are known, the volume of the system occupied by the fluid ϵV may be readily calculated. Vice versa, if both ϵV and v are known one may check the consistency of the residence-time distribution curve as determined in the tracer experiment by the use of equations (4) and (5).

Combining equations (3) and (4) we may write simply:

$$\vartheta = \int_0^\infty t E(t)\, dt \tag{6}$$

Referring to Figure 2 we see that on the basis of equation (6), the

average residence-time θ can also be regarded as the first moment of the distribution function about the ordinate axis since it is the summation of all the differential elements of the area $E(t)dt$ multiplied by the abscissa t.

In general, we define the nth moment of the distribution function as the summation of the differential elements of area multiplied by the abscissa raised to the nth power:

$$\text{nth moment} = \int_0^\infty t^n E(t)\,dt \tag{7}$$

Comparison Between The Response Of Two Systems, The Variance

When it is required to compare the pulse response for two systems having different mean residence-times the time scale for the two systems will be different since in the one for which the residence-time is larger, the tracer elements* will spend a longer time in flowing through even though their relative distribution with respect to the average time spent in the system may be the same as Figure 3 shows. In this case, it is useful to use as the abscissa the dimensionless time t/θ and as the ordinate the dimensionless function $\theta E(t)$ so that equation (3) becomes:

$$\int_0^\infty \theta E(t)\,d(t/\theta) = 1 \tag{3-a}$$

* The word "elements" is used to identify small but discrete portions of the flowing fluid. Depending upon the scale of interest (smoothing out of the response curves) or the nature of the detecting apparatus one may identify such elements with molecules or segments of the flowing stream of various dimensions down to a molecular scale.

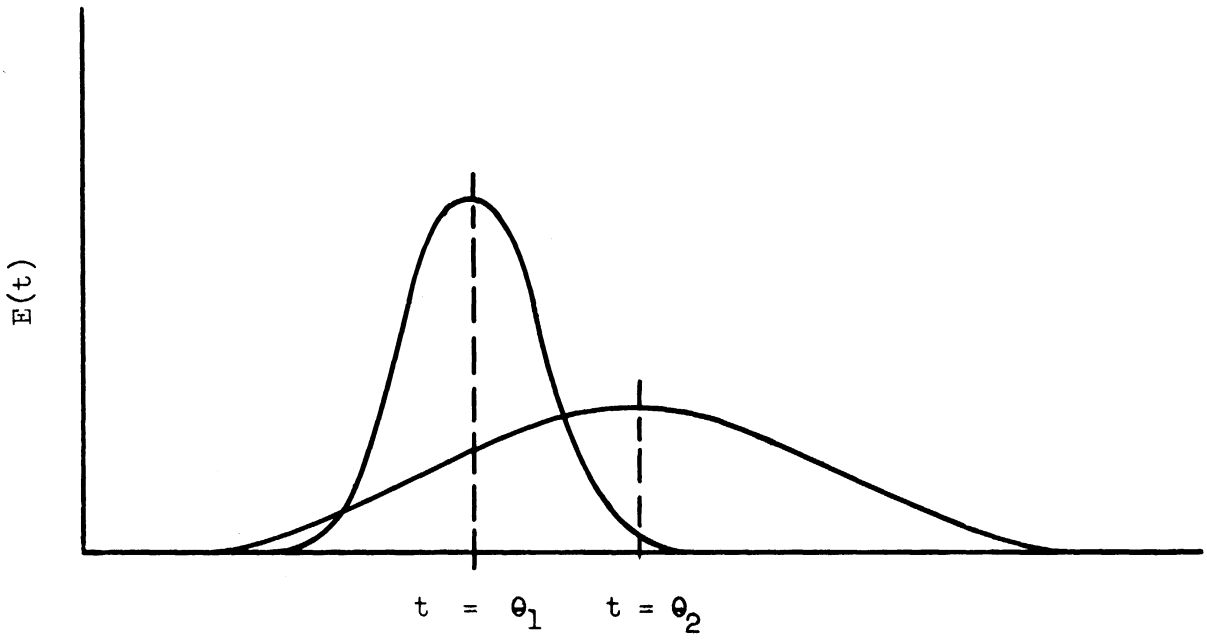

Figure 3

Distribution of Residence-Times Plot
For Two Systems Having Different Average Residence-Time

and equation (6) gives:

$$\int_0^\infty (t/\theta)\, \theta E(t)\, d(t/\theta) = 1 \qquad (6\text{-a})$$

If the dimensionless plot $\theta E(t)$ versus t/θ is the same for the two systems being compared, then the two systems exhibit the same transient behavior.

It is apparent that the shape of the residence-times plot will vary with the nature of the flow taking place in the column depending upon the flow path followed by each tracer element. Two limiting possibilities may be visualized: One is the piston flow case in which tracer

elements which enter the vessel at the same moment proceed through it with constant and equal velocity in parallel flow paths; the other is the case of perfect mixing in which the fraction of tracer elements which escape the system immediately after injection is a maximum. This condition is achieved when the concentration throughout the vessel is the same as the concentration of the effluent. Consequently, at the moment of injection:

$$t = o \qquad \text{and} \qquad Q = \epsilon V_c$$

so that:

$$\vartheta E(t) = \frac{\epsilon V_c}{Q} = 1$$

therefore, the dimensionless time-distribution curve has a value of 1 at $t/\theta = 0$ and as seen in Appendix II, pp. 185 it decays at a rate equal to $1/\theta$.

Between these two limiting cases as illustrated in Figure 4, there are various degrees of mixing depending upon the manner of propagation of the impulse signal through the system.

Figure 4 clearly shows that the major difference between the various degrees of mixing is the degree of dispersion of the impulse signal about the mean residence-time. For piston flow the tracer signal at the outlet is concentrated about $t/\theta = 1$ and the dispersion is zero. The dispersion increases as the mixing increases until for perfect mixing the dispersion is greatest and equal to 1 (See pp. 49).

The second moment of the dimensionless distribution of residence-times curve about $t/\theta = 1$ gives a suitable measure of the degree of dispersion.

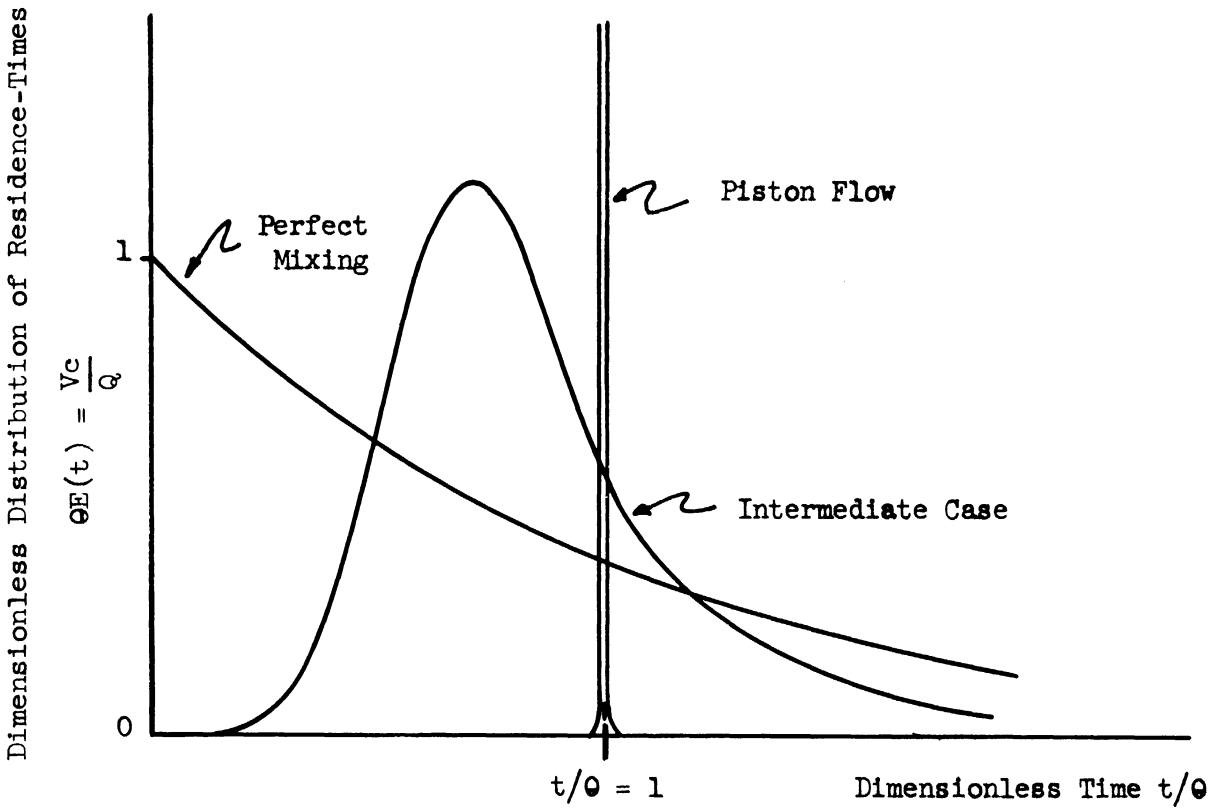

Figure 4

Dimensionless Residence-Times Plot Showing Various Degrees of Mixing

From our definition of the nth moment (see page 15) we have for the second moment of $\theta E(t)$ about the origin:

$$\int_0^\infty (t/\theta)^2 \theta E(t)\, d(t/\theta) \tag{8}$$

similarly, the second moment about $t/\theta = 1$ is:

$$\int_0^\infty (t/\theta - 1)^2 \theta E(t)\, d(t/\theta) \tag{9}$$

by use of equation (3a) and (6a), this reduces to:

$$\sigma^2 = \int_0^\infty (t/\theta)^2 \theta E(t)\, d(t/\theta) - 1 \quad (10)$$

Equation (10) gives the desired quantity which we shall call "variance" and designate it by the symbol σ^2 because of its similarity with an analogous quantity used in statistics /10/, /21/, /24/.

The Skewness, Correlation of Distribution Curves

While the variance of the residence-times distribution typifies the extent of mixing taking place in a flow system by giving a measure of the dispersion of the fluid elements about the average residence-time, no clue is obtained as to the "asymmetry" of the dispersion. In fact, two impulse response curves may have the same average residence-time and variance as shown in Figure 5 and yet they are not completely congruent because one is symmetric about the axis $t/\theta = 1$ and the other is not.

If the distribution curve were symmetric about the $t/\theta = 1$ axis, all central moments of odd order would vanish. It is practice in statistics and probability theory /10/ to use the departure from zero of the third central moment as a measure of the asymmetry of the distribution. We shall call this quantity "skewness" and designate it by the symbol ν. By analogy with equation (9) the third central moment

* In some hypothetical models of flow systems, the average residence-time θ as calculated from the computed response of the model to an impulse may not be equal to the true residence-time $\epsilon V/v$. In this case, if one desires to calculate the variance about the true residence-time $\epsilon V/v$ equation (10) becomes:

$$\sigma^2 = \left(\frac{v}{\epsilon V}\right)^2 \int_0^\infty t^2 E(t)\, dt - \left(\frac{v}{\epsilon V}\right)^2 \left[\int_0^\infty t E(t) dt\right]^2 \quad (10\text{-a})$$

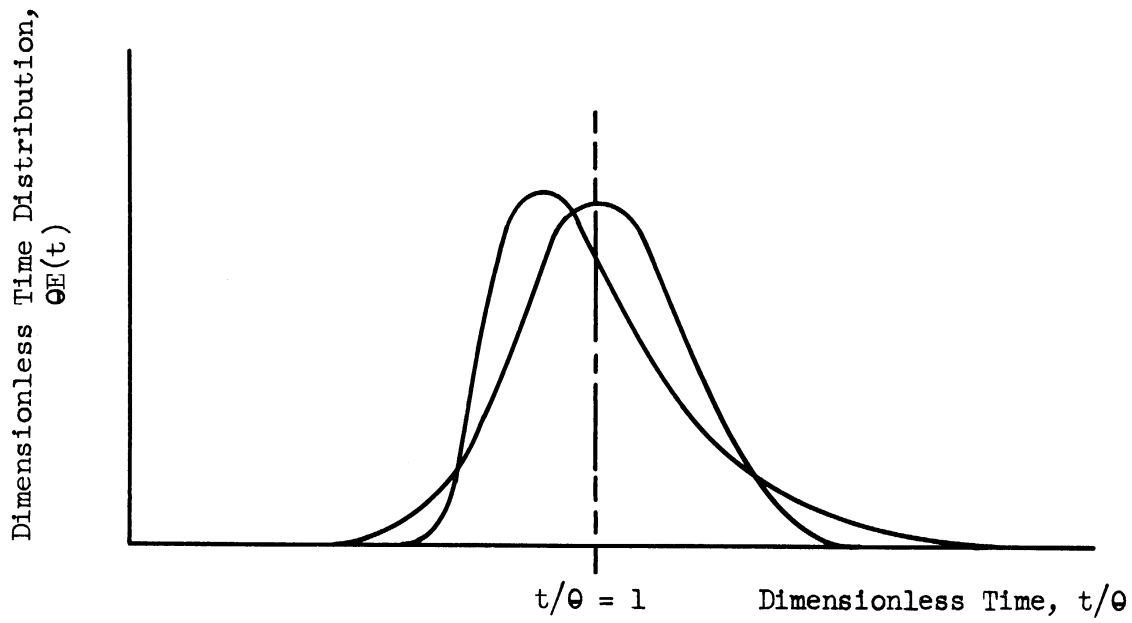

Figure 5

Dimensionless Residence-Times Plot
Showing Asymmetry About The $t/\theta = 1$ Axis

is:

$$\nu = \int_0^\infty \left(t/\theta - 1\right)^3 \theta E(t)\, d(t/\theta) \tag{11}$$

By simplifying:

$$\nu = \int_0^\infty \left(t/\theta\right)^3 \theta E(t)\, d(t/\theta) - 3\int_0^\infty \left(t/\theta\right)^2 \theta E(t)\, d(t/\theta) + 2 \tag{12}$$

The skewness of the distribution function is used in the experimental section of this work to indicate the degree of agreement of experimental residence-times distribution curves with a given correla-

tion model.

The fourth moment of the distribution function is also needed to completely define a distribution curve /24/; however, in practical analysis the evaluation of the variance and skewness may already prove to be a tedious task.

Empirical methods of correlation based on the various moments of the distribution curve have been developed to fit all sorts of statistical distributions. The Gram-Charlier series, for example, is capable of fitting a distribution curve. The coefficient of each term of the series is a moment of the distribution curve in question. The degree of accuracy of the series increases as terms containing moments of higher and higher order are added. For a description of this series and other methods of correlation, reference is made to Fry's excellent work on probability and its engineering uses /24/.

Step Input

The foregoing information about the residence-time distribution function can also be obtained by the introduction in the flow system of a step (or discontinuity) in tracer concentration. For a step function input, a continuous analysis of the effluent fluid will yield a plot of tracer concentration versus time.

When the displacing fluid contains no tracer while the fluid being displaced has a tracer concentration equal to c_o, the response curve will have the general shape shown by the solid line in Figure 6.

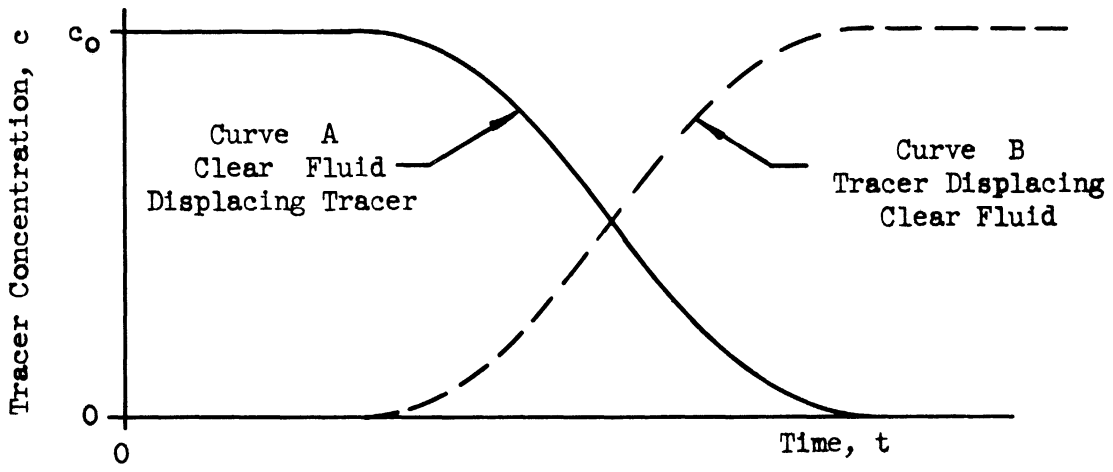

Figure 6

Response To A Step In Tracer Concentration

No matter what the shape of the curve, the material balance:

$$\int_0^\infty v\,c\,dt = c_o(\epsilon V) \tag{13}$$

must hold. Here t is the time from the moment of discontinuing the tracer flow, c_o is the initial tracer concentration, c is the concentration at any time t, ϵV is the volume of the system occupied by the fluid, v is the volumetric fluid velocity.

If the displacing fluid has a tracer concentration equal to c_o while the leading fluid does not, the response curve would have the form as shown by Curve B in Figure 6. The material balance for the tracer is now:

$$\int_0^\infty v(c_o - c)dt = c_o(\epsilon V) \tag{14}$$

On rearranging equations (13) and (14) and substituting for $\epsilon V/v$ the average residence-time θ, we obtain respectively:

$$\int_0^\infty \frac{c}{c_o}\, d(t/\theta) = 1 \qquad (13\text{-a})$$

and

$$\int_0^\infty \left(1 - \frac{c}{c_o}\right) d(t/\theta) = 1 \qquad (14\text{-a})$$

A plot of c/c_o versus t/θ will thus be independent of the mean residence-time. In addition, equations (13-a) and (14-a) clearly show that Curves A and B are one the complement of the other since for any value of t/θ as shown in Figure 7, the sum of the ordinate of Curves A and B is equal to unity.

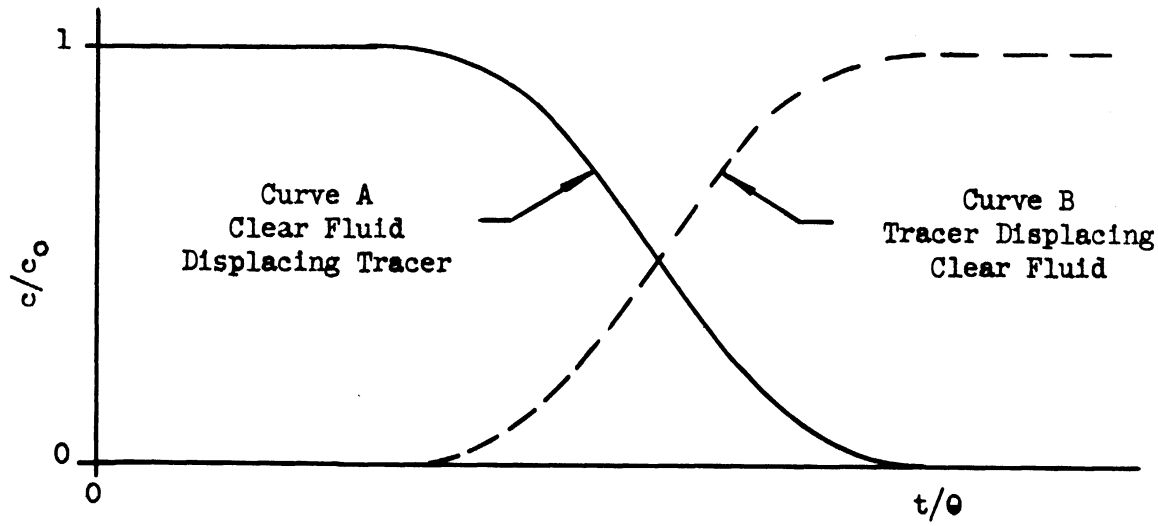

Figure 7

Dimensionless Step Function Response

For the sake of mathematical consistency in the treatment that follows, we shall be concerned with response curves of the type represented by Curve B, i.e., with experiments in which the step function input is produced by a sudden change in concentration from 0 to c_o. The conclusions which we shall obtain will be equally applicable to the complementary case as presented by Curve A.

The step function response must be in some simple way related to the distribution of residence-times function since for the same system, the only difference in the two response curves lies in the input signal.

By intuitive reasoning we may argue that since a step in tracer concentration results from the summation of an infinite number of impulses introduced in the system over a continuous interval of time, the response to a step function ought to be obtained by integration of the distribution of residence-times curve or vice versa, the distribution of residence-times curve should be obtained by differentiation of the step input response.

A verification of this statement is obtained by the following reasoning:

For a step input in tracer concentration at time zero, the flowing stream at the inlet of the system is suddenly changed from 0 to c_o. At any time t thereafter, the rate of flow of tracer in the effluent stream is cv and the molecules of tracer in the effluent stream have been in the system for a period of time anywhere from 0 to t. At time $t + dt$ the rate of outflow of tracer is $cv + \frac{d(vc)}{dt}dt$ and the tracer molecules in the effluent have been in the system for a

period of time anywhere from 0 to t + dt.

The increment in tracer outflow $\frac{d(vc)}{dt}dt$ is due to molecules of feed which have been in the system for an interval of time between t and t + dt. Therefore, the fraction of entering feed emerging at the outlet in the interval of time t + dt and which has been in the system for an interval of time from t to t + dt is:

$$\frac{\frac{d(vc)}{dt}dt}{v c_o} = \frac{d\frac{c}{c_o}}{dt}dt$$

The fraction of entering feed which has been in the reactor for an amount of time between t and t + dt emerging at the outlet for unit of time, i.e., $\frac{d\, c/c_o}{dt}$ corresponds to the distribution of residence-times function E(t) as defined on page 13

$$E(t) = \frac{vc}{Q} = \frac{d\frac{c}{c_o}}{dt} \qquad (15)$$

From the foregoing we have established the fact that the response to a step function is the integral of the distribution of residence-times curve. If it were required to obtain information about the distribution from a step function experiment a differentiation of the response curve would be necessary. Numerical methods of differentiation are rather inaccurate, however, so that one may recur to the evaluation of the moments of the distribution of residence-times curve which are obtainable from the step function response by an integration procedure.

Thus, the material balance from a step function experiment as given in equation (14) is the first moment of the distribution of residence-times:

$$\int_0^\infty tE(t)dt = \int_0^\infty \left(1-\frac{c}{c_o}\right)dt \tag{16}$$

this equality can be verified on integration by parts of the right hand side of equation (16) by using the relationship between E(t) and $\frac{c}{c_o}$ given in equation (15).

In an analogous manner, one may prove that:

$$\sigma^2 = \int_0^\infty (t/\vartheta)^2 \vartheta E(t) d(t/\vartheta) - 1 = \frac{2\int_0^\infty t\left(1-\frac{c}{c_o}\right)dt}{\vartheta^2} - 1 \tag{17}$$

and also:

$$\nu = \int_0^\infty (t/\vartheta)^3 \vartheta E(t) d(t/\vartheta) - 3\int_0^\infty (t/\vartheta)^2 \vartheta E(t) d(t/\vartheta) + 2$$

$$= \frac{3\int_0^\infty t\left(1-\frac{c}{c_o}\right)dt}{\vartheta^3} - \frac{6\int_0^\infty t\left(1-\frac{c}{c_o}\right)dt}{\vartheta^2} + 2 \tag{18}$$

A summary of the relationships between impulse, and step input response with the distribution of residence-times function E(t) is given in Table I, page 27.

Comparison of The Two Methods of Signal Introduction

Whenever it is desired to correlate the distribution of residence-times in terms of mechanistic models, one is confronted with

TABLE I

QUANTITIES CHARACTERIZING A SYSTEM IN TERMS OF ITS TRANSIENT RESPONSE

Moments of the Distribution of Residence-Times Function E(t)		Relationships in Terms of Outflow Concentration	
		Step Input from 0 to c_0	Impulse Input (Amount Q of Tracer Injected Instantaneously)
Zero Moment of E(t) vs. t About t = 0 axis	$\int_0^\infty E(t)dt = 1$	$\int_0^\infty d\, c/c_0 = 1$	$\int_0^\infty cdt = \frac{Q}{v}$
First Moment of E(t) vs. t About t = 0 axis	$\int_0^\infty tE(t)dt = \theta = \frac{\epsilon V}{v}$	$\int_0^\infty (1 - c/c_0)dt = \theta = \frac{\epsilon V}{v}$	$\frac{v}{Q}\int_0^\infty tcdt = \theta = \frac{\epsilon V}{v}$
Variance Second Moment of $\theta E(t)$ vs. t/θ About t/θ = 1 axis	$\sigma^2 = \int_0^\infty (t/\theta)^2 \theta E(t)d(t/\theta) - 1$	$\sigma^2 = \frac{2\int_0^\infty t(1 - c/c_0)dt}{\theta^2} - 1$	$\sigma^2 = \frac{\left(\frac{v}{Q}\right)^2 \int_0^\infty t^2 cdt}{\theta^2} - 1$
Skewness Third Moment of $\theta E(t)$ vs. t/θ About t/θ = 1 axis	$\nu = \int_0^\infty (t/\theta)^3 \theta E(t)d(t/\theta) - 3\int_0^\infty (t/\theta)^2 \theta E(t)d(t/\theta) + 2$	$\nu = \frac{3\int_0^\infty t^2(1 - c/c_0)dt}{\theta^3} - \frac{6\int_0^\infty t(1 - c/c_0)dt}{\theta^2} + 2$	$\nu = \frac{\left(\frac{v}{Q}\right)^3 \int_0^\infty t^3 cdt}{\theta^3} - \frac{3\left(\frac{v}{Q}\right)^2 \int_0^\infty t^2 cdt}{\theta^2} + 2$

the solution of "systems" of differential equations which simulate the behavior of the experimental system. In this case, the step signal lends itself more readily to the mathematical solution of the problem by elementary methods /35/ and, in most cases, the solutions are reported in terms of step function response. The impulse response can be readily obtained by differentiating such solutions.

Another important advantage of the response to a step input experiment is that the volume of the system occupied by the fluid stream which carries the tracer is readily obtained from the value of the area under the response curve as equations (13) and (14) clearly show. When a response to an impulse is available instead, one must evaluate the first moment of the response curve. When this is done by graphical means, the procedure is more laborious and less accurate*.

In many cases, especially in the study of large equipment, the impulse signal may prove to be more advantageous because it requires much smaller quantities of tracer which may be injected just ahead of that portion of equipment under study thus avoiding entrance problems and the problem of obtaining a sharp transition from tracer to ordinary process stream as required in the step input method. On the passive side, however, is the high sensitivity required by the detection equipment since the amount of tracer injected in a pulse will be small in comparison to the volumetric flow rate of the clear fluid so that the tracer concentration at the outlet will be relatively small even at its peak

* In the event that a continuous analysis of the effluent is feasible, one may feed the output signal of the analyzer to suitable electronic integrators to obtain the various moments of the distribution to any desired degree of accuracy.

value. Instruments of high sensitivity and suitable for this purpose, such as a mass spectrograph, are very costly and make the impulse technique less accessible to the experimenter.

Lastly, it is worth mentioning that in special systems it may be advantageous to use both methods of signal introduction. Lapidus, in a recent article /39/ reported a transient study of a reactor packed with porous catalyst pellets and pointed out that impulse response did not detect the intraparticle voids because the rate of tracer transfer in and out of the pores of the catalyst occurred at a much lower rate than the speed of propagation of the impulse throughout the system. In this case, comparison between impulse and step experiments may lead to the evaluation of intraparticle void volume.

Frequency Response

This unsteady state method of experimentation consists of using as input a purely sinusoidal signal. No direct information is obtained, however, about the volume of the system occupied by the fluid or about the distribution of residence-times.

Frequency response is valuable when a mathematical model which approximates the system is already available*. In this case, the mathematical analysis is greatly simplified since the phase shift and amplitude attenuation of the response, as exemplified in Figure 8, permit a direct evaluation of the constants involved in the "system" of differential equations which simulates the physical situation.

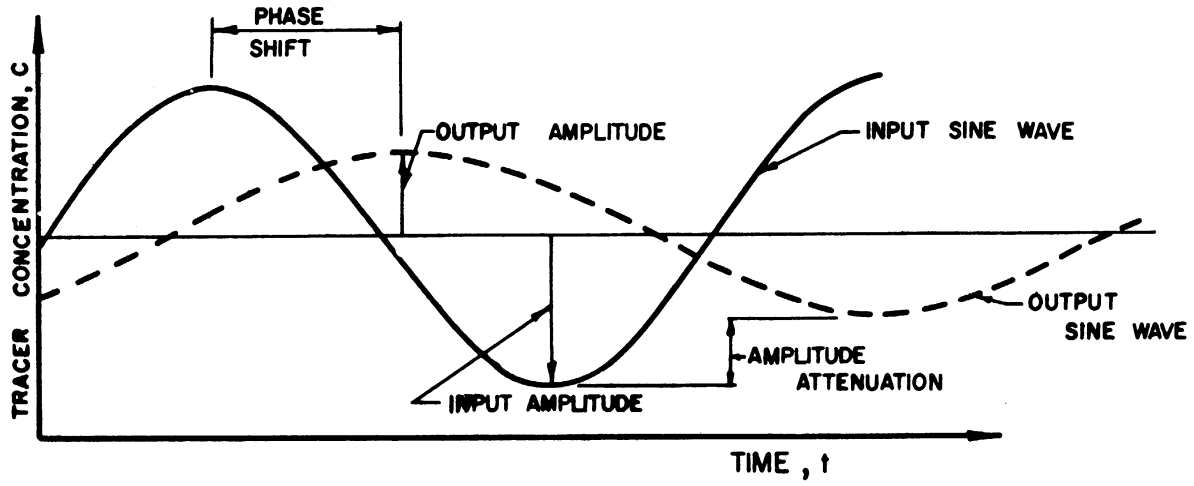

Figure 8

Frequency Response

* This is generally the case in electric networks and instrument loops where frequency response finds its widest application.

Frequency response has found some application in chemical engineering investigations, notably in the study of longitudinal diffusion occurring in one phase flow through packed beds /17/, /18/, /36/ /47/, /38/, and in the study of heat transfer /8/. However, in addition to the one mentioned above, three other disadvantages to this method of analysis as applied to process systems are:

1. A great deal of specialized equipment is necessary to obtain an experimental frequency response on a particular process since the equipment must be capable of applying a sinusoidal disturbance upon one of the intensive properties of the process stream.
2. If the signal is not purely sinusoidal, the mathematical analysis is greatly complicated, thus offsetting the primary advantage of frequency response /18/.
3. If the differential equations which simulate the dynamics of the system are not linear, this method of mathematical analysis breaks down /35/.

Because of the disadvantages enumerated above, the experimental work undertaken in the present investigation was limited to the use of transient response and we shall no longer be concerned with frequency response analysis.

Axial Mixing In Packed Beds, Correlation Models

In this study we are concerned with the mechanism by which mass is dispersed in a packed bed through which it is flowing in the absence of absorption or chemical reaction.

In all cases of practical interest, the dispersion mechanism, which is usually referred to as mixing, involves turbulence. The intermingling of turbulent eddies is apparently responsible for a "coarse scale" of mixing while the ultimate homogenization to a molecular scale is effected by molecular diffusion.*

The Diffusion Model

Numerous authors /2/, /3/, /13/, /38/, /42/, have treated the mixing taking place in a packed bed as a diffusional process in which the rate of mass transfer is described by the relation:

$$r = -D \, \text{grad } c \tag{19}$$

where:

D = Effective diffusivity sq. ft/sec.

grad c = $\frac{\partial c}{\partial x}\,\bar{i} + \frac{\partial c}{\partial y}\,\bar{j} + \frac{\partial c}{\partial z}\,\bar{k}$ moles/cu.ft./ft.

r = Mass transfer rate, moles/sec.sq.ft.

Assuming that the bed can be treated as a continuum, we obtain the following expression for the accumulation in a differential element:

---

* This point is just mentioned here to render the reader aware that the "concentration at the point" has a significance only upon the scale of interest. And, the mixing rate may be dependent upon how fine a mixing is detectable by available instruments /12/.

$$\frac{\partial c}{\partial t} = -\,\mathrm{div}\,(D\ \mathrm{grad}\,c + uc) \qquad (20)$$

where u is the average velocity through the interstices of the bed.

The effective diffusivity has been found to be anisotropic, i.e., it is sensibly greater in the longitudinal than in the radial direction. Bernard and Wilhelm /3/ and Singer and Wilhelm /56/ have shown experimentally that at sufficiently high Reynolds numbers and tube-to-particle-diameter ratio, the radial Peclet number (the dimensionless quantity $\frac{du}{D_r}$) is approximately 11. Baron /2/ from a statistical treatment of the random side-stepping deflections of the fluid in the bed estimated that the radial Peclet number is between 5 and 13. The average length of each step was assumed by Baron to be dependent on the characteristics of the packing, the Reynolds number and the kinematic viscosity. Ranz /49/ calculated that the radial Peclet number in rhomboehedrally packed beds of spheres is 11.2. More recently, measurements of longitudinal mixing by Kramers and Alberda /38/ and McHenry and Wilhelm /47/ showed that the longitudinal Peclet number (the dimensionless quantity $\frac{du}{D_L}$) is between 1 and 2 for gases. Ebach's /18/ measurements for liquids gave values of 0.5 to 1. Despite the discrepancy in reported results, it can be stated with some certainty that the Peclet number in the radial direction is significantly higher. We shall discuss the possible reasons for the anisotropy of the effective diffusivity later (see page 55).

It suffices now to say that we restrict our discussion to longitudinal mixing alone since we assume that the transient concentration signal is introduced in such a manner that the concentration in the direction normal to flow is uniform.

For this particular case, equation /20/ reduces to:

$$\frac{\partial c}{\partial t} = -D_L \frac{\partial^2 c}{\partial x^2} + u \frac{\partial c}{\partial x} \qquad (21)$$

The solution of equation (21) involves a suitable choice of boundary conditions which will completely specify the problem. The choice depends on how detailed or complex a physical model is desired; of course, the resulting solutions become correspondingly more complex and consequently more difficult to use.

Solutions of The Diffusion Equation, Boundary Conditions

Here we shall briefly review the solutions of the diffusion equation (21) as reported in the literature /1/, /6/, /40/, /64/, in order of complexity of the physical model and thereby discuss their shortcomings for the correlation of the experimental data.

The simplest choice of boundary conditions is obtained by assuming continuity of fluid concentration at the inlet of a packed bed of infinite extent. The solution to this problem /6/, /40/, shall be referred to as solution "A". The conditions of continuity at the bed entrance, i.e., at $x = 0$ are:

$$c(0-) = c(0+) \qquad (22)$$

also for a bed of infinite extent:

$$\lim_{x \to \infty} c = 0 \tag{23}$$

A step input in tracer concentration from 0 to c_o may be described as follows:

$$\begin{aligned} c &= 0 \quad \text{at} \quad t < 0 \\ c &= c_o \quad \text{at} \quad t = 0 \\ c &= c_o \quad \text{at} \quad t > 0 \end{aligned} \tag{24}$$

The set of boundary conditions which satisfies equations (22), (23) and (24) is, therefore:

$$\begin{aligned} &\text{1-a)} \quad c(0,t) = c_o \\ &\text{2-a)} \quad \lim_{x \to \infty} c(x,t) = 0 \\ &\text{3-a)} \quad c(x,t) = 0 \end{aligned} \tag{25}$$

The solution of the diffusion equation with this set of boundary conditions evaluated at the outlet where $x = L$ is:*

$$\frac{c}{c_o} = \frac{1}{2}\left[\operatorname{erfc}\left(\frac{L-ut}{2\sqrt{D_L t}}\right) + e^{\frac{uL}{D_L}} \operatorname{erfc}\left(\frac{L+ut}{2\sqrt{D_L t}}\right)\right] \tag{26}$$

By differentiation of the step input response as given by equation (26) above, one obtains the impulse response or distribution of residence-times function:

$$E(t) = \frac{d\frac{c}{c_o}}{dt} = \frac{u}{2\sqrt{\pi t^3 D_L}} e^{-\left(\frac{ut-L}{2\sqrt{tD_L}}\right)} \tag{27}$$

* See derivation details in Appendix I, pp. 164

It may be shown that the zero moment of the distribution of residence-times as given by equation (27) is equal to unity*. Moreover, the second moment of the distribution is equal to L/u^* or the average residence-time. Therefore, solution "A" appears to be consistent with the conditions required by the time distribution of an actual system as specified in equation (3), page 13 and equation (6), page 14 .

Aris and Amundson have recently pointed out /1/ however, that the space distribution ** of this solution does not behave correctly because its zero moment is greater than one, due to the simplicity of the model which does not take into account the diffusion flux at the inlet boundary. For this reason, solution "A" should not be used when the extent of mixing is large (large values of the effective diffusivity).

A somewhat more complex model results when such a diffusion flux is considered to be present immediately at the entrance of a packed bed of infinite extent. We shall call the solution to this problem, recently given by Aris and Amundson /1/, solution "B".

---

* See derivation details in Appendix I, pp. 166 and 167 .

** Note that equation (27) is really a function of space (x) and time (t) and that the space variable was kept constant by letting x = L thus obtaining a distribution in time (or residence-times distribution as we have called it). By maintaining the time variable constant it is possible to study the space distribution as it was done by Aris and Amundson.

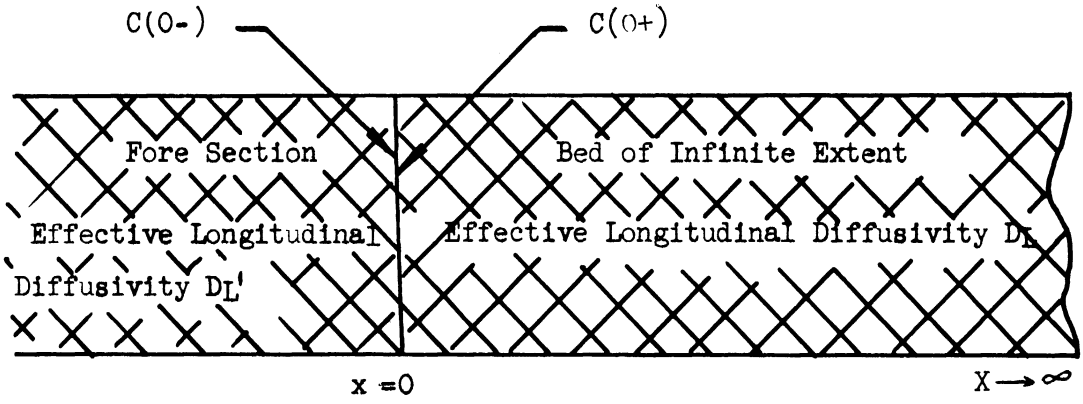

Figure 9

Conditions At Inlet Of Packed Bed

The physical situation at the inlet to the semi-infinite bed is shown schematically in Figure 9. To the left of the boundary x = 0, we have:

$$\frac{\partial c}{\partial t} = uc(0-) - D_L' \frac{\partial c(0-)}{\partial x}$$

to the right:

$$\frac{\partial c}{\partial t} = uc(0+) - D_L \frac{\partial c(0+)}{\partial x}$$

so that a material balance gives the required inlet condition:

$$uc(0-) - D_L' \frac{\partial c(0-)}{\partial x} = uc(0+) - D_L \frac{\partial c(0+)}{\partial x} \qquad (28)$$

For a semi-infinite column as for solution "A", we have:

$$\lim_{x \to \infty} c = 0 \tag{23}$$

and for a step function in tracer concentration from 0 to c_o as before we can write:

$$\begin{aligned} c &= 0 \quad \text{at} \quad t < 0 \\ c &= c_o \quad \text{at} \quad t = 0 \\ c &= c_o \quad \text{at} \quad t > 0 \end{aligned} \tag{24}$$

If the step function is applied immediately at the boundary of the packed bed as we would obviously like to assume for simplicity, then $\frac{D'_L \partial c(o-)}{\partial x}$ in equation (28) must be equal to zero as dictated by the discontinuity in the step function. This essentially means that in order to obtain a sharp step input, the diffusivity in the fore-section D'_L must be zero. Thus the set of boundary conditions which satisfies equations (28), (23) and (24), is:

$$\begin{aligned} &\text{1-b)} \quad uc_o = uc(o,t) - D_L \frac{\partial c}{\partial x}(o,t) \\ &\text{2-b)} \quad \lim_{x \to \infty} c(x,t) = o \\ &\text{3-b)} \quad c(x,o) = o \end{aligned} \tag{29}$$

The solution of the diffusion equation evaluated at the

outlet, i.e., at x = L is:*

$$\frac{c}{c_o} = \int_o^t \frac{u e^{-\frac{(L-ut)^2}{4D_L t}}}{\sqrt{\pi D_L t}} dt + \int_o^t \frac{u^2 e^{\frac{uL}{D_L}}}{2D_L} \operatorname{erfc}\left(\frac{L+ut}{2\sqrt{D_L t}}\right) dt \qquad (30)$$

and the impulse response*:

$$E(t) = \frac{d\frac{c}{c_o}}{dt} = u e^{-\frac{(L-ut)^2}{4D_L t}} - \frac{u^2 e^{\frac{uL}{D_L}}}{2D_L} \operatorname{erfc}\left(\frac{L+ut}{2\sqrt{D_L t}}\right) \qquad (31)$$

The zero moment of the residence-times distribution as given by equation (31) above is equal to unity*. However, for the first moment we find*:

$$\int_o^\infty tE(t)dt = \int_o^\infty \left[\frac{u}{\sqrt{\pi D_L t}} e^{-\frac{(L-ut)^2}{4tD_L}} - \frac{u^2 e^{\frac{uL}{D_L}}}{2D_L} \operatorname{erfc}\left(\frac{L+ut}{2\sqrt{D_L t}}\right)\right] dt = \frac{L}{u} + \frac{D_L}{u^2} \qquad (32)$$

Therefore, the distribution of residence-times given by this model does not correspond to that of an actual system. Normalizing equation (32) i.e., dividing throughout by the residence-time θ or L/u we obtain:

$$\int_o^\infty (t/\theta)\theta E(t)\, d(t/\theta) = 1 + \frac{D_L}{uL} \qquad (33)$$

---

* See derivation details in Appendix I, pp. 172 and 175

A comparison of this result with equation (6-a) clearly shows that the first moment of the time distribution as given by solution "B" will approximate that of an actual system within 1% when:

$$\frac{D_L}{uL} \leq .01 \tag{34}$$

A third solution which we shall refer to as "C" has been reported by Yagi and Miyauchi /64/. The boundary value problem not only takes into account the flux due to diffusion at the entrance but also at the exit from the bed which is now considered to be of finite extent. The physical conditions at the bed outlet are schematically shown in Figure 10.

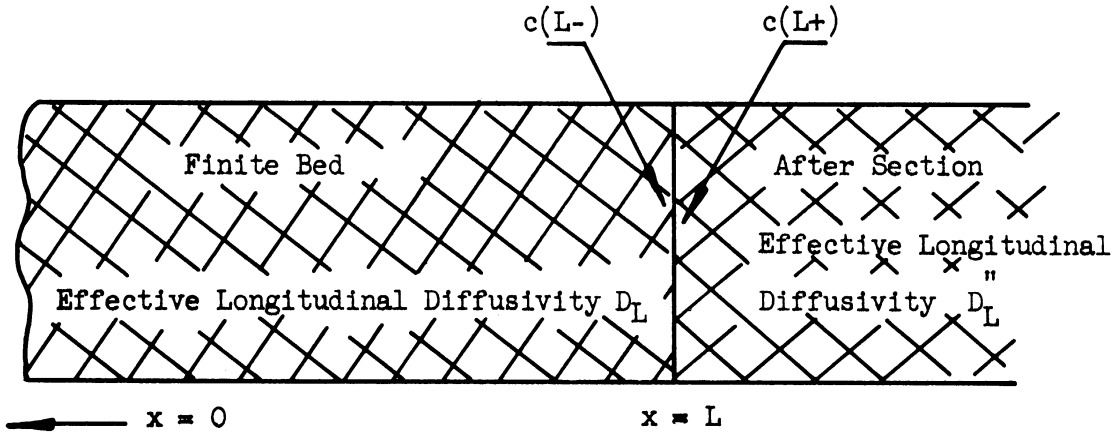

Figure 10

Conditions At Outlet Of Packed Bed

At the boundary between the aftersection and the packed bed we have to the left:

$$\frac{\partial c}{\partial t} = uc(L-) - D_L \frac{\partial c}{\partial x}$$

and to the right:

$$\frac{\partial c}{\partial t} = uc(L+) - D_L'' \frac{\partial c}{\partial x}$$

the exchange of tracer across the boundary is, therefore:

$$uc(L-) - D_L \frac{\partial c}{\partial x} = uc(L+) - D_L'' \frac{\partial c}{\partial x} \qquad (35)$$

If continuity of concentration is assumed in the outlet stream:

$$uc(L-) = uc(L+)$$

so that equation (35) reduces to:

$$D_L \frac{\partial c(L-)}{\partial x} = D_L'' \frac{\partial c(L+)}{\partial x} \qquad (36)$$

Equation (36) is considered a perfectly general representation of the outlet boundary for a transient problem such as this /59/. Yagi and Miyauchi, however, used at the outlet a more restrictive condition, that is:

$$D_L \frac{\partial c(L-)}{\partial x} = 0 \qquad (37)$$

As equation (36) shows, this condition amounts to saying that the flow past the bed exit is perfectly piston-like, ($D''_L = 0$), which is certainly quite arbitrary. Had one assumed that:

$$D_L = D''_L$$

the model would be reduced to that of a semi-infinite columm and solution "B" would have again resulted.

At any rate, the set of boundary conditions which satisfies the outlet condition as given by equation (37), the inlet condition of equations (28), and the step function input, equation (24) is:

$$\begin{aligned} &\text{1-c)} \quad uc_o = uc(o,t) - D_L(o,t) \\ &\text{2-c)} \quad \frac{\partial c}{\partial x}(L,t) = 0 \\ &\text{3-c)} \quad c(x,o) = 0 \end{aligned} \tag{38}$$

The solution of the diffusion equation evaluated at $x = L$ is:

$$\frac{c}{c_o} = 4 \sum_{n=1}^{\infty} \frac{U\mu_n (U\sin\mu_n + \mu_n \cos\mu_n)}{(U^2 + 2U + \mu_n^2)(U^2 + \mu_n^2)} e^{\left[U - \left(\frac{U^2+\mu_n}{2U}\right)\frac{ut}{L}\right]} \tag{39}$$

where:

$$U = \frac{uL}{2D_L} \qquad \text{and} \qquad \cot\mu = \frac{1}{2}\left(\frac{\mu}{U} - \frac{U}{\mu}\right)$$

and the impulse response:

$$E(t) = \frac{d\frac{c}{c_o}}{dt} = 2 \sum_{n=1}^{\infty} \frac{u\mu_n (U\sin\mu_n + \mu_n \cos\mu_n)}{L(U^2 + 2U + \mu_n^2)} e^{\left[U - \left(\frac{U^2+\mu_n}{2U}\right)\frac{ut}{L}\right]} \tag{40}$$

It is easy to see that the resulting expressions are complex and the fact that the eigenvalues μ_n cannot be expressed in an explicit form makes the study of the behavior of this solution difficult.

It is possible that this model may be capable of correlating more accurately the performance of an actual packed bed, since the authors, Yagi and Miyauchi /64/ claim solution "C" reduces to the perfect mixing case when the group $\frac{uL}{D_L}$ tends to zero, a behavior which is not exhibited by solutions "A" and "B". However, to state this with certainty, one should check the moments of its space and time distributions. This proves to be a tedious task and again underlines the fact that equations (39) and (40) are devoid of practical significance in the correlation of experimental data because of their complexity.

The boundary conditions, step and impulse response for solutions "A", "B", and "C" are summarized in Table II. The zero, first moment and variance of the respective distributions are also listed for solutions "A" and "B". Table II includes the Normal Distribution which also satisfies equation (21). The Normal Distribution, ordinary designation in statistics and probability for the Gaussian error curve /24/, is directly obtained from the random walk theory (see Chandrasekhar /4/, pp. 3) using a suitable bias on each random step to account for the superimposed longitudinal velocity and letting the number of steps approach infinity. It can be shown that both solutions "A" and "B" approach the Normal Distribution* as the dimensionless group $\frac{D_L}{uL}$ becomes small $(\frac{D_L}{uL} < .01)$.

On this basis, one may conclude that solutions "A", "B" and the normal distribution are all usable correlation models when the value

* See Appendix I, pp. 177

TABLE II

SOLUTIONS OF DIFFUSION EQUATION

Solution	"A"	"B"	"C"	Normal Distribution
Boundary Conditions For a Step Input From 0 to c_0	1-a) $c(o,t) = c_0$ 2-a) $\lim_{x\to\infty} c(x,t) = 0$ 3-a) $c(x,0) = 0$	1-b) $uc_0 = uc(0,t) - D_L \frac{\partial c}{\partial x}(0,t)$ 2-b) $\lim_{x\to\infty} c(x,t) \neq 0$ 3-b) $c(x,0) = 0$	1-c) $uc_0 = uc(0,t) - D_L \frac{\partial c}{\partial x}(0,t)$ 2-c) $\frac{\partial c}{\partial x}(L,t) = 0$ 3-c) $c(x,0) = 0$	Asymptotic Approximation of Solution "A" and "B" as $\frac{D_L}{uL} \to 0$ Also Arises from Random Walk
Step Function Response	$c/c_0 = \frac{1}{2}\left[\operatorname{erfc}\left(\frac{L-ut}{2\sqrt{D_L t}}\right) + e^{\frac{uL}{D_L}} \operatorname{erfc}\left(\frac{ut+L}{2\sqrt{D_L t}}\right)\right]$	$c/c_0 = \int_0^t \frac{ue^{-\frac{(L-ut)^2}{4D_L t}}}{\sqrt{\pi D_L t}}\,dt + \int_0^t \frac{u^2 e^{\frac{uL}{D_L}}}{2D_L} \operatorname{erfc}\left(\frac{L+ut}{2\sqrt{D_L t}}\right) dt$	$c/c_0 = \sum_{n=1}^{\infty} \frac{U\mu_n(U\sin\mu_n + \mu_n\cos\mu_n)}{(U^2+2U+\mu_n^2)(U^2+\mu_n^2)} \cdot e^{\left[U-\left(\frac{U^2+\mu_n}{2U}\right)\frac{ut}{L}\right]}$ $U = \frac{uL}{2D_L}$ $\quad \cot\mu = \frac{1}{2}\left(\frac{\mu}{U} - \frac{U}{\mu}\right)$	$c/c_0 = \int_0^t \frac{u}{2\sqrt{\pi D_L t}} e^{-\frac{(L-ut)^2}{4D_L t}}\,dt$
Impulse Response Also Residence-Times Distribution Function E(t)	$\frac{d\,c/c_0}{dt} = \frac{u}{2\sqrt{\pi t^3 D_L}} e^{-\left(\frac{ut-L}{2\sqrt{tD_L}}\right)}$	$\frac{d\,c/c_0}{dt} = \frac{ue^{-\frac{(L-ut)^2}{4D_L t}}}{\sqrt{\pi D_L t}} + \frac{u^2 e^{\frac{uL}{D_L}}}{2D_L} \operatorname{erfc}\left(\frac{L+ut}{2\sqrt{D_L t}}\right)$	$\frac{d\,c/c_0}{dt} = 2\sum_{n=1}^{\infty} \frac{u\mu_n(U\sin\mu_n + \mu_n\cos\mu_n)}{L(U^2+2U+\mu_n^2)} \cdot e^{\left[U-\left(\frac{U^2+\mu_n}{2U}\right)\frac{ut}{L}\right]}$	$\frac{d\,c/c_0}{dt} = \frac{u}{2\sqrt{\pi D_L t}} e^{-\frac{(L-ut)^2}{4D_L t}}\,dt$
$\int_0^\infty E(t)dt$	1	1	———	1
$\int_0^\infty tE(t)dt$	L/u	$L/u + D_L/u^2$	———	$L/u + \frac{2D_L}{u^2}$
Variance σ^2	$\frac{2D_L}{uL}$	$\frac{2D_L}{uL} + \frac{3D_L^2}{L^2u^2}$	———	$\frac{2D_L}{uL} + \frac{8D_L^2}{u^2L^2}$
References	R. Aris and N. R. Amundson AIChE Journal 3, 280(1957). For derivation details see Appendix I,	R. V. Churchill "Mod. Op. Math. for Eng." L. Lapidus and N. Amundson, J. of Phys. Chem, 56, 984(1952). For derivation details see Appendix I,	S. Yag and T. Myauchs, Chem. Eng. (Japan) 17, 382(1953).	O. Levenspiel and W. K. Smith Chem. Eng. Sci. 6, 227(1957) For derivation details see Appendix I,

of the dimensionless group $\frac{D_L}{uL}$ is small. However, when $\frac{D_L}{uL}$ is greater than .01, an appreciable disagreement is to be expected as exemplified by the dimensionless distributions of residence-times shown in Figure 11. Moreover, we note from the variance for solutions "A", "B" and the normal distribution that as D_L tends to infinity (perfect mixing) the limit for the variance is zero rather than one as would be expected for an actual system under conditions of complete mixing.

A Packed Bed As A Series of Perfectly Mixed Stages

It is useful to think of a packed bed as a series of stages or cells. We imagine that in each stage perfect mixing exists. As defined in page 17 this requires that the concentration in each stage be uniform and equal to the concentration in the effluent.

Consequently, the differential equation which characterizes each cell is:

$$-\frac{dc_i}{dt} = \frac{v_i'}{V_i'}\left(c_{i-1} - c_i\right) \qquad (41)$$

where c_{i-1} and c_i are the concentrations at the inlet and outlet respectively, v_i' is the volumetric velocity of the fluid through the ith cell and V_i' is its volume. For n such stages in series the effluent concentration from the nth stage is obtained from the simultaneous solution of n equations analogous to equation (41)*. More specifically, if all stages have the same volume V', the response

* See details of these derivations in Appendix II, pp. 187

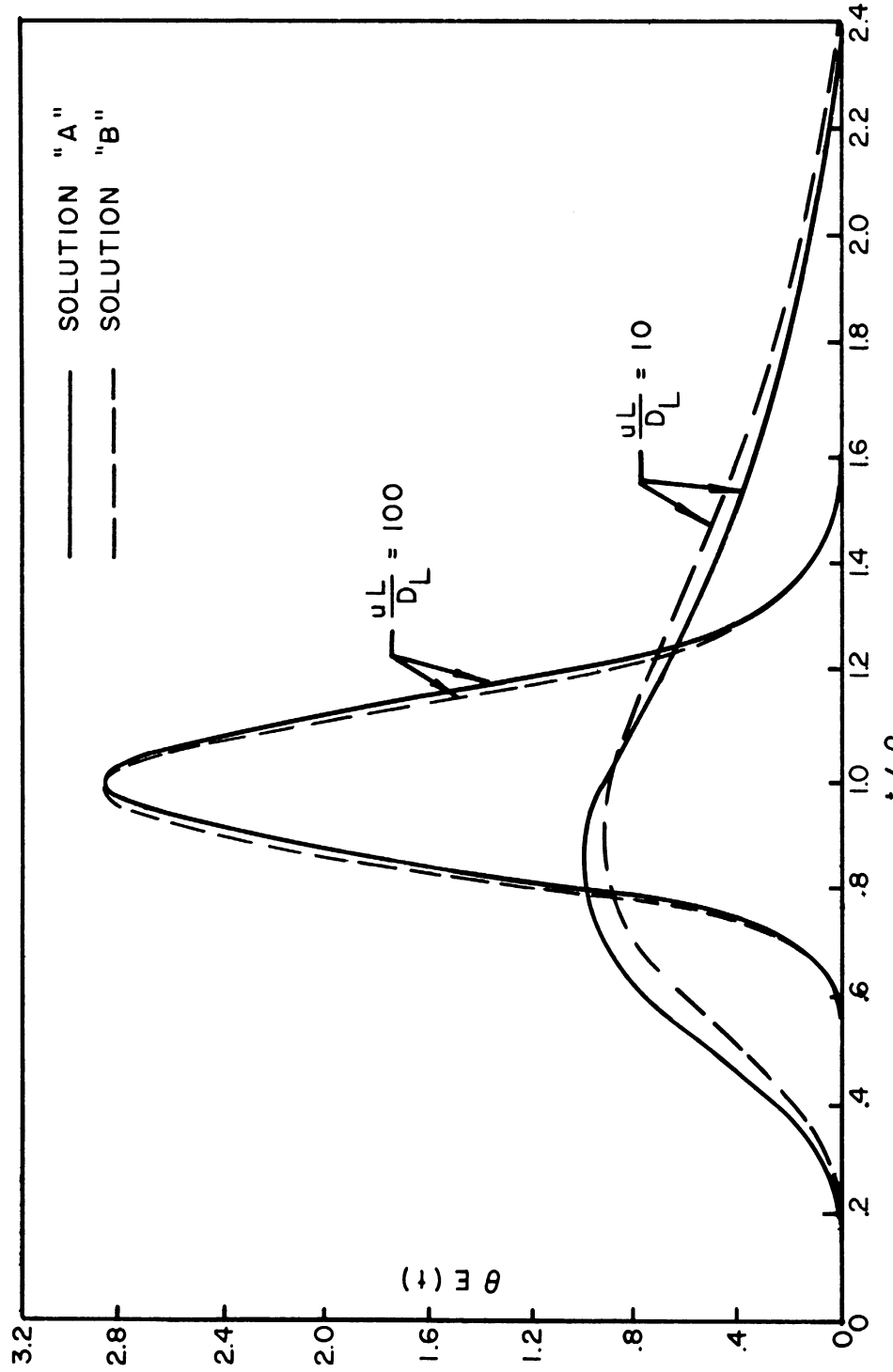

Figure 11. Time Distribution Curves For Solutions "A" and "B" Of The Diffusion Equation

to a step input in concentration is:

$$\frac{c}{c_o} = \left(\frac{v'}{V'}\right)^n \int_0^t \frac{\tau^{(n-1)}}{(n-1)!} e^{-\frac{v'}{V'}\tau} d\tau = 1 - \sum_{i=1}^{n} \frac{e^{-\frac{v'}{V'}t}}{(i-1)!} \left(\frac{v't}{V'}\right)^{i-1} \qquad (42)$$

The corresponding response to an impulse may be obtained by differentiating equation (42) with respect to t:

$$E(t) = \frac{d\frac{c}{c_o}}{dt} = \left(\frac{v'}{V'}\right)^n \frac{t^{n-1}}{(n-1)!} e^{-\frac{v'}{V'}t} \qquad (43)$$

Equation (43) is the distribution of residence-times for the fluid flowing through n stages in series. We shall now show that, under certain conditions this distribution is consistent with the material balance requirements and mixing behavior of an actual system. Taking the integral from zero to infinity of equation (43) we find that:*

$$\int_0^\infty E(t)dt = \int_0^\infty \left(\frac{v'}{V'}\right)^n \frac{t^{n-1}}{(n-1)!} e^{-\frac{v'}{V'}t} dt = 1 \qquad (44)$$

Thus, the zero moment of the time distribution fulfills the material balance of an impulse signal response for an actual system (see eq. (3) pp. 13)provided that the number of stages n be greater than zero. We note further that the integral in equation (44) is none other than the Laplace transform of the function $t^{n-1} / (n-1)!$, thus the number n

* See derivation details in Appendix II, pp. 189

need not be restricted to a whole number greater than zero since $(n - 1)!$ can be expressed as the Gamma function of n, any real number greater than zero /63/. Since it appears meaningless to speak of less than one mixing stage we may arbitrarily restrict the number n to any real number from one to infinity.

In an analogous manner we find that the first moment of the function $E(t)$ of equation (43) is*:

$$\int_0^\infty t\,E(t)\,dt = \int_0^\infty \left(\frac{v'}{V'}\right)^n \frac{t^n}{(n-1)!}\, e^{-\frac{v'}{V'}t}\, dt = n\,\frac{V'}{v'} \tag{45}$$

From the above equality we establish, therefore, the obvious fact that if the cells are all equal the overall residence-time of the system is given by:

$$\frac{\epsilon V}{v} = \frac{nV'}{v'}$$

$$\vartheta = n\vartheta' \tag{46}$$

If we visualize a packed bed as made up of m mixing cells, the overall residence-time of the bed is given by equation (45) only if the cells are disposed in $\frac{m}{n}$ parallel banks, each bank having n cells in series such that:

$$\frac{m}{n}v' = v$$

$$mV' = \epsilon V \tag{47}$$

---

* See derivation details in Appendix II, pp. 190

In other words, in order to make use of equations (45) and (46), we must assume that the flow of fluid through the bed is uniformly distributed. In this case the height of a mixed stage is:

$$H = \frac{V}{nA} = \frac{L}{n} \tag{48}$$

where A is the cross sectional area of the empty column.

Using the same procedure, we obtain the variance of the dimensionless distribution function $\theta E(t)$ about the mean residence-time $n\frac{V'}{v'}$ *:

$$\sigma^2 = \frac{\int_0^\infty \left(\frac{v'}{V'}\right)^n \frac{t^{n+1}}{(n-1)!} e^{-\frac{v'}{V'}t} dt}{\left[\int_0^\infty \left(\frac{v'}{V'}\right)^n \frac{t^n}{(n-1)!} e^{-\frac{v'}{V'}t} dt\right]^2} - 1 = \frac{1}{n} \tag{49}$$

Consequently, the dispersion about the mean residence-time is equal to the reciprocal of the number of mixing stages and it is found to vary from 0 for the case of piston flow where $n = \infty$ to the value of one for the case of perfect mixing when $n = 1$. The variance, therefore, gives a convenient method for the evaluation of the number of mixing stages in series that can be associated with a packed bed from the response of the bed to a step function or an impulse signal input.

Finally, to verify the correctness of the assumption that the flow is distributed uniformly across the bed, we can calculate the skewness of the dimensionless residence-times distribution curve $\theta E(t)$

* See derivation details in Appendix II, pp. 190

vs. t/O. This is*:

$$\nu = \frac{\int_0^\infty \left(\frac{v'}{V'}\right)^n \frac{t^{n+2}}{(n-1)!} e^{-\frac{v'}{V'}t} dt}{\left[\int_0^\infty \left(\frac{v'}{V'}\right)^n \frac{t^n}{(n-1)!} e^{-\frac{v'}{V'}t} dt\right]^3} \quad \frac{3\int_0^\infty \left(\frac{v'}{V'}\right)^n \frac{t^{n+1}}{(n-1)!} e^{-\frac{v'}{V'}t} dt}{\left[\int_0^\infty \left(\frac{v'}{V'}\right)^n \frac{t^n}{(n-1)!} e^{-\frac{v'}{V'}t} dt\right]^2} + 2 = \frac{2}{n^2} \qquad (50)$$

Thus, if $n\frac{V'}{v'}$ is the true residence-time, the skewness will be twice the square of the variance. In the affirmative case, the proposed model of m mixing cells with $\frac{m}{n}$ banks of cells in parallel each bank having n cells, is adequate in simulating the response of the packed bed. We note further that the transient response expressions we have discussed would only give the number of stages in series and the residence-time for each stage or the height of each stage but no information can be obtained on the actual volume of each stage unless the total number of cells m is determined independently.

In the event that the variance and skewness are in disagreement one might postulate that the flow in the packed bed is not uniformly distributed, i.e., a certain degree of channeling occurs. The difference between the skewness and twice the square of the variance would be a measure of such channeling. Theoretically, one could set up alternate models for the packed bed in which the flow rate v' through parallel banks of cells is different in each bank. The additional relationships necessary may be furnished by calculating higher moments of the distribution of residence-times curves.

---

* See derivation details in Appendix II, pp. 191

By referring to Appendix II, pp. 184 , it is apparent that one of the outstanding advantages of perfectly mixed stages as building blocks of packed bed models is the ease by which the moments of the resulting response functions can be predicted by the use of the Laplace transform because of the presence of an exponential term. The moments of the experimental response curves could also be readily obtained if the response of a continuous analyzer at the outlet of the system were fed to a number of integrators, each giving higher moments of the distribution of residence-times.

So far in this discussion we have concerned ourselves with series of perfectly mixed stages all having the same volume such that the overall contact time of the column is given by the product of n with the contact time of a single stage. If the stages are unequal, one can show* that the first moment of the resulting distribution of residence-times function gives the relation:

$$\theta = \sum_{i=1}^{n} \theta_i' \tag{51}$$

and that the variance of the distribution yields:

$$\sigma^2 = \sum_{i=1}^{n} \left(\frac{\theta_i'}{\theta}\right)^2 \tag{52}$$

In this case the variance σ^2 is not equal to the reciprocal of the total number of stages in series except when the volume of each stage

* See derivation details in Appendix II, pp. 196

is not widely different. In fact, by letting:

$$\sigma^2 = \frac{1}{\bar{n}}$$

equation (52) can be rewritten in the form:

$$\frac{\vartheta}{\bar{n}} = \sum_{i=1}^{n} (\vartheta_i')^2$$

multiplying both sides by $\frac{1}{\bar{n}}$ and taking the square root:

$$\frac{\vartheta}{\bar{n}} = \sqrt{\frac{\sum_{i=1}^{n} (\vartheta_i')^2}{\bar{n}}} \qquad (53)$$

It follows from equation (53) that $\bar{n}$ is not equal to the total number of stages present in the system but rather it is equal to a number such that by dividing the total contact time by $\bar{n}$ the mean square average of the contact time for each of the $\bar{n}$ stages is obtained.

If on the other hand, the volume of each stage in series is not widely different:

$$\vartheta_1' \simeq \vartheta_2' \simeq \ldots\ldots \simeq \vartheta_n' \simeq \vartheta'$$

we have:

$$\sum_{i=1}^{n} \vartheta_i^2 \simeq n(\vartheta')^2$$

so that:

$$\bar{n} \simeq n$$

substituting these last two equalities in (53) we find that:

$$\frac{\vartheta}{n} \simeq \vartheta'$$

Comparison with equation (46) shows that this is the ordinary case of an equal number of stages.

When a column is made up of packed sections having different properties or large empty sections interposed with the packing, we may conclude that:

$$\sigma^2 \neq \sigma_1^2 + \sigma_2^2 + \cdots + \sigma_n^2$$

or in terms of mixed stages:

$$\frac{1}{\bar{n}} \neq \frac{1}{n_1} + \frac{1}{n_2} + \cdots + \frac{1}{n_n}$$

where $\bar{n}$ as before refers to the apparent number of stages calculated as the reciprocal of the variance and the subscripts 1 to n refer to different sections making up the total system. But rather the variance contribution for each section to the variance of the residence-times distribution of the whole system is:

$$\sigma^2 = \sigma_1^2 \left(\frac{\vartheta_1}{\vartheta}\right)^2 + \sigma_2^2 \left(\frac{\vartheta_2}{\vartheta}\right)^2 + \cdots \sigma_n^2 \left(\frac{\vartheta_n}{\vartheta}\right)^2 \qquad (54)$$

The same relationship in terms of number of mixing stages is:

$$\frac{1}{\bar{n}} = \frac{1}{n_1}\left(\frac{\vartheta_1}{\vartheta}\right)^2 + \frac{1}{n_2}\left(\frac{\vartheta_2}{\vartheta}\right)^2 + \cdots + \frac{1}{n_n}\left(\frac{\vartheta_n}{\vartheta}\right)^2 \qquad (54\text{-a})$$

Table III gives a summary of the various relationships discussed in the previous pages.

TABLE III

RESPONSE OF A NUMBER OF MIXED STAGES IN SERIES
AND MOMENTS OF THE TIME DISTRIBUTION

QUANTITY	SERIES OF n EQUAL STAGES	n_1 STAGES HAVING VOLUME V_1' IN SERIES WITH n_2 STAGES HAVING VOLUME V_2'
Step Input Response c/c_o	$\left(\frac{v'}{V'}\right)^n \int_0^t \frac{\tau^{n-1}}{(n-1)!} e^{\frac{-v'}{V'}\tau} d\tau$	$\int_0^t \int_0^\tau \left(\frac{v'}{V_1'}\right)^{n_1} \frac{\lambda^{(n_1-1)}}{(n_1-1)!} e^{\frac{-v'}{V_1'}\lambda} \cdot \left(\frac{v'}{V_2'}\right)^{n_2} \frac{(\tau-\lambda)^{(n_2-1)}}{(n_2-1)!} e^{\frac{-v'}{V_2'}(\tau-\lambda)} d\tau d\lambda$
Impulse Response (Residence-Times Distribution)	$\left(\frac{v'}{V}\right)^n \frac{t^{n-1}}{(n-1)!} e^{\frac{-v'}{V'}t}$	$\int_0^t \left(\frac{v'}{V_1'}\right)^{n_1} \frac{\tau^{(n_1-1)}}{(n_1-1)!} e^{\frac{-v'}{V_1'}\tau} \left(\frac{v'}{V_2'}\right) \frac{(t-\tau)}{(n_2-1)!} e^{\frac{-v'}{V_2'}(t-\tau)} d\tau$
$\frac{cv}{Q} = E(t)$		
$\int_0^\infty E(t)dt$	1	1
$\int_0^\infty tE(t)dt$	$\frac{nv'}{V'}$	$\frac{n_1 v'}{V_1'} + \frac{n_2 v'}{V_2'}$
σ^2	$\frac{1}{n}$	$\frac{1}{n_1}\frac{\theta_1^2}{\theta^2} + \frac{1}{n_2}\frac{\theta_2^2}{\theta^2}$
ν	$\frac{2}{n^2}$	———

Comparison Of The Two Models

The similarity between the frequency responses of a series of perfect mixers and of a system which combines plug flow and axial diffusion has already been considered by Kramers and Alberda /38/. On the basis of this similarity and by observing that the longitudinal Peclet Number for gas flowing through beds of spheres is about 2, McHenry and Wilhelm /47/ concluded that the height of a mixed stage is approximately equal to the diameter of each sphere. Aris and Amundson /1/ investigated this point further and found both mechanisms to give comparable results at least in the neighborhood of $t = \theta$ and more generally for low values of the effective diffusivity.

Ranz /49/ in predicting the radial Peclet number for a bed of spheres considered a series of perfectly mixed stages in the radial direction even though not stating so. His calculations show that for a bed of spheres of infinite extent the ratio of the mean residence-time of the fluid proceeding through a cell interconnected longitudinally with that of a cell interconnected by radial openings is .179. Thus, for generally accepted values of longitudinal and radial Peclet numbers, we have:

$$\frac{Pe_L}{Pe_r} = \frac{2}{11} = .183 \qquad (55)$$

The agreement between these two ratios may be fortuitous but not devoid of significance since the Peclet number, consistent with the series of mixed stages mechanism, is inversely proportional to the mean residence-time through each cell mixer. Consequently, one can consider a packed

bed as a matrix of mixing cells connected some in the radial and some in the longitudinal direction through which the flowing medium undergoes complete mixing. This mechanism is equivalent to assuming a mean value of the concentration and of the mass transfer rate within the cells. Even though this assumption may not be exact the resulting mathematical expressions are greatly simplified. While we have limited ourselves to the treatment of this model in the longitudinal direction, it should be possible to extend it to two and three dimensional flow with the presence of absorption and chemical reaction. Such an approach is exemplified in a recent article by Churchill, Abbrecht and Chu /7/ on a heat transfer problem through porous media. The authors have shown that such a model yields a solution of striking simplicity.

From equation (43) we see that the dimensionless residence-times distribution function for a single stage $\theta'E(t)$ is:

$$\vartheta' E(t) = \left(\frac{v'}{V'}t\right)^{n-1} \frac{e^{-\frac{v'}{V'}t}}{(n-1)!} \tag{56}$$

Equation (56) is the familiar Poisson distribution of probability (See Feller /21/ page 110.) It expresses the fraction of those tracer molecules introduced at the inlet at time t over a time interval dt which are in the nth cell at time t or, alternatively it expresses the probability that a tracer molecule introduced at the inlet at time t over a time interval dt may be in the nth cell at time t. The Poisson distribution in probability theory arises in two ways (see Fry /24/ page 214 through 227):

1. As an approximation of the Binomial law governing the distribution of random numbers or steps as arising for instance in the random walk theory /4/, we note that the Normal distribution is also an approximation of the Binomial law. However, probability theory tells us that when $\frac{v'}{V'}t$ of equation (56) is small only the Poisson distribution is a good approximation. On the other hand, if $\frac{v'}{V'}t$ is large both the Poisson and the Normal distribution can be used.

2. The second way in which the Poisson distribution arises is as an exact solution of a system of differential equations of the same form as the one in equation (41). Many other physical systems such as the splitting of physical particles and the arriving of telephone calls at an exchange behave in the same manner as the series of mixed stages discussed in the previous paragraph. In this case, however, no information whatever is required about the number t or $\frac{v'}{V'}$ and no knowledge is required of the number of steps in any interval large or small in contrast with the random walk theory. The only two necessary requirements of the physical processes which obey the Poisson law are that the events described by the basic differential equation (41) be all of the same nature and their occurrence be in no way related to previous or past ones. Thus, the Poisson law possesses a large degree of flexibility in fitting various physical situations.

It is well known that the Poisson distribution converges to the Normal distribution at least for a large number of steps (see Chandrasekhar /4/ pp. 81). Equating the two distributions, one may arrive at some relationship between the number of mixed stages and the effective diffusivity coefficient. For a more direct comparison, with the solutions of the diffusion equations mentioned in previous paragraphs, however, we have chosen to look at the moments of the time distribution function which are listed on Table IV.

As we have already noted, the zero moment is in all cases equal to one. Since the sum of all probabilities for a system must equal unity, it is no surprise that the two models are in agreement on this point.

As far as the first moment is concerned, this should be equal to the residence-time. From Table IV we note that this is so in all cases provided that the dimensionless group $\frac{D_L}{uL}$ is small enough. The reason for the discrepancy presented by solution "B" and the Normal distribution is probably due to the fact that the Normal distribution and, therefore, the diffusion mechanism, does not give an adequate approximation of the probability unless there is an appreciable number of random steps in a given interval of time. Solution "A" gives perhaps fortuitously the proper residence-time because the approximation error is compensated by neglecting the diffusion flux at the entrance of the bed.

Passing to a comparison of the variance of the time distribution we see that the relationship sought between the number of stages

TABLE IV

COMPARISON BETWEEN SERIES OF MIXED STAGES AND THE DIFFUSION MODELS

Moments Of The Time Distribution Function E(t)	n Mixed Stages In Series	Solution "A"	Solution "B"	Normal Distribution
$\int_0^\infty t\,E(t)dt$	1	1	1	1
$\int_0^\infty t^2\,E(t)dt$	θ	θ	$\theta + \frac{D_L}{u^2}$	$\theta + \frac{2D_L}{u^2}$
σ^2	$\frac{1}{n}$	$\frac{2D_L}{uL}$	$\frac{2D_L}{uL} + \frac{3D_L^2}{L^2u^2}$	$\frac{2D_L}{uL}$ $\frac{8D_L^2}{u^2L^2}$

and the effective longitudinal diffusion coefficient is:

$$n \simeq \frac{uL}{2D_L} \tag{57}$$

This relationship is valid within one per cent for $\frac{uL}{D_L}$ greater than ten as far as the variances for the distributions of solution "B" and the Normal approximation are concerned.

Graphical comparison between the diffusional model and the mixing stage model is furnished by Figure 12 where distribution curves for a series of mixed stages and the solution "B" of the diffusion equation are shown.

As one would expect, the agreement is not very good for a small number of mixed stages but it rapidly improves as the number of mixed stages is increased. One may also note that for values of t/θ larger than one the agreement is generally better even for small values of uL/D_L as the theory of probability predicts (/21/,pp. 144). From this point of view, the series of mixed stage mechanism, i.e., the Poisson distribution should furnish, in any case, a better approximation for values of t/θ less than one.

In absence of data on mixing for shallow beds or in which the number of mixing stages is small, we are really not justified in any statement concerning which model gives a more precise representation of the mixing process over the whole range of conditions from plug flow to complete mixing.

While the diffusion model considers the overall effects produced by a very fine mixing scale, the series of mixed stages model

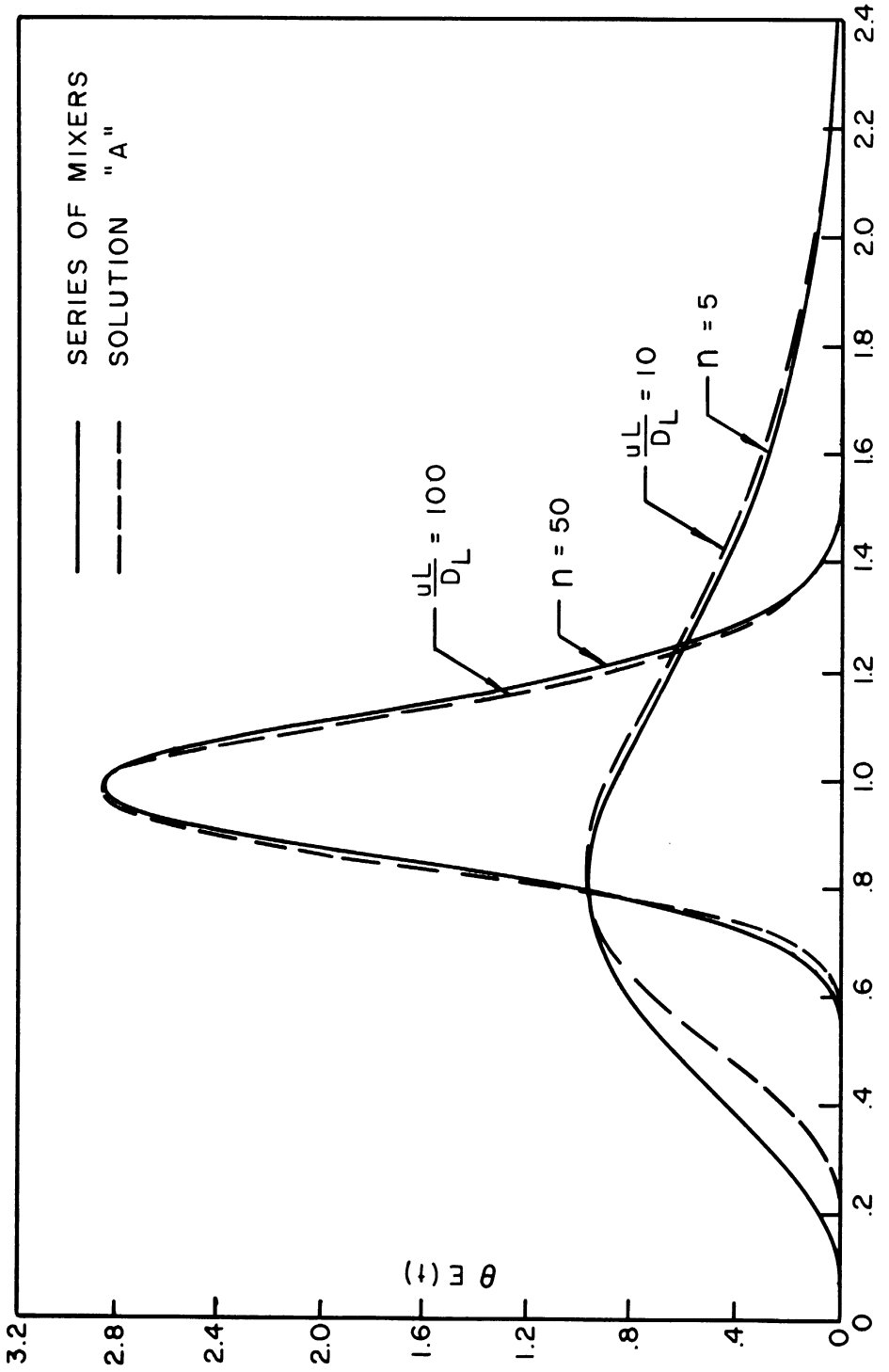

Figure 12. Time Distribution Curves For Solution "B" And A Series Of Mixers

amounts to assuming average conditions over discrete volume fractions of the bed. In addition, the former model gives rise to fairly cumbersome equations to describe the system. The latter instead, yields much simpler relationships which may be easily modified to fit possible anomalies in the behavior of the bed.

CHAPTER IV

EXPERIMENTAL

The prime objective of the experimental work was the collection of data on the gas porosity of an irrigated packed column and on the extent of mixing of the gas phase through the irrigated bed as function of liquid and gas flow rates and column geometry. The transient response method was chosen because, as discussed in the theory, it readily yields such information.

The experimental apparatus was designed with the intent of introducing a signal of helium tracer in the inlet gas stream of an absorption column of suitable dimension and recording the composition of the outlet gas stream continuously and with minimum delay. The equipment, therefore, consists of a liquid supply system, a gas and tracer supply system, a packed test column and a gas analyzer. The details on the various pieces of apparatus are not essential to the presentation of the results except where pertinent data and dimensions are needed. The reader may, therefore, omit the section entitled: Equipment which follows and continue on page 76.

Equipment

Flow System

A flow diagram showing liquid, gas and tracer supply systems and the packed test column is given in Figure 13.

The liquid supply system handles water flow rates from .1 to 1.1 gal/min and is arranged as to make possible the introduction of a step function or a pulse of dye in the water stream even though the

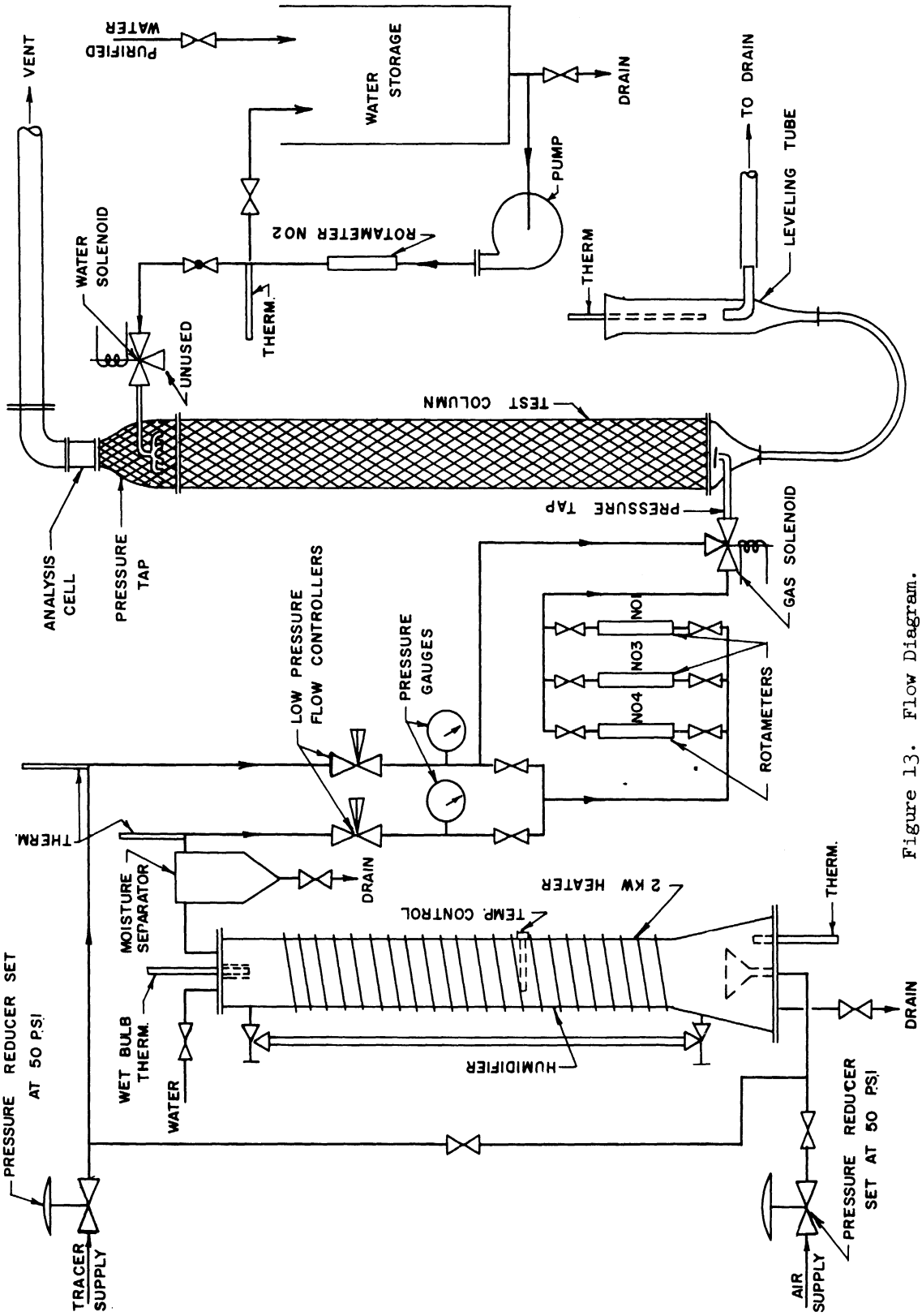

Figure 13. Flow Diagram.

experimental work is only limited to the tracer study of the gas stream. City water is softened and purified in a Bruner 60,000 grain capacity water softener and transferred to a 100 gallon storage tank where it is allowed to come to equilibrium with the temperature of the room.

The gas system allows air flow rates from .1 to 4 SCF/minute. Compressed air at 50 psi pressure is humidified in a brass column 4 inches in diameter and 4' 8" in height. The column is heated by a 2 Kwatt wire coil wound on the outer surface of the column. A Fenwall temperature controller maintains the temperature of the water such that the gas leaving the humidifier has a dry bulb temperature approximately equal to the temperature of the water flowing down the packed column. The air rate is measured through a bank of three rotameters in parallel. The air rate is adjusted and maintained constant by a pancake low pressure regulator ahead of the rotameters.

Pure helium or a mixture of helium in N_2 (15% He - 85% N_2) are used as tracers and are available in pressurized tanks. The tracer flow after a primary reduction in pressure is maintained at a constant rate by means of a second pancake low pressure regulator. A three-way solenoid valve immediately before the inlet to the test column permits replacing the air flow to the column with tracer or the introduction of a pulse of tracer as slugs of short duration in the air stream. An automatic timer and switching assembly controls the operation of the solenoid valve and supplies an electric impulse marker to the recorder. Details of the electric wiring for the timer and manual switches are shown in Figure 14.

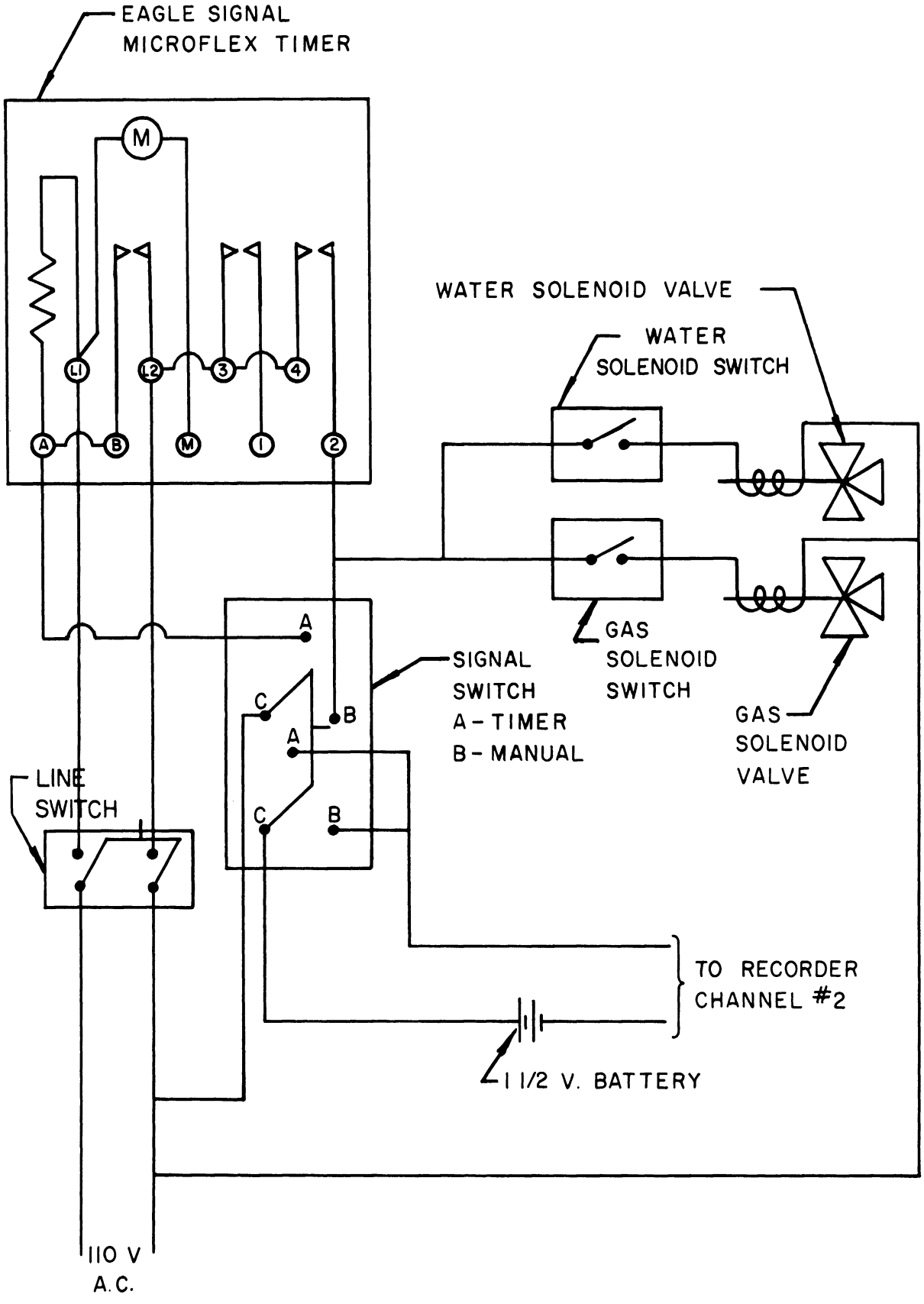

Figure 14. Timer and Solenoids Wiring.

The test column is made out of 4" I.D. flanged Pyrex glass pipe. The mid-section of the column is interchangeable in lengths of 3' and 4'. The bottom section of the column is conical and a 3/4" I.D. liquid outlet is located at the vertex of the cone. An adjustable liquid level device is used to maintain an adequate liquid seal to allow the outgoing liquid to disengage any gas bubbles before going to the drain. A 3/4" I.D. gas inlet is located at right angles with the bottom section and it is surmounted by a hood to protect the gas line from any splashing liquid. A packing support screen is fastened between gaskets and flanges which connect the column's bottom with the mid-section. The screen mesh is of the same dimension as the nominal diameter of the packing used. The total volume of the bottom section from the three-way solenoid valve to the beginning of the packing is .0065 cu.ft. and it constituted 1.5 to 2% of the total volume of the column depending on the height of the mid-section.

The upper extremity of the column is reduced in diameter down to 2" I.D. for connection with the gas analyzer. The liquid is introduced on a side inlet and is distributed by six jets made of 1-1/2 mm. capillary tubing evenly spaced on a 3" radius. The volume of the upper section is .0437 cu.ft. The mid and upper column sections are completely filled with packing up to the gas analysis cell, thus that portion of packing which is in the upper section remains dry during the gas-liquid runs because it is above the liquid distributor.

The column is packed with Raschig rings of 1/4", 3/8" and 1/2" nominal diameter. The rings, made of unglazed porcelain, were supplied through the courtesy of the United States Stoneware Co.

Continuous Gas Analyzer

A rapid monitoring system capable of producing a continuous and accurate recording of the tracer concentration in the gas stream is the most important component of the experimental equipment. For this purpose an alpha particle ionization cell was constructed. This device is frequently used in vacuum practice as a vacuum gauge and leak detector. Deisler, McHenry and Wilhelm /16/ first used it as an analyzer for binary and ternary gas mixtures at pressures above atmospheric.

The ionization cell utilizes the alpha particles emitted by a radium source to ionize the gas passing through it. The number of ions produced per unit time depends on the nature of the gas which is being analyzed. The ions can be collected between two electrodes immersed in the flowing stream to produce a current. For a binary mixture of gases at constant temperature and pressure, the rate of production of ions by the alpha particles is function of the gas composition only. If the voltage impressed upon the electrodes is maintained constant, then the current produced is also a function of gas composition only, and measurement and recording of this current makes possible the measurement and recording of the gas composition. Further details on the theory and design considerations for this instrument may be found in the paper on this subject by Deisler, McHenry and Wilhelm /16/.

The electrodes of the cell are two rectangular stainless steel plates 1-1/4" x 1-11/16", 1/32" thick. The one used as the alpha particle emitter has on one side an active area of 1-1/8" x 1-1/8"

covered with 100 micrograms of Ra^{226} rolled in gold foil. The other plate is the ion collector. The plates are spaced at a distance of one inch within a 2" O.D. Teflon mount specially streamlined to minimize extraneous mixing of the gas entering the cell. The assembly is housed in a specially fabricated glass flanged tube 3" long which is inserted between two 2" Pyrex brand pipe flanges forming the connection between the top of the test column and the exhaust pipe as shown in Figure 15. Electric leads are clamped on the electrodes by means of copper clips and sealed through the glass housing by means of rubber vial caps. The glass housing and high impedance lead are shielded with brass foil.

The accessory equipment to the analyzer consists of a high voltage D.C. Supply, a 187 megohm resistor circuit between the collecting plate and the ground, a Keithley Model 210 Electrometer which matches the high impedance of the cell resistor combination and a two channel Brush amplifier and direct writing oscillograph. Details of the analyzer and recorder cell circuit are shown in Figure 16.

The rectangular cell geometry was chosen to give most favorable current stability and noise characteristics. In fact, when using pure helium as the tracer, the output is exceedingly stable and completely free of stray noise.

The output current of the ionization chamber for air and helium as functions of the applied voltage at the electrodes is shown in Figure 17. It can be seen here that a potential of about 1000 volts across the electrodes is necessary to collect all the ions formed by the alpha particles. Thus, this voltage was selected as standard throughout the experimental work. The variable high voltage D.C. power supply

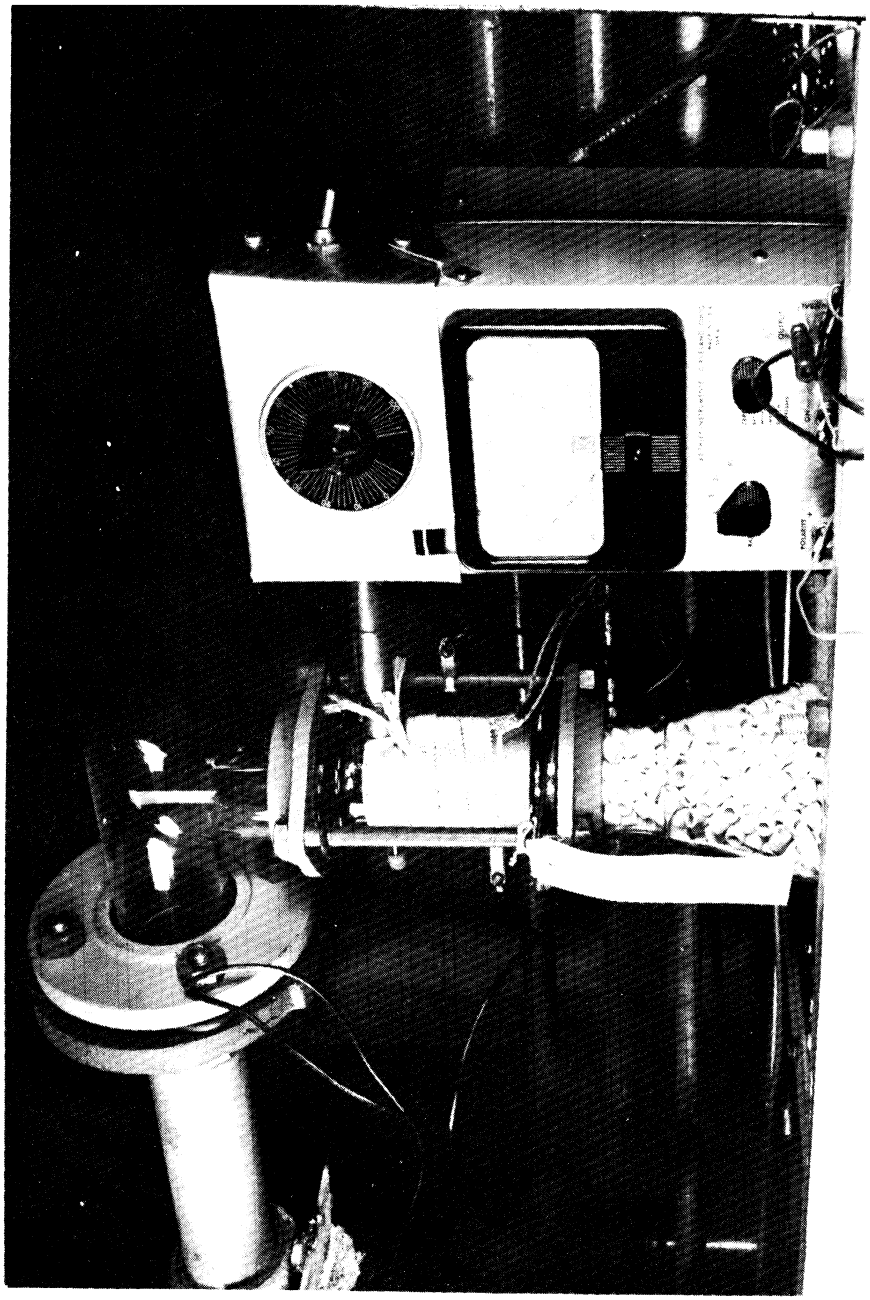

Figure 15

Gas Analyzer Assembly

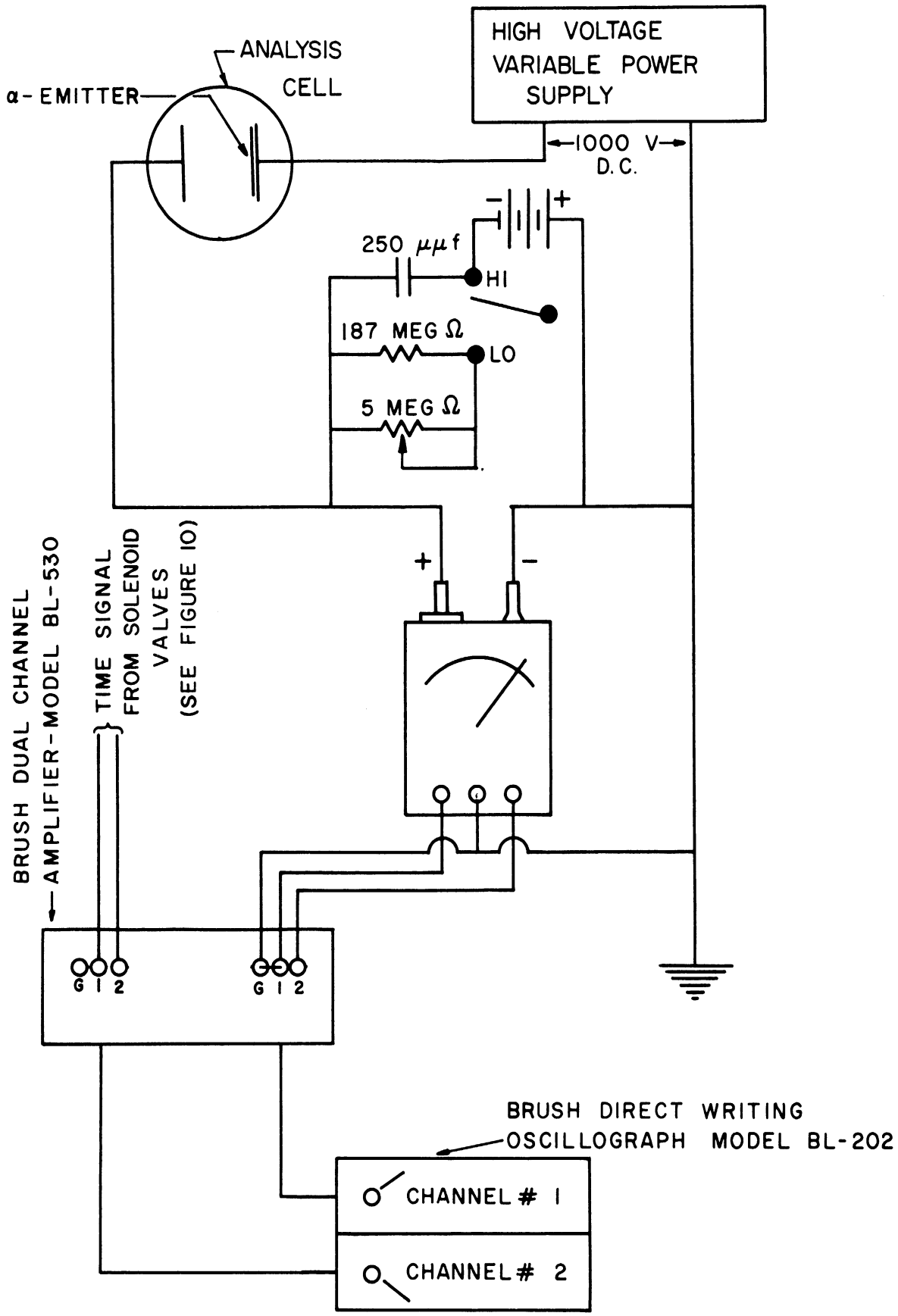

Figure 16. Assembly of Gas Analyzer and Accessories.

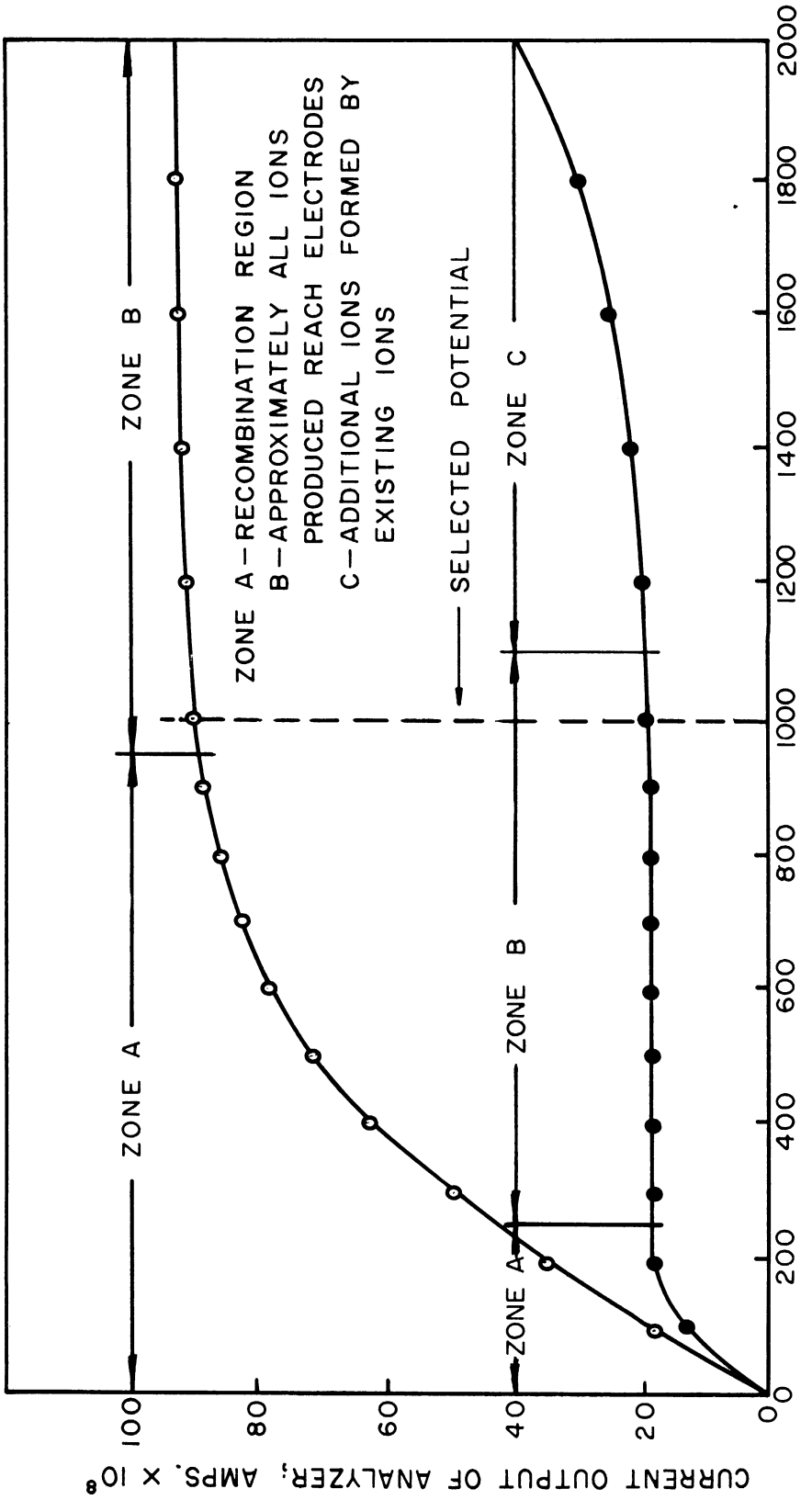

Figure 17. Current Output of Gas Analyzer with Impressed Potential.

was built using a high voltage transformer and a thermionic rectifier. The power supply circuit is shown in Figure 18.

The output current of the electrodes at 1000 volts potential varies linearly with helium concentration from a value of 1.9×10^{-8} amps for pure helium to 9.1×10^{-8} for air. The output current vs. concentration shown in Figure 19 was obtained by passing through the cell known gas mixtures. The overall precision of the measurement is better than one per cent.

The low output current from the electrode is boosted by a 187 megohm resistor across the ion collector plate and the ground to a maximum potential drop of 17 volts. To allow the use of 15% helium--85% N_2 mixture as a tracer a current blocking circuit is inserted in series with the resistor. This consists of a 15 volt mercury battery connected with inverted polarity so that this constant voltage is subtracted from the output voltage of the resistor. Thus, when the battery is inserted in the high resistance circuit, the maximum output voltage corresponding to 100% air is two volts. The high sensitivity circuit causes a certain amount of noise to be detected in the cell output, thus a 250 μμfarad capacitor was added across the high sensitivity circuit to damp some of it out (see circuit details in Figure 16, page 71 .

The cell-resistor combination results in an impedance of the order of 10^8 ohms so that a matching circuit is provided to measure the output voltage. This purpose is served by the Keithley Model 210 Electrometer which is capable of measuring input voltages having an impedance as high as 10^{14} ohms. The electrometer features five scales from 0 to .8, 2, 8, 20 and 80 volts. The 0 to 2 volt scale is used with the high sensitivity circuit while the 0 to 20 volt scale is

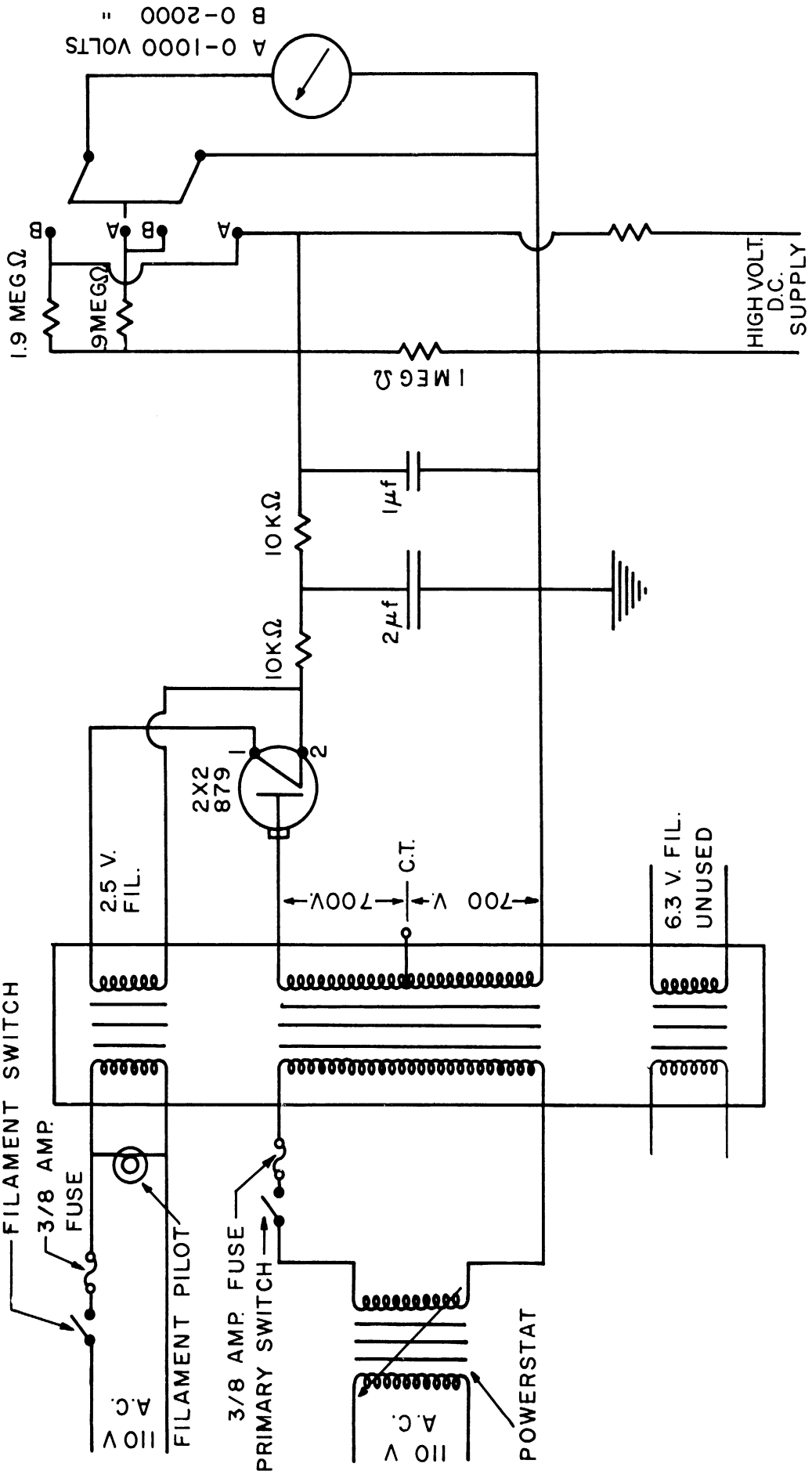

Figure 18. High Voltage D.C. Supply.

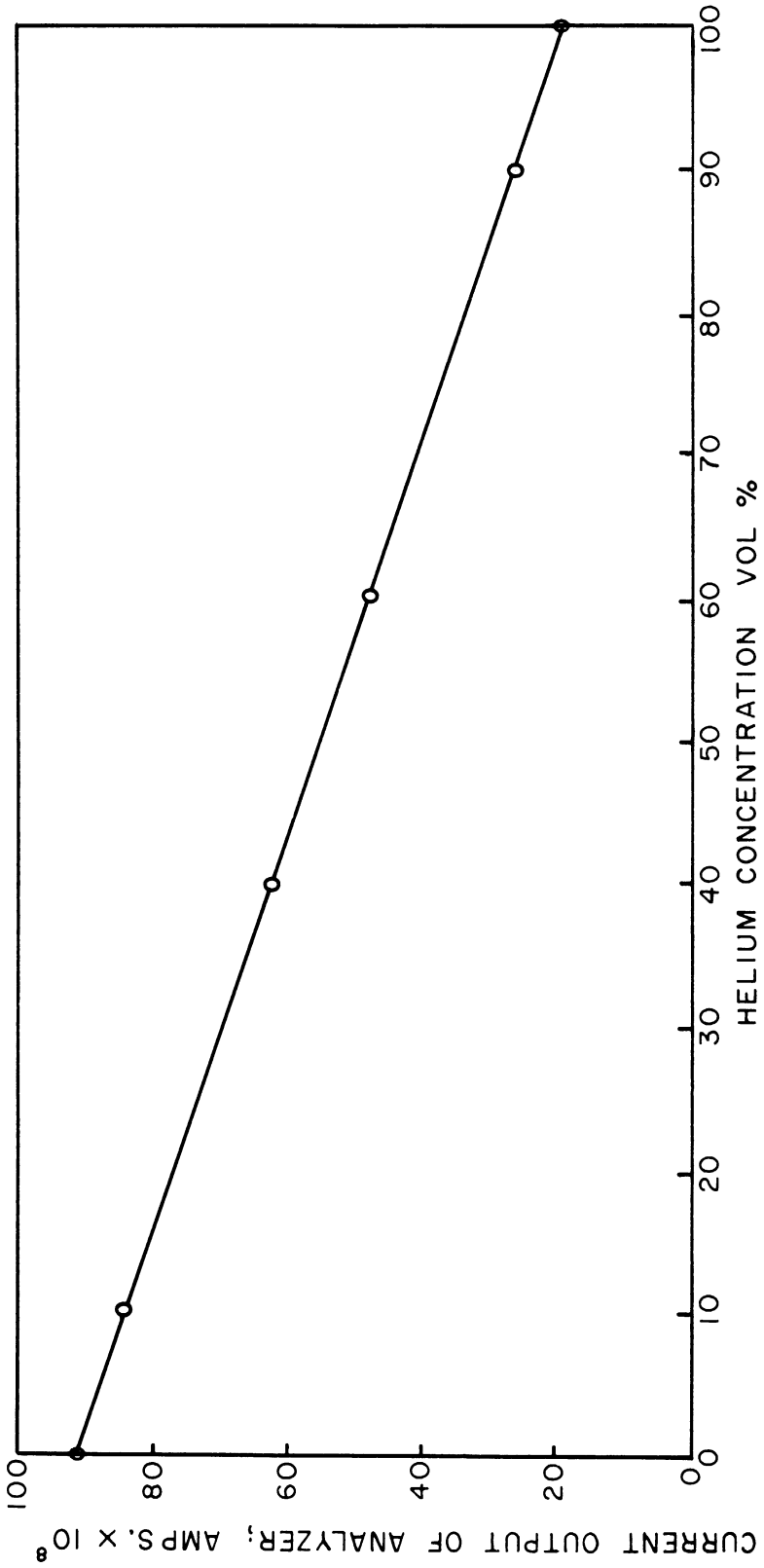

Figure 19. Current Output of Gas Analyzer with Helium Concentration.

used for the normal sensitivity. The electrometer contains an output amplifier which develops 10 volts in a balanced connection for full scale reading of the meter and a 1.0 milliampere current to drive the recorder.

The output of the electrometer is fed to a Brush dual channel direct-writing oscillograph model BL 202 through a Brush model BL530 amplifier by means of a balanced connection to the electrometer.

Procedure

Preliminary Tests

A number of test runs were performed to give preliminary estimates of the limitations of the equipment and to establish a consistent and reproducible experimental procedure.

The manner of introduction of the tracer at the column inlet was soon limited to step changes in concentration since it was found impossible to inject an appreciable amount of tracer in an interval of time short compared with the contact time of the gas flowing through the column in order to approximate an impulse signal. The contact time through the column was varied from 2 to 40 seconds, thus a time of injection as short as .02 to .04 seconds was required. In the runs at low gas velocity some impulse responses were recorded and the first moments and variance of the resulting distributions were found to be within 1% of those obtained by a step change in tracer concentration.

Pure helium was first used as a tracer in preliminary work. It was found, however, that when the helium displaced the air through the column, the recorder traces (which we shall also call response curves) were severely distorted, especially at low flow rates. This phenomenon

is clearly detectable in the reproduction of the Brush recording for Run D-23 shown on Figure 23, pp. 87 where the gas flow rate was .482 cu.ft./second. No distortion is visible when air displaces helium however. As the gas flow rate was increased, the distortion became less pronounced. These observations led to the belief that convective currents were produced by the eightfold difference in density between helium and air and disturbed the smooth displacement of the air by the helium. Since the flow was upward, such currents would not be present when air displaced helium; in addition when the average gas velocity was presumably well above the convective velocity, the disturbing effect was much less pronounced. On further experiments, carbon dioxide was used as tracer and for this gas, the distortion appeared in the response curves recorded when air displaced the carbon dioxide. Since this gas is about 1.5 times heavier than air, the convective currents set up by the difference in density were, indeed, responsible for the observed phenomenon.

It was, therefore, decided to carry out the experimental work using as tracer a mixture of 15 volumes of helium and 85 volumes of nitrogen. This mixture was prepared in standard gas cylinders at a total pressure of 1000 psi. The difference in density with air is about 16% and the resulting response curves for the tracer displacing the air and for the air displacing the tracer were in reasonable agreement as discussed in Chapter V.

The high sensitivity circuit for the analyzer described previously (see pp. 73) was added at this time to permit both the use of 15% helium or pure helium as tracer whenever desired. When helium

was used, the output from the analyzer through the normal sensitivity circuit was practically free of noise as Figure 23, pp. 87 shows. With 15% helium used as a tracer, the high sensitivity circuit was required to allow full deflection of the meter whenever 100% tracer was present in the analysis cell. Due to the sevenfold magnification, the cell output was more sensitive to slight pressure fluctuations and/or stray currents so that a certain amount of random noise was registered at the recorder. To filter out some of this noise, a 250 x 10^{-12} μμ farad capacitor was added across the high sensitivity circuit, a slight amount of random noise was, however, still detectable as exemplified by a typical run record reproduced in Figure 21, pp. 85 .

The increased capacitance of the high sensitivity circuit resulted in an increase in the time constant* of the analyzer recorder system from .005 to .05 seconds. To insure that this increase of the time constant would not disturb the response curves, the data was checked for consistency as discussed on page 110 , Chapter V.

The analyzer cell, especially at higher sensitivity was found to be somewhat susceptible to pressure fluctuations, thus changes in flow rate would alter the analyzer calibration. This factor was eliminated by calibrating the analyzer-recorder system each time a different flow rate was used. Once the system was properly warmed up, no appreciable drift was noticed for the entire duration of any one run. The pressure sensitivity of the analyzer was found useful as a check to insure that the air and tracer would produce the same flow conditions through the system since for unequal flow conditions at the moment of

---

* The time constant referred to here is the time required for the pen to travel .632% of the total width of the paper.

switching the flow from air to tracer or vice versa, the recording would register slight deviations from normal setting due to a pressure change at the analyzer cell.

During the experiments performed with irrigated packing or humidified gas, some moisture would deposit on the electrodes of the analysis cell and the output of the cell would gradually be shorted out. This problem was completely corrected by maintaining the analyzer at a temperature of approximately 100°F with a heating tape wound around the glass housing and shield.

To investigate the effect of the degree of humidification of the air and tracer upon the response curves, test runs were made by alternately routing the air stream or the gas stream through the humidifier with or without liquid descending over the packing. No detectable effect of the degree of humidification of either stream on the response curves was noticed as long as the temperatures of the flowing streams were kept approximately the same. It was noticed that the temperature of the tracer was usually within a degree of room temperature. The liquid was kept in the storage tank and allowed to come to equilibrium with the temperature of the room. Consequently, only the air temperature needed occasional adjustment and this was done by conditioning it through the humidifier.

Standard Experimental Technique

Raschig rings of the desired size were introduced into the column by partially filling the column with water, then slowly pouring the rings from the top. The water prevented breakage and provided slow and even settling of the rings. The column was then reassembled.

Column and packing were dried out by allowing dry air to flow through the column overnight. The porosity of the dry bed was measured by back filling the column with water to a level two inches above the packing support screen. 1600 cc. of water were then added and the increment of the water level in the column measured by means of a cathetometer. This procedure was repeated by successively adding 1600cc. of water until the top of the column was reached. The porosity was calculated for each increment knowing the net amount of water added to the column and the resulting increase of the liquid level. The porosity of the bed was taken as the average of the total number of determinations. The deviation from the average was for all packing sizes within 0.5% indicating reasonable uniformity of the porosity throughout. Column and packing were again dried prior to a series of runs.

A typical run was started by turning on the high voltage generator, amplifier, recorder, and the heaters for the analysis cell and humidifier. Warmup of the analyzer-recorder system required about two hours.

If a series of dry packing runs were executed, the required gas and tracer flow rates were preset by adjusting the low pressure regulators and measuring the flow rates through the bank of rotameters. The flow rates of the two streams were adjusted so as to give approximately the same pressure drop through the column. The temperatures of the flowing streams were adjusted within one or two degrees Fahrenheit. The liquid seal level at the bottom of the column was set at a reference mark by means of the leveling tube. The electrometer was set to zero and the sensitivity and proper voltage scale selected. The recorder was calibrated by allowing air to flow through the column and setting the

recorder pen to coincide with the zero line of the chart. Tracer was then allowed to flow through the column and the full deflection of the pen was adjusted by proper setting of the Brush amplifier controls. The chart speed was selected and air and tracer flow rates were again checked. A run was started by turning on the switch for the three-way solenoid valve which interrupts the air flow and replaces it with tracer. When the response curve for the tracer displacing the air was completed at the recorder, the flow was switched back to air and a response curve for the air displacing the tracer was recorded. The air and tracer flow rates, all the temperatures and the pressures were then rechecked and recorded.

For an irrigated packing run, the packing was first thoroughly wetted by turning the water to 6000 lb/hr.sq.ft. for about one hour. Then a series of runs was performed by adjusting the liquid flow to the desired rate and following the same procedure described above for the gas. For each liquid flow rate, the column was allowed to reach equilibrium for about a half-hour, then response curves were recorded at 15-minute intervals and compared by superposition to note if the curves were exactly congruent. In the negative case the gas and liquid flow rates were checked and the procedure repeated until two successive sets of curves were in agreement. When flooding was reached, the flow conditions through the column were too erratic to obtain consistent response curves so that no data was obtained on or about this range of conditions. Only for Run W-19 was a reasonable agreement for successive response curves obtained even though the column was flooded. Whenever a second person was available, the dynamic liquid holdup was measured at the end of an irrigated packing run by interrupting simultaneously the gas and liquid

flow and collecting the total amount of liquid drained from the column.

When a series of runs was completed and a changeover of packing was necessary, the porosity was again checked. Then the packing was removed and weighed in such a manner as to determine the total number of particles.

Experimental Data

Dry Packing

The experimental effort was first directed to the study of the gas phase mixing through the dry bed in order to verify the suitability of the equipment and method of analysis against existing data obtained by the frequency response /47/. Since it was possible to measure the void volume of the dry packing independently, the precision of the gas holdup information furnished by the transient response could also be determined.

A total of 28 experiments were performed with gas flowing over dry Raschig rings. Figures 20 through 24 are typical examples of data collected during these experiments.

The variables and the ranges covered are:

	Variables	Ranges
1.	Column Length	3, 4 Ft.
2.	Tracer	Pure helium and 15% He-85% N_2
3.	Average gas interstitial flow rate	0.06 - 1.0 ft./sec.
4.	Nominal Particle diameter	1/4, 3/8, 1/2 in.
5.	Packing Arrangement	Random and Oriented

Other variables which were held constant are:

6.	Column Diameter	0.334 Ft.
7.	Packing Type	Unglazed Porcelain Raschig Rings
8.	Method of Signal Introduction	Step Function

Figure 20. Dry Packing, Run No. D-8

Date: 7/15/57

Room Temperature: 78.8°F

Chart Speed: 5 divisions/second

Column Properties:

Nominal Particle Size	1/4 in.
Height of Packed Bed	3.42 ft.
Porosity of Dry Bed	0.633

Tracer:

Rotameter No. 3 Reading	70
Temp. of Flowing Stream	79.4°F
Pressure at Rotameter	15.7 psia

Air:

Rotameter No. 3 Reading	70
Heater Temperature	79.2°F
Dry Bulb Temperature	78.3°F
Wet Bulb Temperature	78.5°F
Pressure at Rotameter	15.7 psia

RECORDER TRACES:

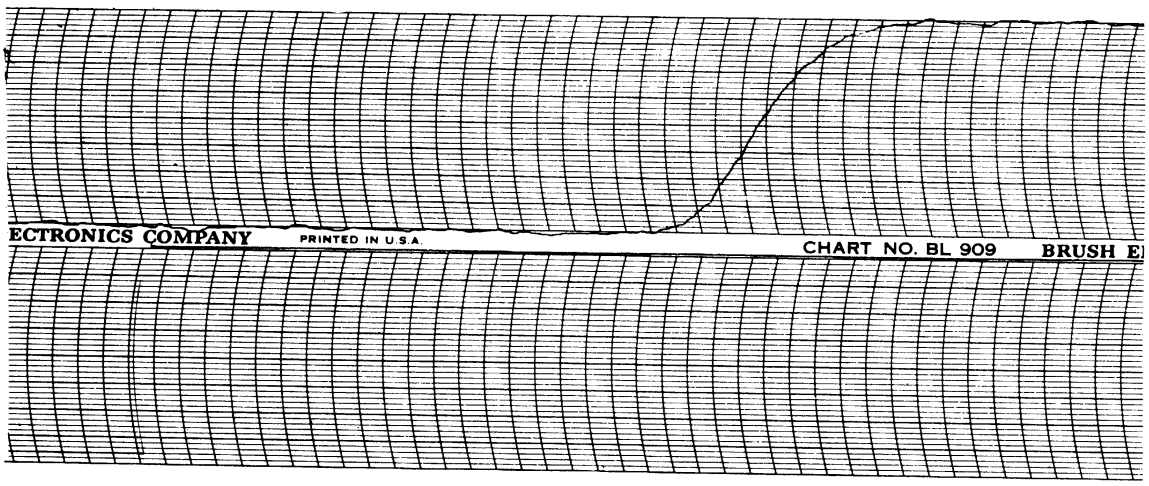

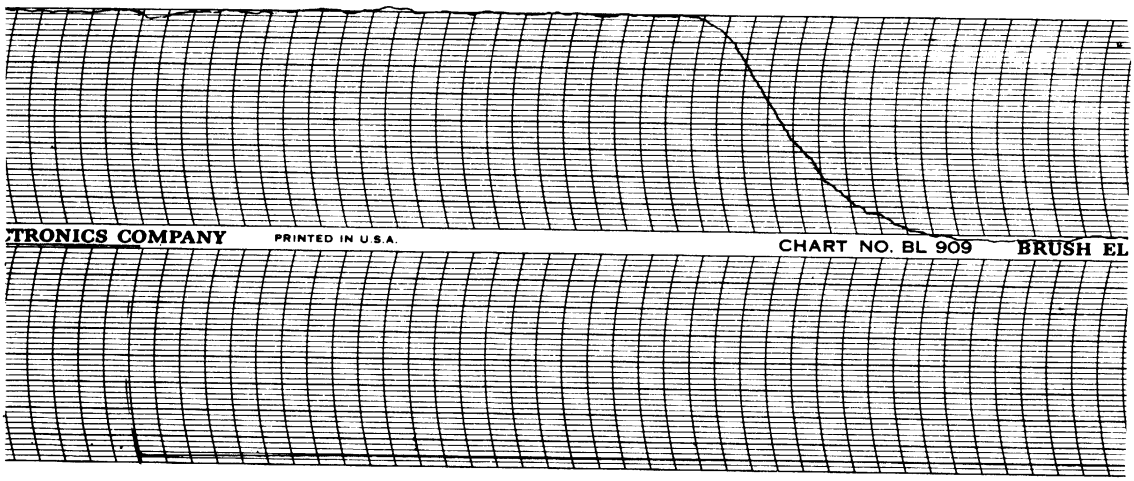

Figure 21. Dry Packing, Run No. D-12

Date: 8/26/57

Room Temperature: 73.4°F

Chart Speed: 1 division/second

Column Properties:

Nominal Particle Size	1/4 in.
Height of Packed Bed	4.45 ft.
Porosity of Dry Bed	.685

Tracer:

Rotameter No. 1 Reading	9.6
Temp. of Flowing Stream	73.2°F
Pressure at Rotameter	14.7 psia

Air:

Rotameter No. 1 Reading	10
Heater Temperature	73.0°F
Dry Bulb Temperature	72.8°F
Wet Bulb Temperature	72.3°F
Pressure at Rotameter	14.7 psia

RECORDER TRACES:

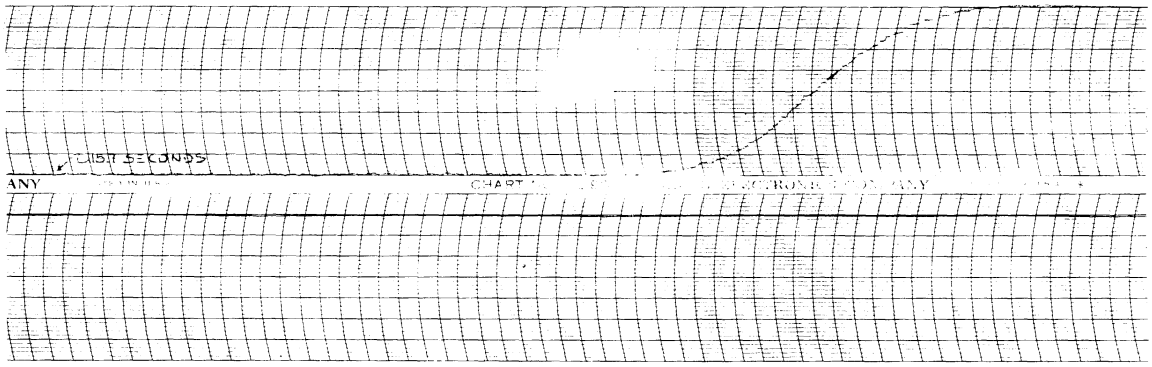

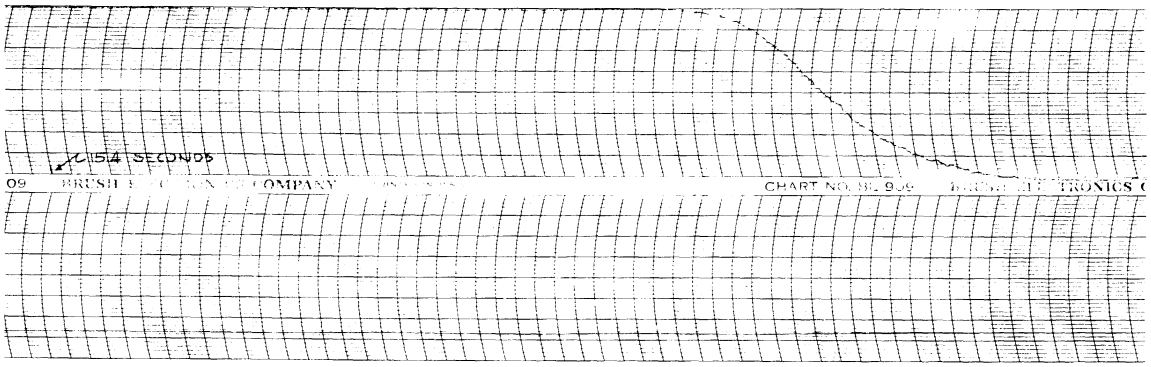

Figure 22. Dry Packing, Run No. D-16

Date: 8/22/57

Room Temperature: 77.4°F

Chart Speed: 5 divisions/second

Column Properties:

Nominal Particle Size	1/4 in.
Height of Packed Bed	3.42 ft.
Porosity of Dry Bed	.666

Tracer:

Rotameter No. 3 Reading	68
Temp. of Flowing Stream	77.2°F
Pressure at Rotameter	15.8 psia

Air:

Rotameter No. 3 Reading	70
Heater Temperature	77.2°F
Dry Bulb Temperature	76.5°F
Wet Bulb Temperature	76.0°F
Pressure at Rotameter	15.9 psia

RECORDER TRACES:

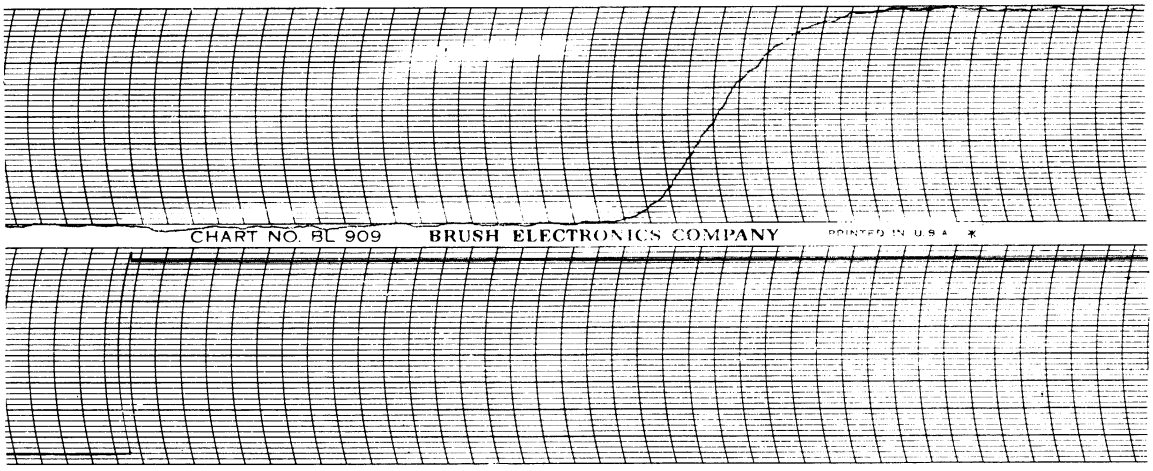

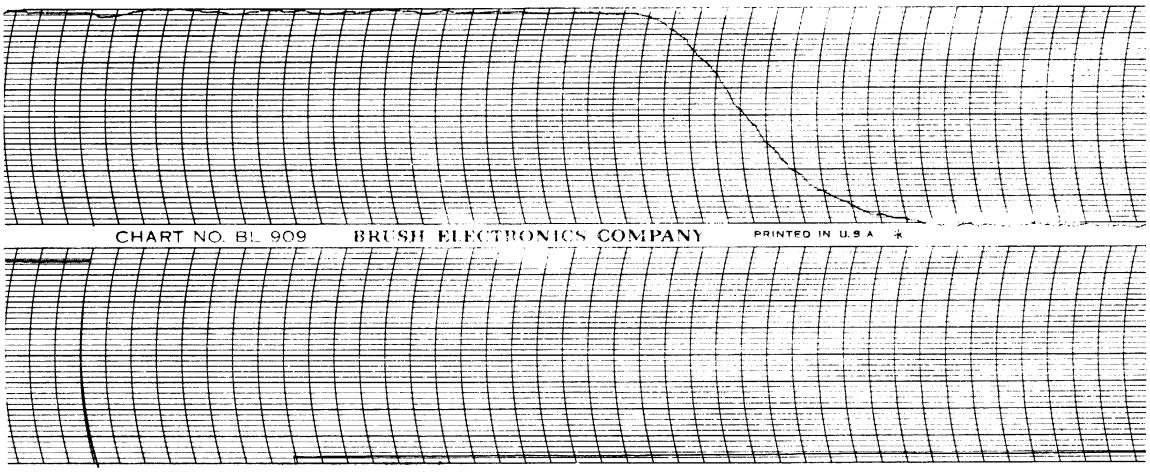

Figure 23. Dry Packing, Run No. D-23

Date: 9/7/57

Room Temperature: 70.6°F

Chart Speed: 1 division/second

Column Properties:

Nominal Particle Size	3/8 in.
Height of Packed Bed	4.45 ft.
Porosity of Dry Bed	.660

Tracer:

Rotameter No. 1 Reading	18.0
Temp. of Flowing Stream	69.8°F
Pressure at Rotameter	14.7 psia

Air:

Rotameter No. 1 Reading	15.3
Heater Temperature	71.0°F
Dry Bulb Temperature	69.5°F
Wet Bulb Temperature	69.0°F
Pressure at Rotameter	14.7 psia

RECORDER TRACES:

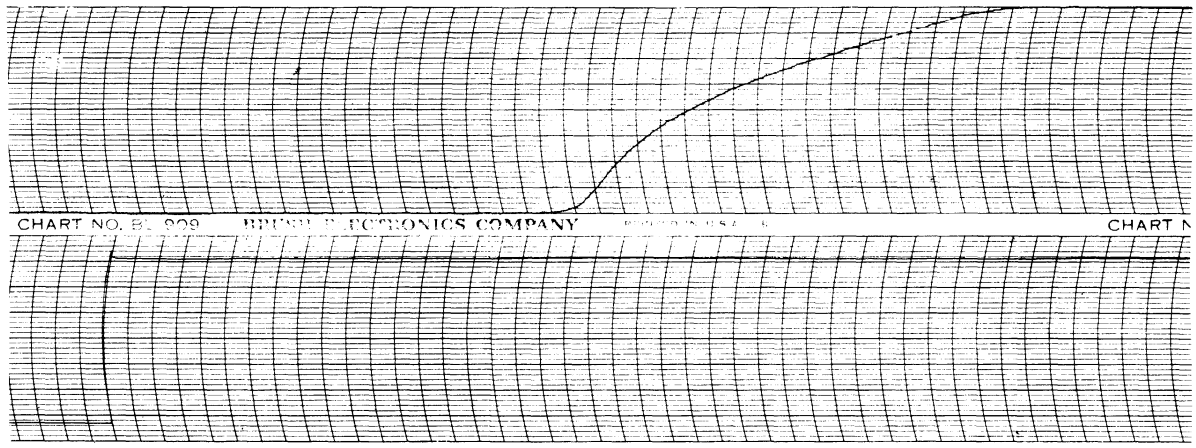

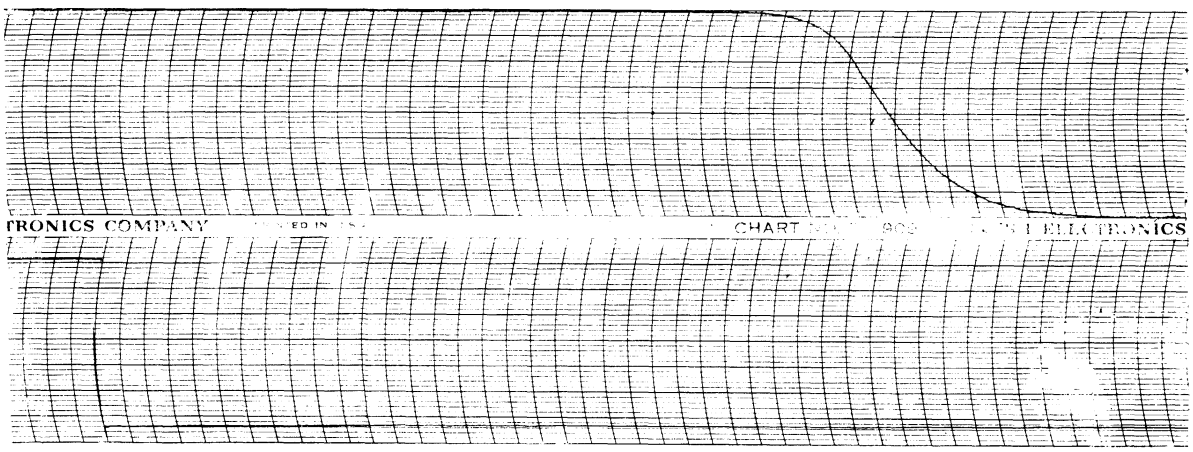

Figure 24. Dry Packing, Run No. D-27

Date: 9/17/57

Room Temperature: 71.7°F

Chart Speed: 1 division/second

Column Properties:

Nominal Particle Size	1/2 in.
Height of Packed Bed	4.45 ft.
Porosity of Dry Bed	.703

Tracer:

Rotameter No. 1 Reading	15
Temp. of Flowing Stream	71.5°F
Pressure at Rotameter	14.7 psia

Air:

Rotameter No. 1 Reading	15
Heater Temperature	72.0°F
Dry Bulb Temperature	69.7°F
Wet Bulb Temperature	69.2°F
Pressure at Rotameter	14.7 psia

RECORDER TRACES:

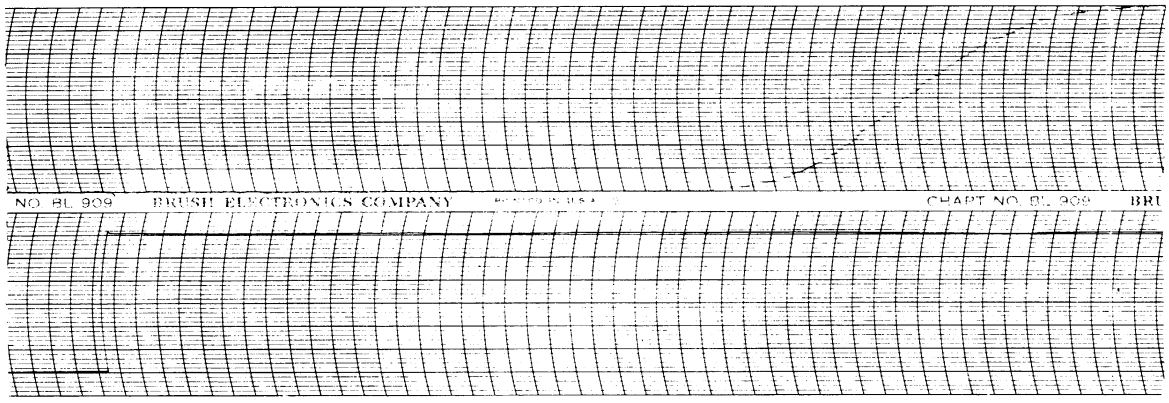

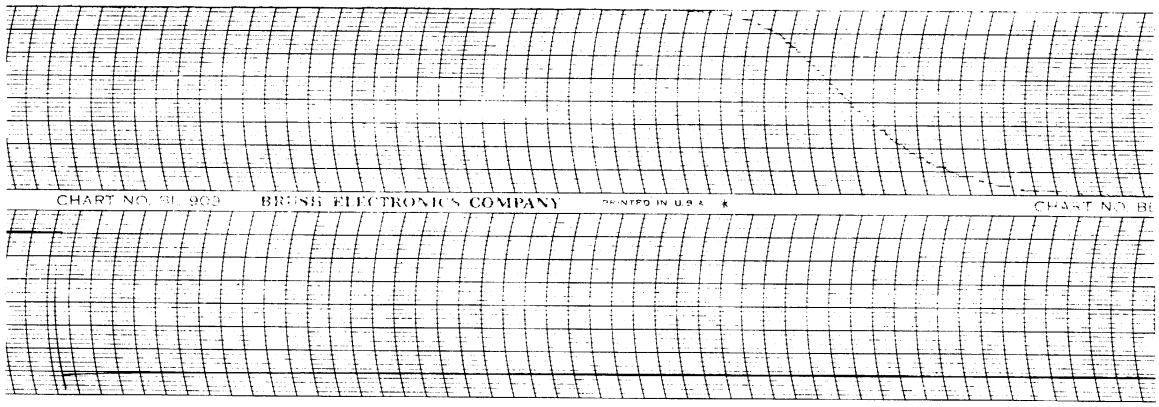

Irrigated Packing

Having determined the effect of column geometry, manner of signal introduction and tracer composition by means of experiments on the dry packing, the porosity of the wet packing and the extent of mixing taking place in the gas stream were measured in a series of 42 runs employing a step input of tracer having a composition of 15% He and 85% N_2. Figures 25 through 33 are typical examples of the data collected.

The variables considered and the ranges investigated are:

Variables	Range
1. Gas rate lb/hr ft^2	19.2 - 198
2. Liquid rate lb/hr ft^2	0 - 6200
3. Particle diameter	1/4, 3/8, 1/2 in.

Beds of 1/4" Raschig rings, three and four feet deep, were used to ascertain the effect of a section of packing which remained dry at the top of the column. The remaining variables which were kept constant are:

4. Column Diameter	.334 ft.
5. Packing Type	Unglazed Porcelain Raschig Rings
6. Surface Tension of the Liquid	~ 70 dynes/cm.

Figure 25. Irrigated Packing, Run No. W-1

Date: 7/25/57
Room Temperature: 78.8°F
Chart Speed: 1 division/second

Column Properties:

Nominal Particle Size	1/4 in.
Height of Irrigated Section	3.0 ft.
Porosity of Dry Bed	.693

Tracer:

Rotameter No. 3 Reading	21.5
Temp. of Flowing Stream	79.2°F
Pressure at Rotameter	14.7 psia

Water:

Rotameter No. 2 Reading	.30
Temperature In	78.9°F
Temperature Out	78.5°F

Air:

Rotameter No. 1 Reading	15
Heater Temperature	79.5°F
Dry Bulb Temperature	79.2°F
Wet Bulb Temperature	78.7°F
Pressure at Rotameter	14.7 psia

RECORDER TRACES:

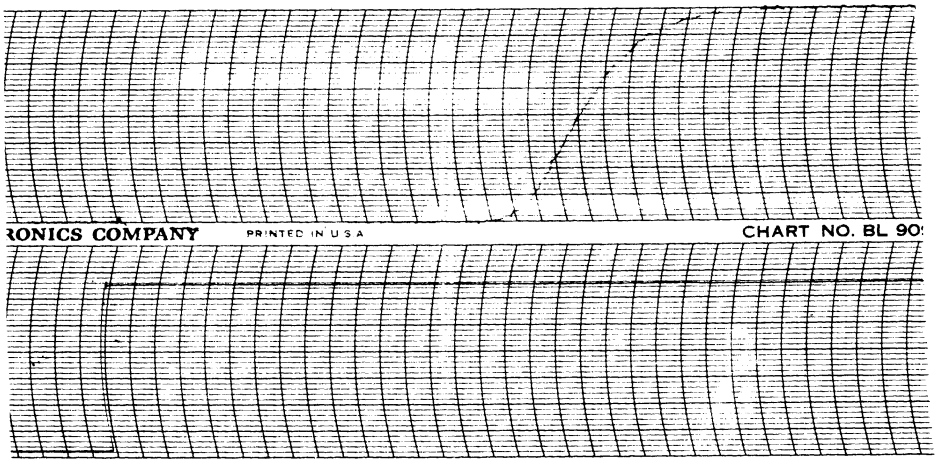

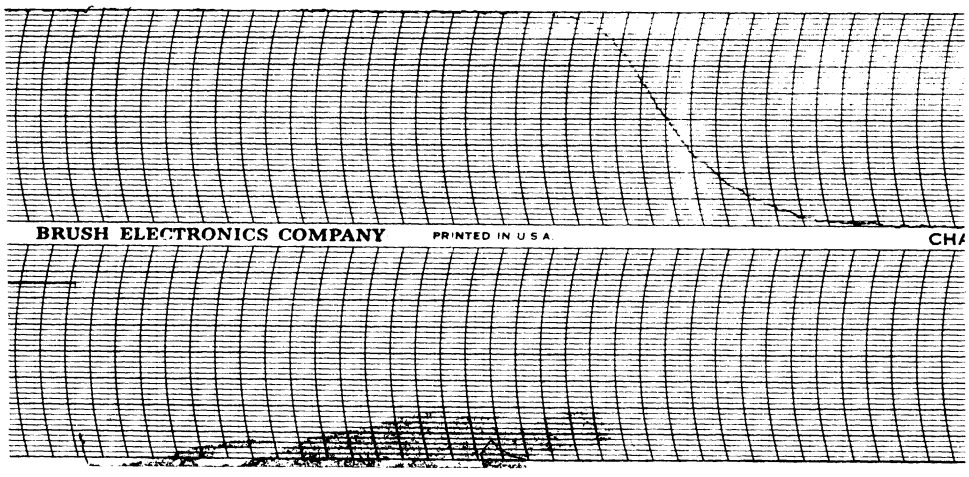

Figure 26. Irrigated Packing, Run No. W-5

Date: 7/29/57
Room Temperature: 85.2°F
Chart Speed: 1 division/second

Column Properties:

Nominal Particle Size	1/4 in.
Height of Irrigated Section	3.0 ft.
Porosity of Dry Bed	.693

Tracer:

Rotameter No. 1 Reading	13.7
Temp. of Flowing Stream	84.2°F
Pressure at Rotameter	14.7 psia

Water:

Rotameter No. 2 Reading	.60
Temperature In	84.9°F
Temperature Out	84.7°F

Air:

Rotameter No. 1 Reading	15
Heater Temperature	86.0°F
Dry Bulb Temperature	85.3°F
Wet Bulb Temperature	84.7°F
Pressure at Rotameter	14.7 psia

RECORDER TRACES:

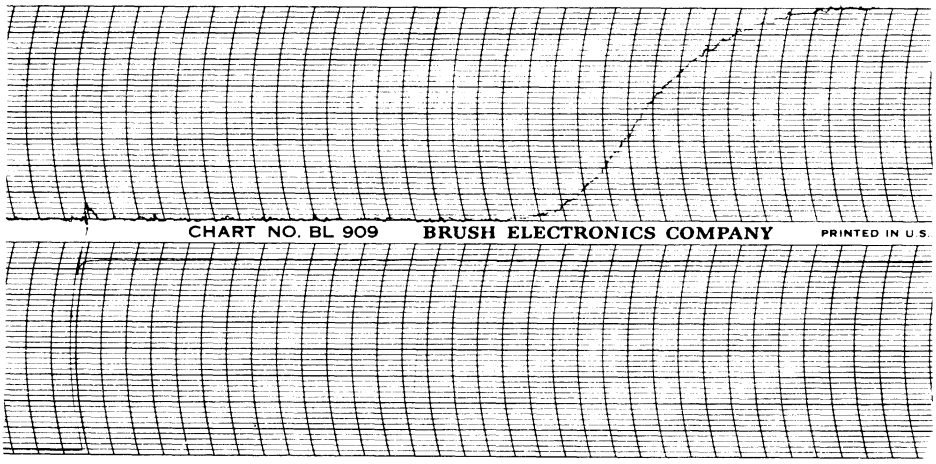

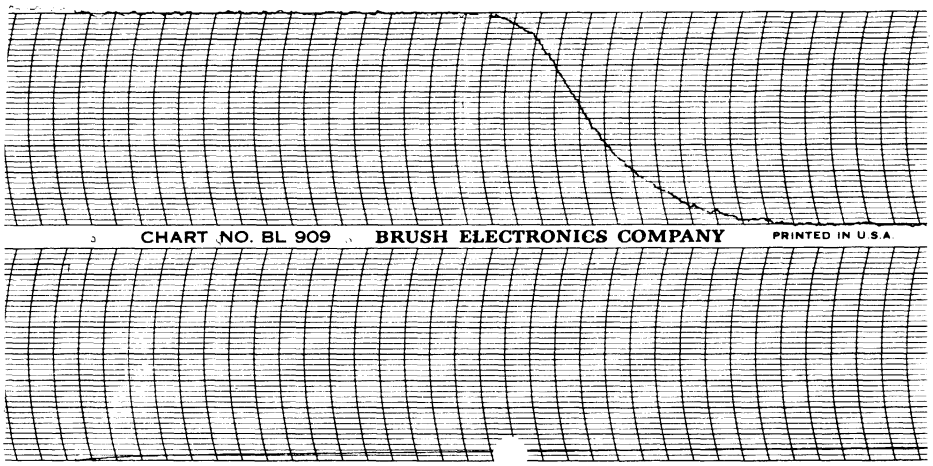

Figure 27. Irrigated Packing, Run No. W-8

Date: 7/19/57
Room Temperature: 87.8°F
Chart Speed: 5 divisions/second

Column Properties:

Nominal Particle Size	1/4 in.
Height of Irrigated Section	3.0 ft.
Porosity of Dry Bed	.693

Tracer:

Rotameter No. 3 Reading	29
Temp. of Flowing Stream	88.0°F
Pressure at Rotameter	14.85 psia

Water:

Rotameter No. 2 Reading	.40
Temperature In	88.5°F
Temperature Out	88.2°F

Air:

Rotameter No. 3 Reading	30
Heater Temperature	88.0°F
Dry Bub Temperature	87.8°F
Wet Bulb Temperature	86.9°F
Pressure at Rotameter	14.9 psia

RECORDER TRACES:

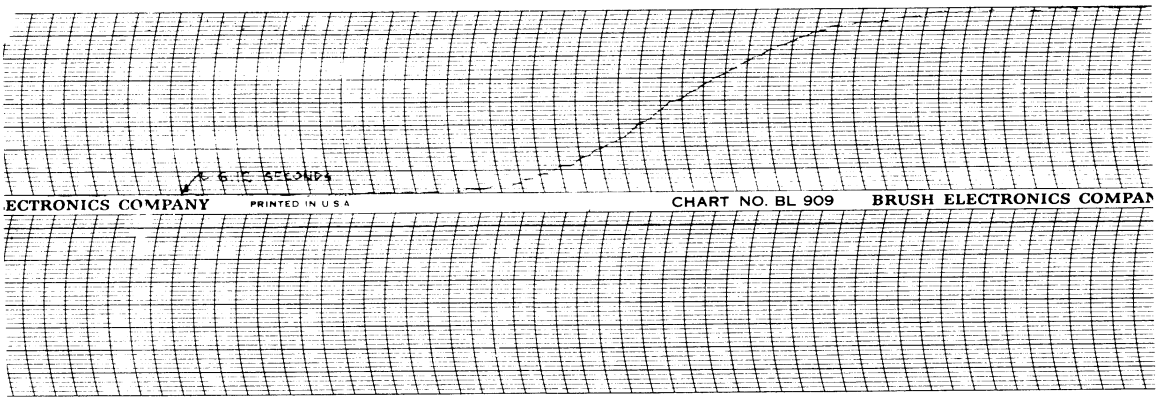

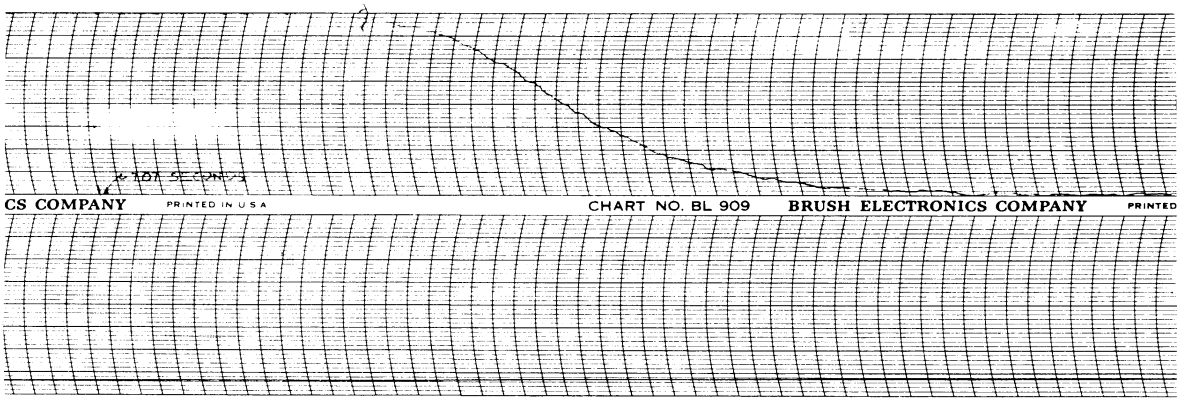

Figure 28. Irrigated Packing, Run No. W-11

Date: 7/30/57
Room Temperature: 86.5°F
Chart Speed: 5 divisions/second

Column Properties:

Nominal Particle Size	1/4 in.
Height of Irrigated Section	3.0 ft.
Porosity of Dry Bed	.693

Tracer:

Rotameter No. 3 Reading	28
Temp. of Flowing Stream	85.6
Pressure at Rotameter	14.9 psia

Water:

Rotameter No. 2 Reading	.30
Temperature In	86.2°F
Temperature Out	85.8°F
Volume Drained From Column	.0118 cu.ft.

Air:

Rotameter No. 3 Reading	30
Heater Temperature	87.8°F
Dry Bulb Temperature	86.7°F
Wet Bulb Temperature	86.3°F
Pressure at Rotameter	14.9 psia

RECORDER TRACES:

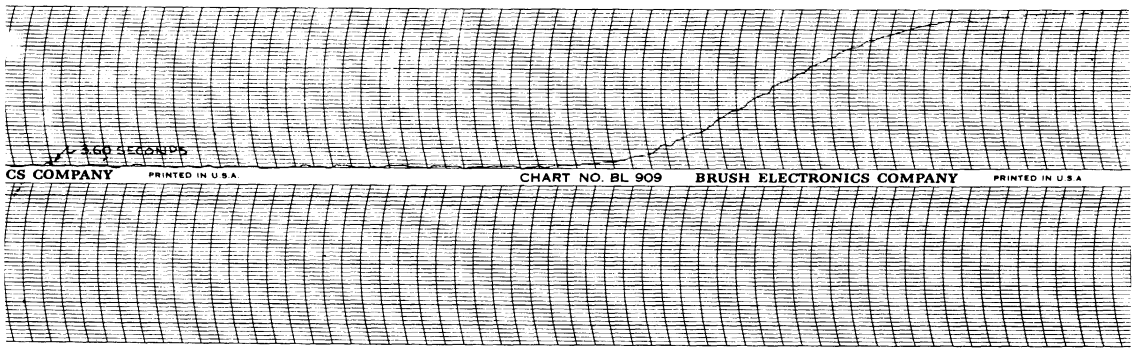

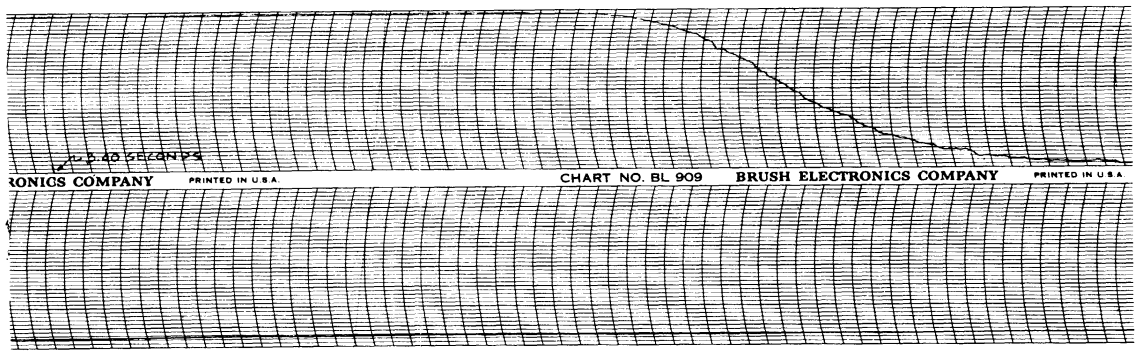

Figure 29. Irrigated Packing, Run No. W-17

Date: 8/3/57
Room Temperature: 81.2°F
Chart Speed: 5 divisions/second

Column Properties:

Nominal Particle Size	1/4 in.
Height of Irrigated Section	
Section	3.0 ft.
Porosity of Dry Bed	.693

Tracer:

Rotameter No. 3 Reading	28
Temp. of Flowing Stream	81.9°F
Pressure at Rotameter	14.9 psia

Water:

Rotameter No. 2 Reading	.90
Temperature In	81.7°F
Temperature Out	81.4°F
Volume Drained From Column	.0385 cu. ft.

Air:

Rotameter No. 3 Reading	30
Heater Temperature	82.0°F
Dry Bulb Temperature	81.8°F
Wet Bulb Temperature	81.5°F
Pressure at Rotameter	14.9 psia

RECORDER TRACES:

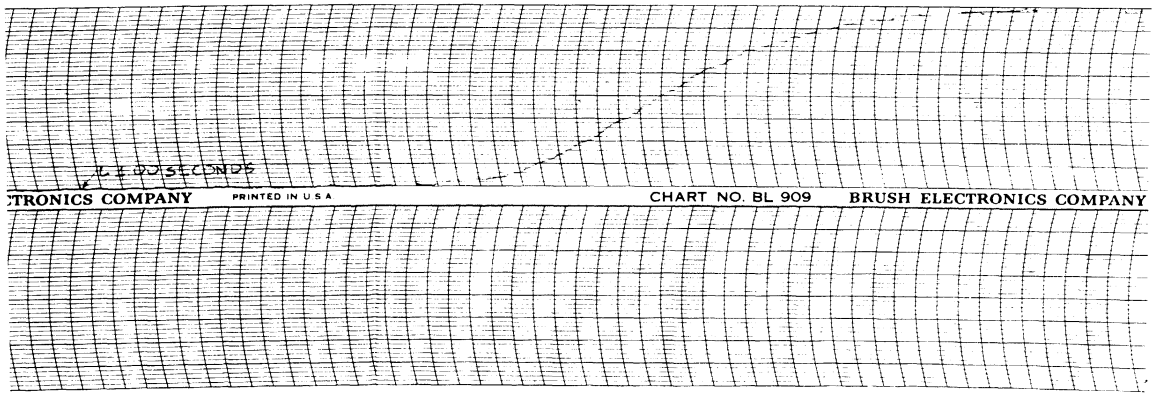

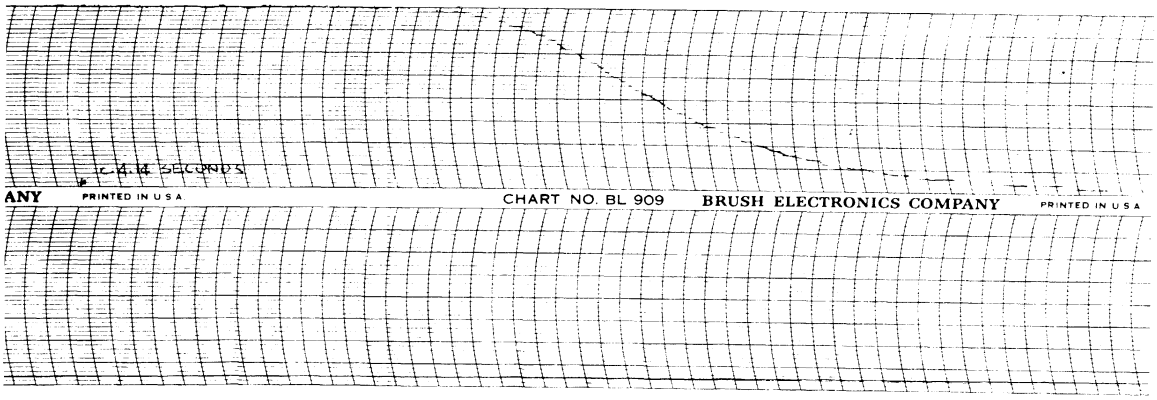

Figure 30. Irrigated Packing, Run No. W-26

Date: 8/31/57
Room Temperature: 76.2°F
Chart Speed: 1 division/second

Column Properties:

Nominal Particle Size	1/4 in.
Height of Irrigated Section	4.0 ft.
Porosity of Dry Bed	.685

Tracer:

Rotameter No. 1 Reading	12
Temp. of Flowing Stream	76.4°F
Pressure at Rotameter	14.7 psia

Water:

Rotameter No. 2 Reading	.90
Temperature In	76.0°F
Temperature Out	75.6°F

Air:

Rotameter No. 1 Reading	15
Heater Temperature	76.6°F
Dry Bulb Temperature	76.2°F
Wet Bulb Temperature	75.7°F
Pressure at Rotameter	14.7 psia

RECORDER TRACES:

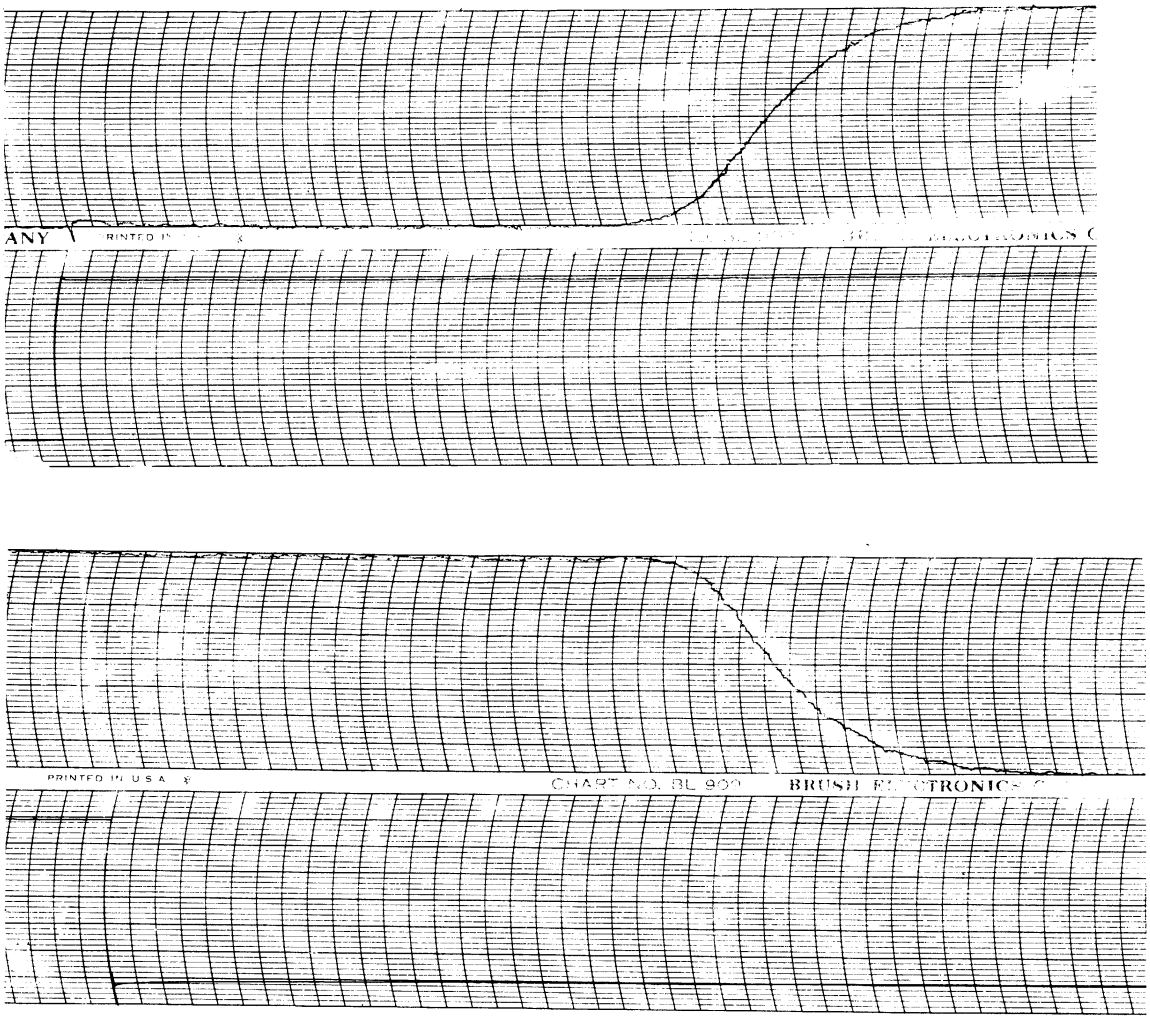

Figure 31. Irrigated Packing, Run No. W-30

Date: 10/29/57
Room Temperature: 77.0°F
Chart Speed: 1 division/second

Column Properties:

Nominal Particle Size	3/8 in.
Height of Irrigated Section	4.0 ft.
Porosity of Dry Bed	.658

Tracer:

Rotameter No. 1 Reading	13
Temp. of Flowing Stream	77.4°F
Pressure at Rotameter	14.7 psia

Water:

Rotameter No. 2 Reading	0.0
Temperature In	---
Temperature Out	---

Air:

Rotameter No. 1 Reading	15
Heater Temperature	78.0°F
Dry Bulb Temperature	77.6°F
Wet Bulb Temperature	77.1°F
Pressure at Rotameter	14.7 psia

RECORDER TRACES:

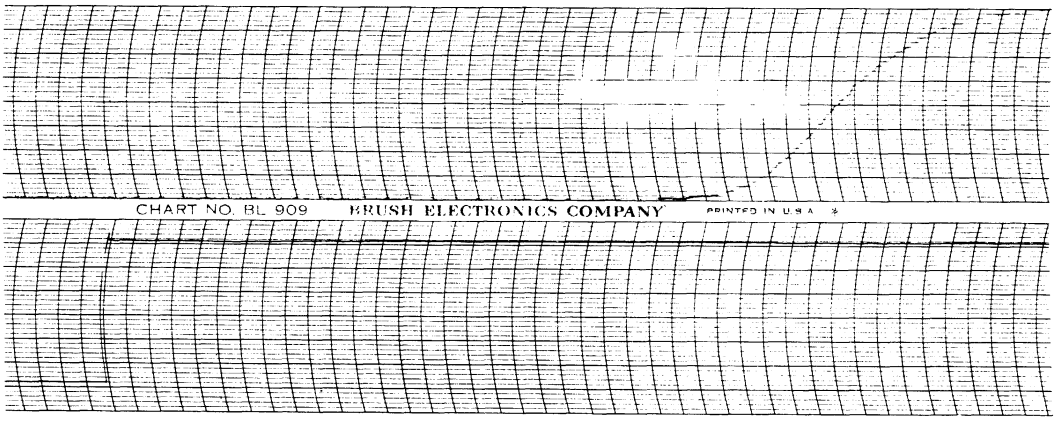

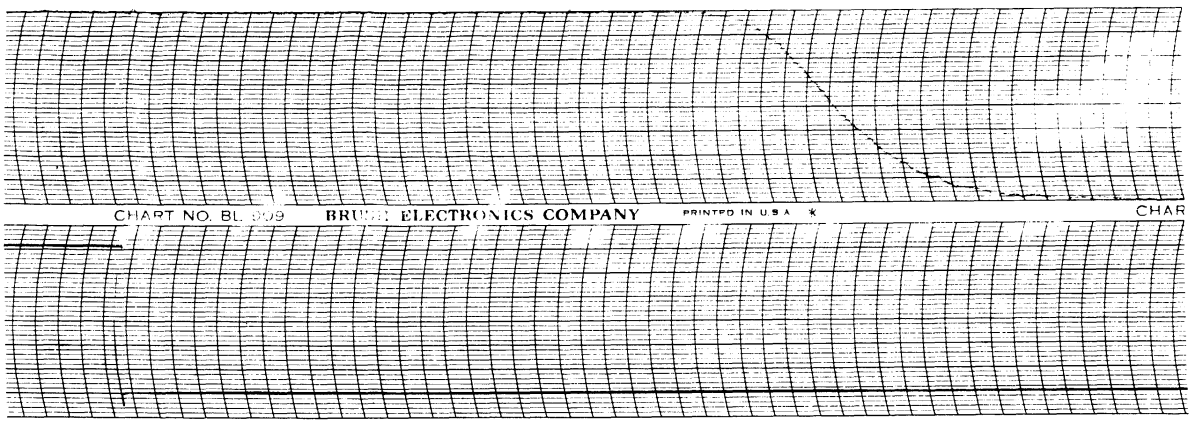

Figure 32. Irrigated Packing, Run No. W-32

Date: 10/30/57
Room Temperature: 75.6°F
Chart Speed: 5 divisions/second

Column Properties:

Nominal Particle Size	3/8 in.
Height of Irrigated Section	4.0 ft.
Porosity of Dry Bed	.658

Tracer:

Rotameter No. 3 Reading	64
Temp. of Flowing Stream	75.0°F
Pressure at Rotameter	15.8 psia

Water:

Rotameter No. 2 Reading	.60
Temperature In	75.8°F
Temperature Out	75.3°F

Air:

Rotameter No. 3 Reading	70
Heater Temperature	76.2°F
Dry Bulb Temperature	75.6°F
Wet Bulb Temperature	75.2°F
Pressure at Rotameter	15.9 psia

RECORDER TRACES:

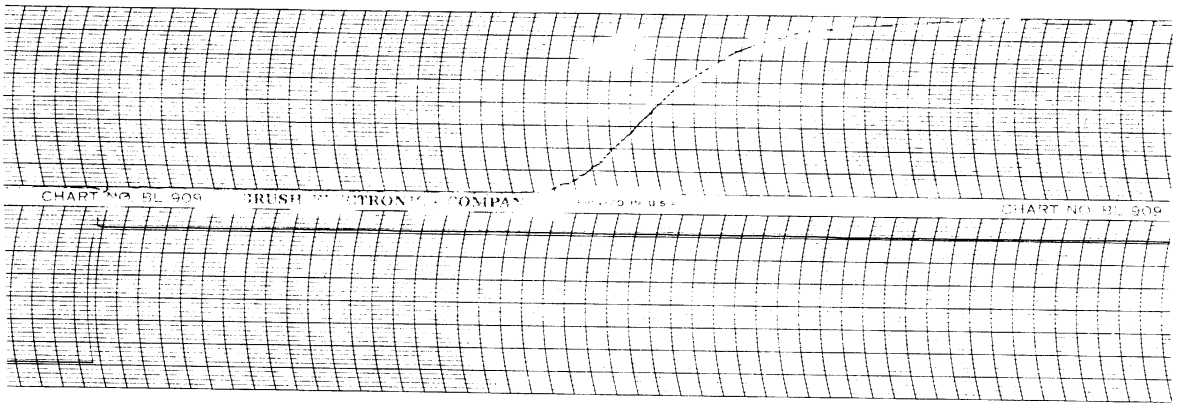

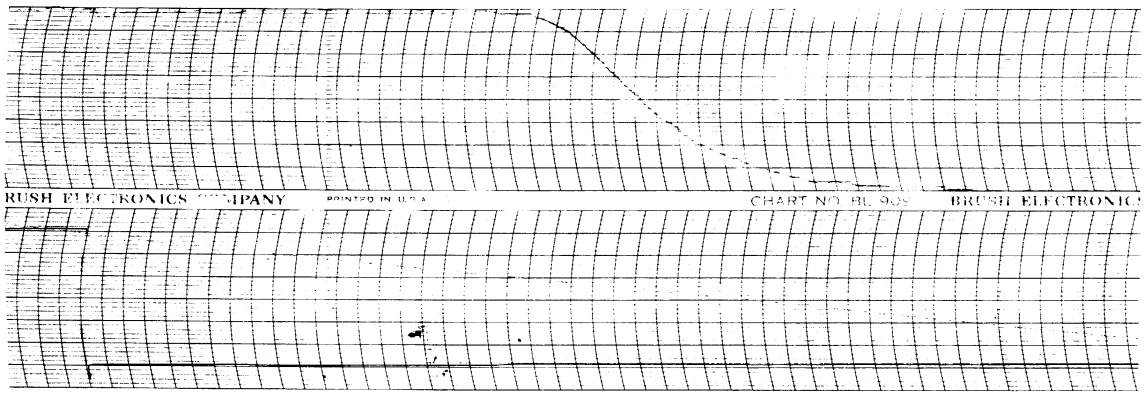

Figure 33. Irrigated Packing, Run No. W-39

Date: 11/4/57
Room Temperature: 77.0°F
Chart Speed: 5 divisions/second

Column Properties:

Nominal Particle Size	1/2 in.
Height of Irrigated Section	4.0 ft.
Porosity of Dry Bed	.705

Tracer:

Rotameter No. 3 Reading	66
Temp. of Flowing Stream	77.1°F
Pressure at Rotameter	15.8 psia

Water:

Rotameter No. 2 Reading	1.10
Temperature In	77.4°F
Temperature Out	76.8°F

Air:

Rotameter No. 3 Reading	70
Heater Temperature	78.0°F
Dry Bulb Temperature	77.7°F
Wet Bulb Temperature	77.3°F
Pressure at Rotameter	15.9 psia

RECORDER TRACES:

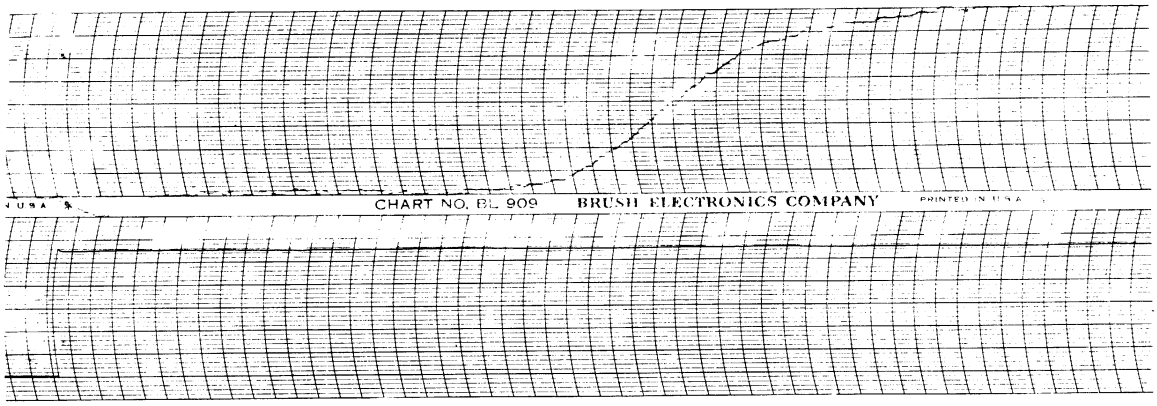

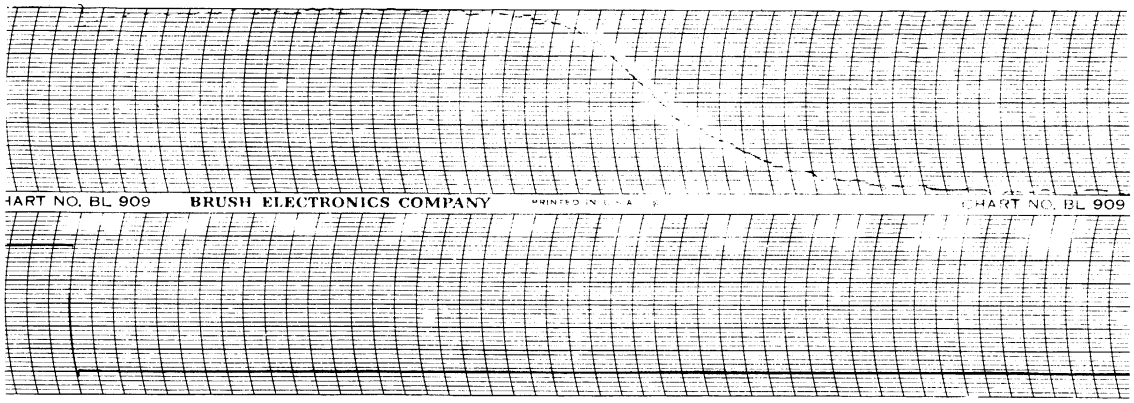

Calculated Results

Calculated results and experimental conditions for the 28 runs performed with dry packing are listed in Table V, pp. 100. Table VI, pp. 101 gives an analogous tabulation for the 42 experiments performed with wet packing.

Standard run calculations consisted of obtaining liquid and gas flow rates and respective Reynolds numbers, also in estimating various moments and appropriate mixing parameters from the recorder traces as described below.

Gas and Liquid Reynolds Numbers were calculated from the measured flow rates converted to superficial mass velocities in the unpacked column, nominal diameter of Raschig rings and viscosities.

The Residence-Time was evaluated by integration of the area bounded by the response curve from the time at which the step input in concentration is introduced. This quantity is:

for tracer displacing air: $\vartheta = \int_0^\infty \left(1 - \frac{c}{c_0}\right) dt$ (See Eq. 14, pp. 22)

for air displacing tracer: $\vartheta = \int_0^\infty \frac{c}{c_0}\, dt$ (See Eq. 13, pp. 22)

The ratio of the residence-time calculated as above with that calculated from the total void free volume and the gas flow rate was designated as Material Balance, i.e.

TABLE V

EXPERIMENTAL CONDITIONS AND RESULTS FOR GAS FLOWING THROUGH DRY PACKING

1	2	3	4	5	6	7	8	9	10	11	12	13	14	15	16	17	18	19	20	21	22	23	24	25	26	27	28	29	30	31	32	33	34
	BED PROPERTIES				AIR						AIR DISPLACING TRACER								TRACER							TRACER DISPLACING AIR							
Run No.	Nominal Particle size a, Ft.	Bed Porosity ϵ	Bed Height L, Ft.	Total Free Volume $\epsilon V_D + V_E$ Cu. Ft.	Pressure, Psia	Temperature, °F	Volumetric Flow Rate v, Cu.Ft./sec.	Mass Flow Rate G, Lb/Hr. Sq.Ft.	Viscosity μ, Lb./Ft.Hr.	Reynolds No. Ga/μ	Residence Time θ, sec.	Material Balance $\theta v/\epsilon V_D + V_E$	Calculated Variance $\sigma^2 = 4/\pi$	Average Number of Stages π	Estimated $uL/2D_L$	Corrected Variance $\sigma_D^2 - \frac{1}{\pi D}$	Height of Mixed Stage H, Ft.	Peclet No.	Composition Vol.% Helium	Pressure Psia	Temperature, °F	Volumetric Flow Rate v, Cu.Ft./sec.	Mass Flow Rate G, Lb./Hr.Sq.Ft.	Viscosity μ, Lb./Ft.Hr.	Reynolds No. Ga/μ	Residence Time θ	Material Balance $\theta v/\epsilon V_D + V_E$	Calculated Variance $\sigma^2 = 4/\pi$	Average Number of Stages π	Estimated $uL/2D_L$	Corrected Variance $\sigma_D^2 = 1/\pi D$	Height of Mixed Stage H, Ft.	Peclet No.
D-1	.0208	.693	3.42	.217	14.7	86	.00568	17.0	.0440	8.05	38.07	.995	.00773	129	140	.00712	.0244	1.71	15	14.7	86	.00519	13.1	.0438	6.22	43.26	1.036	.00778	128	130	.00707	.0242	1.72
D-2	.0208	.693	3.42	.217	14.7	86	.00568	17.0	.0440	8.05	38.60	1.011	.00903	111	110	---	---	---	100	14.7	86	.00521	2.15	.0439	.98	41.80	1.002	.02971	42	---	---	---	---
D-3	.0208	.693	3.42	.217	14.7	77	.00934	28.5	.0435	13.6	22.81	.984	.00760	131	135	.00709	.0242	1.72	15	14.7	77	.01016	26.1	.0433	12.5	22.63	1.054	.00776	129	130	.00726	.0248	1.68
D-4	.0208	.693	3.42	.217	14.7	77	.00934	28.5	.0435	13.6	22.86	.986	.00750	133	140	.00699	.0239	1.74	15	14.7	77	.01016	26.1	.0433	12.5	23.07	1.078	.00746	134	135	.00694	.0238	1.75
D-5	.0208	.693	3.42	.217	14.7	78	.00786	24.0	.0435	11.5	27.28	.992	.00602	166	150	.00541	.0185	2.25	15	14.7	78	.0817	21.0	.0433	10.10	25.15	0.947	.00660	152	150	.00604	.0207	2.01
D-6	.0208	.693	3.42	.217	14.8	77	.0166	51.0	.0435	24.4	13.51	1.033	.00714	140	140	.00661	.0226	1.84	15	14.8	77	.01703	44.0	.0433	21.2	12.96	1.016	.00713	140	140	.00659	.0225	1.85
D-7	.0208	.693	3.42	.217	14.8	77	.0166	51.0	.0435	24.4	12.61	.965	.00835	120	120	---	---	---	100	14.7	77	.01501	6.32	.0454	2.90	14.34	.994	.01824	55	---	---	---	---
D-8	.0208	.693	3.42	.217	15.7	79	.0400	129.6	.0436	62.0	5.21	.961	.00763	131	140	.00713	.0244	1.71	15	15.7	79	.0435	118.9	.0434	57.1	4.87	.976	.00746	134	140	.00694	.0238	1.75
D-9	.0208	.693	3.42	.217	16.0	79	.0403	133.2	.0436	63.7	5.29	.984	.00890	112	120	---	---	---	100	15.9	79	.0326	17.1	.0454	7.83	5.18	.922	.02179	46	---	---	---	---
D-10	.0208	.693	3.42	.217	14.7	78	.00416	12.6	.0435	6.02	53.40	1.022	.00665	150	150	.00609	.0208	2.00	15	14.7	78	.00458	11.71	.0433	5.63	45.61	.962	.00642	156	150	.00584	.0200	2.08
D-11	.0208	.693	3.42	.217	17.2	79	.0645	230.0	.0436	110	3.39	1.006	.00742	135	135	.00690	.0236	1.77	15	17.1	79	.0663	199.0	.0434	95.5	3.11	.951	.00695	144	140	.00641	.0220	1.89
D-12	.0208	.685	4.45	.276	14.7		.00480	14.7	.0433	7.07	55.51	.966	.00508	197	200	.00477	.0212	1.97	15	14.7	73	.00493	12.77	.0431	6.16	54.72	.977	.00478	209	200	.00445	.0198	2.10
D-13	.0208	.685	4.45	.276	14.9		.01676	52.1	.0433	25.1	16.07	.976	.00530	189	195	.00500	.0223	1.87	15	14.9	73	.01699	44.5	.0431	21.5	16.32	1.005	.00452	220	200	.00419	.0187	2.23
D-14	.0208	.685	4.45	.276	15.9		.0401	133.0	.0434	63.7	6.95	1.009	.00507	197	200	.00476	.0212	1.97	15	15.8	75	.0399	110.6	.0432	53.3	6.57	.952	.00591	169	175	.00564	.0252	1.65
D-15	.0208	.666	3.42	.206			.00822	22.1	.0435	10.6	25.28	1.008	.00831	120	130	.00785	.0269	1.55	15	14.7	77	.00775	19.9	.0433	9.56	26.64	1.001	.00822	122	130	.00776	.0266	1.57
D-16	.0208	.666	3.42	.206			.0402	132.5	.0435	63.4	5.31	1.031	.00954	105	115	.00917	.0314	1.33	15	15.8	77	.0423	115.6	.0433	55.6	4.74	.973	.01013	99	110	.00979	.0335	1.24
D-17	.0208	.666	3.42	.206			.0402	132.5	.0435	63.4	5.31	1.031	.00979	102	115	.00944	.0323	1.29	15	15.8	77	.0423	115.6	.0433	55.6	4.72	.971	.01007	100	100	.00973	.0333	1.25
D-18	.0312	.660	4.45	.266	14.7	73	.00358	11.0	.0433	7.94	73.97	.996	.00630	159	155	.00604	.0269	2.32	15	14.7	73	.00429	11.1	.0431	8.04	60.45	.975	.00620	161	160	.00594	.0264	2.36
D-19	.0312	.660	4.45	.266	14.7	68	.00796	24.8	.0430	18.0	35.58	1.066	.00606	165	160	.00579	.0258	2.42	15	14.7	68	.00796	20.8	.0428	15.16	31.00	.930	.00590	145	160	.00669	.0298	2.10
D-20	.0312	.660	4.45	.266	15.8	67	.0392	130.8	.0429	95.2	6.63	.976	.00723	138	130	.00703	.0313	2.00	15	15.7	67	.00469	130.5	.0427	95.5	5.46	.965	.00695	144	155	.00672	.0300	2.08
D-21	.0312	.660	4.45	.266	17.2	67	.0632	228.0	.0429	165.9	4.32	1.029	.00687	145	140	.00665	.0296	2.11	15	17.1	67	.0652	197.0	.0427	144	4.07	.999	.00716	140	140	.00695	.0310	2.02
D-22	.0312	.660	4.45	.266	14.9	70	.01670	51.6	.0431	37.4	16.35	1.021	.00654	153	160	---	---	---	100	14.7	70	.01865	7.97	.0449	5.53	14.23	1.000	.01313	66	---	----	----	---
D-23	.0312	.660	4.45	.266	14.7	70	.00803	24.9	.0431	18.0	32.94	.994	.00628	161	160	---	---	---	100	14.7	70	.00970	4.14	.0449	2.88	25.44	.929	.03993	25	---	----	----	---
D-24	.0416	.703	4.45	.283	14.9	71	.01667	52.1	.0432	50.3	17.76	1.045	.01088	92	105	.01084	.0483	1.72	15	14.9	71	.01502	39.8	.0430	38.6	18.06	.961	.01088	92	110	.01084	.0482	1.73
D-25	.0416	.703	4.45	.283	15.6	72	.0396	127.9	.0432	123.3	7.13	.999	.01065	94	95	.01060	.0472	1.76	15	15.6	72	.03706	102.2	.0431	99.0	7.84	1.027	.00947	106	100	.00936	.0417	2.00
D-26	.0416	.703	4.45	.283	16.7	72	.0553	193.5	.0432	186.8	5.11	.993	.00885	91	85	.00873	.0388	2.14	15	16.6	72	.0618	181.0	.0431	175.0	4.49	.982	.01092	92	90	.01068	.0484	1.72
D-27	.0416	.703	4.45	.283	14.7	71	.0079	24.5	.0432	23.6	36.81	1.031	.00920	109	110	.00909	.0404	2.06	15	14.7	71	.00761	19.8	.0430	19.2	37.14	.999	.01210	83	80	.01210	.0538	1.55
D-28	.0416	.703	4.45	.283	14.7	71	.00340	10.5	.0432	10.1	85.38	1.021	.00848	118	120	.0834	.0371	2.24	15	14.7	71	.00328	8.65	.0430	8.38	92.16	.954	.00936	107	100	.00926	.0412	2.02

TABLE VI

EXPERIMENTAL CONDITIONS AND RESULTS FOR GAS FLOWING THROUGH IRRIGATED PACKING

1	2	3	4	5	6	7	8	9	10	11	12
	BED PROPERTIES					AIR					
RUN NO.	Nominal Particle Size d, Ft.	Porosity of Dry Bed ε	Height of Irrigated Section L, Ft.	Empty Column Volume of Irrigated Section V_W, Cu. Ft.	Void Volume Not Wetted $\epsilon V_{DT}+V_E$, Cu.Ft.	Pressure, Psia	Temperature, °F	Volumetric Flow Rate v, cu.ft/sec	Mass Flow Rate G, Lb/Hr Sq.Ft.	Viscosity μ_G, Lb/Hr.Ft.	Reynolds No. G d/ μ_G
W-1	.0208	.693	3.00	.259	.0369	14.7	79	.00788	24.0	.0436	11.5
W-2	.0208	.693	3.00	.259	.0369	14.7	79	.00788	24.0	.0436	11.5
W-3	.0208	.693	3.00	.259	.0369	14.7	79	.00788	24.0	.0436	11.5
W-4	.0208	.693	3.00	.259	.0369	14.7	85	.00784	23.6	.0439	11.2
W-5	.0208	.693	3.00	.259	.0369	14.7	85	.00784	23.6	.0439	11.2
W-6	.0208	.693	3.00	.259	.0369	14.7	85	.00784	23.6	.0439	11.2
W-7	.0208	.693	3.00	.259	.0369	14.7	85	.00784	23.6	.0439	11.2
W-8	.0208	.693	3.00	.259	.0369	14.9	88	.0165	50.0	.0441	23.6
W-9	.0208	.693	3.00	.259	.0369	16.0	88	.0398	129	.0441	60.9
W-10	.0208	.693	3.00	.259	.0369	17.0	88	.0560	196	.0441	92.5
W-11	.0208	.693	3.00	.259	.0369	14.9	86	.0165	50.0	.0440	23.7
W-12	.0208	.693	3.00	.259	.0369	16.0	86	.0390	130	.0440	61.5
W-13	.0208	.693	3.00	.259	.0369	17.0	86	.0566	194	.0440	91.9
W-14	.0208	.693	3.00	.259	.0369	14.9	88	.0165	50.0	.0441	23.6
W-15	.0208	.693	3.00	.259	.0369	16.0	88	.0398	129	.0441	60.9
W-16	.0208	.693	3.00	.259	.0369	17.0	82	.0566	198	.0438	94.0
W-17	.0208	.693	3.00	.259	.0369	14.9	82	.0165	50.8	.0438	24.2
W-18	.0208	.693	3.00	.259	.0369	16.0	86	.0398	130	.0440	61.5
W-19	.0208	.693	3.00	.259	.0369	17.0	86	.0566	194	.0440	91.9
W-20	.0208	.693	3.00	.259	.0369	14.9	86	.0165	50.1	.0440	23.7
W-21	.0208	.693	3.00	.259	.0369	16.0	86	.0398	130	.0440	61.5
W-22	.0208	.693	3.00	.259	.0369	16.0	73	.0398	133	.0433	64.0
W-23	.0208	.685	4.00	.349	.0366	14.7	76	.00789	24.2	.0434	11.5
W-24	.0208	.685	4.00	.349	.0366	14.7	76	.00789	24.2	.0434	11.5
W-25	.0208	.685	4.00	.349	.0366	14.7	76	.00789	24.2	.0434	11.5
W-26	.0208	.685	4.00	.349	.0366	14.7	76	.00789	24.2	.0434	11.5
W-27	.0312	.658	4.00	.349	.0355	14.7	75	.00788	24.2	.0434	17.4
W-28	.0312	.658	4.00	.349	.0355	14.7	77	.00788	24.0	.0435	17.2
W-29	.0312	.658	4.00	.349	.0355	14.7	77	.00786	24.0	.0435	17.2
W-30	.0312	.658	4.00	.349	.0355	14.7	77	.00771	23.5	.0435	16.9
W-31	.0312	.658	4.00	.349	.0355	15.9	75	.0402	133	.0434	95.6
W-32	.0312	.658	4.00	.349	.0355	15.9	75	.0402	133	.0434	95.6
W-33	.0312	.658	4.00	.349	.0355	15.9	75	.0402	133	.0434	95.6
W-34	.0312	.658	4.00	.349	.0355	15.9	75	.0402	133	.0434	95.6
W-35	.0416	.705	4.00	.349	.0374	14.7	75	.00788	24.2	.0434	23.2
W-36	.0416	.705	4.00	.349	.0374	14.7	77	.00788	24.0	.0434	23.0
W-37	.0416	.705	4.00	.349	.0374	14.7	77	.00788	24.0	.0435	23.0
W-38	.0416	.705	4.00	.349	.0374	14.7	77	.00788	24.0	.0435	23.0
W-39	.0416	.705	4.00	.349	.0374	15.9	77	.0402	132	.0435	126
W-40	.0416	.705	4.00	.349	.0374	15.9	77	.0402	132	.0435	126
W-41	.0416	.705	4.00	.349	.0374	15.9	77	.0402	132	.0435	126
W-42	.0416	.705	4.00	.349	.0374	15.9	77	.0402	132	.0435	126

1	13	14	15	16	17	18	19	20	21	22	23	24	25	26	27
	AIR DISPLACING TRACER									TRACER					
RUN NO.	Total Residence Time θ, Sec.	Residence-Time in Irrigated Section θ_W, Sec.	Porosity of Wet Packing, ϵ_W	Calculated Variance $\sigma^2 = \frac{1}{n}$	Corrected Variance $\sigma_D^2 = \frac{1}{n_W}$	Height of Mixed Stage, H_W, Ft	Peclet No. $2d/H_W$	Skewness ν	Departure From Uniform Flow $\nu - 2\sigma^4$	Pressure, Psia	Temperature, °F	Volumetric Flow Rate, v, Cu.Ft/Sec	Mass Flow Rate G, Lb/Hr.Sq.Ft.	Viscosity μ_G, Lb/Hr.Ft.	Reynolds No. G d/μ_G
W-1	24.10	19.42	.590	.01144	.01383	.0415	1.00	.0003	.0000	14.7	79	.00964	24.6	.0434	11.8
W-2	22.26	17.58	.535	.01330	.01670	.0501	0.830	.0004	.0000	14.7	79	.00964	24.6	.0434	11.8
W-3	20.75	16.07	.489	.01625	.02156	.0647	0.643	.0030	.0025	14.7	79	.00964	24.6	.0434	11.8
W-4	24.99	20.29	.614	.00793	.00854	.0256	1.62	.0000	.0000	14.7	85	.00800	20.2	.0437	9.65
W-5	22.29	17.59	.532	.01306	.01633	.0490	0.849	.0005	.0002	14.7	85	.00761	19.2	.0437	9.15
W-6	20.11	15.41	.467	.01690	.02273	.0682	0.610	.0031	.0021	14.7	85	.00761	19.2	.0437	9.15
W-7	25.15	20.45	.620	.00767	.00817	.0245	1.69	.0002	.0001	14.7	85	.00761	19.2	.0437	9.15
W-8	11.67	9.43	.601	.01118	.01346	.0404	1.03	.0007	.0003	14.9	88	.0175	44.5	.0439	21.1
W-9	4.78	3.85	.592	.01286	.01602	.0481	0.866	.0004	.0000	15.9	88	.0406	111	.0439	52.6
W-10	3.26	2.61	.570	.01603	.02099	.0630	0.661	.0020	.0015	16.9	88	.0610	176	.0439	83.5
W-11	11.43	9.19	.585	.01011	.01178	.0353	1.177	.0003	.0001	14.9	86	.0167	42.6	.0438	20.2
W-12	4.65	3.72	.573	.01355	.01710	.0513	0.811	.0009	.0005	15.9	86	.0406	111	.0438	52.6
W-13	3.21	2.56	.560	.01551	.02021	.0606	0.686	.0020	.0015	16.9	86	.0610	177	.0438	84.0
W-14	10.39	8.15	.518	.01358	.01716	.0515	0.808	.0010	.0006	14.9	88	.0175	44.5	.0439	21.1
W-15	4.21	3.28	.504	.01674	.02234	.0670	0.621	.0013	.0007	15.9	88	.0370	101	.0439	47.9
W-16	2.89	2.24	.491	.02404	.03457	.1037	0.401	.0055	.0044	16.9	82	.0571	167	.0436	79.9
W-17	9.80	7.58	.484	.01847	.02526	.0758	0.549	.0014	.0007	14.9	82	.0167	42.9	.0436	20.5
W-18	3.92	3.00	.462	.02072	.02929	.0879	0.473	.0019	.0011	15.9	86	.0075	126	.0438	59.9
W-19	2.47	1.82	.399	.02853	.04430	.1329	0.313	.0073	.0057	16.9	86	.0610	177	.0438	84.0
W-20	9.45	7.21	.460	.02065	.02921	.0876	0.475	.0019	.0011	14.9	86	.0167	42.6	.0438	20.2
W-21	3.83	2.90	.445	.02968	.04503	.1351	0.308	.0021	.0003	15.9	86	.0475	126	.0438	59.9
W-22	4.95	4.02	.618	.00780	.00838	.0345	1.21	.0002	.0001	15.9	73	.0406	114	.0431	55.2
W-23	31.85	27.21	.616	.00612	.00650	.0260	1.60	.0003	.0002	14.7	76	.00750	19.3	.0434	9.26
W-24	30.39	25.75	.582	.00895	.01038	.0415	1.00	.0000	.0000	14.7	76	.00750	19.3	.0434	9.26
W-25	28.22	23.58	.534	.01133	.01372	.0549	0.758	.0009	.0007	14.7	76	.00750	19.3	.0434	9.26
W-26	26.82	22.10	.501	.01357	.01701	.0680	0.611	.0009	.0005	14.7	76	.00750	19.3	.0434	9.26
W-27	28.71	24.21	.546	.02209	.02834	.0850	0.735	.0031	.0021	14.7	75	.00725	18.7	.0432	13.5
W-28	27.45	22.96	.518	.02744	.03618	.1447	0.432	.0029	.0014	14.7	77	.00725	18.6	.0433	13.4
W-29	30.23	25.74	.581	.01252	.01484	.0594	1.05	.0006	.0003	14.7	77	.00725	18.6	.0433	13.4
W-30	31.99	27.38	.605	.01032	.01183	.0473	1.32	.0004	.0002	14.7	77	.00742	19.0	.0433	13.7
W-31	5.34	4.46	.504	.02687	.03543	.1417	0.441	.0045	.0031	15.8	75	.0400	111	.0432	80.2
W-32	5.32	4.49	.517	.02253	.02922	.1169	0.535	.0023	.0012	15.8	75	.0400	111	.0432	80.2
W-33	5.79	4.91	.571	.01456	.01769	.0708	0.883	.0010	.0006	15.8	75	.0400	111	.0432	80.2
W-34	5.90	5.02	.584	.01307	.01561	.0624	1.00	.0006	.0003	15.8	75	.0400	111	.0432	80.2
W-35	31.59	26.85	.607	.01838	.02240	.0896	0.931	.0018	.0011	14.7	75	.00725	18.7	.0432	18.0
W-36	31.24	26.50	.599	.02338	.02930	.1173	0.711	.0034	.0023	14.7	77	.00725	18.6	.0433	17.9
W-37	32.42	27.68	.625	.01285	.01476	.0590	1.41	.0007	.0004	14.7	77	.00725	18.6	.0433	17.9
W-38	33.32	28.58	.645	.01376	.01601	.0640	1.30	.0008	.0004	14.7	77	.00725	18.6	.0433	17.9
W-39	5.58	4.65	.534	.02832	.03688	.1475	0.565	.0026	.0010	15.8	77	.0410	113	.0433	108.6
W-40	5.99	5.06	.583	.02132	.02658	.1063	0.784	.0017	.0008	15.8	77	.0410	113	.0433	108.6
W-41	6.42	5.49	.633	.01855	.02257	.0903	0.924	.0017	.0010	15.8	77	.0410	113	.0433	108.6
W-42	6.38	5.45	.628	.01700	.02045	.0818	1.02	.0008	.0002	15.8	77	.0410	113	.0433	108.6

1	28	29	30	31	32	33	34	35	36	37	38	39	40	41	42
	TRACER DISPLACING AIR									WATER					
RUN NO.	Total Residence Time θ, Seconds	Residence-Time In Irrigated Section θ_W, Sec	Porosity of Wet Packing, ϵ_W	Calculated Variance $\sigma^2 = \frac{1}{n}$	Corrected Variance $\sigma_D^2 = \frac{1}{n_W}$	Height of Mixed Stage, H_W, Ft	Peclet No $2d/H_W$	Skewness ν	Departure From Uniform Flow $\nu - 2\sigma^4$	Temperature, °F	Density, ρ, Lb/Cu.Ft.	Viscosity μ_W Lb/Ft.Hr.	Volumetric Flow Rate, v Gal/Min	Mass Flow Rate W, Lb/Hr.Sq.Ft.	Reynolds No. W d/μ_W
W-1	19.48	15.65	.582	.01199	.01466	.0440	.946	.0006	.0003	79	62.23	2.11	.279	1600	15.8
W-2	18.19	14.36	.534	.01324	.01659	.0498	.836	.0005	.0002	79	62.23	2.11	.584	3340	33.0
W-3	17.27	13.44	.500	.01581	.02080	.0624	.667	.0013	.0008	79	62.23	2.11	.886	5070	50.1
W-4	24.88	19.77	.611	.00803	.00869	.0261	1.60	.0003	.0002	85	62.17	1.96	.078	446	4.75
W-5	22.91	18.06	.530	.01412	.01802	.0541	0.770	.0004	.0000	85	62.17	1.96	.584	3340	35.6
W-6	21.00	16.15	.474	.01643	.02190	.0657	0.633	.0017	.0012	85	62.17	1.96	1.083	6190	65.9
W-7	26.30	21.45	.631	.00751	.00796	.0239	1.74	.0000	.0000	85	62.17	1.96	.000	0	.0
W-8	10.92	8.81	.595	.01038	.01220	.0366	1.14	.0002	.0002	88	62.13	1.89	.078	446	4.91
W-9	4.70	3.79	.594	.01274	.01584	.0475	0.875	.0004	.0001	88	62.13	1.89	.078	446	4.91
W-10	3.05	2.45	.574	.01598	.02088	.0626	0.664	.0017	.0012	88	62.13	1.89	.078	446	4.91
W-11	11.38	9.17	.590	.00992	.01147	.0344	1.21	.0002	.0000	86	62.16	1.94	.279	1590	17.1
W-12	4.60	3.69	.580	.01252	.01549	.0465	.895	.0005	.0002	86	62.16	1.94	.279	1590	17.1
W-13	2.97	2.37	.557	.01855	.02499	.0750	.555	.0015	.0008	86	62.16	1.94	.279	1590	17.1
W-14	9.80	7.69	.520	.01495	.01936	.0581	.716	.0006	.0002	88	62.13	1.89	.584	3340	36.8
W-15	4.60	3.60	.515	.01454	.01870	.0561	.742	.0007	.0003	88	62.13	1.89	.584	3340	36.8
W-16	2.82	2.18	.480	.02295	.02692	.0808	.515	.0033	.0023	82	62.20	2.06	.584	3340	33.8
W-17	9.61	7.40	.477	.01630	.02164	.0649	.641	.0009	.0004	82	62.20	2.06	.886	5060	51.2
W-18	3.40	2.62	.467	.02339	.03358	.1007	.413	.0022	.0011	86	62.16	1.94	.886	5050	54.3
W-19	2.36	1.76	.412	.03552	.05646	.1694	.246	.0075	.0050	86	62.16	1.94	.886	5050	54.3
W-20	9.17	6.96	.450	.02207	.03169	.0951	.438	.0018	.0009	86	62.16	1.94	1.083	6190	66.5
W-21	3.20	2.42	.444	.02081	.02959	.0888	.469	.0014	.0006	86	62.16	1.94	1.083	6190	66.5
W-22	4.84	3.93	.616	.01106	.01329	.0399	1.04	.0003	.0000	73	62.28	2.28	.000	0	.0
W-23	32.98	28.10	.604	.00620	.00659	.0264	1.58	.0000	.0000	76	62.25	2.19	.078	447	4.25
W-24	31.70	26.82	.577	.00950	.01113	.0445	.934	.0000	.0000	76	62.25	2.19	.279	1600	15.2
W-25	29.60	23.86	.524	.00999	.01179	.0472	.882	.0002	.0000	76	62.25	2.19	.584	3340	31.8
W-26	28.38	23.50	.504	.01193	.01462	.0585	.711	.0005	.0000	76	62.25	2.19	.886	5070	48.3
W-27	30.88	25.99	.539	.01924	.02435	.0974	.642	.0013	.0006	75	62.26	2.22	.584	3340	47.0
W-28	29.31	24.42	.506	.02719	.03599	.1440	.434	.0056	.0041	77	62.24	2.16	1.083	6200	89.8
W-29	33.50	28.61	.593	.01175	.01379	.0552	1.13	.0003	.0000	77	62.24	2.16	.078	447	6.47
W-30	32.60	27.82	.592	.00966	.01092	.0437	1.43	.0010	.0009	77	62.24	2.16	.000	0	.0
W-31	5.22	4.33	.496	.02529	.03336	.1334	.468	.0054	.0041	75	62.26	2.22	1.083	6200	87.4
W-32	5.49	4.60	.529	.02400	.03118	.1247	.501	.0039	.0028	75	62.26	2.22	.584	3340	47.0
W-33	6.04	5.15	.585	.01394	.01679	.0672	.931	.0010	.0006	75	62.26	2.22	.078	447	6.29
W-34	6.10	5.21	.591	.01268	.01506	.0602	1.038	.0007	.0004	75	62.26	2.22	.000	0	.0
W-35	33.55	25.99	.589	.01996	.02465	.0986	0.846	.0025	.0017	75	62.26	2.22	.584	3340	62.8
W-36	32.91	24.42	.575	.02200	.02757	.1103	0.756	.0024	.0014	77	62.24	2.16	1.083	6200	120.0
W-37	36.35	28.61	.646	.01431	.01676	.0670	1.24	.0009	.0005	77	62.24	2.16	.078	447	8.64
W-38	36.39	28.55	.648	.01390	.01621	.0648	1.29	.0005	.0001	77	62.24	2.16	.000	0	0.0
W-39	5.84	4.93	.579	.02656	.03401	.1360	.613	.0016	.0002	77	62.24	2.16	1.083	6200	120.0
W-40	6.05	5.14	.604	.02387	.03005	.1202	.694	.0015	.0004	77	62.24	2.16	.584	3340	64.5
W-41	6.22	5.31	.624	.01875	.02288	.0915	.911	.0011	.0004	77	62.24	2.16	.078	447	8.64
W-42	6.26	5.35	.629	.01940	.02376	.0950	.878	.0005	.0000	77	62.24	2.16	.000	0	.0

for tracer displacing air: $$\frac{\int_0^\infty \left(1-\frac{c}{c_0}\right)dt}{\frac{\epsilon V_P + V_E}{v}}$$

for air displacing tracer: $$\frac{\int_0^\infty \frac{c}{c_0}\,dt}{\frac{\epsilon V_P - V_E}{v}}$$

where ϵV_P is the volume available to gas flow in the packed section, V_E is the volume of the empty bottom section and v is the volumetric flow rate of the follow-up gas. The above ratios must be equal to unity for a perfect material balance. Since the free volume was known independently only for the dry bed, the material balance was calculated for the dry packing runs only.

The porosity of the irrigated packing can be calculated from the mean residence-time of the gas flowing through the irrigated portion of the bed (i.e., $\vartheta - \vartheta_D - \vartheta_E$) divided by the residence-time which the gas would require to flow through the same section of empty column $\frac{V_W}{v}$. This quantity is, therefore:

for tracer displacing air: $$\epsilon_W = \frac{\int_0^\infty \left(1-\frac{c}{c_0}\right)dt - \frac{\epsilon V_D}{v} - \frac{V_E}{v}}{\frac{V_W}{v}} = \frac{\vartheta - \vartheta_D - \vartheta_E}{\frac{V_W}{v}} \quad (58)$$

for air displacing tracer: $$\epsilon_W = \frac{\int_0^\infty \frac{c}{c_0}\,dt - \frac{\epsilon V_D}{v} - \frac{V_E}{v}}{\frac{V_W}{v}} = \frac{\vartheta - \vartheta_D - \vartheta_E}{\frac{V_W}{v}} \quad (58a)$$

where ϵ_w is the porosity of the irrigated packing, ϵV_D is the free volume of that portion of the column which remains dry and V_w is the empty volume of the irrigated portion. Again v refers to the volumetric flow rate of the displacing gas.

The Variance was evaluated as:

for tracer displacing air: $$\sigma^2 = \frac{2\int_0^\infty t\left(1-\frac{c}{c_o}\right)dt}{\left[\int_0^\infty \left(1-\frac{c}{c_o}\right)dt\right]^2}$$ (See Eq. (17), pp. 26)

for air displacing tracer: $$\sigma^2 = \frac{2\int_0^\infty t\,\frac{c}{c_o}\,dt}{\left[\int_0^\infty \frac{c}{c_o}\,dt\right]^2}$$ (Complementary to above)

The variance as calculated by the above method measures the mixing produced by the entire system. For the dry packing experiment, this includes a packed section and an empty section. According to the mixing stage model (see pp. 53 eq. (54) and (54a) the variance of the total system is:

$$\sigma^2 = \sigma_p^2\left(\frac{\vartheta_p}{\vartheta}\right)^2 + \sigma_E^2\left(\frac{\vartheta_E}{\vartheta}\right)^2 = \frac{1}{n_p}\left(\frac{\vartheta_p}{\vartheta}\right)^2 + \frac{1}{n_E}\left(\frac{\vartheta_E}{\vartheta}\right)^2$$

where σ, n and Θ are the variance, number of mixed stages and average residence-time for the total system and the subscripts P and E refer to the packed and empty portions respectively. Since we are interested in the variance or number of mixed stages for the packed section alone and we assume that the empty section is perfectly mixed,

$$\text{i.e.,} \quad \sigma_E^2 = \frac{1}{n_E} = 1$$

the corrected variance for dry packing runs is therefore:

$$\sigma_p^2 = \sigma^2 \left(\frac{\vartheta}{\vartheta_p}\right)^2 - \left(\frac{\vartheta_E}{\vartheta_p}\right)^2 \qquad (59)$$

Since the volumetric flow rate is the same in each section, equation (59) can be rewritten in terms of the free volume of the packed section ϵV_P and the volume of the empty bottom section V_E (.0065 cu.ft.)

$$\sigma_p^2 = \sigma^2 \left(\frac{\epsilon V_P + V_E}{\epsilon V_p}\right)^2 - \left(\frac{V_E}{\epsilon V_p}\right)^2 \qquad (59a)$$

For the irrigated packing experiments the packed bed was in turn made up of two sections: an irrigated portion and a portion remaining dry above the liquid distributor so that according to the mixing stage model (see pp. 53 eq. (54) and (54a)

$$\sigma^2 = \sigma_W^2 \left(\frac{\vartheta_W}{\vartheta}\right)^2 + \sigma_D^2 \left(\frac{\vartheta_D}{\vartheta}\right)^2 + \sigma_E^2 \left(\frac{\vartheta_E}{\vartheta}\right)^2$$

where the subscripts w, D and E refer to those portions of the column containing wet packing, dry packing and no packing respectively. Since in this case we are interested in the variance or number of mixed stages for the irrigated packed section alone and as before, we assume that $\sigma_E = \frac{1}{n_E} = 1$, the corrected variance for irrigated packing runs is, therefore:

$$\sigma_W^2 = \sigma^2 \left(\frac{\vartheta}{\vartheta_W}\right)^2 - \sigma_D^2 \left(\frac{\vartheta}{\vartheta_W}\right)^2 - \sigma_E^2 \left(\frac{\vartheta_E}{\vartheta_W}\right)^2 \qquad (60)$$

The number of mixed stages contributed by the dry section of packing above the liquid distributor n_D is estimated from the results of previous experiments on dry packing. Values of n_D used for various groups of runs are listed in Table VII.

The height of a perfectly mixed stage is obtained from the variance which after appropriate correction as described above is multiplied by the effective height of the packed section being considered, (See Eq. (48), pp. 49). The effective height of the bed was taken equal to the empty volume of the column occupied by packing, divided by the average cross sectional area of the column.

The dimensionsless group $\frac{uL}{2D_L}$ was estimated for dry packing runs by graphical comparison of actual recorder traces with the solution "A" of the diffusion equation giving the response to a step input (eq. (26), pp. 35). This was done by superimposing a graph of c/c_o vs t/θ as obtained from a given recorder trace over previously prepared graphs of solution "A" evaluated for increments of the group $\frac{uL}{2D_L}$ of 10 units from $\frac{uL}{2D_L} = 80$ to $\frac{uL}{2D_L} = 200$*. An example of this procedure is shown in Figure 34 where the points plotted were taken from the response curve for Run D-4 when tracer displaces air. The superimposed curves were calculated for $\frac{uL}{2D_L}$ equal to 120, 140, 160. The estimated value of $\frac{uL}{2D_L}$ for the experimental points was chosen to be 140.

---

* A tabulation of this data can be found in Appendix IV, Table XVIII, pp. 215

TABLE VII

NUMBER OF MIXED STAGES FOR DRY PACKING SECTION
ABOVE LIQUID DISTRIBUTOR

Run No.	Nominal Packing Diameter In.	Modified Peclet No. From Eq. (63b) pp. 120 $\frac{}{Pe''_L}$	Packing Porosity ϵ	Hydraulic Mean Diam. d_m	Height of Mixed Stage $H = \frac{2d_m}{Pe''_L}$	Equilavent Height of Dry Packed Section Ft.	Number of Mixed Stages For Packed Section Above Liquid Distributor N_D
W-1 through W-22	1/4	.338	.693	.00371	.0220	.45	20.4
W-23 through W-26	1/4	.338	.685	.00362	.0214	.45	21.0
W-27 through W-34	3/8	.338	.658	.00512	.0303	.45	14.8
W-35 through W-42	1/2	.338	.705	.00748	.0442	.45	10.2

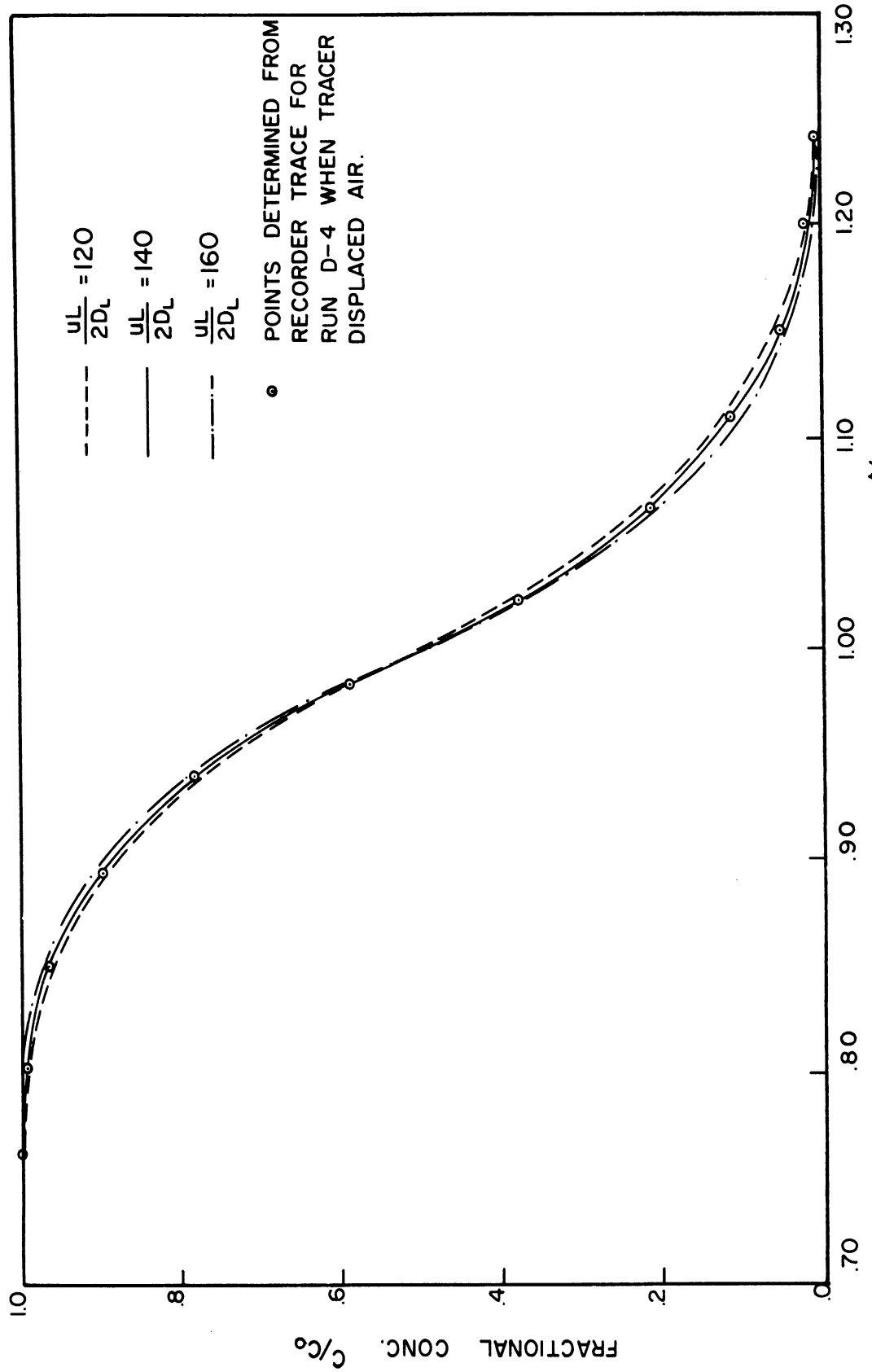

Figure 34. Estimation of the Dimensionless Group $\frac{uL}{2D_L}$ For Dry Packing Runs.

The Peclet Number is generally defined as:

$$Pe_L = \frac{du}{D_L} \tag{61}$$

using the relationship found earlier (Eq. (57), pp. 60) between the number of stages and the effective longitudinal diffusivity the Peclet number can be expressed as the ratio of the particle diameter with the height of a mixed stage.

$$Pe_L = \frac{2d}{L/n} = \frac{2d}{H} \tag{62}$$

The equation above is used to calculate the basic value of the longitudinal Peclet number. A modified Peclet number is also used in Chapter V for correlation purposes where the nominal particle diameter is replaced by other characteristic lengths.

The skewness of the time distribution function was evaluated for wet packing runs as a measure of the departure from uniform flow. This quantity is:

for tracer displacing air: $$\nu = \frac{3\int_0^\infty t^2\left(1-\frac{c}{c_o}\right)dt}{\left[\int_0^\infty\left(1-\frac{c}{c_o}\right)dt\right]^3} - \frac{6\int_0^\infty t\left(1-\frac{c}{c_o}\right)dt}{\left[\int_0^\infty\left(1-\frac{c}{c_o}\right)dt\right]^2} + 2 \tag{18}$$

for air displacing tracer: (complementary to above) $$\nu = \frac{3\int_0^\infty t^2\frac{c}{c_o}dt}{\left[\int_0^\infty\frac{c}{c_o}dt\right]^3} - \frac{6\int_0^\infty t\frac{c}{c_o}dt}{\left[\int_0^\infty\frac{c}{c_o}dt\right]} + 2$$

If the flow of gas through the column is not uniform, then:

$$2(\sigma^2)^2 \neq \nu$$

For an illustration of detailed calculations for the various quantities, a sample calculation for Run No. W-8 is given in Appendix III, pp. 199

CHAPTER V

DISCUSSION

Dry Packing

We examine first the reported results to seek a confirmation of the conclusions drawn from theoretical considerations and the validity of the experimental technique.

Material Balance

The first requirement of the step input technique is that the area bounded by the response curve from the time at which the step input in concentration is introduced must coincide with the time required for the gas to replenish itself through the system. The degree of agreement is given by the material balance listed in columns 13 and 28 of Table V, pp. 100. It may be observed that this quantity fluctuates about unity with a maximum deviation of $\pm$ 8%. The uncertainty of the flow rate measurements (the precision of the rotameter calibrations was about 3%) and the precision of reading the recorder traces (the recorder chart can be estimated within $\pm$ 1/2 line or 2.5%) with subsequent graphical integration give ample justification for the reported fluctuations of the material balance. We may thus conclude that the step input used gives the true response of the system. It may further be noted that if the time lag of the analyzer-recorder system did affect the response curves then the material balances would have to be consistently greater than one because of the additional delay of the output signal caused by the analyzer system and not due to the gas flow through the system. Thus both the normal sensitivity operation using helium as tracer and the high sensitivity operation are consistent on

this point.

Effect of Tracer Composition

The second point concerning the validity of the experimental technique was to discover whether the signal output was affected by changes in tracer composition or by the manner in which the step signal in tracer concentration was introduced.

From the preliminary experiments, some doubt was created on whether the use of pure helium would alter the shape of the response curves not only for the tracer displacing the air which was quite evident in Figure 23, pp. 87 but also for the air displacing the helium. Table VIII gives a comparison for analogous runs carried out with both 15% helium and pure helium as tracer.

From the variance for helium displacing air, we see that the discrepancy in the response curves is quite large and this can be explained by the convective effect already discussed on page 77. For the air displacing the helium, this effect should be non-existent however. Nevertheless, a comparison of the variance calculated from these response curves shows a significant difference for Runs D-2, D-7, D-9, D-20, and D-23 as compared with runs executed at similar volumetric flow rates but with 15% helium. Thus, some other effect concurs to increase the variance of the distribution. A plausible cause of the increased mixing may be found in the difference in line pressure necessary to obtain comparable volumetric flow rates for air and pure helium. Because of this difference it is possible that a certain amount of extraneous mixing takes place at the solenoid valve when the tracer flow is interrupted and replaced with air. At any rate, this point was

TABLE VIII

EFFECT OF TRACER COMPOSITION

Run No.	Nominal Packing Diameter, in.	Tracer Composition Vol. % H_e	Flow Rate cu.ft./sec.	Calculated Variance For Air Displacing Tracer	Calculated Variance For Tracer Displacing Air
D-1	1/4	15	.00519	.00773	.00778
D-2	1/4	100	.00521	.00903	.02971
D-6	1/4	15	.01703	.00714	.00713
D-7	1/4	100	.01501	.00835	.01824
D-8	1/4	15	.0435	.00763	.00746
D-9	1/4	100	.0458	.00890	.02179
D-18	3/8	15	.00429	.00630	.00620
D-21	3/8	15	.0652	.00606	.00716
D-20	3/8	100	.01865	.00654	.01513
D-23	3/8	100	.00970	.00620	.03998

not investigated further. Having noted the undesirable effect of the helium air system on both air and tracer response curves, it was decided to base all the subsequent conclusions on results obtained with 15% helium as tracer.

For the runs made using 15% helium, Table VIII shows no consistent difference between the value of the variance for air displacing helium and that for helium displacing air. Thus, both values of the variance were used in the subsequent treatment.

Relationship Between Number of Stages and Diffusion Coefficient

A third point which was verified experimentally is the relationship between the number of stages and the longitudinal diffusion coefficient. The average number of stages in series can be obtained directly as the inverse of the variance and is listed in Columns 15 and 30 of Table V, pp. 100 for displacing air and helium respectively. The group $\frac{uL}{2D_L}$ was estimated by means of solution "A" as described on page 105 and is listed in Columns 16 and 31 of the table mentioned above for air and helium respectively as the displacing gases. By comparing column 15 with 16, and 30 with 31, it can be seen that the agreement between these two quantities is within 10%. On considering that the uncertainty in the estimation of the group $\frac{uL}{2D_L}$ is probably not better than 10%, one may conclude that the relationship:

$$n \simeq \frac{uL}{2D_L} \tag{57}$$

is valid at least for the range investigated. This fact lends addition-

al proof to the validity of the step function technique for measuring longitudinal mixing because it is in substantial agreement with the theory (see pp. 55-62). Because the variance as calculated from the response curves was considered more precise than the estimation of the group $\frac{uL}{2D_L}$ it was decided to adopt the number of mixing stages or the inverse of the variance as a measure of the extent of mixing taking place in the column.

Effect of Bed Height, Correction For End Effects

Lastly, we may consider the consistency of the data with respect to bed height and end effects.

According to the correlation model in which the packed bed is considered as made up of a series of perfectly mixed stages, one might expect that the height of a mixed stage:

$$H = \frac{V}{nA} = \frac{L}{n} \qquad (48)$$

be independent of bed height.

A tabulation of the data showing the effect of the packing height on the variance and on the height of a mixed stage is given on the following page. The variance was corrected as described on page 104 to account for entrance effects produced by the bottom empty section. Table IX shows the variance and height of a mixed stage before and after correction.

Assuming that there is no effect of flow rate or packing porosity, the height of a mixed stage appears in fair agreement for both bed heights. Before correction the average of all the runs for

TABLE IX

EFFECT OF BED HEIGHT

		AIR DISPLACING TRACER				TRACER DISPLACING AIR			
Run No.	Effective Bed Height Ft.	Calculated Variance	Height of a Mixed Stage Before Correction Ft.	Corrected Variance	Actual Height of A Mixed Stage Ft.	Calculated Variance	Height of a Mixed Stage Before Correction Ft.	Corrected Variance	Actual Height of A Mixed Stage Ft.
D-1	3.42	.00773	.0265	.00712	.0244	.00778	.0267	.00707	.0242
D-3	3.42	.00760	.0260	.00709	.0242	.00776	.0266	.00726	.0248
D-4	3.42	.00750	.0257	.00699	.0239	.00746	.0259	.00694	.0238
D-5	3.42	.00602	.0206	.00541	.0185	.00660	.0226	.00604	.0207
D-6	3.42	.00714	.0244	.00661	.0226	.00713	.0244	.00659	.0225
D-8	3.42	.00763	.0262	.00713	.0244	.00746	.0256	.00694	.0238
D-10	3.42	.00665	.0228	.00609	.0208	.00642	.0220	.00584	.0200
D-11	3.42	.00742	.0254	.00690	.0236	.00695	.0238	.00641	.0220
D-12	4.45	.00508	.0226	.00477	.0212	.00478	.0213	.00445	.0198
D-13	4.45	.00530	.0236	.00500	.0223	.00452	.0202	.00419	.0187
D-14	4.45	.00507	.0226	.00476	.0212	.00591	.0264	.00564	.0252

the shorter bed gives a height of a mixed stage equal to .0247 ft. as compared with .0228 ft. for the longer bed. After correction, the averages are .0228 and .0214 for the shorter and longer bed respectively.

Comparison of the above data shows that the correction for the bottom empty section amounts to about 7-8% for the shorter bed and 5-6% for the longer bed. Consequently, while the height of a mixed stage for the two bed lengths before correction differs by 8%, the difference is only 6% after the end correction was applied. This type of behavior is expected if the correction is real. On this basis, we may conclude, therefore, that the height of a mixed stage is independent of column height. Moreover, the correction for the extraneous mixing introduced by the empty portion of the column, although small, appears justified.

Having established in the above discussion that the equipment and experimental technique yield reliable and consistent results, we wish to compare the present results with analogous data of previous authors. The discussion that follows also offers the basis for the overall correlation of the data.

Comparison with Previous Investigators

An extensive study of axial mixing for gases flowing through packed beds of spheres is reported by McHenry and Wilhelm /47/, who used a frequency response technique. Their findings can be summarized as follows:

1. The Peclet number calculated as $\frac{du}{D_L}$, where d is the spherical diameter and u is the interstitial velocity, is essentially independent of Reynolds number.
2. For 21 determinations of Peclet number in the Reynolds number range from 10 to 400, the mean Peclet number

was found to be 1.88. Expressed in statistical language, their reported result is:

$$Pr \quad (2.03 > \overline{Pe} > 1.73) = 95\%$$

where Pr is read, "the probability of" and $\overline{Pe}$ is the true mean of 21 determination.

3. No detectable effect of gas density was found for the two gas systems studied. These were, methane-nitrogen and hydrogen-nitrogen.

The data of these authors is represented in Figure 35 as a shaded band indicating the 95% confidence limits for the Peclet number. The data for the Raschig rings as obtained in the present work are listed in Table V, columns 19 and 34, and are also shown graphically in Figure 35. In this case, the Peclet number is calculated as the ratio of twice the nominal particle diameter to the height of a perfectly mixed stage and it is entirely analogous to the Peclet number used by McHenry and Wilhelm except that the nominal ring diameter is used in place of the diameter of spheres. The gross agreement between the two sets of data as shown by Figure 35 may be quite fortuitous because clearly there is little hydrodynamic relation between Raschig rings and spheres having the same diameter. However, Figure 35 serves to point out that the Peclet number is of the same order of magnitude in both sets of experimental data for both techniques of signal input, i.e., step function response and frequency response.

An analogous conclusion was also obtained by Ebach /18/ who has extensively studied axial mixing of liquids, packed beds of spheres and other packing shapes. The dotted line in the lower region of Figure

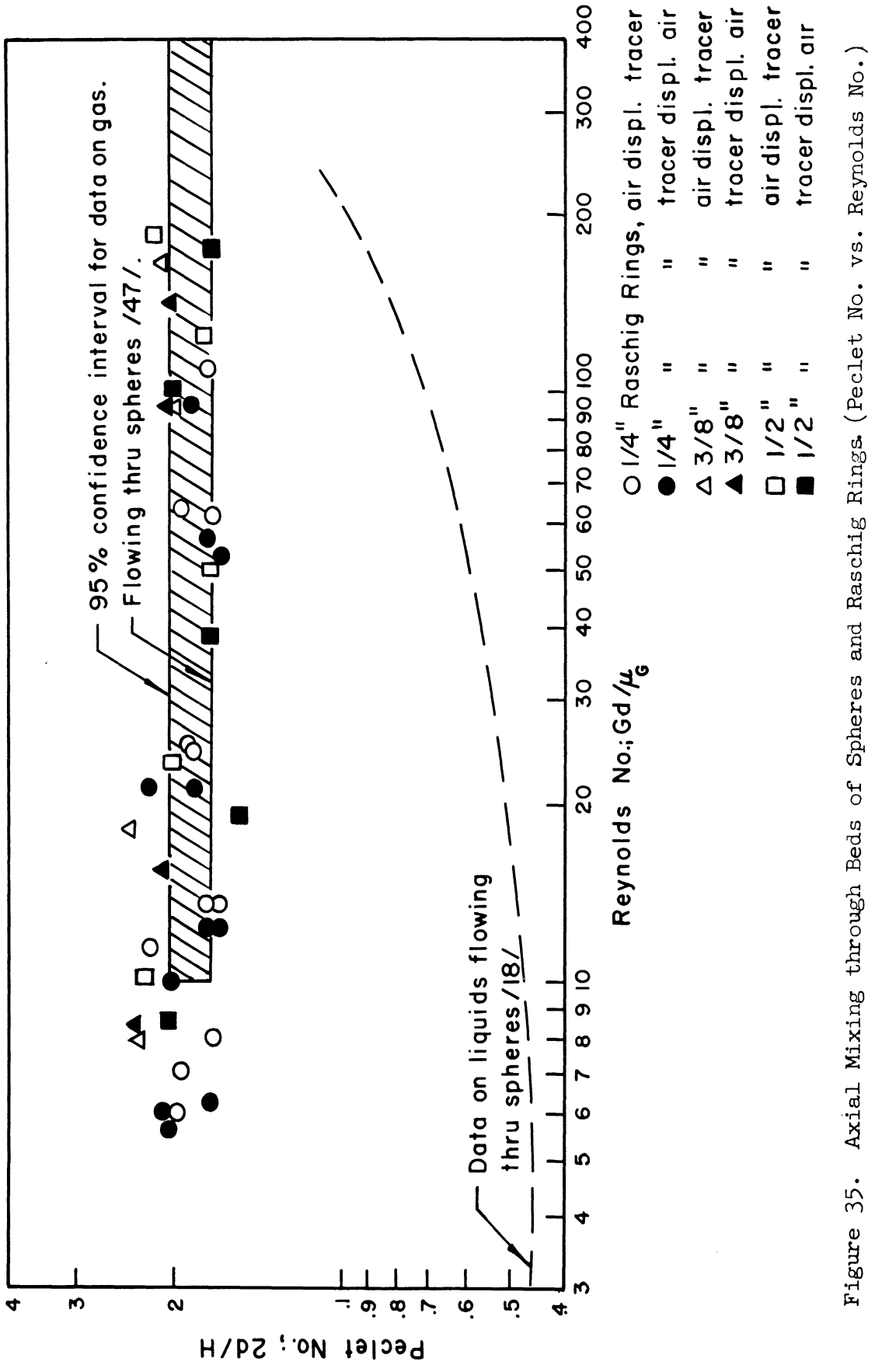

Figure 35. Axial Mixing through Beds of Spheres and Raschig Rings (Peclet No. vs. Reynolds No.)

35 is representative of data obtained in his experiments using two types of unsteady state techniques, i.e., transient and frequency response. Other data for liquids obtained by Danckwerts /13/ and Kramers and Alberda /38/ also fall in the neighborhood of the dotted line.

A statistical analysis of the data obtained on Raschig rings with the exception of Runs D-15, D-16 and D-17 on oriented packing, shows that a least squares straight line through the points plotted on Figure 35 has no significant slope. Thus, no apparent effect of Reynolds number in the investigated range is detectable. Therefore, the Peclet number can be expressed as the true mean of forty points and is found to be equal to $1.94 \pm .07$. In statistical language the foregoing can be expressed as:

$$\Pr\ (2.01 > \bar{Pe} > 1.87) = 95\%^{*} \qquad (63)$$

These results compare well with those of McHenry and Wilhelm, thus the principal objective of the first part of this work concerning the dry packing was reached.

Effect of Particle Diameter and Packing Orientation

In the preceding paragraph it was tacitly assumed that the Peclet number computed as the ratio of the nominal Raschig rings diameter to the height of the mixing stage was independent of particle diameter.

---

* In terms of height of a mixed stage we have:

$$\bar{H} = 1.03d \pm .07 \qquad (63a)$$

However, this dimension is seldom used to characterize Raschig rings. More frequently, the equivalent spherical diameter d_p (diameter of spheres having the same volume as the Raschig rings) is used /41/. Ebach /18/ employed this quantity in the study of axial mixing of liquid flowing through a bed of Raschig rings. For pressure drop through granular beds Kozeny /37/ suggested as hydraulic mean diameter the quantity:

$$d_m = \frac{\epsilon}{(1-\epsilon)S} = \frac{\epsilon}{a} \qquad (64)$$

where ϵ is the void fraction, S is the specific surface of the material and a is the surface area of the material in the bed. For spheres, this quantity is:

$$d_m = \frac{\epsilon d}{6(1-\epsilon)} \qquad (65)$$

Since the porosity for a packed bed of spheres varies about a value of 0.4, the value of d_m is approximately 1/10 of the actual diameter of the sphere.

To compare the suitability of each of these quantities in the correlation of the data, Table X was prepared.

On the basis of the foregoing results, it is apparent that the hydraulic mean diameter d_m is the best correlation parameter for the effect of particle size and porosity on Peclet number. Using the modified Peclet number computed with the above characteristic length, the results for 40 determinations can be summarized as follows:

$$Pr\left(.349 > \overline{Pe}'' > .327\right) = 95\% \qquad (63b)$$

TABLE X

CHARACTERISTIC LENGTHS FOR PECLET NUMBER CORRELATION

Nominal Particle Diameter In.	Particle to Bed Diameter Ratio d/dt	Number of Runs Using Random Packing	MEAN PECLET NUMBER $Pe_L = \frac{2d}{H}$	$Pe'_L = \frac{2dp}{H}$	$Pe''_L = \frac{2dm}{H}$
1/4	.0625	22	1.87	1.73	.331
3/8	.0938	8	2.18	2.04	.357
1/2	.1250	10	1.89	1.82	.335
Mean Value of Above Numbers.....			1.98	1.86	.340
Mean Square Deviation.....			.03006	.02543	.00043

Since no trend is detectable in the Peclet numbers of Table X with particle size irrespective of characteristic length used, one may assume that the variation of particle diameter to bed diameter ratio from .0625 to .1250 does not appreciably affect the longitudinal mixing.

The packing properties for all the dry runs listed in Table V are summarized in Table XI. As seen here, Runs D-15, D-16 and D-17 were performed with oriented packing. The orientation, visually very noticeable, was produced by flooding the column so that the packing was lifted by the severe pulsation in the gas flow and rearranged anew. The longitudinal mixing observed in this type of bed is appreciably greater than that for a bed packed as described on page 79 . Figure 36 gives a graphical comparison of the mean values of the Peclet number as determined for the random Raschig rings, the oriented Raschig rings and Wilhelm and McHenry's data for spheres.

Summary

1. The material balance for the step function technique employed in these experiments appears consistent with the precision of the measurements. The area bounded by the response curves can thus safely be used in the irrigated packing experiments as a measure of the volume of the system occupied by the gas.
2. Because of extraneous mixing effects detected when pure helium was used as the tracer stream, all subsequent work was limited to the use of 15% helium.
3. The relationship between number of mixing stages and diffusion coefficient is as predicted by the theory

TABLE XI

PACKING PROPERTIES

Runs	Nominal Particle d, In.	Surface of Particle In.^{2}	Packing Arrangement	Total No. of Particles	Bed Porosity ϵ	Surface Area Per Unit Vol. of Bed Q, Sq.Ft/Cu.Ft.	Hydraulic Mean Diameter $d_m = \frac{\epsilon}{a}$
D-1 through D-11	1/4	.375	random	21500	.693	187	.00371
D-12 through D-14	1/4	.375	random	28300	.685	189	.00362
D-15 through D-17	1/4	.375	oriented	22800	.666	199	.00335
D-18 through D-23	3/8	.767	random	9440	.660	129	.00512
D-24 through D-28	1/2	1.38	random	3880	.703	95.4	.00736

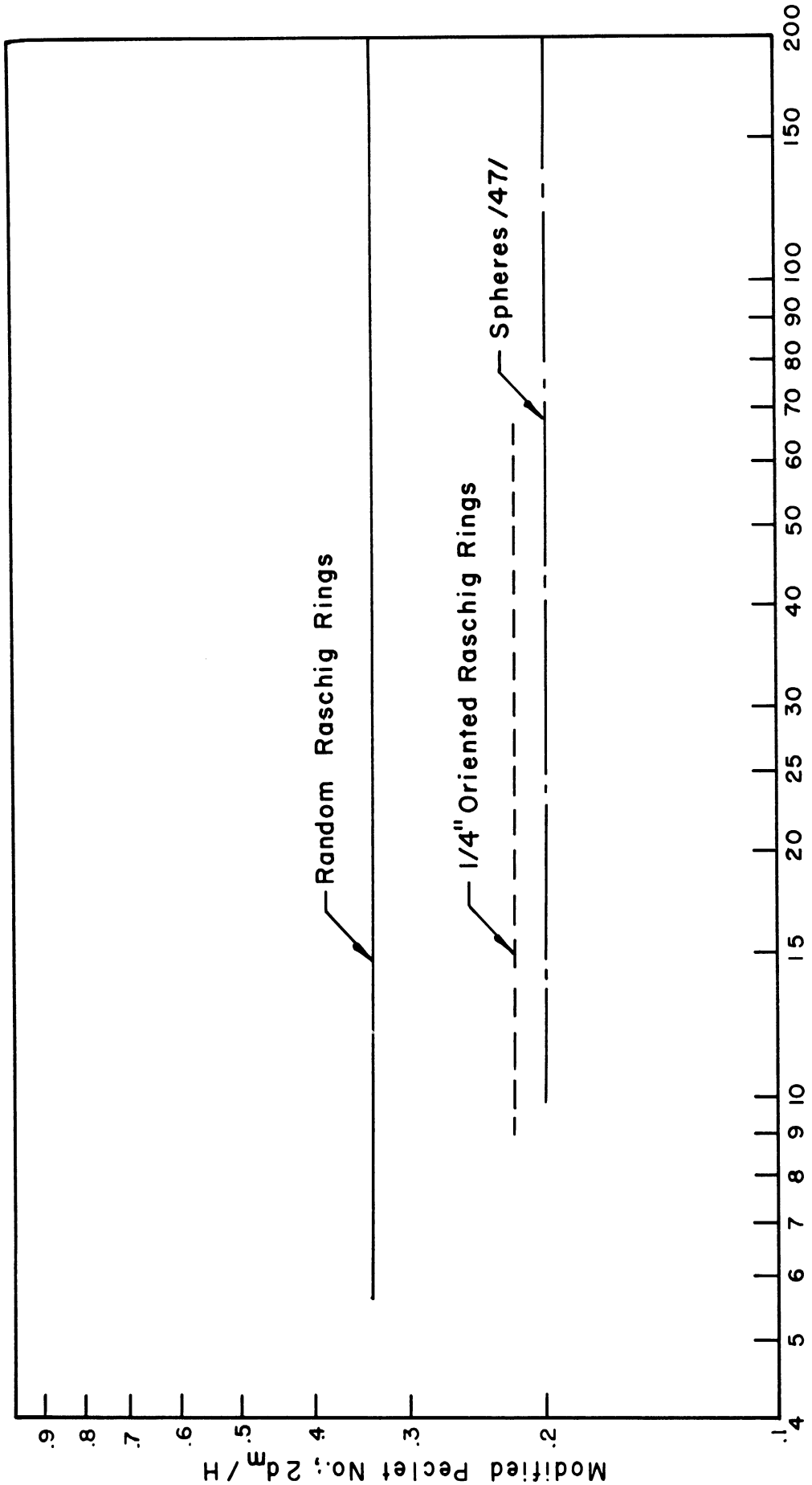

Figure 36. Axial Mixing for Gas Flowing through Beds of Spheres and Raschig Rings. (Average value of Modified Peclet No. vs. Reynolds No.)

(eq. (57), pp.60) at least in the range investigated when values of $\frac{uL}{2D_L}$ were fairly large.

4. The corrections for end effects introduced by the presence of an empty portion of column at the entrance of the bed appear adequate. On this basis, a similar correction will be used for irrigated packing experiments.

5. The longitudinal mixing for beds of Raschig rings as measured by the present data can be expressed as follows:

$$Pr \quad (2.01 > \overline{Pe} > 1.87) = 95\%$$

In order of magnitude of the Peclet number and in the precision of the data, this result is comparable with data of previous investigators.

6. The effect of particle diameter and packing porosity appears best accounted for by the use of the hydraulic mean diameter ($d_m = \frac{\epsilon}{a}$) as the characteristic length in the Peclet number. On this basis, the result of the overall correlation is:

$$Pr = (.349 > \overline{Pe}'' > .327) = 95\%$$

Irrigated Packing

Porosity of Irrigated Packing

As described on page 102, the fractional volume of the wet bed occupied by the gas or the porosity of the irrigated packing was calculated as the ratio of the actual residence-time of the flowing gas to the residence-time which the gas would have required to flow through the same section of empty column.

The wet porosity is presumably dependent on the mass flow rates and viscosities of the flowing streams, on the size and shape of the packing as well as on the surface tension of the liquid. The liquid used was water so that variations in surface tension do not enter into consideration for the correlation of the data. Raschig rings were the only packing shape investigated, thus:

$$\epsilon_w = F\ (G, W, \mu_G, \mu_w, d)$$

where ϵ_w is the porosity of the irrigated packing, G is the superficial mass flow rate for the gas, W is the superficial mass flow rate for the liquid, μ_G and μ_w are the viscosities for the liquid and gas respectively and d is the diameter of the Raschig rings. We choose for convenience to express the independent variables in the form of dimensionless Reynolds number and particle to bed diameter ratio. The influence of the variables on the data is shown in Figure 37 where the wet porosity is plotted versus the Reynolds number of the liquid. This Figure indicates that the liquid rate is the most important variable and that the relationship between the liquid rate and porosity may be

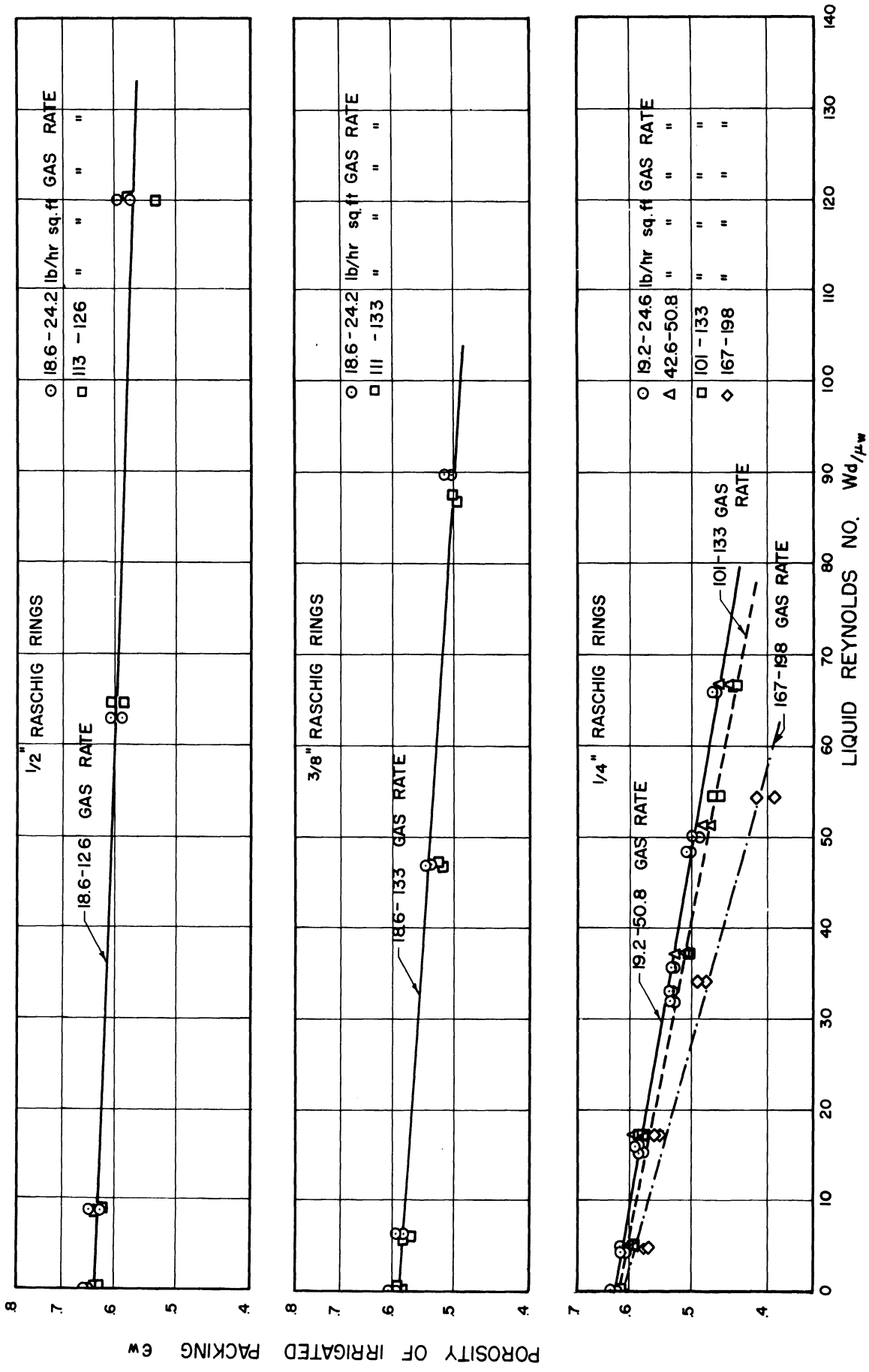

FIGURE 37. EFFECT OF LIQUID FLOW RATE ON POROSITY OF IRRIGATED BED.
(POROSITY vs LIQUID REYNOLDS NO.)

represented by the equation:

$$\epsilon_w = \epsilon_{wo}\, 10^{-MRe_w} \qquad (66)$$

where ϵ_{wo} is the intercept, M the slope of the lines shown in Figure 37 and Re_w is the Reynolds number for the liquid.

The constants ϵ_{wo} and M were determined by the method of least squares for the group of runs listed in Table XII. Each run in a group was performed with packing of the same size; also a statistical test showed that the effect of gas rate for each run in the same group could not be distinguished from the random scatter of the data. On this basis, the effect of gas rate was only noticeable for beds packed with 1/4" Raschig rings and for gas rates greater than 50 lb/hr ft.^{2} It can be noticed from Figure 37 that for 1/4" Raschig rings, an increase in gas rate above 50 lb/hr.ft^2 does not affect the value of the intercept ϵ_{wo}, whereas the value of the slope M increases rapidly at gas flow rates in the loading zone range (167 to 198 lb/hr. ft^2).

Considering the effect of particle diameter, it can be noted from the last column of Table XII that the ratio $\frac{\epsilon_{wo}}{\epsilon}$ is independent of particle diameter. Moreover, the slope M varies proportionally with the 2.31 power of the particle diameter as is clearly shown in Figure 39. On this basis, equation (66) was extended to comprise the effect of particle diameter as follows:

$$\frac{\epsilon_w}{\epsilon} = .900 \times 10^{-3.43 \times 10^{-6}\left(\frac{d}{dt}\right)^{2.31} Re_w} \qquad (67)$$

TABLE XII

COEFFICIENTS FOR POROSITY CORRELATION

RUN NUMBER	Nominal Particle Diameter d, Ft	Particle Diameter to Column Diameter d/dt	Range of Liquid Flow Rates lb/hr. ft.^{2}	Range of Gas Flow Rates lb/hr. ft.^{2}	Porosity of Dry Packing ϵ	Total Number of Points	COEFFICIENTS				
							ϵ_o	95% Confidence Interval	M	95% confidence Interval	$\frac{\epsilon_o}{\epsilon}$
W-1 through W-17 W-8, W-11, W-14, W-17 and W-20 W-23 through W-26	1/4	.0625	0-6190	19.2-50.8	.068-.693	32	.623	±.002	.00200	±.00003	.899-.909
W-9, W-12, W-15, W-18, W-21, and W-22.	1/4	.0625	0-6190	101-133	.693	12	.616	±.004	.00218	±.00015	.890
W-10, W-13 W-16, W-19	1/4	.0625	446-5050	167-198	.693	8	.612	±.012	.00315	±.00064	.883
W-27 through W-34	3/8	.0938	0-6200	18.6-133	.658	16	.589	±.005	.000783	±.00013	.896
W-35 through W-42	1/2	.125	0-6200	18.6-132	.705	16	.636	±.006	.000402	±.00013	.902

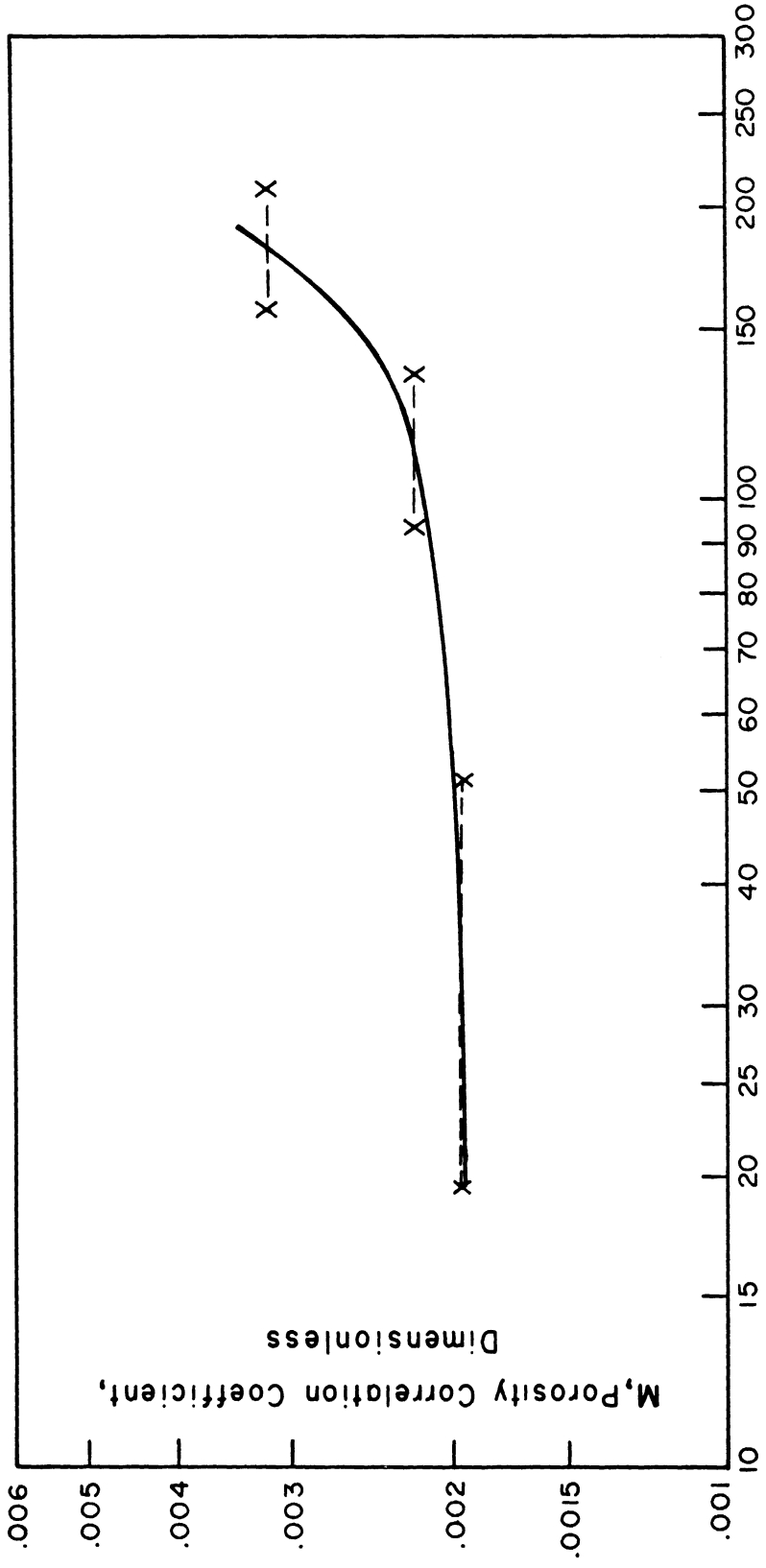

Figure 38. Effect of Gas Flow Rate on Wet Porosity for 1/4" Raschig Rings.

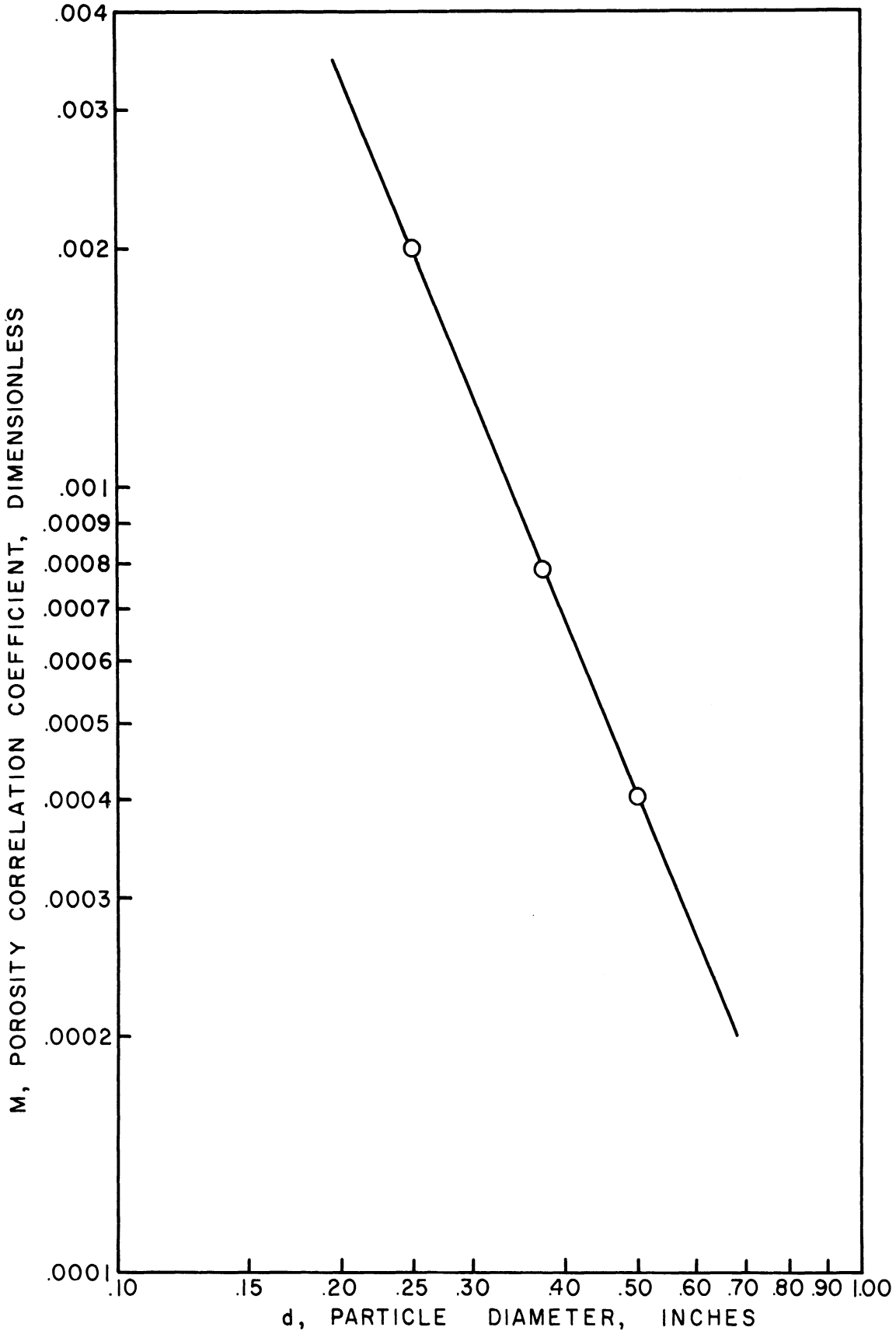

Figure 39. Effect of Particle Diameter on Wet Porosity.

The intercept ϵ_{wo} of the wet porosity versus liquid Reynolds number plot (Figure 37) represents the porosity of the wet packing at zero liquid flow rate, thus the difference $\epsilon_{wo} - \epsilon_w$ should correspond to the dynamic holdup. This quantity is compared in Table XIII with the amount of liquid drained from the column when both liquid and gas rates were suddenly interrupted. As seen here, such data was obtained only for nine runs in which 1/4" packing was used. However, the agreement is as good as could be expected from the precision of the experimental technique (see page 110). Since the measurements were made at the most drastic flow conditions, least favorable to experimental precision (Runs W-16, W-18, W-19 were conducted in the loading region), the agreement can be considered quite general. The values of $\epsilon_{wo} - \epsilon_w$ for 3/8" and 1/2" rings are also in fair agreement with operating holdup data of Shulman, Ullrich, and Wells /54/, and Jesser and Elgin /34/ considering slightly different packing dimensions, differences in porosities of the dry packing and differences in drainage time.

TABLE XIII

AGREEMENT BETWEEN LIQUID HOLD UP AND POROSITY
OF IRRIGATED PACKING

	Superficial Liquid Flow Rate W Lb./Hr. Sq.Ft.	Volume Of Liquid Collected From Draining Column Cu.Ft.	Dynamic Liquid Holdup	AIR DISPLACING TRACER			TRACER DISPLACING AIR		
				Superficial Air Mass Flow Rate G Lb./Hr. Sq. Ft.	Wet Porosity ϵ_w	$\epsilon_{wo} - \epsilon_w$	Superficial Tracer Mass Flow Rate G Lb./Hr. Sq.Ft.	Wet Porosity ϵ_w	$\epsilon_{wo} - \epsilon_w$
W-11	1590	.0118	.045	50.1	.585	.038	42.6	.590	.042
W-12	1590	.0118	.045	130	.573	.050	111	.580	.043
W-13	1590	.0146	.055	194	.560	.063	177	.557	.066
W-14	3340	.0286	.110	50.0	.518	.098	44.5	.520	.096
W-15	3340	.0279	.108	129	.504	.112	101	.515	.101
W-16	3340	.0336	.130	198	.491	.125	167	.480	.136
W-17	5060	.0385	.149	50.8	.484	.128	42.9	.477	.135
W-18	5050	.0380	.147	130	.462	.150	126	.467	.145
W-19	5050	.0540	.208	194	.399	.213	177	.412	.200

Correlation of Experimental Response Curves

In the study of the gas mixing through the irrigated packing, it was noted that as the liquid and gas flow rates were increased, the response of the system could no longer be correlated in terms of any of the models discussed in the theory in which uniformity of flow is assumed.

In absence of any information on the actual flow distribution in the column, the variance of the distribution of residence-times is still to be considered the most appropriate measure of the mixing process since it expresses the dispersion of the gas elements as they flow through the column.

The variance, however, says nothing about the relative weight that the various fractions of feed have on the total dispersion. Therefore, the skewness as defined by equation (12), page 20 was introduced.

In accordance with the series of mixing stage mechanism, as discussed previously (see page 50), the skewness is equal to $\frac{2}{n^2}$, provided that the flow through the column is uniformly distributed. It follows, therefore, that the difference between the skewness and twice the square of the variance should be a measure of the degree of departure from uniform flow. Figures 40, 41 and 42 give a graphical representation of the distortion in the response curves by comparing a theoretical curve for which the quantity $\nu - 2\sigma^4$ is zero with an experimental curve having the same variance but for which $\nu - 2\sigma^4$ is increasingly important.

The distortion as produced in the experimental curve appears to show that the "younger" elements of gas (i.e., those elements which have been in the system for a time less than the average) replace them-

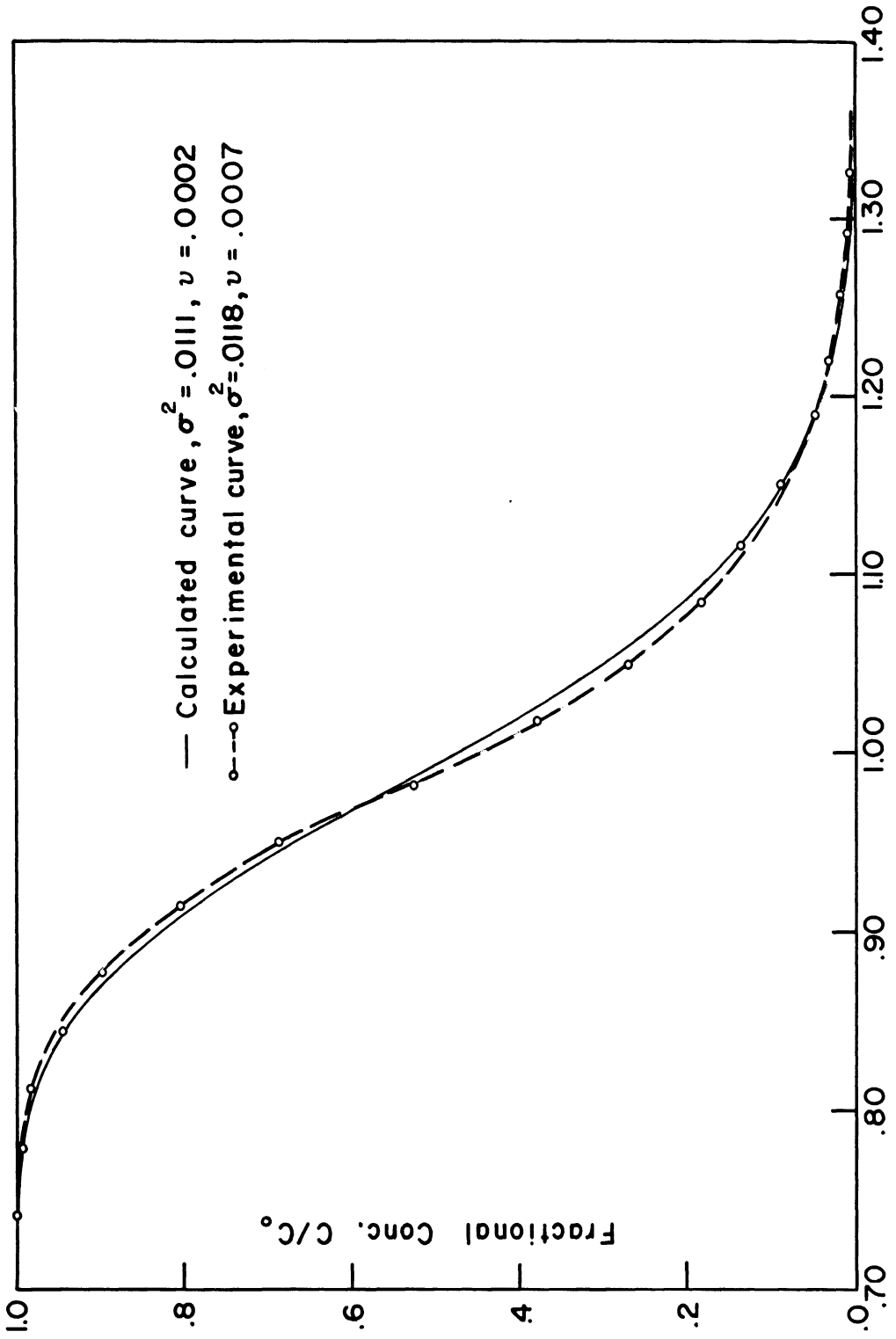

Figure 40. Response Curve Showing Departure from Uniform Flow ($v - 26^4 = .0003$) for Run No. W-8 Air Displacing Tracer.

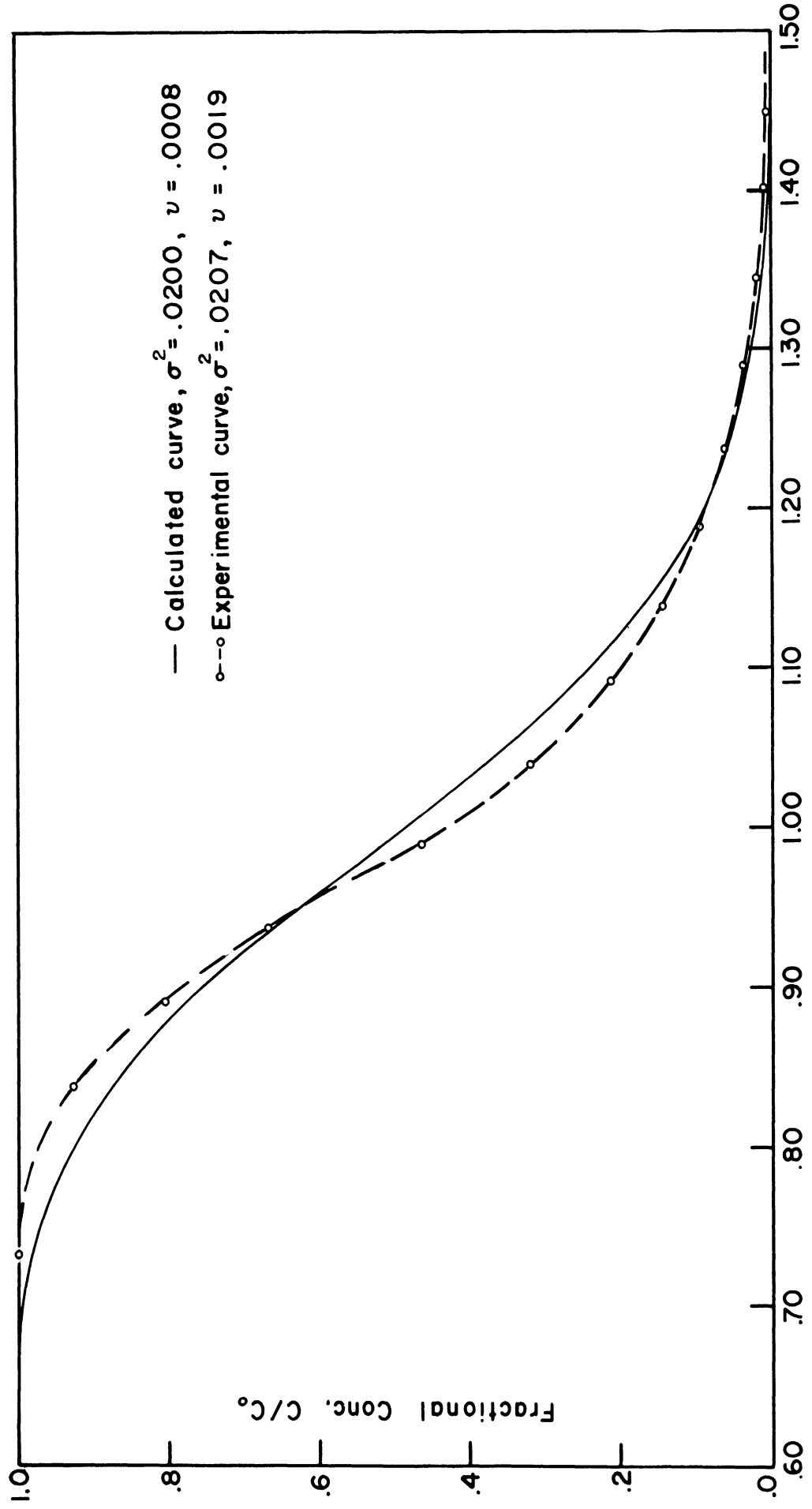

Figure 41. Response Curve Showing Departure from Uniform Flow ($v - 2\sigma^4 = .0011$) for Run No. W-18 Air Displacing Tracer.

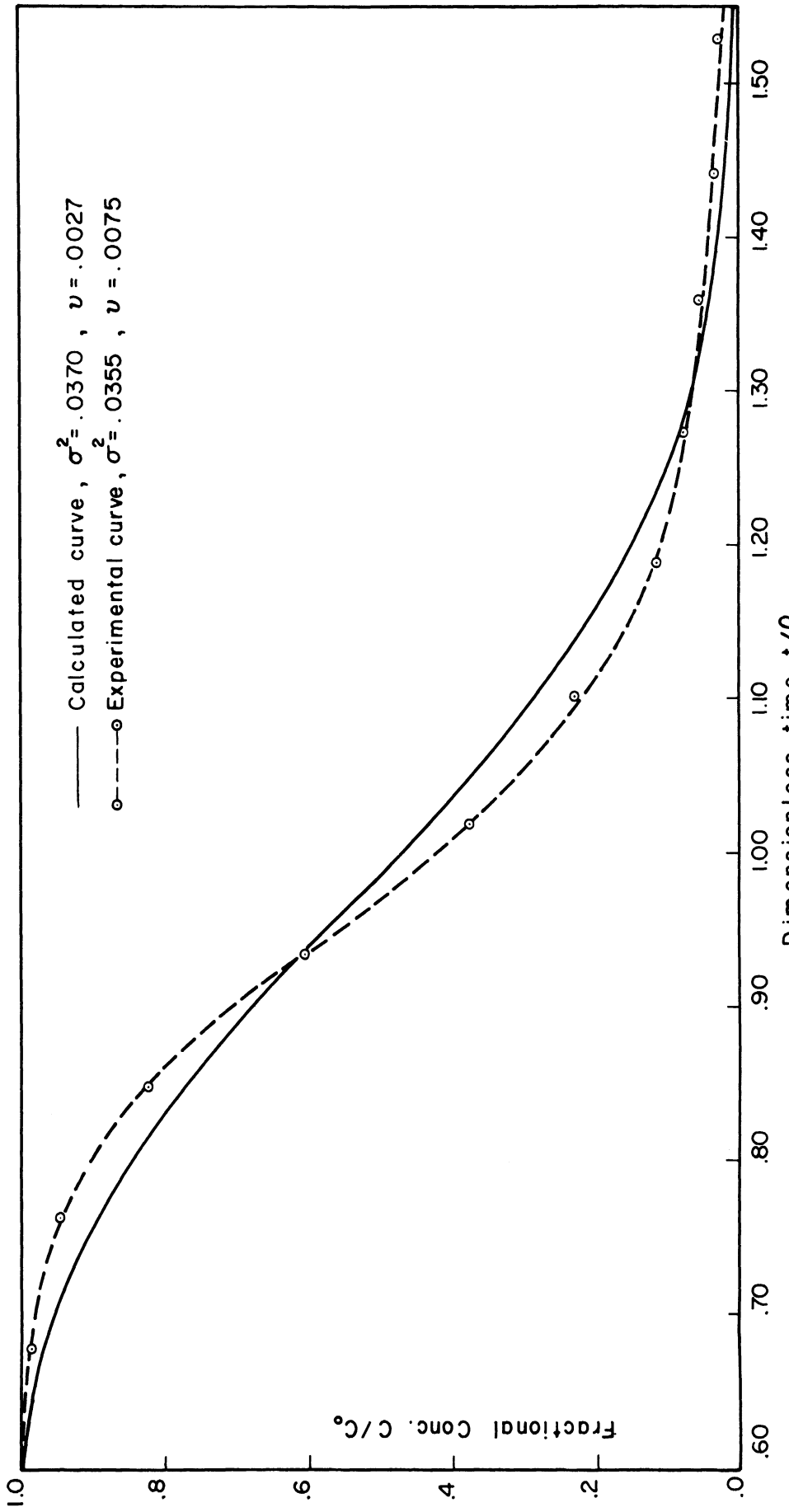

Figure 42. Response Curve Showing Departure from Uniform Flow ($v - 2\sigma^4 = .0050$) for Run No. W-19 Tracer Displacing Air.

selves at a greater rate, or in other words, have a greater probability of leaving the system than the "older" elements of gas. This, of course, is essentially what happens when we speak of "channeling" or "by-passing". What is generally meant by these terms is that a substantial fraction of the fluid entering the system finds its way out through inner channels or by-passes much before the average residence time has elapsed while the remaining feed is held back and appears at the effluent at a much slower rate.

By referring to Table VI, pp. 101 columns 21 and 36 where the quantity $\nu-2\sigma^4$ is listed, one can make the following observations:

1. The magnitude of this quantity is somewhat erratic. Although this is partly due to the difference of two numbers σ^4 and ν of the same order of magnitude both subject to inaccuracy in their numerical evaluation, it is evident that the departure from uniform flow may fluctuate greatly for any one run as evidenced by large variations in the value of $\nu-2\sigma^4$ when air displaces helium from corresponding values when helium displaces air.
2. The departure from uniform flow appears to be most affected by increase in liquid flow rates.
3. Gas flow rates appear also to have an effect but while this is not detectable for liquid loadings below 3,000 lb/hr.sq.ft. it becomes more pronounced above this flow rate.
4. The departure from uniform flow is greatest for Run No. W-19 where flooding was observed.

The above qualitative information gives some indication that the distortion in the response curve is perhaps due to the random occlusion of the gas flow channels by the liquid resulting in maldistribution of the gas through the bed. Consistent with this hypothesis, the departure from uniform flow would increase with liquid flow rates until a point is reached in which the liquid forms a continuous phase throughout the bed (flooding). When this occurs, the gas is compelled to lift the liquid from the pores in a pulsating manner and will proceed through the column in the form of bubbles rather than a continuous stream. Consequently, uniformity of gas distribution can hardly be expected.

The skewness of the response curve and the departure from uniform flow as measured by the difference $\nu - 2\sigma^4$ have only been introduced here to give a qualitative indication of the nature of the flow taking place in the bed. Having done so, we shall continue to use the variance of the distribution of residence-times curve as the only practical measure of the mixing process in the discussion that follows.

End Effects

The variance of the residence-times distribution was calculated from the recorded response curves as outlined on page 104. Because of the presence of end effects due to a section of dry packing at the upper extremity of the column and of an empty section at the bottom, the calculated variance was corrected as discussed on page according to equation (60).

The significance of the correction as applied to the variance is best understood when data on beds of different depths are compared.

This is done in Table XIV where data obtained from 1/4" Raschig ring beds having irrigated depths of 3 and 4 feet are compared under similar operating conditions. For each run, the height of a perfectly mixed stage as calculated from the variance before and after correction is reported. It may be readily seen that a more satisfactory agreement is obtained after the correction is applied. On this basis, the end effects are adequately accounted for and the bed depth is no longer considered as a pertinent variable.

Axial Mixing Correlation

In a manner analogous to the previous correlation for mixing of the gas through the dry packing, we choose to express the axial mixing in terms of the Peclet number defined as the ratio of twice the nominal particle diameter to the height of a mixed stage. Having concluded from the previous discussion that the height of a mixed stage is independent of bed depth, the remaining variables, the effects of which need to be considered in the correlation of the experimental data, are liquid and gas flow rates and particle diameter.

Gas and liquid flow rates are expressed as before, in terms of the respective Reynolds number and particle-to-bed-diameter ratio.

The data in question are shown in Figure 43 where the Peclet number is plotted versus the Reynolds number of the liquid at constant gas rate for all three different packing sizes investigated. The lines drawn through the points are calculated by the least squares method

TABLE XIV

EFFECT OF IRRIGATED BED DEPTH
ON LONGITUDINAL MIXING

Run Number	Nominal Packing Diameter - Inches	Depth of Irrigated Packing - L, ft.	Liquid Flow Rate W, lb./hr. sq.ft.	AIR DISPLACING TRACER					TRACER DISPLACING AIR				
				Air Flow Rate G lb./hr. sq.ft.	Calculated Variance σ^2	Height of Mixed Stage (Uncorrected) $H = \sigma^2 \times L$, ft.	Corrected Variance σ_W^2	Height of Mixed Stage (Corrected) $H_W = \sigma_W^2 \times L$, ft.	Tracer Flow Rate - G lb./hr. sq.ft.	Calculated Variance σ^2	Height of Mixed Stage (Uncorrected) $H = \sigma^2 \times L$, ft.	Corrected Variance σ_W^2	Height of Mixed Stage (Corrected) $H_W = \sigma_W^2 \times L$, ft.
W-4	1/4	3	446	23.6	.00793	.0238	.00854	.0256	20.2	.00803	.0241	.00869	.0261
W-23	1/4	4	447	24.2	.00612	.0245	.00650	.0260	19.3	.00620	.0248	.00659	.0264
W-1	1/4	3	1600	24.0	.01144	.0343	.01383	.0415	24.6	.01199	.0360	.01466	.0440
W-24	1/4	4	1600	24.2	.00896	.0358	.01038	.0415	19.3	.00950	.0380	.01113	.0445
W-2	1/4	3	3340	24.0	.01330	.0399	.01670	.0501	24.6	.01324	.0397	.01659	.0498
W-25	1/4	4	3340	24.2	.01133	.0453	.01372	.0549	19.3	.00999	.0400	.01179	.0472
W-3	1/4	3	5070	24.0	.01625	.0488	.02156	.0647	24.6	.01581	.04743	.02080	.0624
W-26	1/4	4	5070	24.2	.01357	.0543	.01701	.0680	19.3	.01193	.0477	.01462	.0585

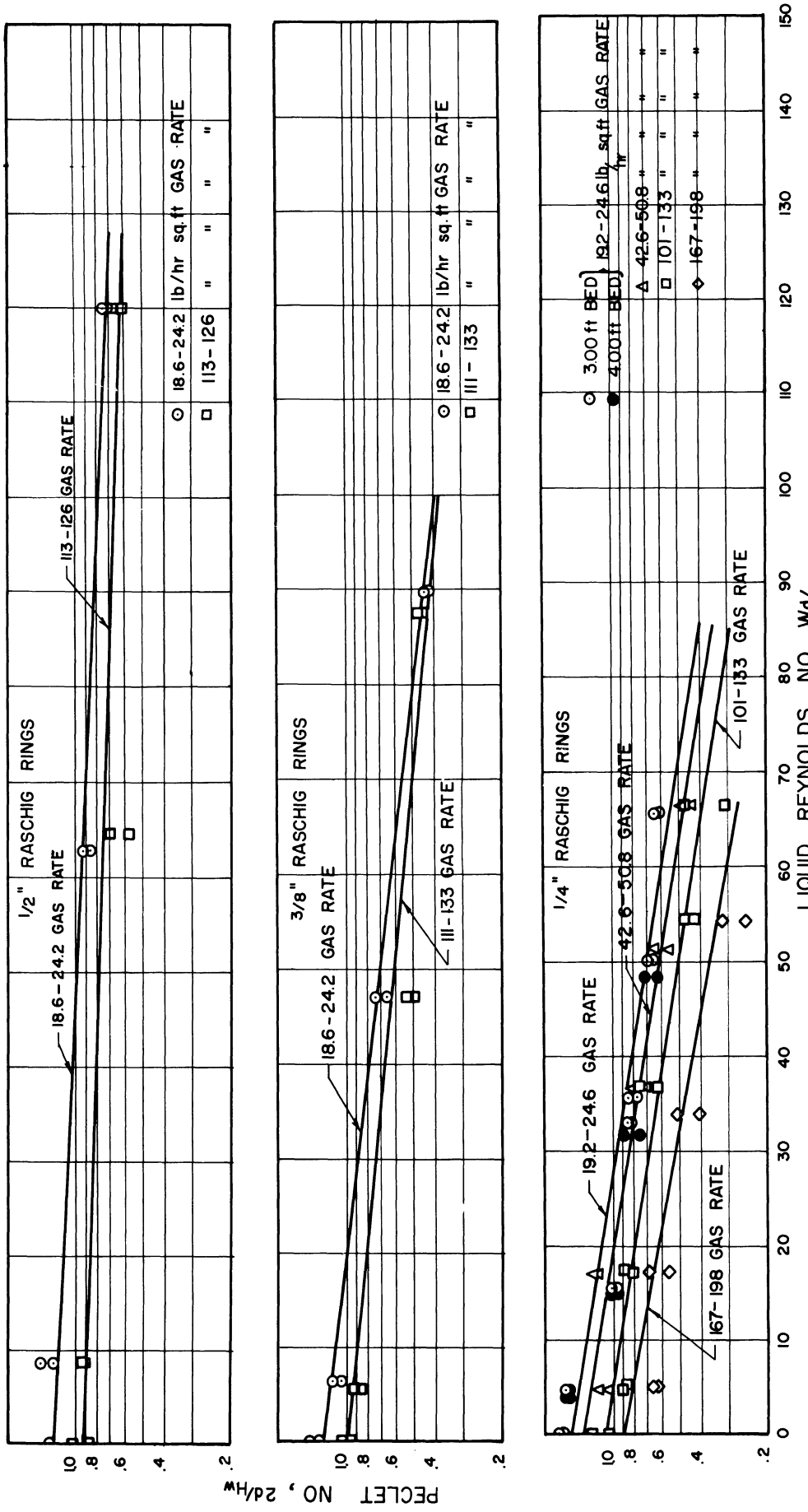

FIGURE 43. EFFECT OF LIQUID FLOW RATE ON PECLET NO. FOR IRRIGATED BED.
(PECLET NO. vs LIQUID REYNOLDS NO.)

according to the equation:

$$Pe_w = Pe_{wo}\ 10^{-NRew} \tag{68}$$

where Pe_w is the longitudinal Peclet number for the irrigated packing.

The constants Pe_{wo} and N were evaluated separately for nine groups of runs during each of which the bed properties, i.e., particle diameter and bed porosity were the same and the gas flow rate varied over a narrow range so that its effect could be assumed negligible. Table XV gives a list of the constants and the groups of runs for which they were evaluated. From an inspection of Figure 43, it appears that due to the scatter of the data, the slope of the least squares line, i.e., the constant N in Table XV can be considered independent of particle diameter. A statistical test of this hypothesis shows that the average value of N for all runs having the same particle size is no different than the least squares value for individual groups of runs reported on Table XV. Figure 44 shows the effect of particle size on the constant N of equation (68). A similar test indicates that the intercept Pe_{wo} of the Peclet number vs. Reynolds number plot can be considered a function of gas Reynolds number only. Figure 45 gives the relationship between Pe_{wo} and the gas Reynolds number.

From the foregoing assumptions, the data can be represented

TABLE XV

COEFFICIENTS FOR MIXING CORRELATION

RUN NO.	Nominal Particical Diameter In.	Range of Liquid Flow Rates lb/hr. ft.^{2}	Range of Gas Flow Rates lb/hr. ft.^{2}	Average Gas Reynolds No.	Total Number of Points	COEFFICIENTS			
						P_{Wo}	95% Confidence Interval	N	95% Confidence Interval
W-1 through W-7	1/4	0-6190	19.2 - 24.0	10.8	14	1.528	±.030	.0069	±.0013
W-23 through W-26	1/4	447-5070	19.3 - 24.2	10.4	8	1.500	±.064	.0079	±.0038
W-8, W-11 W-14, W-17 and W-20	1/4	446-6190	42.6 - 50.8	22.2	10	1.334	±.038	.0068	±.0017
W-9, W-12 W-15, W-18 W-21, W-22	1/4	0-6190	101 - 133	58.2	12	1.072	±.035	.0067	±.0014
W-10, W-13 W-16, W-19	1/4	446-5050	167 - 198	87.7	8	.895	±.053	.0079	±.0027
W-27 through W-30	3/8	0-6200	18.6 - 24.2	15.3	8	1.265	±.032	.0053	±.0009
W-31 through W-34	3/8	0-6200	111 - 133	87.9	8	.979	±.045	.0041	±.0013
W-35 through W-38	1/2	0-6200	18.6 - 24.2	20.5	8	1.254	±.021	.0020	±.0004
W-38 through W-42	1/2	0-6200	113 - 126	117.5	8	.928	±.060	.0014	±.0012

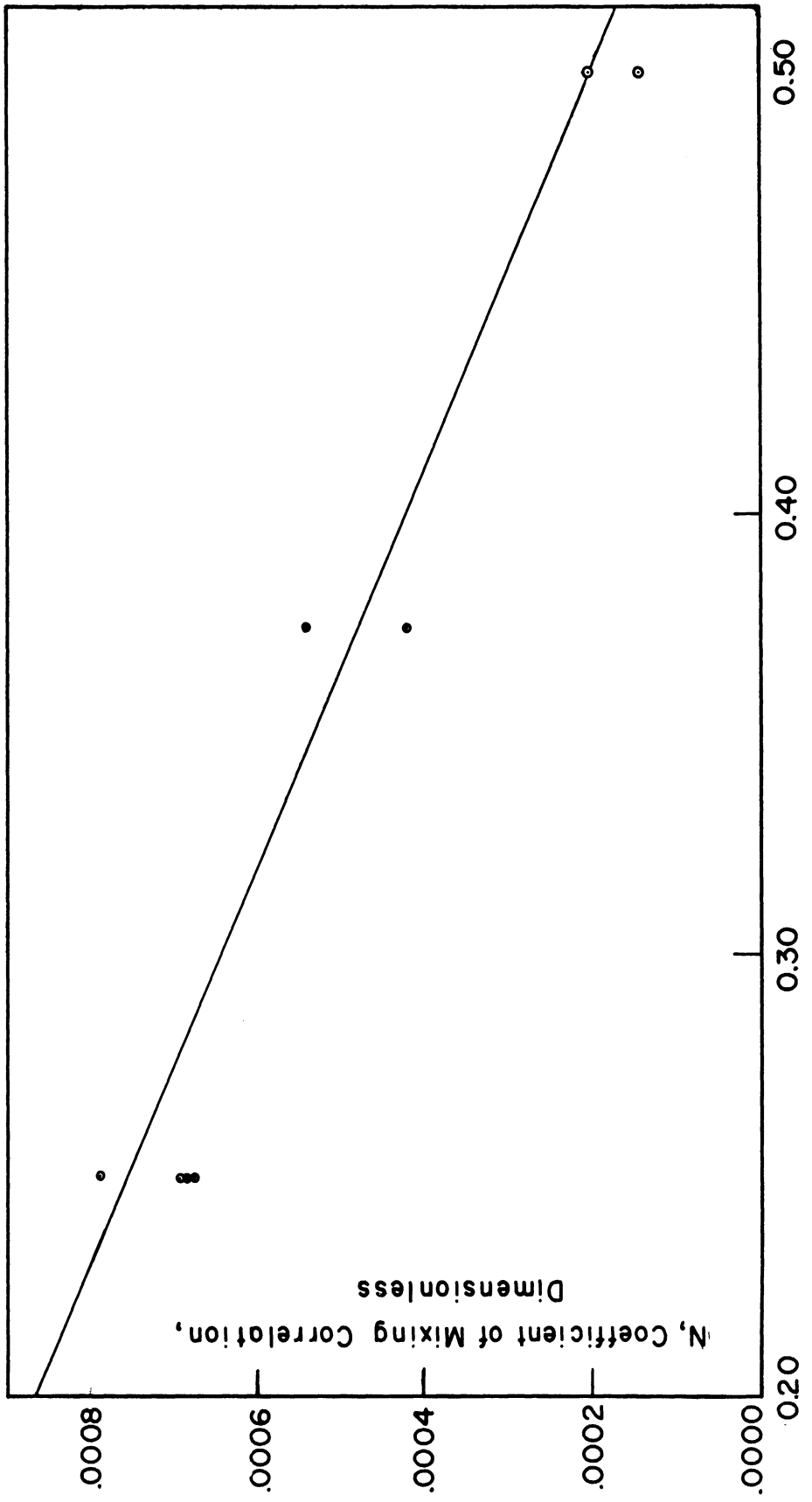

Figure 44. Effect of Particle Diameter on Longitudinal Mixing.

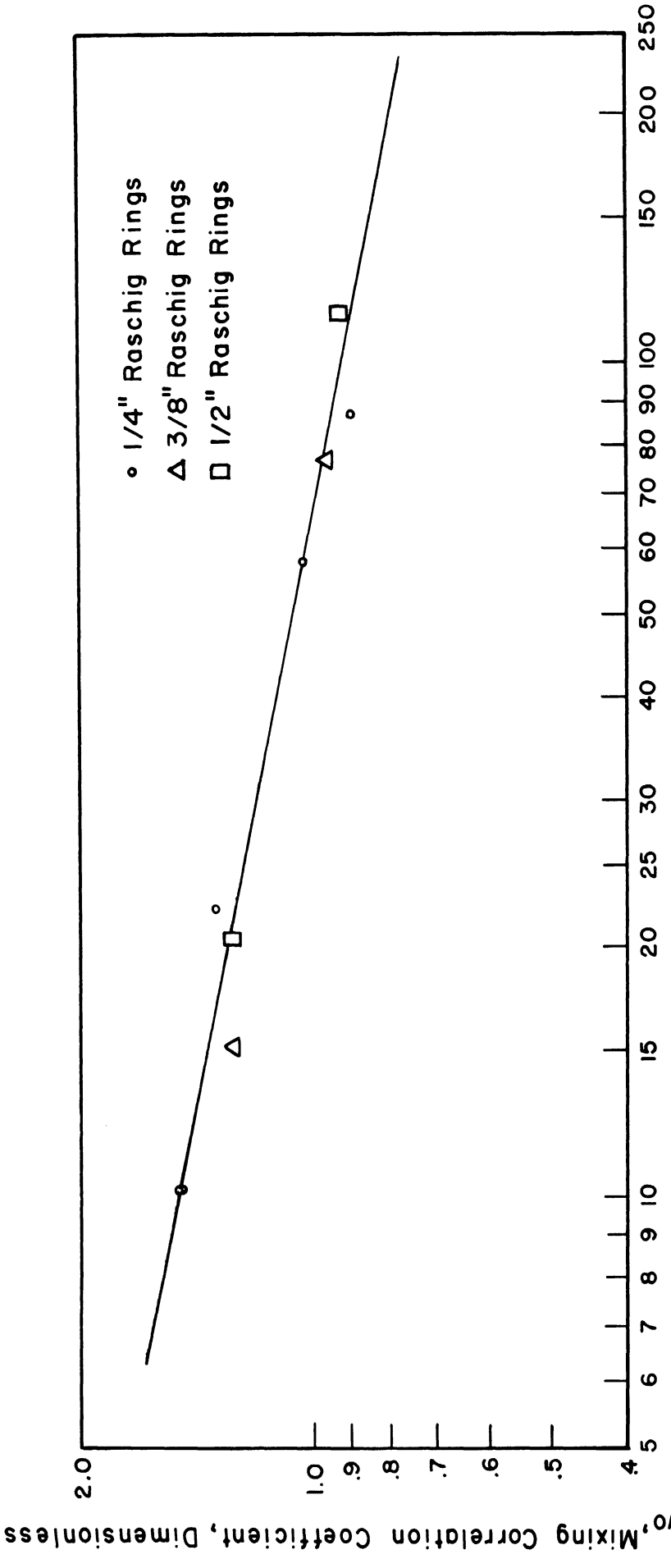

Figure 45. Effect of Gas Flow Rate on Longitudinal Mixing.

by the equation:

$$Pe_w = 2.4\ (Re_G)^{-.20}\ 10^{-(\ .013\ -\ .088\ \frac{d}{dt}\ )Re_w} \qquad (69)$$

Equation (67) can also be written in terms of the height of perfectly mixed stages:

$$H_w = .83d\ (Re_G)^{.20}\ 10^{(.013\ -\ .088\ \frac{d}{dt}\ )Re_w} \qquad (69a)$$

Interpretation of Mixing Data

If one uses the series of perfectly mixed stages model to interpret the results pertaining to the mixing taking place in the bed, one observes that the height of a mixed stage is smaller for dry packing than it is for wet packing. Since the height of a mixed stage is, as seen in the dry packing correlation, proportional to the particle diameter, one may postulate that as the liquid descends on the packing, it envelops several packing elements to form larger aggregates, thus

increasing the apparent diameter of the particles or in an equivalent manner, increasing the height of a mixed stage H. Consistent with this interpretation, equation (69a) shows that H increases with liquid flow rate.

An idea of the validity range of equation (69) is given by Figure 46 where the average Peclet number for dry Raschig rings is compared with data on irrigated packing. The line for wet packing calculated from equation (69) for a liquid flow rate equal to zero is representative of all three packing sizes used in the experiments. It is apparent that equation (69) cannot be used to extrapolate mixing data for Reynolds number much less than ten since from what we remarked before, one would expect the Peclet number for wet packing to remain always below that for dry packing. The lower line shows 1/4" packing data for a liquid flow rate from 5050 to 5070 lb/hr.sq.ft. The points on the extreme right of this line are for Run W-19 which was conducted under flooding conditions. One may infer, therefore, that in the flooding region, equation (69) yields higher values of the Peclet number than those observed.

A more interesting but highly speculative interpretation of the Peclet number may be given by assuming that the ratio of hydraulic mean diameter to height of a mixed stage is a constant. As seen from Table X page 123, this is quite true generally for dry packing. We may assume, therefore:

$$Pe''_L = Pe''_W = \frac{2\overline{\epsilon}}{H} = \frac{2\overline{\epsilon}_W}{H_W} = \text{Constant}$$

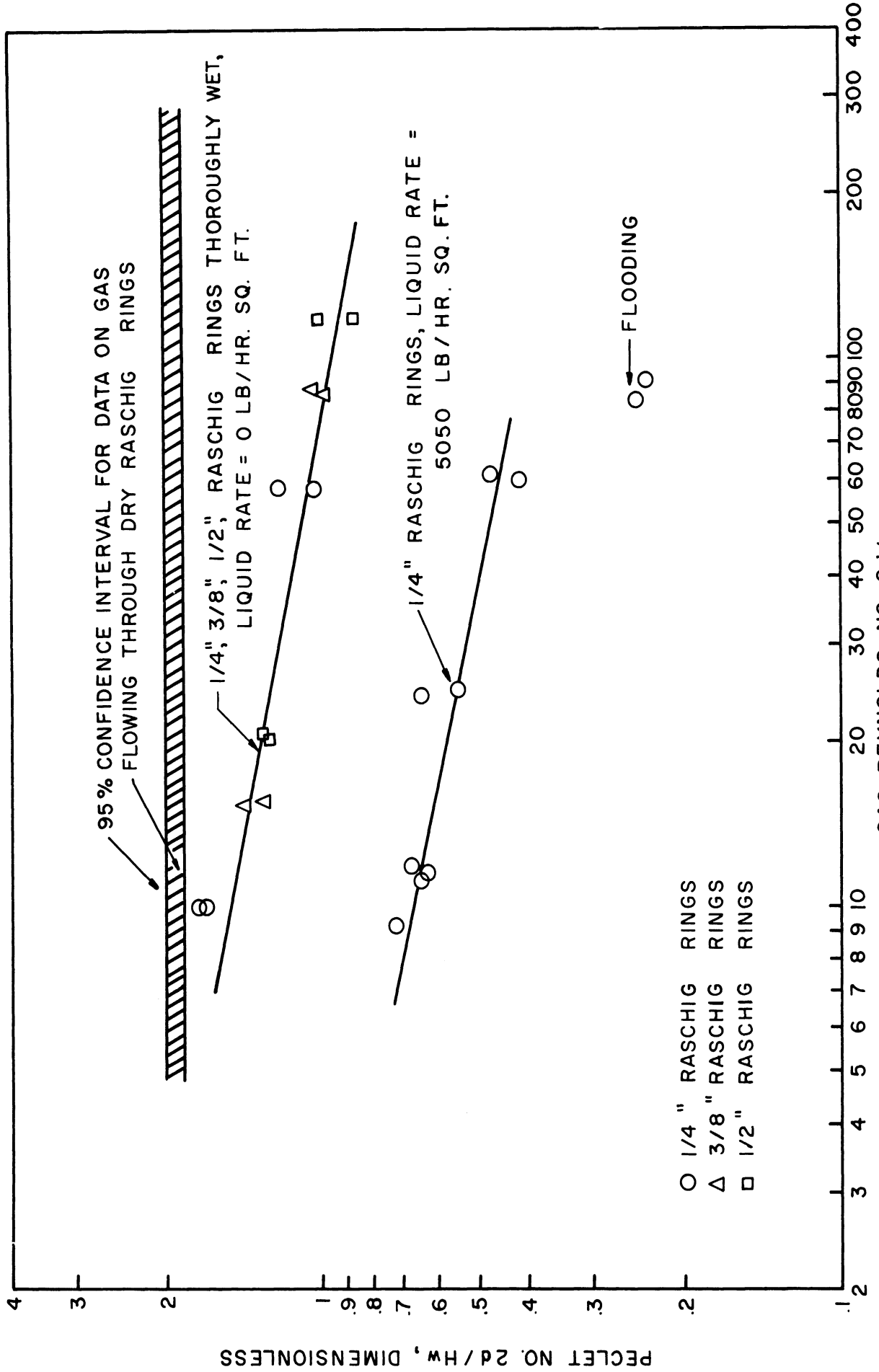

Figure 46. Longitudinal Mixing for Gas Flowing through Irrigated Beds of Raschig Rings.

Accordingly, by dividing equation (69a) by H as given by equation (63a) pp. 119 we find that:

$$\frac{H_w}{H} = \frac{\epsilon_w}{\epsilon} \times \frac{a}{a_w} = 0.81\ (Re_G)^{0.20}\ 10^{(0.013 - 0.088\ \frac{d}{dt})\ Re_w} \qquad (70)$$

so that the ratio of total wet packing area to dry area is obtained by dividing equation (67) pp. 128 by (70):

$$\frac{a_w}{a} = 1.11\ (Re_G)^{-0.20}\ 10^{-\left[0.013 - 0.088\ \frac{d}{dt} \quad -3.43 \times 10^{-6}\left(\frac{d}{dt}\right)^{-2.31}\right] Re_w} \qquad (71)$$

Equation (71) although highly speculative, indicates that the wetted area would decrease rapidly with liquid flow rate and at faster rate, in fact, than the porosity of the wet packing. In addition, the rate of decrease in area is much more pronounced for the smaller size packing than it is for larger sizes. The wetted area could also be affected, but to a lesser extent by the gas Reynolds number. This may be due to the fact that higher gas flow rates tend to make the liquid-packing aggregate more compact so that it presents less surface area to gas flow.

The cumulative result of these effects is to reduce the wetted surface area in inverse proportion of the particle size so that the area of the packed bed exposed to gas flow may, at high liquid flow rates, be larger for large packing sizes than for the smaller packing. Figure 47 shows the relationship between the total area of the bed in contact with flowing gas as estimated by equation (71) together with estimates of effective mass transfer area /22/, /45/, /62/. The uncertainty of data on effective mass transfer area is illustrated by the low and high values reported for 1/2" Raschig rings. The data of Mayo, Hunter and Nash /45/ obtained by measuring the colored surface area of Raschig rings made of paper over which water containing a red dye was circulated appear in line with the total surface area as given by equation (71). In fact, one would expect the mass transfer area to be only a fraction of the total surface area exposed to gas flow and that the former increases with increasing liquid flow rates so that the two quantities approach each other asymptotically.

It is possible that the area which the bed presents to liquid flow is more directly related to the effective mass transfer area. If the reasoning followed in the derivation of equation (71) is valid, (this could be verified by obtaining mixing data on other packing shapes) then the surface area which the bed presents to gas flow could be evaluated by a study analogous to the present one for the liquid phase.

Comparison With Previous Investigators

In connection with the previous discussion, it is interesting to compare the present data on the gas phase mixing with the results reported in graphical form by Kramers and Alberda /38/ on a number of

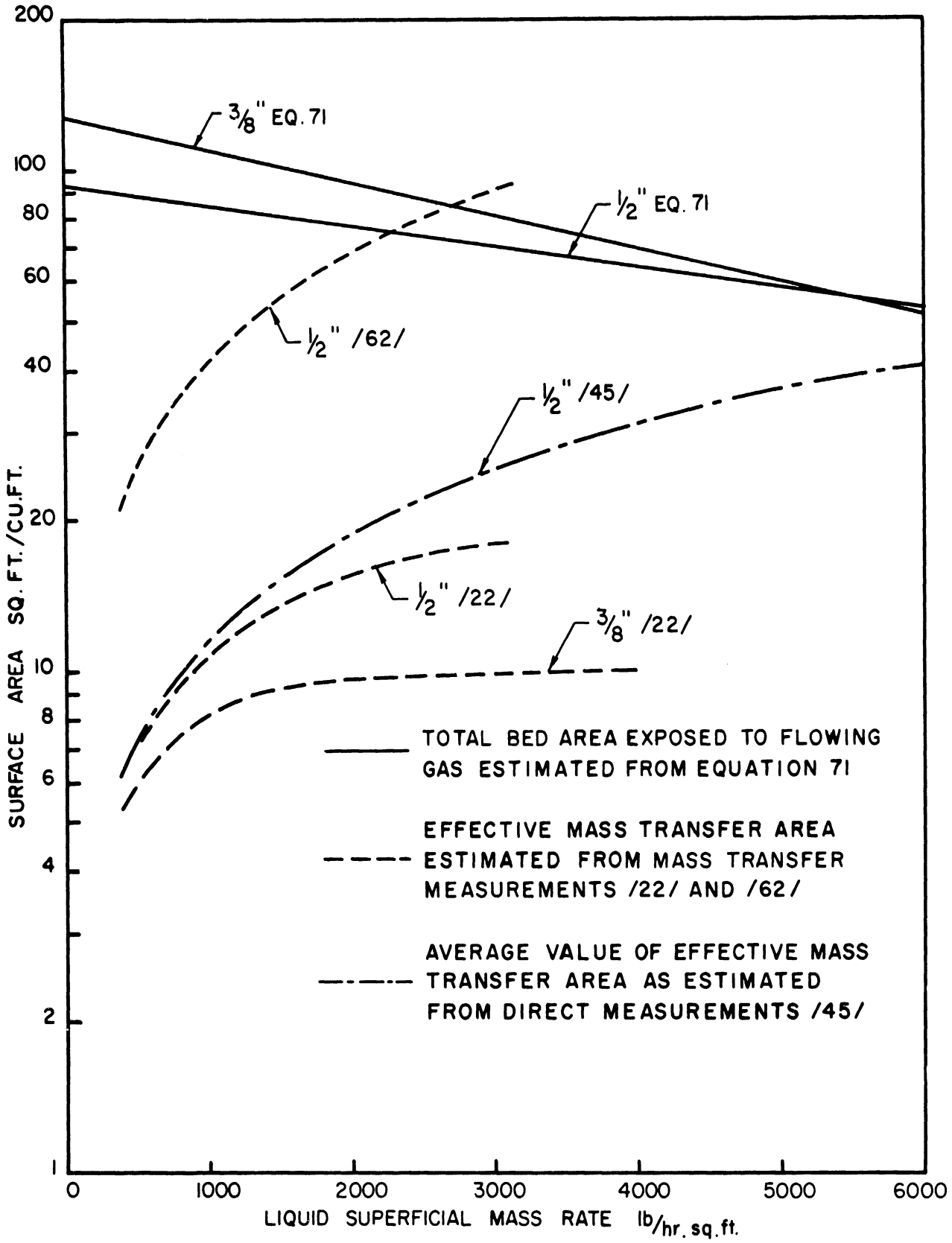

Figure 47. Total Bed Area Exposed to Flowing Gas and Effective Mass Transfer Area as Function of Liquid Flow Rate.

experiments in which the mixing of water running over 10mm. Raschig rings in an absorption column with a countercurrent air flow was measured by frequency response.

Figure 48 shows the Peclet number for the gas as measured in the present work for 3/8" rings (closest dimension to 10mm) with analogous Peclet numbers for the liquid as estimated roughly from the graphical data reported by the above authors. It is apparent from this Figure that while mixing in the gas phase increases both with liquid and gas rates, in the liquid phase instead, mixing decreases with increasing liquid rates. The results on the liquid phase have to be accepted with some reservation because of their scarcity and because Kramers and Alberda do not give details about the experimental technique used. However, they seem to show that according to the discussion of the previous paragraph, the area which the bed presents to the flow of liquid does, indeed, behave in a similar manner to the effective mass transfer area.

Another interesting aspect of this comparison is that according to Figure 48, the Peclet number and, thus the height of the mixing stage for both phases is of the same order of magnitude in the practical range of liquid flow rates. This fact may have some importance in greatly simplifying the interpretation of mass transfer data as we briefly discuss in the next section.

Lapidus' data on countercurrent flow of liquid and gas over spheres and porous pellets /39/ is not sufficient to be used for comparisons of the sort shown previously.

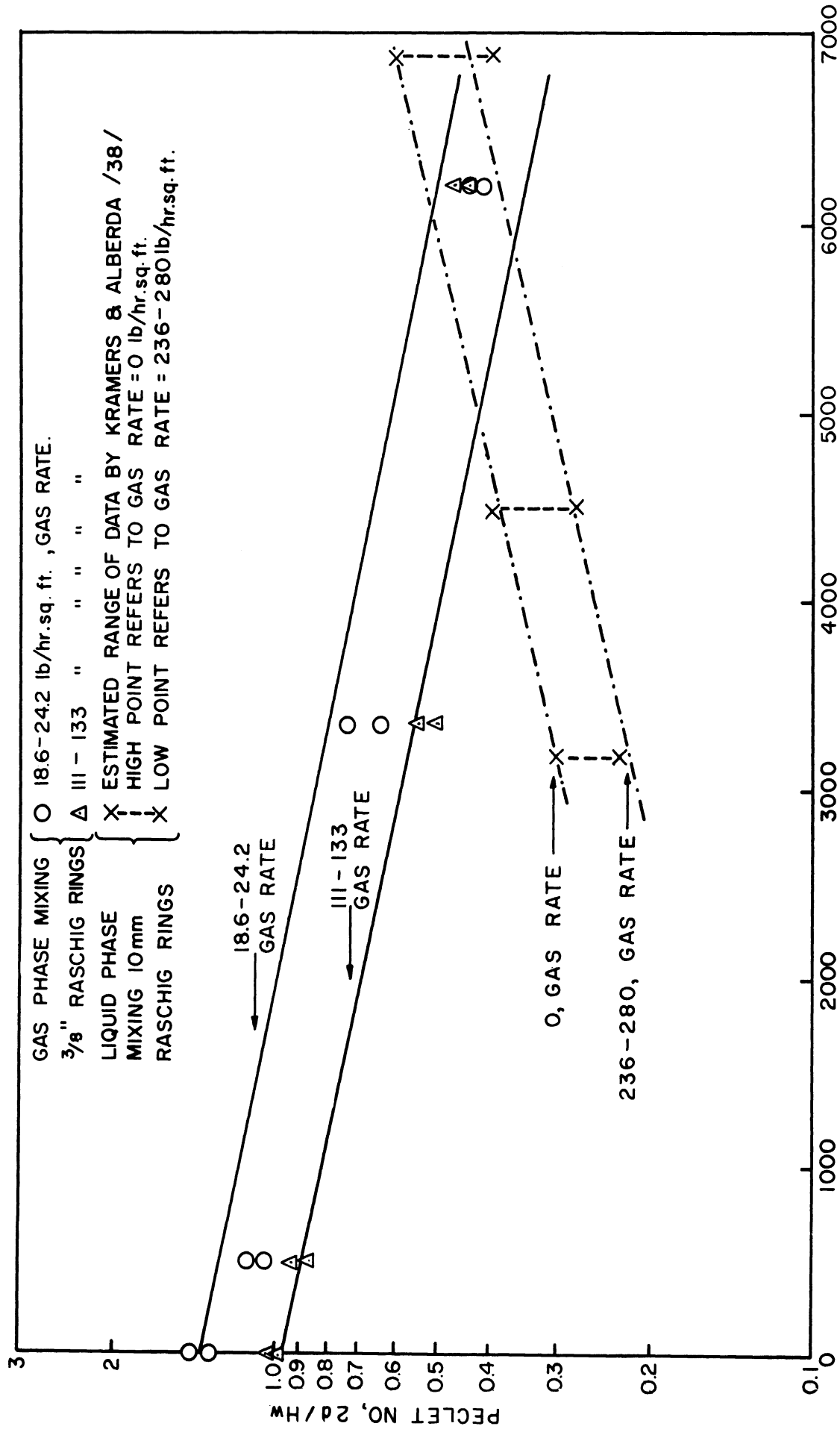

Figure 48. Peclet Number for the Liquid and Gas Phases Flowing Counter Currently through a Packed Bed of Raschig Rings.

Significance Of Time Distribution Data As Applied To Mass Transfer

It is interesting to speculate on the significance of the mixing stage concept in interpreting the exchange of mass taking place between the liquid and gas stream in the packed absorber. If the gas and liquid phase effectively undergo a series of complete mixing through discrete intervals of bed (a perfectly mixed stage), the rate of renewal of the fluid through the stage might have some relationship with the rate of surface renewal as visualized in the modern penetration theory of mass transfer.

The penetration theory originally conceived by Higbie /32/ and later developed by Danckwerts /11/, /14/, supposes that turbulence generated in both flowing streams extends to the mass transfer surface so that there is a constant renewal of both surfaces. Consequently, the rate of absorption in each phase would depend upon the time distribution of the elements of surface. Depending on what distribution function one assumes for the liquid and gas surface, one obtains various expressions for the liquid and gas film transfer coefficients respectively. Danckwerts suggests that the time distribution function for elements of surface is of the form:

$$\Psi(t) = \psi e^{-\psi t}$$

where ψ is the fractional rate of surface renewal. This equation is identical in form to the rate of change of concentration in a perfectly mixed stage where ψ is now the rate of renewal of the fluid contained in the stage $\frac{v'}{V'}$. Hanratty /31/ in a recent study of mass and momentum transfer of fluid with a solid boundary found that an analogous time distribution for the elements of fluid in contact with the wall

permitted an accurate prediction of the concentration profile in the fluid.

Danckwerts has also pointed out/11/ that mass transfer data from actual packed beds of Raschig rings may be rationalized by supposing that the time distribution of the elements of surface area is distorted to favor relatively higher rates of replacement of the "younger" elements of surface. A phenomenon of this kind (see page 134) has actually been observed in the course of this research.

It is possible, therefore, that the residence-time distribution data of the kind presented in this work may be of value in the interpretation of mass transfer data. In this case, and in the event that the penetration theory gives a sufficiently accurate representation of the mass transfer process in packed beds, simple measurements of mass transfer and chemical reaction rates as occurring through a stagnant surface and distribution of residence-time data would be all that is required in the prediction of gas and liquid film coefficients.

SUMMARY

1. The porosity of the irrigated bed for which no other method of measurement is presently known is calculated from a knowledge of the mean residence-time of the gas and the corresponding volumetric flow rate. For flow conditions up to loading, the porosity of the irrigated bed is correlated by equation (67) pp. 128

2. For liquid loadings above 3000 lb/hr. sq. ft. the experimental response curves can no longer be satisfactorily correlated by assuming uniform flow through the column. This condition is apparently brought about by "channeling" or "by-passing" of the gas through the irrigated bed. While the variance is still the most appropriate measure of the extent of mixing, the difference between the skewness and twice the square of the variance gives a measure of the deviation from uniform flow.

3. The presence of an empty portion of column at the entrance of the bed and of a dry packing portion above the liquid distributor is accounted for by a correction analogous to the one used for dry packing. On this basis the depth of the packed bed does not affect the height of a perfectly mixed stage.

4. The axial mixing through the bed as expressed by the Peclet number is dependent on liquid and gas flow rates as well as particle diameter as expressed by equation (69) pp. 147

5. Since the height of a mixed stage (see eq. (69a) pp. 147) increases markedly with liquid flow rates, one may postulate that as the liquid descends on the packing, it envelops several packing elements to form larger and larger obstacles to the flow of gas.

6. If one assumes that the ratio of hydraulic mean diameter to the height of a mixed stage is constant, one may obtain information on the area of the wet packing exposed to the gas flow as given by eq. (71) pp. 150.

7. Comparison of the present data with results reported by Kramers and Alberda/38/ shows that while mixing in the gas phase increases both with liquid and gas rates, in the liquid phase instead, mixing decreases with increasing liquid rates. In the practical range of flow rates the height of a mixed stage for both phases is of the same order of magnitude.

8. It is possible that residence-time distribution data of the kind presented in this work may be of value in the application of the Higbie - Danckwerts penetration theory of mass transfer.

Recomendations

In the previous discussion we have seen that there is an appreciable amount of mixing occurring in the longitudinal direction for the gas phase flowing through irrigated packing. This may have considerable effect on processes of simultaneous absorption and chemical reaction especially for the final exposure of the gas where presumably the conversion for the gas phase is fairly large. In addition, the large dispersion and the poor distribution of the gas in the loading and flooding region as revealed by the experimental response curves are perhaps the major factors responsible for the poor performance of packed absorbers in this operating range.

The brief account given of the consequences which are derivable from a knowledge about residence-times distribution of the flowing streams has served to point out the desirability of an extensive study of the liquid running over the packing. The existing evidence seems to show that the extent of mixing in both phases is of the same order of magnitude. Since minor changes in the magnitude of the mixing parameter (i.e., variance, height of mixing stage or diffusivity) do not greatly affect the overall behavior of the system, one may hope to simply apply the penetration theory of mass transfer to a system as complex as a packed absorber.

Moreover, the mixing in the liquid phase appears to increase with decreasing flow rates. This is rather interesting since, accordingly, it would imply a restricted flow region for most efficient operation of an absorber.

Lastly, we wish to recall that the characterization of the residence-times distribution by means of the moments of the distribution is believed to be most general since it is not restricted to any one specific correlation model. While the computation of these moments from experimental concentration-time records is rather tedious since it involves numerical methods of integration, we strongly suggest that automatic methods of computation be applied to the output of the continuous analyzer. If this suggestion is workable, it would enable the experimenter to analyze a large number of data and to obtain all the desired moments of the distribution with the same uniform degree of accuracy.

It is hoped that the present work has furnished the student of "rate processes" a glimpse of the numerous possibilities offered by transient response as a method of chemical engineering experimentation, and that the increased interest in this field may serve in the long range to adequately resolve scale-up and automation problems in the chemical industry.

Conclusions

By the use of unsteady state experiments, the present research has resulted in the evaluation of gas holdup and distribution of residence-times spent by the elements of the gas stream flowing through an irrigated bed of Raschig rings.

Dry packing experiments served to verify that the mean residence-time, as obtained from recorded concentration-time response curves can be used to calculate the volume of the bed occupied by the gas. On this basis, the porosity of the irrigated bed for which no other method of measurement is presently known is calculated from a knowledge of the mean residence-time of the gas and the corresponding volumetric flow rate. For flow conditions up to leading, the porosity of the irrigated bed is correlated by equation (67), pp 128.

The variance of the residence-time distribution was used as a measure of the logitudinal mixing of the gas phase flowing through the bed. This quantity obtained from the recorded response curves for dry packing was compared with various mixing models. The relationship between the variance σ^2, the number of perfectly mixed stages n and the effective diffusivity coefficient D_L is:

$$\sigma^2 = \frac{1}{n} \simeq \frac{uL}{2D_L}$$

Two bed depths were studied to evaluate the magnitude of end effects on the overall response. On the basis of the series of perfectly mixed state model, an adequate correction for end effects was obtained.

For a dry bed of Raschig rings, the ratio of the height of a mixed stage to the nominal packing diameter is essentially a constant at least in the investigated range of gas flow rates. For irrigated packing, the height of a mixed stage is both affected by liquid and gas flow as expressed by equation (69a) pp. 147.

APPENDIX I
Solution "A"

The problem in terms of longitudinal diffusion and superimposed plug flow is given by eq. (21) pp. 34 which is transcribed here:

$$\frac{\partial c}{\partial t} = -D_L \frac{\partial^2 c}{\partial^2 x} + u \frac{\partial c}{\partial x}$$

The boundary conditions for a step input in concentration from 0 to c_o for a packed bed of infinite extent assuming continuity of fluid concentration at the inlet are (see Chapter III pp. 34-38):

(1a) $c(0,t) = c_o$

(2a) $\lim_{x \to \infty} c(x,t) = 0$

(3a) $c(x,0) = 0$

taking the Laplace transform of eq. (21)

(1-AI)

$$s\bar{c}(x,s) - c(x,0) = D_L \bar{c}_{xx}(x,s) - u\bar{c}_x(x,s)$$

and the boundary conditions become:

1-a') $\bar{c}(0,s) = \frac{c_0}{s}$

2-a') $\lim_{x \to \infty} \bar{c}(x,s) = 0$

3-a') $c(x,0) = 0$

applying 3-a') to eq. (1-AI) we get:

$$\bar{c}_{xx}(x,s) - \frac{u}{L}\bar{c}_x(x,s) - \frac{s}{D_L}\bar{c}(x,s) = 0 \qquad \text{(2-AI)}$$

Eq. (2-AI) is an ordinary differential equation, the general solution of which is:

$$\bar{c}(x,s) = \phi e^{\left(\frac{u}{2D_L} + \frac{\sqrt{u^2/4D_L + s}}{\sqrt{D_L}}\right)x} + \chi e^{\left(\frac{u}{2D_L} - \frac{\sqrt{u^2/4D_L + s}}{\sqrt{D_L}}\right)x} \qquad \text{(3-AI)}$$

where φ and χ are arbitrary functions of s since $\bar{c}(x,s)$ is bounded, (condition 2-a') φ must be zero also to satisfy condition 1-a'):

$$\chi = \frac{c_0}{s} \qquad \text{(4-AI)}$$

thus, the solution of equation (2-AI) is:

$$\bar{c}(s) = \frac{c_o}{s} e^{\left(\frac{u}{D_L} - \frac{\sqrt{u^2/4D_L + s}}{\sqrt{D_L}}\right)x} \qquad (5\text{-AI})$$

to find the inverse transform we write eq. (5-AI) in the form:

$$\frac{\bar{c}(s)}{c_o} = \frac{1}{s} e^{\frac{ux}{2D_L}} \cdot e^{\frac{x\sqrt{u^2/4D_L + s}}{\sqrt{D_L}}} \qquad (6\text{-AI})$$

the inverse transforms are:

$$\mathcal{L}^{-1}\left\{\frac{e^{\frac{ux}{2D_L}}}{s}\right\} = e^{\frac{ux}{2D_L}} \mathcal{L}^{-1}\left\{\frac{1}{s}\right\} = e^{\frac{ux}{2D_L}} \qquad (7\text{-AI})$$

$$\mathcal{L}^{-1}\left\{e^{\frac{-x\sqrt{u^2/4D_L + s}}{\sqrt{D_L}}}\right\} = e^{-\frac{u^2 t}{4D_L}} \mathcal{L}^{-1}\left\{e^{-\frac{x\sqrt{s}}{\sqrt{D_L}}}\right\}^{*} = e^{\frac{u^2 t}{4D_L}} \frac{x e^{-\frac{x^2}{4D_L t}}}{2\sqrt{\pi D_L t^3}} \qquad (8\text{-AI})$$

* This latter transform is obtained from /6/, pp. 299 eq. (82)

Thus, by the convolution theorem (see /6/ pp. 36):

$$\frac{c}{c_o} = e^{\frac{ux}{2D_L}} \left\{ 1 * \frac{e^{-\left(\frac{u^2t}{4D_L} + \frac{x^2}{4D_Lt}\right)}}{2\sqrt{\pi D t^3}} \right\}$$

$$= \int_o^t \frac{x e^{\left(\frac{ux}{2D_L} - \frac{u^2t}{4D_L} - \frac{x^2}{4D_Lt}\right)}}{2\sqrt{\pi D_L t^3}} dt \qquad (9\text{-AI})$$

$$= \int_o^t \frac{x e^{-\frac{(x-ut)^2}{4D_Lt}} dt}{2\sqrt{\pi D_L t^3}}$$

In order to integrate eq. (9-AI) above, we write it in the form:

$$\frac{c}{c_o} = \int_o^t \left(\frac{x+ut}{\sqrt{\pi D_L t^3}}\right) e^{-\left(\frac{x-ut}{2\sqrt{D_Lt}}\right)^2} dt + e^{\frac{ux}{D_L}} \int_o^t \left(\frac{x-ut}{\sqrt{\pi D_L t^3}}\right) e^{\left(\frac{x+ut}{2\sqrt{D_Lt}}\right)^2} dt \qquad (10\text{-AI})$$

Now we let:

$$\alpha = \frac{x-ut}{2\sqrt{D_Lt}} \qquad d\alpha = -\left(\frac{x+ut}{\sqrt{D_Lt^3}}\right) dt$$

$$\beta = \frac{x+ut}{2\sqrt{D_Lt}} \qquad d\beta = -\left(\frac{x-ut}{\sqrt{D_Lt^3}}\right) dt$$

also as $t \to o \quad \alpha \to \infty$ and $\beta \to \infty$

thus we can write eq. (10-AI) in the form:

$$\frac{c}{c_o} = \frac{1}{2}\left(-\int_{\infty}^{\alpha}\frac{2e^{-\alpha^2}}{\sqrt{\pi}}d\alpha - e^{\frac{ux}{D_L}}\int_{\infty}^{\beta}\frac{2e^{-\beta^2}}{\sqrt{\pi}}d\beta\right)$$

$$= \frac{1}{2}\left(erfc\,\alpha + e^{\frac{ux}{D_L}}erfc\,\beta\right) \qquad (11\text{-AI})$$

and substituting back the values of α and β we get:

$$\frac{c}{c_o} = \frac{1}{2}\left[erfc\left(\frac{x-ut}{2\sqrt{D_L t}}\right) + erfc\left(\frac{x+ut}{2\sqrt{D_L t}}\right)\right] \qquad (12\text{-AI})$$

We are interested in the response of the system at the outlet, i.e., $x = L$ thus, equation (12-AI) becomes:

$$\frac{c}{c_o} = \frac{1}{2}\left[erfc\left(\frac{L-ut}{2\sqrt{D_L t}}\right) + erfc\left(\frac{L+ut}{2\sqrt{D_L t}}\right)\right] \qquad (13\text{-AI})$$

The response to an impulse signal or the distribution of residence-times function at the outlet is:

$$E(t) = \frac{d\frac{c}{c_o}}{dt} = \frac{L}{2\sqrt{\pi D_L t^3}}e^{-\frac{(L-ut)^2}{4D_L t}} \qquad (14\text{-AI})$$

We thus proceed in evaluating the zero and first moment of E(t) and the central second moment or the variance of $\theta E(t)$ vs. t/θ curve.

For the zero moment we have:

$$\int_0^\infty E(t)\,dt = \int_0^\infty \frac{L e^{-\frac{(L-ut)^2}{4D_L t}}}{2\sqrt{\pi D_L t^3}}\,dt = e^{\frac{uL}{2D_L}} \int_0^\infty \frac{L e^{-\frac{L}{4D_L t}}}{2\sqrt{\pi D_L t^3}} e^{-\frac{u^2}{4D_L}t}\,dt \qquad (15\text{-AI})$$

We may evaluate the integral on the right hand side of equation (15-AI) by regarding it as a Laplace transform in which the parameter s is equal to $\frac{u^2}{4D_L}$. Accordingly we write formally:

$$\int_0^\infty E(t)\,dt = e^{\frac{uL}{2D_L}} \cdot \left\{ \frac{L e^{-\frac{L^2}{4D_L t}}}{2\sqrt{\pi D_L t^2}} \right\} \qquad (16\text{-AI})$$

From a table of transforms /6/ pp. 299 eq. (82) we find that:

$$\mathcal{L}\left\{ \frac{L e^{-\frac{L^2}{4D_L t}}}{2\sqrt{\pi D_L t^3}} \right\} = e^{-\frac{L\sqrt{s}}{\sqrt{D_L}}}$$

By substituting this relation in equation (16-AI):

$$\int_0^\infty E(t)\,dt = e^{\frac{uL}{2D_L}} \cdot e^{-\frac{L\sqrt{s}}{\sqrt{D_L}}} \qquad (17\text{-AI})$$

and substituting for s the value $\frac{u^2}{4D_L}$ we obtain:

$$\int_0^\infty E(t)\,dt = 1 \qquad (18\text{-AI})$$

as required for the zero moment of the residence-times distribution (see eq. (3) pp. 13).

The <u>first moment</u> of the distribution function is according to the definition given on page 14:

$$\int_0^\infty tE(t)\,dt = \int_0^\infty \frac{Lt}{2\sqrt{\pi D_L t^3}}\, e^{\frac{-(L-ut)^2}{4D_L t}}\, dt \qquad (19\text{-AI})$$

Here again we may evaluate the integral by use of the Laplace transform. Since multiplication of a function by t corresponds to differentiating and changing the sign of the transform of said function we obtain from equations (16-AI) and (17-AI):

$$\int_0^\infty tE(t)\,dt = -e^{\frac{uL}{2D_L}} f'\left\{\frac{Le^{\frac{-L^2}{4D_L t}}}{2\sqrt{\pi D_L t}}\right\} = e^{\frac{uL}{2D_L}} \frac{d}{ds}\left(e^{\frac{-L\sqrt{s}}{\sqrt{D_L}}}\right) \qquad (20\text{-AI})$$

and by carrying out the differentiation with respect to s:

$$\int_0^\infty tE(t)\,dt = e^{\frac{uL}{2D_L}} \left(\frac{Le^{\frac{-L\sqrt{s}}{\sqrt{D_L}}}}{2\sqrt{D_L s}}\right) \qquad (21\text{-AI})$$

Hence, by substituting $s = \frac{u^2}{4D_L}$:

$$\int_0^\infty t\,E(t)\,dt = \frac{L}{u} \qquad (22\text{-AI})$$

Since L/u is equal to the true mean residence-time equation (22-AI) satisfies the requirements of an actual system (see eq. (5) pp. 14, and eq. (6) pp. 14)

The variance of the dimensionless distribution $\theta E(t)$ vs. t/θ is according to equation (10) pp. 19:

$$\sigma^2 = \int_0^\infty (t/\theta)^2\,\theta E(t)\,d(t/\theta) - 1 = \int_0^\infty \frac{u^2 t^2 e^{-\frac{(L-ut)^2}{4D_L t}}}{L\sqrt{\pi D_L t^3}}\,dt - 1 \qquad (23\text{-AI})$$

We let $s = \frac{u^2}{4D_L}$ and as before we use the Laplace transform to evaluate the integral on the right hand side of equation (23-AI):

$$\sigma^2 = \frac{u^2}{L^2} e^{\frac{uL}{2D_L}} f''\left\{\frac{Le^{-\frac{L^2}{4D_L t}}}{2\sqrt{\pi D_L t^3}}\right\} - 1 = \frac{u^2 e^{\frac{uL}{2D_L}}}{L^2}\frac{d^2}{ds^2}\left(e^{-\frac{L\sqrt{s}}{\sqrt{D_L}}}\right) \qquad (24\text{-AI})$$

by evaluating the differential, we get:

$$\sigma^2 = \frac{u^2}{4L^2} e^{\frac{uL}{2D_L}} - \frac{L\sqrt{s}}{\sqrt{D_L}} \left(\frac{L}{\sqrt{D_L s^3}} + \frac{L^2}{sD_L} \right) - 1 \qquad (25\text{-AI})$$

by substituting $s = \frac{u^2}{4D_L}$ and simplifying, we find that the variance is:

$$\sigma^2 = \frac{2D_L}{uL} \qquad (26\text{-AI})$$

Solution "B"

Equation (21) pp. 34 can also be solved for another set of boundary conditions which take into account the flux due to diffusion at the inlet of a semi-infinite bed (see Chapter III pp. 37 to 38) These are:

1-b) $$u c_o = u\, c(o,t) - D_L \frac{\partial c}{\partial x}(o,t)$$

2-b) $$\lim_{x \to \infty} c(x,t) = o$$

3-b) $$c(x,o) = o$$

The Laplace transform of eq. (21) pp. 34 is again:

$$s\bar{c}(x,s) - c(x,o) = D_L \bar{c}_{xx}(x,s) - u\bar{c}_x(x,s) \qquad \text{(1-AI)}$$

and the boundary conditions become:

1-b') $$\frac{uc_o}{s} = u\bar{c}(o,s) - D_L \bar{c}_x(o,s)$$

2-b') $$\lim_{x \to \infty} \bar{c}(x,s) = o$$

3-b') $$c(x,o) = o$$

applying condition 3-b') to eq. (1-AI):

$$\bar{c}_{xx}(x,s) - \frac{u}{D_L}\bar{c}_x(x,s) - \frac{s}{D_L}\bar{c}(x,s) = o \qquad \text{(2-AI)}$$

the general solution for equation (2-AI) is as before:

$$\bar{c}(x,s) = \phi e^{\left(\frac{u}{2D_L} + \frac{\sqrt{u^2/4D_L + s}}{\sqrt{D_L}}\right)x} + \chi e^{\left(\frac{u}{2D_L} - \frac{\sqrt{u^2/4D_L + s}}{\sqrt{D_L}}\right)x} \qquad (3\text{-AI})$$

where φ and χ are arbitrary functions of s. In order that condition 2-b') be satisfied φ must be zero, also to satisfy condition 1-b'):

$$\chi = \frac{uc_o}{D_L s\left(\frac{u}{2D_L} + \frac{\sqrt{u^2/4D_L + s}}{\sqrt{D_L}}\right)} \qquad (27\text{-AI})$$

Hence, the solution of equation (3-AI) for the new set of boundary conditions is:

$$\frac{\bar{c}(s)}{c_o} = \frac{ue^{\left(\frac{ux}{2D_L} - \frac{x\sqrt{u^2/4D_L + s}}{\sqrt{D_L}}\right)}}{D_L s\left(\frac{u}{2D_L} + \frac{\sqrt{u^2/4D_L + s}}{\sqrt{D_L}}\right)} \qquad (28\text{-AI})$$

To find the inverse transform, we write eq. (28-AI) in the form:

$$\frac{\bar{c}(s)}{c_o} = \frac{ue^{\frac{ux}{2D_L}}}{s\sqrt{D_L}} \cdot \frac{e^{-d\sqrt{\gamma+s}}}{\beta + \sqrt{\gamma+s}} \qquad (29\text{-AI})$$

where in the second factor on the right hand side we have made the substitutions:

$$\alpha = \frac{x}{\sqrt{D_L}} \quad ; \quad \beta = \frac{u}{2\sqrt{D_L}} \quad ; \quad \gamma = \frac{u^2}{4D_L} \tag{30-AI}$$

the inverse transforms are:

$$f^{-1}\left\{\frac{ue^{-\alpha\sqrt{s}}}{s\sqrt{D_L}}\right\} = \frac{ue^{\frac{ux}{2D_L}}}{\sqrt{D_L}} f^{-1}\left\{\frac{1}{s}\right\} = \frac{u}{\sqrt{D_L}} e^{\frac{ux}{2D_L}} \tag{31-AI}$$

$$f^{-1}\left\{\frac{e^{-\alpha\sqrt{\gamma+s}}}{\beta+\sqrt{\gamma+s}}\right\} = e^{-\gamma t} f^{-1}\left\{\frac{e^{-\alpha\sqrt{s}}}{\beta+\sqrt{s}}\right\}^{*}$$

$$= e^{-\gamma t}\left[\frac{e^{-\frac{\alpha^2}{4t}}}{\sqrt{\pi t}} - \beta e^{-\alpha\beta+\beta^2 t}\, \operatorname{erfc}\left(\frac{\alpha}{2\sqrt{t}}+\beta\sqrt{t}\right)\right] \tag{32-AI}$$

By the convolution theorem (/6/, pp.36) we find that the inverse transform of equation (6-AI) is:

$$\frac{c}{c_o} = \frac{ue^{\frac{ux}{2D_L}}}{\sqrt{D_L}} \int_0^t e^{-\gamma t}\left[\frac{e^{-\frac{\alpha^2}{4t}}}{\sqrt{\pi t}} - \beta e^{-\alpha\beta+\beta^2 t}\, \operatorname{erfc}\left(\frac{\alpha}{2\sqrt{t}}+\beta\sqrt{t}\right)\right] dt \tag{33-AI}$$

---

* This inverse transform is found in the H. Bateman Manuscript Project, Tables of Integral Transform, Volume 1, pp. 246, eq. 12

substituting back the values of α, β and γ and simplifying we find:

$$\frac{c}{c_o} = \int_0^t \left[\frac{ue^{-\frac{(x-ut)^2}{4D_L t}}}{\sqrt{\pi D_L t}} - \frac{u^2 e^{\frac{ux}{D_L}}}{2D_L} \operatorname{erfc}\left(\frac{x+ut}{2\sqrt{D_L t}}\right)\right] dt \qquad (34\text{-AI})$$

Since we are interested in the response of the system at the outlet, we can rewrite the above equation, substituting $x = L$:

$$\frac{c}{c_o} = \int_0^t \left[\frac{ue^{-\frac{(L-ut)^2}{4D_L t}}}{\sqrt{\pi D_L t}} - \frac{u^2 e^{\frac{uL}{D_L}}}{2D_L} \operatorname{erfc}\left(\frac{L+ut}{2\sqrt{D_L t}}\right)\right] dt \qquad (35\text{-AI})$$

the above integral is rather difficult to evaluate analytically. One can resort to the graphical integration of the impulse response function $E(t)$

$$E(t) = \frac{d\frac{c}{c_o}}{dt} = \frac{ue^{-\frac{(L-ut)^2}{4D_L t}}}{\sqrt{\pi D_L t}} - \frac{u^2 e^{\frac{uL}{D_L}}}{2D_L} \operatorname{erfc}\left(\frac{L+ut}{2\sqrt{D_L t}}\right) \qquad (36\text{-AI})$$

We may now proceed to find the moments of the distribution of residence-times.

For the zero moment we have:

$$\int_0^\infty E(t)dt = \int_0^\infty \left[\frac{u}{\sqrt{\pi D_L t}} e^{-\frac{(L-ut)^2}{4D_L t}} - \frac{u^2}{2D_L} e^{\frac{uL}{D_L}} \operatorname{erfc}\left(\frac{L+ut}{2\sqrt{D_L t}}\right)\right]dt \quad (37\text{-AI})$$

we can rewrite the equation above in the form:

$$\int_0^\infty E(t)dt = \frac{ue^{\frac{uL}{2D_L}}}{\sqrt{D_L}} \int_0^\infty \left[\frac{e^{\frac{-\alpha'^2}{4t}}}{\sqrt{\pi t}} \beta e^{-\alpha' t+\beta^2 t} \operatorname{erfc}\left(\frac{\alpha'}{2\sqrt{t}} + \frac{\beta}{\sqrt{t}}\right)\right] e^{-\gamma t} dt \quad (38\text{-AI})$$

where now $\alpha = \frac{L}{\sqrt{D_L}}$, β and γ remaining as defined in (30-AI). We note that the integral on the right side of equation (15-AI) is the Laplace transform of the function enclosed in square brackets having argument γ. Hence, we may write formally:

$$\int_0^\infty E(t)dt = \frac{ue^{\frac{uL}{2D_L}}}{\sqrt{D_L}} f\left\{\frac{e^{\frac{-\alpha'^2}{4t}}}{\sqrt{\pi t}} - \beta e^{-\alpha'\beta+\beta^2 t} \operatorname{erfc}\left(\frac{\alpha'}{2\sqrt{t}} + \frac{\beta}{\sqrt{t}}\right)\right\} \quad (39\text{-AI})$$

The transform can be evaluated with the help of (32-AI), replacing s with γ:

$$\int_0^\infty E(t)dt = \frac{ue^{\frac{uL}{2D_L}}}{\sqrt{D_L}} \left(\frac{e^{-\alpha\sqrt{\gamma}}}{\beta+\sqrt{\gamma}}\right) \quad (40\text{-AI})$$

substituting back the values of α', β and γ we find:

$$\int_0^\infty E(t)\,dt = 1 \qquad (41\text{-AI})$$

as is required for the response to an impulse signal (see eq. (3) pp. 13).

For the first moment of the distribution function E(t), we may write:

$$\int_0^\infty tE(t)\,dt = \frac{ue^{\frac{uL}{2D_L}}}{\sqrt{D_L}}\int_0^\infty t\left[\frac{e^{\frac{-\alpha'^2}{4t}}}{\sqrt{\pi t}} - \beta\, e^{-\alpha'\beta+\beta^2 t}\,\mathrm{erfc}\left(\frac{\alpha'}{2\sqrt{t}}+\beta\sqrt{t}\right)\right]e^{-\gamma t}\,dt \qquad (42\text{-AI})$$

since multiplication of the function by $-t$ corresponds to differentiation of the transform of the function, we may write formally:

$$\int_0^\infty tE(t)\,dt = -\frac{ue^{\frac{uL}{2D_L}}}{\sqrt{D_L}} f'\left\{\frac{e^{\frac{-\alpha'^2}{4t}}}{\sqrt{\pi t}} - \beta\, e^{-\alpha'\beta+\beta^2 t}\,\mathrm{erfc}\left(\frac{\alpha'}{2\sqrt{t}}+\beta\sqrt{t}\right)\right\}$$

$$= -\frac{ue^{\frac{uL}{2D_L}}}{\sqrt{D_L}}\frac{d}{d\gamma}\left(\frac{e^{\alpha'\sqrt{\gamma}}}{\beta-\sqrt{\gamma}}\right) \qquad (43\text{-AI})$$

$$= \frac{ue^{\frac{uL}{2D_L}}}{\sqrt{D_L}}\,\frac{e^{-\alpha'\sqrt{\gamma}}\left(\alpha'\beta+\alpha'\sqrt{\gamma}+1\right)}{2\sqrt{\gamma}\left(\beta+\sqrt{\gamma}\right)^2}$$

substituting the values of α', β and γ we find:

$$\int_0^\infty tE(t)dt = \frac{L}{u} + \frac{D_L}{u^2} \tag{44-AI}$$

which indicates that the first moment approximates the residence-time only when $\frac{D_L}{u^2}$ is small.

Since the average residence-time as given by equation (44-AI) is not equal to the true residence-time L/u or which is the same $\epsilon v/V$. The variance may be evaluated by using Eq. (10-a) (footnote on page 19) thus:

$$\sigma^2 = \left(\frac{v}{\epsilon V}\right)^2 \int_0^\infty t^2 E(t)dt - \left(\frac{v}{\epsilon V}\right)^2 \left[\int_0^t tE(t)dt\right]^2$$

$$= \left(\frac{u}{L}\right)^2 \int_0^\infty t^2 E(t)dt - \left(\frac{u}{L}\right)^2 \left[\int_0^\infty tE(t)dt\right]^2 \tag{45-AI}$$

In a manner analogous to the procedure used in obtaining eq. (38-AI) and by substitution of equation (44-AI) in (45-AI) we obtain:

$$\sigma^2 = \frac{u^3 e^{\frac{uL}{2D_L}}}{L^2\sqrt{D_L}} \int_0^\infty t^2 \left[\frac{e^{-\frac{\alpha'^2}{4t}}}{\sqrt{\pi t}} - \beta e^{-\alpha'\beta+\beta^2 t} \cdot \right. \tag{46-AI}$$

$$\left. \cdot erfc\left(\frac{\alpha'}{2\sqrt{t}} + \beta\sqrt{t}\right)\right] e^{-\sqrt{t} + \frac{u^2}{L^2}\left(\frac{L}{u} + \frac{D_L}{u^2}\right)^2}$$

By use of the Laplace transform we may write formally:

$$\sigma'^2 = \frac{u^3 e^{\frac{uL}{2D_L}}}{L^2\sqrt{D_L}} \frac{d^2}{d\gamma^2}\left(\frac{e^{-\alpha'\sqrt{\gamma}}}{\beta+\sqrt{\gamma}}\right) + \frac{u^2}{L^2}\left(\frac{L}{u}+\frac{D_L}{u^2}\right)^2 \qquad (47\text{-AI})$$

Evaluating the second derivative in gamma, we find:

$$\sigma'^2 = \frac{u^3 e^{\frac{uL}{2D_L}}}{L^2\sqrt{D_L}} \frac{e^{-\alpha'\sqrt{\gamma}}}{4\sqrt{\gamma}(\beta+\sqrt{\gamma})^3}\left[\frac{(\alpha'^2\beta^2+4\alpha'\beta+3}{\sqrt{\gamma}} + \right.$$

$$\left. + \frac{\alpha'\beta^2+\beta}{\gamma} + 2\alpha'^2\beta + 3\alpha' + \alpha'^2\sqrt{\gamma}\right] \qquad (48\text{-AI})$$

Substituting the values of α', β and γ :

$$\sigma' = \frac{2D_L}{uL} + \frac{3D_L^2}{L^2u^2} \qquad (49\text{-AI})$$

The Normal Distribution

Considering the impulse response of solution "B":

$$E(t)=\frac{dc}{c_o dt} = \frac{u e^{-\frac{(L-ut)^2}{4D_L t}}}{\sqrt{\pi D_L t}} - \frac{u^2 e^{\frac{uL}{D_L}}}{2D_L} \operatorname{erfc}\left(\frac{L+ut}{2\sqrt{D_L t}}\right) \qquad (36\text{-AI})$$

and the asymptotic expansion for large values of the argument of the complementary error function:

$$\operatorname{erfc}(\lambda) = \frac{e^{-\lambda^2}}{\lambda\sqrt{\pi}}\left(1-\frac{1}{2\lambda^2}+\frac{1\cdot 3}{(2\lambda^2)^2}-\frac{1\cdot 3\cdot 5}{(2\lambda^2)^3}+\cdots\right) \qquad (50\text{-AI})$$

we can write equation (36-AI) in the form:

$$E(t)=\frac{dc}{c_o dt}=\frac{u e^{-\frac{(L-ut)^2}{D_L t}}}{\sqrt{\pi D_L t}}\left[1-\frac{ut}{L+ut}\left(1-\frac{2D_L t}{(L+ut)^2}+\frac{12D_L^2 t^2}{(L+ut)^4}+\cdots\right)\right] \qquad (51\text{-A})$$

we see that for large values of $L + ut$ and especially for L in the neighborhood ut, that is $\frac{ut}{L} = \frac{t}{\theta} = 1$, equation (51-AI) simplifies to:

$$E(t)=\frac{dc}{c_o dt}=\frac{u}{\sqrt{4\pi D_L t}} e^{-\frac{(L-ut)^2}{4D_L t}} \qquad (52\text{-AI})$$

This is the normal or Gaussian distribution*. It is worth noting that for large values of $\frac{uL}{D_L}$ the response to a step function for solution "A" reduces to:

$$\frac{c}{c_o} = \frac{1}{2}\left[1 + \text{erf}\left(\frac{L-ut}{2\sqrt{D_L t}}\right)\right] \qquad (53\text{-AI})$$

This expression, the approximate response of a packed bed to a step function, was the result of a simplified derivation by Danckwerts /13/. The derivative of eq. (53-AI) with respect to t or the response to an impulse function for large values of $\frac{uL}{D_L}$ is:

$$E(t) = \frac{d\frac{c}{c_o}}{dt} = \frac{u}{2\sqrt{\pi D_L t}}\left(\frac{L+ut}{ut}\right) e^{-\frac{(L-ut)}{4D_L t}} \qquad (54\text{-AI})$$

which again reduces to the normal distribution of equation (52-AI) in the neighborhood of $\frac{t}{\theta} = 1$.

We should like to find the moments of the time distribution function E(t).

Zero Moment:

$$\int_0^\infty E(t)\,dt = \int_0^\infty \frac{u\,e^{-\frac{(L-ut)^2}{4D_L t}}}{2\sqrt{\pi D_L t}}\,dt = \frac{u e^{\frac{uL}{4D_L t}}}{2\sqrt{D_L}} \int_0^\infty \frac{e^{-\frac{L^2}{4D_L t} - \frac{u^2 t}{4D_L}}}{\sqrt{\pi t}}\,dt \qquad (55\text{-AI})$$

---

* Levenspiel and Smith /42/ in their discussion of packed beds use equation (52-AI) as the response to the impulse function.

If we let $\frac{u^2}{4D_L} = s$ we can evaluate the last integral on the right hand side of eq. (55-AI) by finding the Laplace transform of the function $\frac{e^{-L^2/4D_L t}}{\sqrt{\pi t}}$ this is:

$$\mathcal{L}\left\{\frac{e^{-\frac{L^2}{4D_L t}}}{\sqrt{\pi t}}\right\}^{*} = \frac{e^{-\frac{L\sqrt{s}}{\sqrt{D_L}}}}{\sqrt{s}} \qquad (56\text{-AI})$$

Consequently, eq. (55-AI) becomes:

$$\int_0^\infty E(t)dt = \frac{u}{2\sqrt{D_L}} e^{\frac{uL}{2D_L}} \left(\frac{e^{-\frac{L\sqrt{s}}{\sqrt{D_L}}}}{\sqrt{s}}\right) \qquad (57\text{-AI})$$

substituting for s the value $\frac{u^2}{4D_L}$ we find that:

$$\int_0^\infty E(t)\,dt = 1 \qquad (58\text{-AI})$$

---

* This transform is obtained from /6/ pp. 299, eq. (84)

First Moment:

$$\int_0^\infty tE(t)dt = \int_0^\infty \frac{ut}{4\sqrt{\pi D_L t}} e^{-\frac{(L-ut)^2}{4D_L t}} = -\frac{u}{2\sqrt{D_L}} e^{\frac{uL}{2D_L}} f'\left\{\frac{e^{-\frac{L^2}{4D_L t}}}{\sqrt{\pi t}}\right\}$$

$$= -\frac{u e^{\frac{uL}{2D_L}}}{2\sqrt{D_L}} \frac{d}{ds}\left(\frac{e^{-\frac{L\sqrt{s}}{\sqrt{D_L}}}}{\sqrt{s}}\right) \qquad (59\text{-AI})$$

evaluating the differential:

$$\int_0^\infty tE(t)dt = -\frac{u}{4\sqrt{D_L}} e^{\frac{uL}{2D_L} - \frac{L\sqrt{s}}{\sqrt{D_L}}}\left(-\frac{L}{s\sqrt{D_L}} - \frac{1}{\sqrt{s}}\right) \qquad (60\text{-AI})$$

and substituting the value of $s = \frac{u^2}{4D_L}$ we get:

$$\int_0^\infty tE(t)\,dt = \frac{L}{u} + \frac{2D_L}{u^2} \qquad (61\text{-AI})$$

Variance of the dimensionless time distribution:

$$\sigma'^2 = \left(\frac{u}{L}\right)^2 \int_0^\infty t^2 E(t)\,dt - \left(\frac{u}{L}\right)^2 \left[\int_0^\infty t\,E(t)\,dt\right]^2$$

$$= \frac{u^2}{L^2}\int_0^\infty \frac{u t^2\, e^{-\frac{(L-ut)^2}{4D_L t}}}{4\sqrt{\pi D_L t}}\,dt - \frac{u^2}{L^2}\left(\frac{L}{u}+\frac{2D_L}{u^2}\right)^2 \qquad (62\text{-AI})$$

utilizing again the principle of differentiation of the Laplace transform we may formally write:

$$\int_0^\infty \frac{u t^2}{4\sqrt{\pi D_L t}}\, e^{-\frac{(L-ut)^2}{4D_L t}}\,dt = \frac{u}{2\sqrt{D_L}}\, e^{\frac{uL}{2D_L}}\, \frac{d^2}{ds^2}\left(\frac{e^{-\frac{L\sqrt{s}}{\sqrt{D_L}}}}{\sqrt{s}}\right) \qquad (63\text{-AI})$$

hence, eq. (62-AI) becomes:

$$\sigma'^2 = \frac{u^3}{2L^2\sqrt{D_L}}\, e^{\frac{uL}{2D_L}-\frac{L\sqrt{s}}{\sqrt{D_L}}}\left(\frac{L}{2\sqrt{s^3 D_L}}+\frac{1}{s^2}+\frac{L}{2s^3\sqrt{D_L}}+\frac{3}{2\sqrt{s^5}}\right) - \qquad (64\text{-AI})$$

$$-\frac{u^2}{L^2}\left(\frac{L}{u}+\frac{2D_L}{u^2}\right)^2$$

by simplifying and substituting $s = \frac{u^2}{4D_L}$ we obtain the variance:

$$\sigma'^2 = \frac{2D_L}{uL} + \frac{8D_L^2}{u^2L^2} \qquad (65\text{-AI})$$

APPENDIX II

A Number of Mixed Stages in Series Having Equal Volumes

Let us consider a perfectly mixed tank such that the concentration at the outlet is at all times equal to the concentration in the bulk of the tank as shown in Figure 49:

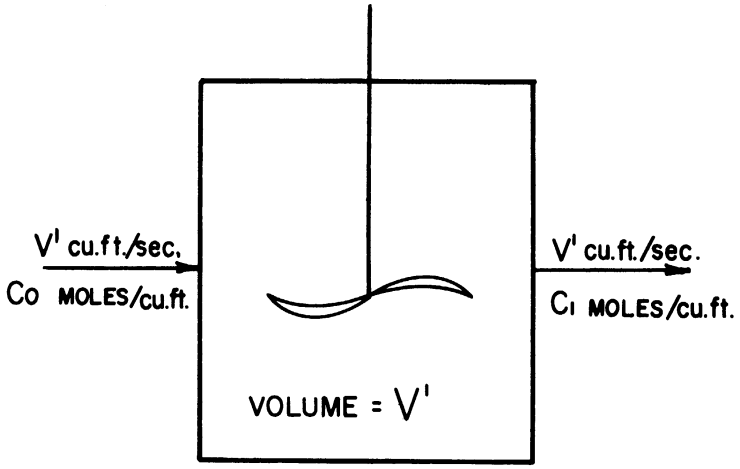

Figure 49
A Perfectly Mixed Tank

If the concentration at the inlet of the tank is suddenly changed from 0 to c_o, we can write that the rate of change of concentration in the bulk of the tank or at the outlet is:

$$-V' \frac{dc}{dt} = v'c_1 - v'c_o \qquad (1\text{-AII})$$

Also the boundary condition at the outlet is:

$$c_1 = 0 \qquad \text{at} \qquad t = 0 \tag{2-AII}$$

which expresses the fact that at the outlet the concentration remains 0 at least up to time $t = 0$. Taking the Laplace transform of (1-AII) we have:

$$s\bar{c}_1(s) - c_1(0) = \frac{v' c_0}{V's} - \frac{v'\bar{c}_1(s)}{V's} \tag{3-AII}$$

since $c(o) = 0$ by (2-AII) we can solve for $\bar{c}_1(s)$:

$$\bar{c}_1(s) = \frac{v'}{V's} = \frac{c_0}{\left(s + \frac{v'}{V'}\right)} \tag{4-AII}$$

the inverse transform of which is:

$$c_1 = c_0\left(1 - e^{-\frac{v'}{V'}t}\right) * \tag{5-AII}$$

---

* Note that in this limiting case the distribution function is:

$$E(t) = \frac{dc/c_0}{dt} = e^{-v't/V'}$$

thus it is an exponential curve decaying at the rate v'/V' or $1/\theta$.

Suppose now that the outlet stream from this tank is admitted to a second tank of equal volume as shown in the Figure below:

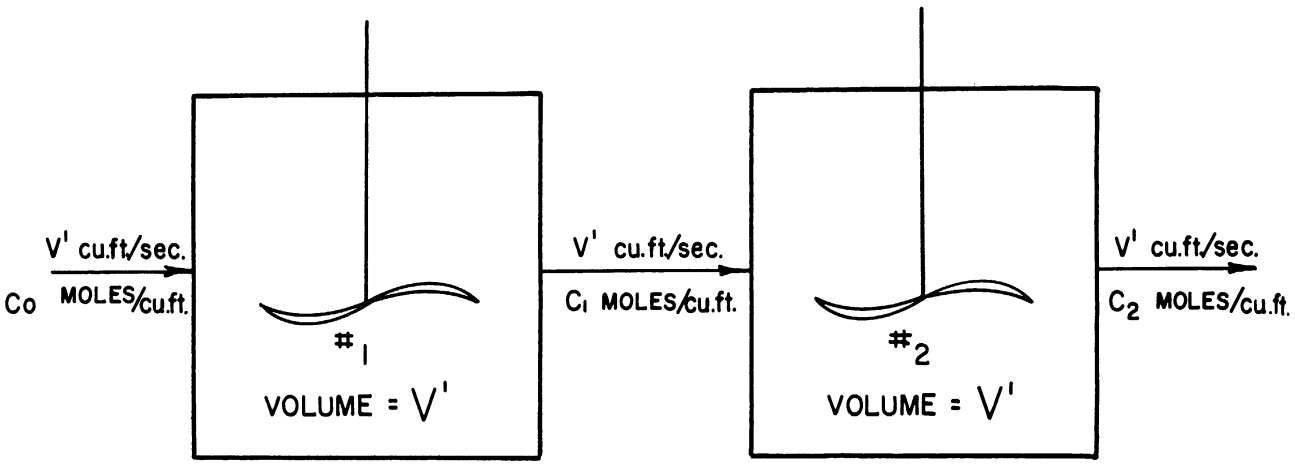

Figure 50
Two Perfectly Mixed Tanks in Series

The rate of change in concentration for tank No. 2 is:

$$-V' \frac{dc_2}{dt} = v'c_2 - v'c_1 \qquad (6\text{-AII})$$

with the boundary condition:

$$c_2 = 0 \quad \text{at} \quad t = 0 \qquad (7\text{-AII})$$

Taking the Laplace transform of (6-AII) we find:

$$s\bar{c}(s) - c_2(0) = \frac{v'}{V'}\bar{c}(s) - \frac{v'}{V'}\bar{c}_2(s) \qquad (8\text{-AII})$$

Since by eq. (7-AII) $c_2(0) = 0$ we can solve for $\bar{c}_2(s)$:

$$\bar{c}_2(s) = \frac{v'}{V'}\frac{\bar{c}_1(s)}{\left(s+\frac{v'}{V'}\right)} \qquad (9\text{-AII})$$

but $\bar{c}_1(s)$ is given by eq. (4-AII) which substituted in (9-AII) gives:

$$\bar{c}_2(s) = \left(\frac{v'}{V'}\right)^2 \frac{c_0}{s\left(s+\frac{v'}{V'}\right)^2} \qquad (10\text{-AII})$$

For the nth tank we have:

$$-V'\frac{dc_n}{dt} = v'c_n - v'c_{n-1} \qquad (11\text{-AII})$$

hence, the Laplace transform of the concentration at the outlet of the nth tank can be written immediately by analogy with eq. (10-AII):

$$\bar{c}_n(s) = \left(\frac{v'}{V'}\right)^n \frac{c_0}{s\left(s+\frac{v'}{V'}\right)^n} \qquad (12\text{-AII})$$

The inverse transform of eq. (12-AII) can be found with the aid of the convolution integral from the following inverse transforms:

$$\mathcal{L}^{-1}\left\{\frac{1}{s}\right\}=1$$

$$\mathcal{L}^{-1}\left\{\frac{1}{\left(s+\frac{v'}{V'}\right)^n}\right\}=e^{-\frac{v'}{V'}t}\,\mathcal{L}^{-1}\left\{\frac{1}{s^n}\right\}=\frac{t^{n-1}}{(n-1)!}e^{-\frac{v'}{V'}t} \qquad \text{(13-AII)}$$

Hence, the inverse transform of (12-AII) is:

$$c=c_0\left(\frac{v'}{V'}\right)^n\left\{1*\frac{t^{-1}}{(n-1)!}e^{-\frac{v'}{V'}t}\right\}=c_0\left(\frac{v'}{V'}\right)^n\int_0^t\frac{\tau^{(n-1)}}{(n-1)!}e^{-\frac{v'}{V'}\tau}d\tau \qquad \text{(14-AII)}$$

Integration of equation (14-AII) for any finite number of stages n greater than 1 yields the equation:

$$\frac{c}{c_0}=1-\sum_{i=1}^{n}\frac{e^{\frac{v'}{V'}}}{(i-1)!}\left(\frac{v't}{V'}\right)^{i-1} \qquad \text{(15-AII)}$$

This form of the response of a number of mixers in series has already been reported by McMullin and Weber /48/; however, eq. (14-AII) is more

general since n need not be restricted to an integral number greater than one but may be any real positive number.

The time distribution function for this model is given directly by differentiation of eq. (14-AII):

$$E(t) = \frac{dc}{c_o dt} = \left(\frac{v'}{V'}\right)^n \frac{t^{n-1}}{(n-1)!} e^{-\frac{v'}{V'}t} \qquad (16\text{-AII})$$

This equation written in the dimensionless form:

$$\frac{v'}{V'} E(t) = \frac{dc}{\frac{dv't}{V'}} = \left(\frac{v'}{V'}t\right)^{n-1} \frac{e^{-\frac{v'}{V'}t}}{(n-1)!} \qquad (17\text{-AII})$$

is the well known Poisson probability distribution. Many of the results derived on the following pages can be derived directly from probabilistic considerations, see Feller /21/.

The zero moment of the time distribution function is obtained by integration of eq. (16-AII) between the limits of zero to infinity:

$$\int_0^\infty E(t)\,dt = \int_0^\infty \left(\frac{v'}{V'}\right)^n \frac{t^{n-1}}{(n-1)!} e^{-\frac{v'}{V'}t}\,dt \qquad (18\text{-AII})$$

By letting $\frac{v'}{V'} = s$ we see that the right hand side is the Laplace transform of the function $\frac{t^{n-1}}{(n-1)!}$. Thus we have immediately:

$$\int_0^\infty E(t)\,dt = \left(\frac{v'}{V'}\right)^n \frac{1}{s^n} = 1 \qquad \text{(19-AII)}$$

The first moment of the distribution can be found in an analogous manner:

$$\int_0^\infty t\,E(t)\,dt = \left(\frac{v'}{V'}\right)^n \int_0^\infty \frac{t^n}{(n-1)!} e^{-\frac{v'}{V'}t} = \left(\frac{v'}{V'}\right)^n \frac{n}{s^{n+1}} = \frac{n V'}{v'} \qquad \text{(20-AII)}$$

This is, therefore, the overall residence-time θ through the series of n stages.

The variance of the distribution is:

$$\sigma^2 = \int_0^\infty (t/\theta)^2\,\theta\,E(t)\,d(t/\theta) - 1 = \left(\frac{V'}{nv'}\right)^2 \left(\frac{v'}{V'}\right)^n \int_0^\infty \frac{t^{n+1}}{(n-1)!} e^{-\frac{v'}{V'}t}\,dt - 1 \qquad \text{(21-AII)}$$

Again with the aid of the Laplace transform, we have:

$$\sigma^2 = \left(\frac{V'}{nv'}\right)^2 \left(\frac{v'}{V'}\right)^n \frac{n(n+1)}{s^{n+2}} - 1 = \frac{1}{n} \qquad \text{(22-AII)}$$

Finally, we may also find the skewness of the distribution function by writing according to Eq. (12) pp. 20:

$$\nu = \int_0^\infty \left(t/\vartheta\right)^3 \vartheta E(t)\, d\left(t/\vartheta\right) - 3\int_0^\infty \left(t/\vartheta\right)^2 \vartheta E(t)\, d\left(t/\vartheta\right) + 2$$

$$= \left(\frac{V'}{n\nu'}\right)^3 \left(\frac{\nu'}{V'}\right)^n \int_0^\infty \frac{t^{n+2}}{(n-1)!} e^{-\frac{\nu'}{V'}t}\, dt - 3\left(\frac{V'}{n\nu'}\right)^2 \left(\frac{\nu'}{V'}\right)^n \int_0^\infty \frac{t^{n+1}}{(n-1)!} e^{-\frac{\nu'}{V'}t}\, dt \qquad (23\text{-AII})$$

we can then write the integrals in Eq. (23-AII) in terms of Laplace transforms:

$$\nu = \left(\frac{V'}{n\nu'}\right)^3 \left(\frac{\nu'}{V'}\right)^n \frac{n(n+1)(n+2)}{s^{n+3}} - 3\left(\frac{V'}{n\nu'}\right)^2 \left(\frac{\nu'}{V'}\right)^n \frac{n(n+1)}{s^{n+2}} + 2 \qquad (24\text{-AII})$$

substituting $s = \frac{\nu'}{V'}$ and simplifying we find:

$$\nu = \frac{2}{n^2} \qquad (25\text{-AII})$$

A Number of Mixed Stages in Series Having Unequal Volumes

Let us suppose that we have n_1 perfectly mixed stages, each having a volume V_1' and n_2 stages, each having volume V_2' connected in series as shown in Figure 51.

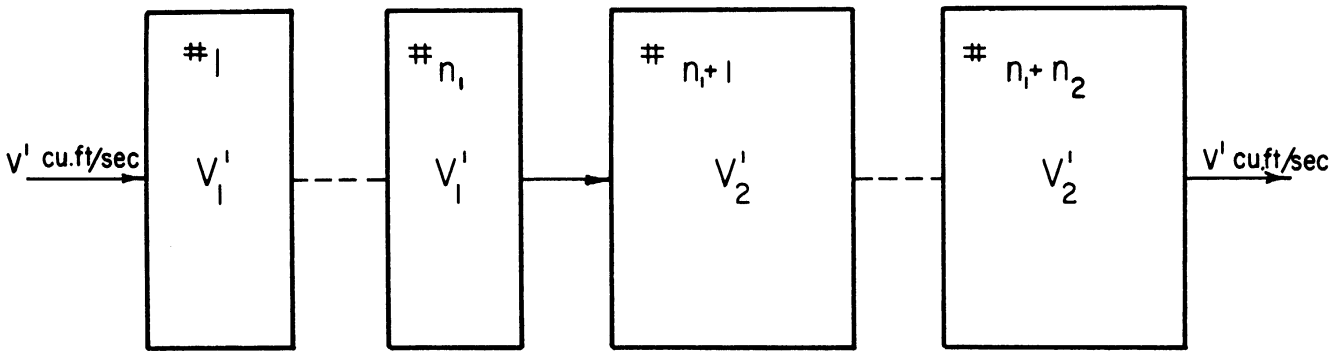

Figure 51
Series of Perfectly Mixed Tanks Having Unequal Volumes

Then if each stage is perfectly mixed, we can immediately write the Laplace transform of the concentration of the stream emerging at the end of the series of tanks by comparison with eq. (12-AII) pp. 187 :

$$c(s)=\left(\frac{v'}{V_1'}\right)^{n_1}\left(\frac{v'}{V_2'}\right)^{n_2}\frac{c_0}{s\left(s+\frac{v'}{V_1'}\right)^{n_1}\left(s+\frac{v'}{V_2'}\right)^{n_2}} \qquad (26\text{-AII})$$

the inverse transforms are:

$$f^{-1}\left\{\frac{1}{s\left(s+\frac{v'}{V_1'}\right)^{n_1}}\right\}=f^{-1}\left\{\frac{1}{s}\right\}*e^{-\frac{v'}{V_1'}}f^{-1}\left\{\frac{1}{s^{n_1}}\right\}=\int_0^{\tau}\frac{\tau^{(n_1-1)}}{(n_1-1)!}e^{-\frac{v'}{V_1'}\tau}d\tau$$

(27-AII)

$$f^{-1}\left\{\frac{1}{\left(s+\frac{v'}{V_2'}\right)^{n_2}}\right\}=e^{-\frac{v'}{V_2'}}f^{-1}\left\{\frac{1}{s^{n_2}}\right\}=\frac{t^{(n_2-1)}}{(n_2-1)!}e^{-\frac{v'}{V_2'}t}$$

by the convolution theorem (see ref. /6/ pp. 36) we see that:

$$\frac{c}{c_0}=\left[\int_0^t\left(\frac{v'}{V_1'}\right)^{n_1}\frac{\tau^{(n_1-1)}}{(n_1-1)!}e^{-\frac{v'}{V_1'}\tau}d\tau*\left(\frac{v'}{V_2'}\right)^{n_2}\frac{t^{(n_2-1)}}{(n_2-1)}e^{-\frac{v'}{V_2'}t}\right] \qquad \text{(28-AII)}$$

Therefore, the response to a step function in concentration for a series of stages having different volumes V_1' and V_2' is:

$$\frac{c}{c_0}=\int_0^t\int_0^{\tau}\left(\frac{v'}{V_1'}\right)^{n_1}\frac{\lambda^{(n_1-1)}}{(n_1-1)!}e^{-\frac{v'}{V_1'}\lambda}\cdot\left(\frac{v'}{V_2'}\right)^{n_2}\frac{(\tau-\lambda)^{(n_2-1)}}{(n_2-1)!}e^{-\frac{v'}{V_2'}(\tau-\lambda)}d\tau d\lambda \qquad \text{(29-AII)}$$

We find the response to the impulse input by differentiating the equation above with respect to time:

$$E(t) = \frac{d\frac{c}{c_o}}{dt} = \int_o^t \left(\frac{v'}{V_1'}\right)^{n_1} \frac{\tau^{(n_1-1)}}{(n_1-1)!} e^{-\frac{v'}{V_1'}\tau} \cdot \cdot \left(\frac{v'}{V_2'}\right)^{n_2} \frac{(t-\tau)^{(n_2-1)}}{(n_2-1)!} e^{-\frac{v'}{V_2'}(t-\tau)} d\tau \qquad (30\text{-AII})$$

We can now calculate the zero moment of the time distribution E(t):

$$\int_o^\infty E(t)dt = \int_o^\infty \int_o^t \left(\frac{v'}{V_1'}\right)^{n_1} \frac{\tau^{(n_1-1)}}{(n_1-1)!} e^{-\frac{v'}{V_1'}\tau} \cdot \cdot \left(\frac{v'}{V_2'}\right)^{n_2} \frac{(t-\tau)^{(n_2-1)}}{(n_2-1)!} e^{-\frac{v'}{V_2'}(t-\tau)} dt\, d\tau \qquad (31\text{-AII})$$

By use of the Laplace transform and by letting $s_1 = \frac{v'}{V_1'}$ and $s_2 = \frac{v'}{V_2'}$, we may write the above equation in the form:

$$\int_o^\infty E(t)dt = \left(\frac{v'}{V'}\right)^{n_1} f(s_1) \cdot \left(\frac{v'}{V_2'}\right) f(s_2) = \left(\frac{v'}{V_1'}\right)^{n_1} \left(\frac{v'}{V_2'}\right)^{n_2} \left(\frac{1}{s_1^{n_1}}\right)\left(\frac{1}{s_2^{n_2}}\right) \qquad (32\text{-AII})$$

By substituting back the values of s_1 and s_2 we get:

$$\int_o^\infty E(t)dt = 1 \qquad (33\text{-AII})$$

The overall contact time through the series of tanks is obtained from the first moment of the time distribution function:

$$\int_0^\infty tE(t)dt = \left(\frac{v'}{V_1'}\right)^{n_1}\left(\frac{v'}{V_2'}\right)^{n_2}\int_0^\infty t\int_0^t \frac{\tau^{(n_1-1)}}{(n_1-1)!}e^{-\frac{v'}{V_1'}\tau}\frac{(t-\tau)^{(n_2-1)}}{(n_2-1)!}e^{\frac{v'}{V_2'}(t-\tau)}\,dt\,d\tau \quad (34\text{-AII})$$

making use of the fact that multiplication of the function by $-t$ is equivalent to differentiating the corresponding transform with respect to s we may write formally:

$$\int_0^\infty tE(t)dt = -\left(\frac{v'}{V_1'}\right)^{n_1}\left(\frac{v'}{V_2'}\right)^{n_2}\left[f'(s_1)\cdot f(s_2)+f(s_1)\cdot f'(s_2)\right]$$

$$= -\left(\frac{v'}{V_1'}\right)^{n_1}\left(\frac{v'}{V_2'}\right)^{n_2}\left[\frac{d}{ds_1}\left(\frac{1}{s_1^{n_1}}\right)\frac{1}{s_2^{n_2}}+\frac{d}{ds_2}\left(\frac{1}{s_2^{n_2}}\right)\frac{1}{s_1^{n_1}}\right]$$

$$= \left(\frac{v'}{V_1'}\right)^{n_1}\left(\frac{v'}{V_2'}\right)^{n_2}\left[\frac{n_1}{s_1^{n_1+1}s_2^{n_2}}+\frac{n_2}{s_1^{n_1}s_2^{n_2+1}}\right] \quad (35\text{-AII})$$

Substituting the values of s_1 and s_2 and simplifying, we get:

$$\int_0^\infty t\,E(t)\,dt = n_1\frac{V_1'}{v'} + n_2\frac{V_2'}{v'} \qquad (36\text{-AII})$$

thus, the overall contact time is the sum of the contact time for each stage as would be expected. We can thus write the general result:

$$\vartheta = \sum_{i=1}^{n} \vartheta_i' \qquad (37\text{-AII})$$

Passing to the variance of the time distribution function:

$$\sigma^2 = \int_0^\infty (t/\vartheta)^2 \vartheta\, E(t)\, d(t/\vartheta) - 1 \qquad (38\text{-AII})$$

$$= \frac{1}{\vartheta^2}\left(\frac{v'}{V_1'}\right)^{n_1}\left(\frac{v'}{V_2'}\right)^{n_2}\int_0^\infty t^2 \int_0^t \frac{\tau^{(n_1-1)}}{(n_1-1)!}\, e^{-\frac{v'}{V_1'}\tau} \cdot \frac{(t-\tau)}{(n_2-1)!}\, e^{-\frac{v'}{V_2'}(t-\tau)}\, dt\, d\tau$$

Again, with the use of the Laplace transform and the chain rule for differentiation we may write eq. (38-AII) in the form:

$$\sigma^2 = \frac{1}{\theta^2}\left(\frac{v'}{V_1'}\right)^{n_1}\left(\frac{v'}{V_2'}\right)^{n_2}\left[f''(s_1)f(s_2)+2f'(s_1)f'(s_2)+f(s_1)f''(s_2)\right]-1 \tag{39-AII}$$

$$= \frac{1}{\theta^2}\left(\frac{v'}{V_1'}\right)^{n_1}\left(\frac{v'}{V_2'}\right)^{n_2}\left[\frac{d^2}{ds_1^2}\left(\frac{1}{s_1^{n_1}s_2^{n_2}}\right)+2\frac{d}{ds_1}\left(\frac{1}{s_1^{n_1}}\right)\frac{d}{ds_2}\left(\frac{1}{s_2^{n_2}}\right)+\frac{d^2}{ds_2^2}\left(\frac{1}{s_1^{n_1}+s_2^{n_2}}\right)\right]$$

hence, by evaluation of the differentials in s_1 and s_2:

$$\sigma^2 = \frac{1}{\theta^2}\left(\frac{v_1'}{V_1'}\right)^{n_1}\left(\frac{v'}{V_2'}\right)^{n_2}\left[\frac{n_1(n_1+1)}{s_1^{n_1+2}s_2^{n_2}}+\frac{2n_1n_2}{s_1^{n_1+1}s_2^{n_2+1}}+\frac{n_2(n_2+1)}{s_1^{n_1}+s_2^{n_2+2}}\right] \tag{40-AII}$$

substituting for s_1 and s_2, $\frac{v'}{V_1'}$ and $\frac{v'}{V_2'}$ respectively, and simplifying:

$$\sigma^2 = \frac{n_1\left(\frac{V_1'}{v'}\right)^2+n_2\left(\frac{V_2'}{v'}\right)^2}{\left(n_1\frac{V_1'}{v'}+n_2\frac{V_2'}{v'}\right)} \tag{41-AII}$$

since:

$$\frac{n_1 V_1'}{V'} + \frac{n_2 V_2'}{V'} = \vartheta \quad \text{and} \quad \frac{n_1 V_1'}{V'} = \vartheta_1 \; ; \; \frac{n_2 V_2'}{V'} = \vartheta_2$$

we may write eq. (41-AII) in the form:

$$\sigma^2 = \frac{\frac{1}{n_1}\vartheta_1^2 + \frac{1}{n_2}\vartheta_2^2}{\vartheta^2} \qquad (42\text{-AII})$$

Generalizing these results for a large number of unequal mixing stages, we have:

$$\sigma^2 = \sum_{i=1}^{n} \left(\frac{\vartheta_i'}{\vartheta}\right)^2 \qquad (43\text{-AII})$$

APPENDIX III

Typical Irrigated Packing Experiment

For experimental record, see Figure 27, pp. 92

a) Bed Properties

1. Average I.D. of column, d_t = .334 ft.
2. Average cross-sectional area, $\frac{\pi}{4} d_t^2$ = .0874 sq.ft.
3. Volume of Empty Column

   Volume of Bottom Section, V_E = .0065 cu.ft.

   Empty Volume of Mid-Section, V_w = .2590 cu.ft.

   Empty Volume of Top Section (above liquid distributor), V_D = .0437 cu.ft.

   Total Empty Volume, $V_E + V_w + V_D$ = .3092 cu.ft.
4. Free Volume of Packed Column

   Volume of Bottom Section, V_E = .0065 cu.ft.

   Volume of Packed Mid-Section (Wetted), ϵV_w
   .693 x .2590 = .180 cu.ft.

   Volume of Top Section, ϵV_D = .0303 cu.ft.

   Total Free Volume, $V_E + \epsilon V_w + \epsilon V_D$ = .217 cu.ft.

   Volume Not Wetted, $V_E + \epsilon V_D$
   .0065 + .0304 = .0369 cu.ft.
5. Nominal Diameter of Raschig Rings = .0208 cu.ft.
6. Surface Area of One Raschig Ring

   Outer Cylindrical Surface Area:
   π x 6.5 mm. x 6mm. = 122.6 mm^2

   Inner Cylindrical Surface Area:
   π x 4.5mm. x 6mm. = 84.9 mm^2

   Bottom Ring Surface:
   $\frac{\pi}{4}$ x $(6.5^2 \times 4.5^2)$ mm^2 = 17.3 mm^2

   Top Ring Surface:
   $\frac{\pi}{4}$ x $(6.5^2 \times 4.5^2)$ mm^2 = 17.3 mm^2

   Total Surface of Particle = 242.1 mm^2 or .375 sq.in.

a) Bed Properties (cont'd)

7. Total Surface Area of Packing

Total Weight of Raschig Rings, Loaded to Column = 6380 gr.

Average Weight of 4 Samples of 200 Rings Each = 59.4 gr.

Total Number of Rings = 21,500

Total Surface Area Per Unit Volume of Bed:

$$a = \frac{21{,}500 \times .375 \text{ sq. in.}}{144 \text{ sq.in./sq.ft.} \times .3027 \text{ cu.ft.}} = 187 \text{ sq.ft./cu.ft.}$$

8. Hydraulic Mean Diameter:

$$d_m = \frac{\epsilon}{a} = \frac{.693}{187 \text{ sq.ft./cu.ft.}} = .00371 \text{ ft.}$$

b) Air Properties

1. Average Temperature of All Flowing Streams is taken to nearest degree = 88°F

2. Air Flow Rate: (from No. 3 Rotameter calibration, Figure 56, pp. 218) = 1.01 cu.ft./min. at 60°F and 14.7 psia

3. True Air Flow Rate:

$$v = \frac{1.01 \text{ cu.ft./min}}{60 \text{ min/sec}} \left(\frac{520 \times 14.9}{548 \times 14.7}\right)^{1/2} = .0165 \text{ cu.ft./sec.}$$

4. Air Density:

$$\rho_G = \frac{29 \text{ lb./mole}}{359 \text{ cu.ft./mole}} \left(\frac{492 \times 14.9}{548 \times 14.7}\right) = .0735 \text{ lb/cu.ft.}$$

5. Superficial Mass Flow Rate:

$$G = \frac{.0735 \text{ lb./cu.ft.} \times .0165 \text{ cu.ft./sec.} \times 3600 \text{ sec./hr.}}{.0874 \text{ sq.ft.}} = 50.0 \frac{\text{lb/hr.}}{\text{sq.ft.}}$$

6. Viscosity:

(From Figure 58, pp. 220 at 88°F), μ_G = .0441 lb/ft.hr.

b) Air Properties (cont'd)

7. Reynolds No.:

$$Re_G = \frac{Gd}{\mu_G} = \frac{50.0 \text{ lb./hr.sq.ft.} \times .0208 \text{ ft.}}{.0441 \text{ lb/ft.hr.}} = 23.6$$

c) Tracer Properties

1. Average Temperature = $88^{\circ}F$

2. Tracer Flow Rate:
(From No. 3 Rotameter calibration, Figure 56, pp. 218) = .98 cu.ft/min at $60^{\circ}F$ and 14.7 psia

3. True Tracer Flow Rate:

$$v = \frac{.98 \text{ cu.ft./min.}}{60 \text{ min./sec.}} \left(\frac{520}{548} \times \frac{14.9}{14.7} \times \frac{29}{24.4}\right)^{1/2} = .0175 \text{ cu.ft./sec.}$$

4. Tracer Density:

$$\rho_G = \frac{24.4 \text{ lb/mole}}{359 \text{ cu.ft./mole}} \left(\frac{492}{548} \times \frac{14.9}{14.7}\right) = .0619 \text{ lb/cu.ft.}$$

5. Superficial Mass Flow Rate:

$$G = \frac{.0619 \text{ lb/cu.ft.} \times .0175 \text{ cu.ft./sec.} \times 3600 \text{ sec./hr.}}{.0874 \text{ sq. ft.}} = 44.5 \text{ lb/hr.sq.ft.}$$

6. Viscosity:

(From Figure 58, pp.220 at $88^{\circ}F$), μ_G = .0439 lb/ft.hr.

7. Reynolds No.:

$$Re_G = \frac{Gd}{\mu_G} = \frac{44.5 \text{ lb./hr.sq.ft.} \times .0208 \text{ ft.}}{.0439} = 21.1$$

d) Response Curve, Air Displacing Tracer

1. Residence-Time

As defined in page 99, the residence-time of the gas phase is evaluated by integration of the area

d) Response Curve, Air Displacing Tracer (cont'd)

bounded by the response curve. Table XVI gives the necessary quantities as obtained from the recorder traces shown in Figure 27, pp. 92 . Figure 52 shows the graphical integration of that part of the response curve which has a significant slope. Values of $\left(\frac{c}{c_o}\right)_{av.}$ are obtained graphically as the average values for small time increments from Figure 52.

The value of $\frac{c}{c_o} = 1$ for $t \leqslant 8.67$, also, $\frac{c}{c_o} = 0$ for $t \geqslant 15.47$, therefore:

$$\int_0^\infty \frac{c}{c_o}\,dt \simeq \int_{t=0}^{t=8.67} dt + \sum_{t=8.67}^{t=15.47} \left(\frac{c}{c_o}\right)_{av} \Delta t$$

$$\simeq 8.67 + 2.992 = 11.67 \text{ seconds}$$

2. Porosity of Irrigated Packing

Residence-time in Empty Section (that which is usually occupied by irrigated packing):

$$\theta = \frac{.259 \text{ cu.ft.}}{.0165 \text{ cu.ft./sec}} = 15.70 \text{ seconds}$$

Residence-time in Sections Not Wetted:

$$\frac{V_E + \epsilon V_P}{v} = \frac{.0369 \text{ cu.ft.}}{.0165 \text{ cu.ft./sec.}} = 2.24 \text{ seconds}$$

Porosity of Irrigated Packing:

$$\epsilon_w = \frac{11.67 - 2.24}{15.7} = .601$$

TABLE XVI

DETERMINATION OF MIXING PARAMETERS FOR RESPONSE CURVE, AIR DISPLACING TRACER

t Seconds	c Chart Divisions	$\frac{c}{c_o}$	Δt	t_{av}	t^2_{av}	$(\frac{c}{c_o})_{av}$	$(\frac{c}{c_o})_{av}\Delta t$
8.67	40.0	1.000					
			.40	8.87	78.6769	.996	.3984
9.07	39.7	.992					
			.40	9.27	85.9329	.984	.3936
9.47	39.0	.975					
			.40	9.67	93.5089	.961	.3844
9.87	37.8	.945					
			.40	10.07	101.4049	.920	.3680
10.27	35.6	.890					
			.40	10.47	109.6209	.850	.3400
10.67	32.2	.805					
			.40	10.87	118.1569	.750	.3000
11.07	27.4	.685					
			.40	11.27	127.0129	.607	.2428
11.47	21.0	.525					
			.40	11.67	136.1889	.447	.1788
11.87	15.2	.380					
			.40	12.07	145.6849	.320	.1280
12.27	10.9	.272					
			.40	12.47	155.5009	.225	.0900
12.67	7.5	.187					
			.40	12.87	165.6369	.158	.0632
13.07	5.3	.132					
			.40	13.27	176.0929	.108	.0432
13.47	3.5	.0875					
			.40	13.67	186.8689	.074	.0296
13.87	2.3	.0590					
			.40	14.07	197.9649	.048	.0192
14.27	1.5	.0375					
			.40	14.47	209.3809	.030	.0120
14.67	1.0	.0250					
			.40	14.87	221.1169	.015	.0060
15.07	0.5	.0125					
			.40	15.27	233.1729	.005	.0020
15.47	0.0	.000					

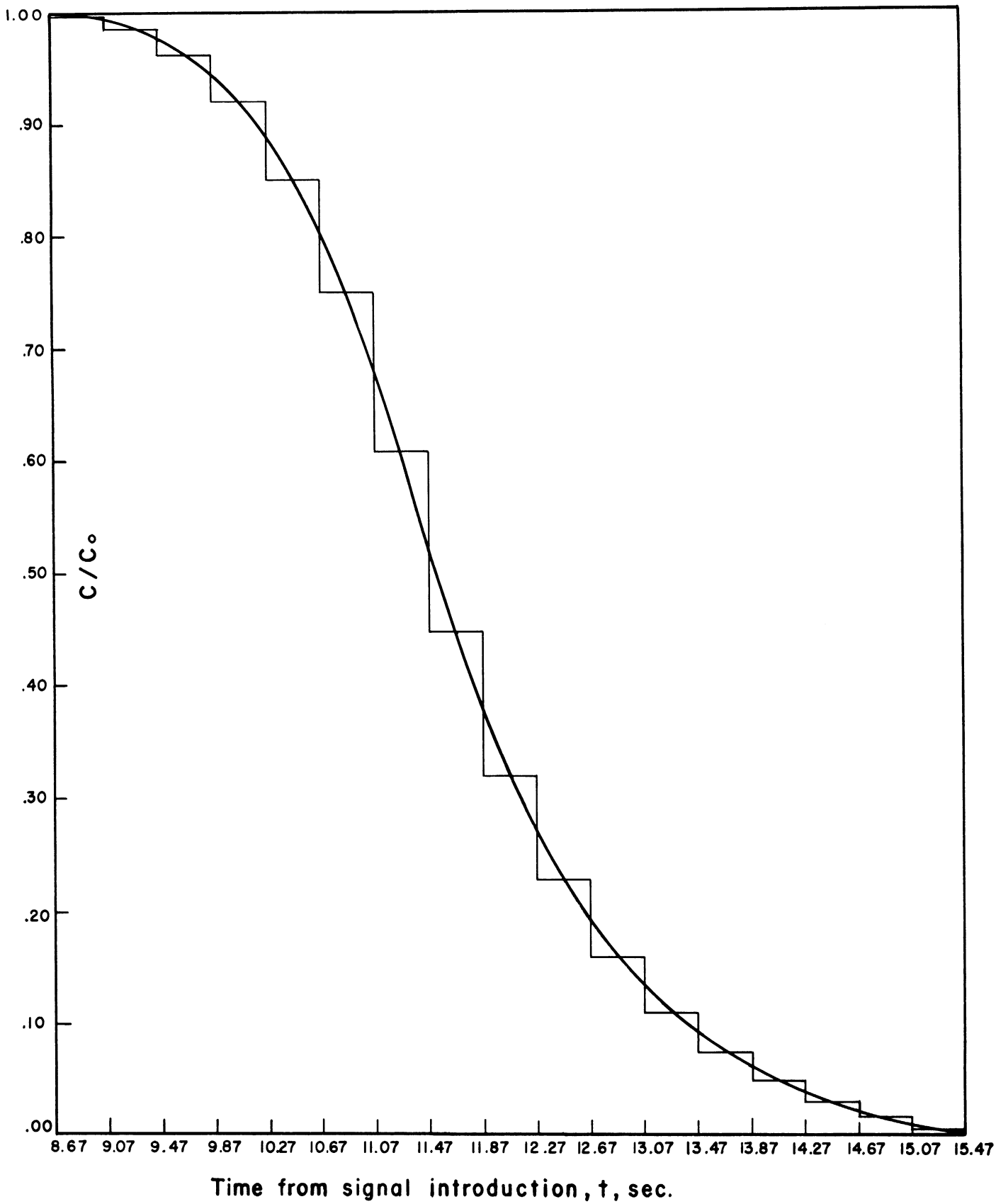

Figure 52. Graphical Integration of Response Curve, Air Displacing Tracer.

d) Response Curve, Air Displacing Tracer (cont'd)

3. Calculated Variance

The variance is calculated as indicated on page 103. By reference to d)1, we assume that:

$$\int_0^\infty t\frac{c}{c_o}\,dt \simeq \int_{t=0}^{t=8.67} t\,dt + \sum_{t=8.67}^{t=15.47} t_{av}\,\left(\frac{c}{c_o}\right)_{av}\,\Delta t$$

where $t_{av} = t + \frac{\Delta t}{2}$

The foregoing formula for graphical integration involves the assumption that for small intervals of time:

$$t_{av}\left(\frac{c}{c_o}\right)_{av} \simeq \left(t\,\frac{c}{c_o}\right)_{av}$$

This was verified by detailed graphical integration of the curve $t\,\frac{c}{c_o}$ vs. t and found to hold for all cases encountered in the experimental work.

$$\int_0^\infty t\,\frac{c}{c_o}\,dt \simeq \frac{8.67^2}{2} + 31.27122 = 68.85567 \text{ sec}^2$$

Variance:

$$\sigma^2 = \frac{2\int_0^\infty t\,\frac{c}{c_o}\,dt}{\int_0^\infty \frac{c}{c_o}\,dt} - 1$$

$$= \frac{2 \times 68.85567}{(11.67)^2} - 1 = .01118$$

d) Response Curve, Air Displacing Tracer (cont'd)

4. Skewness

In a similar manner, as for the calculation of the variance, we may write:

$$\int_0^\infty t^2 \frac{c}{c_o}\,dt \simeq \int_{t=0}^{t=8.67} t^2 dt + \sum_{t=8.67}^{t=15.47} t^2_{av} \left(\frac{c}{c_o}\right)_{av} \Delta t$$

$$\simeq \frac{(8.67)^3}{3} + 330.69345 = 547.9326$$

And the skewness is:

$$\nu = \frac{3 \times 547.9326}{(11.67)^3} - 3(1.01118) + 2 = .00073$$

5. Variance Correction For End Effects

Modified Peclet Number From pp. 120 eq. (63b): = .338

Hydraulic Mean Diameter From a) 8 = .00371 ft.

Height of Mixed Stage:

$$H = \frac{2 \times .00371 \text{ ft.}}{.338} = .0220 \text{ ft.}$$

Equivalent Height of Section Above Liquid Distributor = .45 ft.

Number of Stages in Section Above Distributor:

$$n_D = \frac{.45 \text{ ft.}}{.022 \text{ ft.}} = 20.4$$

d) Response Curve, Air Displacing Tracer (cont'd)

Residence-time in Section Above Distributor:

$$\theta_D = \epsilon\frac{V_D}{v} = \frac{.0303 \text{ cu.ft.}}{.0165 \text{ cu.ft./sec.}} = 1.84 \text{ sec.}$$

Residence-time in Empty Section:

$$\theta_E = \frac{V}{v} E = \frac{.0066 \text{ cu. ft.}}{.0165 \text{ cu.ft./sec.}} = .40 \text{ sec.}$$

Residence-time in Irrigated Section:

$$\theta_w = \theta - \theta_D - \theta_E = 11.67 - 1.85 - 0.39 = 9.43 \text{ sec.}$$

Corrected Variance:

$$\sigma_D^2 = .01118 \left(\frac{11.67}{9.43}\right)^2 - \frac{1}{20.4}\left(\frac{1.84}{9.43}\right)^2 - \left(\frac{0.40}{9.43}\right)^2 = 0.01346$$

6. Height of Mixed Stage

Height of Irrigated Section = 3.00 ft.

Height of Mixed Stage:

$$H_w = .01346 \times 3.00 \text{ ft.} = .0404$$

7. Peclet Number:

$$Pe_w = \frac{2d}{H_w} = \frac{2 \times .0208}{.0404} = 1.03 \text{ ft.}$$

e) Response Curve, Tracer Displacing Air

1. Residence-time

In manner analogous to d)1 (see Table XVII and Figure 53):

$$\int_0^\infty \left(1-\frac{c}{c_o}\right)dt \simeq \int_{t=0}^{t=8.12} dt + \sum_{t=8.12}^{t=14.52} \left(1-\frac{c}{c_o}\right)_{av.} \Delta t$$

$$\simeq 8.12 + 2.8004 = 10.92 \text{ sec.}$$

TABLE XVII

DETERMINATION OF MIXING PARAMETERS FOR RESPONSE CURVE, TRACER DISPLACING AIR

t Seconds	c Chart Divisions	$\frac{c}{c_o}$	$1-\frac{c}{c_o}$	Δt	t_{av}	t^2_{av}	$(1-\frac{c}{c_o})_{av}$	$(1-\frac{c}{c_o})_{av}\Delta t$
8.12	.0	.0000	1.000					
				.40	8.32	69.2224	.997	.3988
8.52	.3	.0075	.993					
				.40	8.72	76.0384	.984	.3936
8.92	.9	.0225	.978					
				.40	9.12	83.1744	.963	.3852
9.32	2.3	.0575	.943					
				.40	9.52	90.6304	.910	.3640
9.72	5.5	.137	.863					
				.40	9.92	98.4064	.822	.3288
10.12	9.6	.240	.760					
				.40	10.32	106.5024	.697	.2788
10.52	15.0	.375	.625					
				.40	10.72	114.9184	.555	.2220
10.92	20.4	.510	.490					
				.40	11.12	123.6544	.417	.1668
11.32	26.0	.650	.350					
				.40	11.52	132.7104	.280	.1120
11.72	31.1	.777	.223					
				.40	11.92	142.0864	.165	.0660
12.12	35.0	.875	.125					
				.40	12.35	151.7824	.100	.0400
12.52	37.0	.925	.075					
				.40	12.72	161.7984	.060	.0240
12.92	38.0	.950	.050					
				.40	13.12	172.1344	.038	.0152
13.32	39.0	.975	.025					
				.40	13.52	182.7904	.022	.0088
13.72	39.3	.983	.017					
				.40	13.92	193.7664	.011	.0044
14.12	39.7	.993	.007					
				.40	14.32	205.0624	.005	.0020
14.52	40.0	1.000	.000					

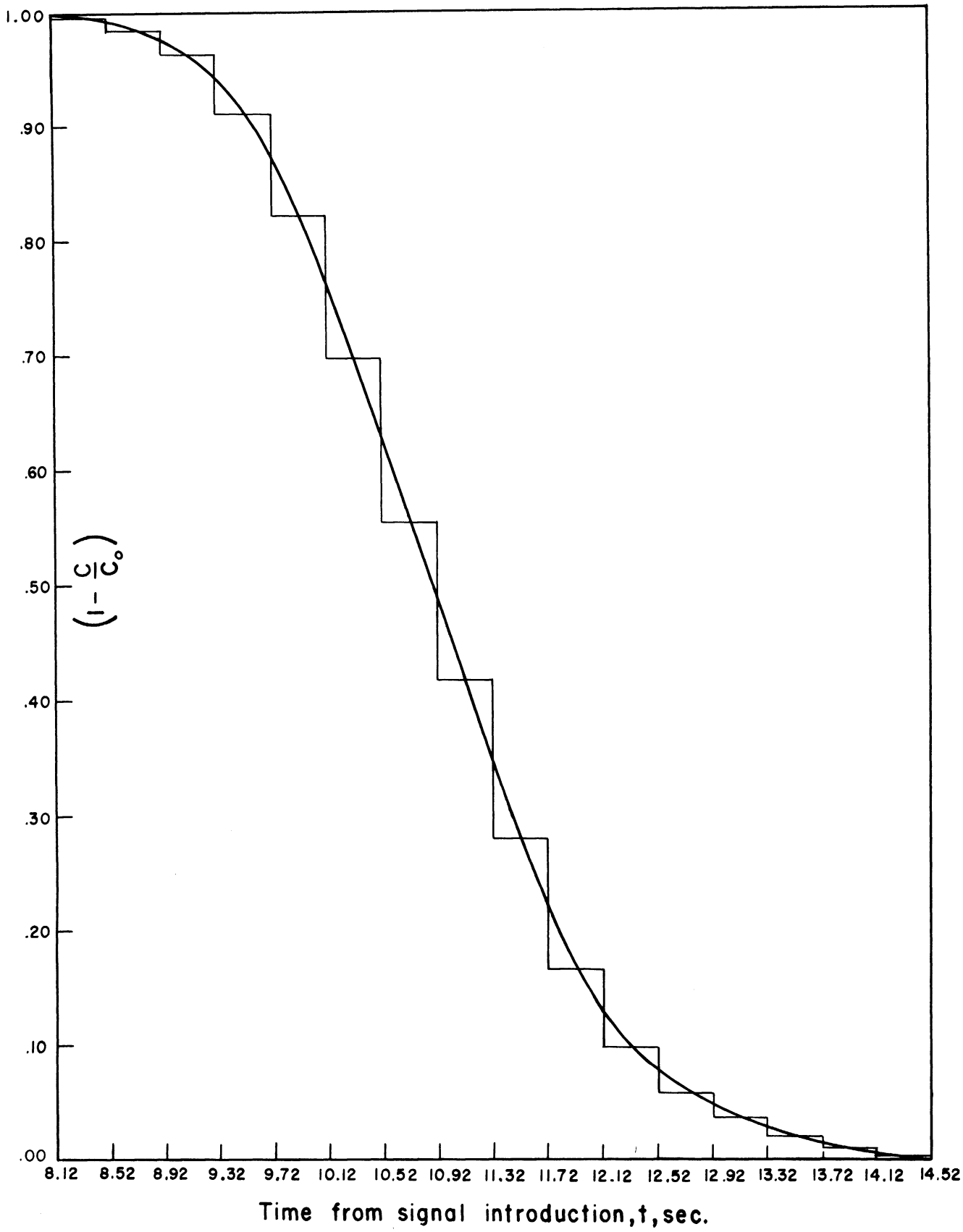

Figure 53. Graphical Integration of Response Curve, Tracer Displacing Air.

e) Response Curve, Tracer Displacing Air (cont'd)

2. Porosity of Irrigated Packing

Residence-time in empty section occupied by irrigated packing only:

$$\theta = \frac{.259 \text{ cu. ft.}}{.0175 \text{ cu.ft./sec.}} = 14.8 \text{ sec.}$$

Residence-time in Section Not Wetted:

$$\frac{V_E + \epsilon V_D}{v} = \frac{.0369 \text{ cu.ft.}}{.0175 \text{ cu.ft./sec.}} = 2.11 \text{ sec.}$$

Porosity of Irrigated Packing:

$$\epsilon_w = \frac{10.92 - 2.11}{14.8} = .595$$

3. Calculated Variance

In manner analogous to d)3 (See Table XVII and Figure 53):

$$\int_0^\infty t\left(1-\frac{c}{c_o}\right)dt \simeq \int_{t=0}^{t=8.12} tdt + \sum_{t=8.12}^{t=14.52} t_{av}\left(1-\frac{c}{c_o}\right)_{av.}\Delta t$$

$$\simeq \frac{(8.12)^2}{2} + 27.38541 = 60.35261 \text{ sec}^2$$

Variance

$$\sigma^2 = \frac{2\int_0^\infty t\left(1-\frac{c}{c_o}\right)dt}{\int_0^\infty \left(1-\frac{c}{c_o}\right)dt} - 1$$

$$\simeq \frac{2 \times 60.35261 \text{ sec}^2}{(10.92)^2 \text{sec}^2} - 1 = .01038$$

e) Response Curve, Tracer Displacing Air (cont'd)

4. Skewness

$$\int_0^\infty t^2\left(1-\frac{c}{c_o}\right)dt \simeq \int_{t=0}^{t=8.12} t^2 dt + \sum_{t=8.12}^{t=14.52} t^2{}_{av}\left(1-\frac{c}{c_o}\right)_{av.}\Delta t$$

$$\simeq \frac{(8.12)^3}{3} + 270.43762 = 448.9000$$

And the skewness is:

$$\nu = \frac{3 \times 448.9000}{(10.92)^3} - 3\ (1.01038) + 2 = .00022$$

5. Variance Correction for End Effects

From d)5, the number of stages above distributor are: = 20.4

Residence-time in section above distributor

$$\theta_D = \frac{\epsilon V_D}{V} = \frac{.0304 \text{ cu.ft.}}{.0175 \text{ cu.ft./sec.}} = 1.74 \text{ sec.}$$

Residence-time in empty section:

$$\theta_E = \frac{V}{v} E = \frac{.0065 \text{ cu.ft.}}{.0175 \text{ cu.ft./sec.}} = .37 \text{ sec.}$$

Residence-time in irrigated section:

$$\theta_w = \theta - \theta_D - \theta_E = 10.92 - 1.59 - 0.52 = 8.81 \text{ sec.}$$

Corrected Variance:

$$= .01038\left(\frac{10.92}{8.81}\right)^2 - \frac{1}{20.4}\left(\frac{1.74}{8.81}\right)^2 - \left(\frac{0.37}{8.81}\right)^2 = .1220$$

6. Height of Mixed Stage

Height of Irrigated Section: = 3.00 ft.

$$H_w = .1220 \times 3.00 \text{ ft.} = .3660 \text{ ft.}$$

7. Peclet Number

$$Pe_w = \frac{2d}{H_w} \quad \frac{2 \times .0208}{.03660} = 1.14$$

f) Water Properties

1. Average Temperature = 88°F

2. Density (see Figure 59, pp. 221), ρ_w = 62.13 lb/cu.ft.

3. Viscosity (see Figure 59, pp. 221), ρ_w = 1.89 lb/ft.hr.

4. Water Flow Rate:

(From No. 2 Rotameter Calibration,

Figure 55, pp.217) = .078 gal/min.

5. Superficial Mass Flow Rate:

$$W = \frac{62.13 \text{ lb/cu.ft.} \times .078 \text{ gal/min} \times .1337 \text{ cu.ft/gal} \times 60 \text{ min/hr}}{.0874 \text{ sq. ft.}}$$

$$= 446 \text{ lb/hr.ft.}^2$$

6. Reynolds Number

$$Re_L = \frac{Wd}{u_w} = \frac{446 \text{ lb/hr.ft.}^2 \times .0208 \text{ ft.}}{1.89 \text{ lb./ft.hr.}} = 4.91$$

APPENDIX IV

TABLE XVIII

RESPONSE TO A STEP FUNCTION FOR SOLUTION "A" OF DIFFUSION EQUATION

$\frac{c}{c_o}$ AS FUNCTION OF $\frac{t}{\theta}$ FOR VALUES OF $\frac{uL}{2D_L}$ FROM 80 to 200

$\frac{t}{\theta}$ \ $\frac{uL}{2D_L}$	80	90	100	110	120	130	140	150	160	170	180	190	200
.6	1.000	1.000	1.000	1.000	1.000	1.000	1.000	1.000	1.000	1.000	1.000	1.000	1.000
.7	.999	1.000	1.000	1.000	1.000	1.000	1.000	1.000	1.000	1.000	1.000	1.000	1.000
.8	.974	.981	.985	.988	.994	.994	.995	.997	.998	.998	.999	.999	.999
.85	.920	.932	.943	.956	.959	.965	.970	.975	.978	.981	.984	.987	.988
.90	.813	.829	.843	.856	.867	.877	.886	.896	.902	.909	.916	.922	.927
.95	.656	.669	.674	.688	.698	.706	.717	.721	.729	.736	.743	.749	.755
1.00	.477	.479	.480	.481	.482	.482	.483	.484	.484	.484	.485	.486	.486
1.05	.311	.303	.294	.288	.281	.274	.268	.261	.256	.250	.245	.244	.254
1.10	.181	.169	.157	.147	.138	.129	.120	.114	.106	.100	.094	.088	.083
1.15	.095	.084	.069	.066	.055	.047	.045	.040	.035	.031	.028	.025	.022
1.20	.046	.037	.030	.025	.020	.017	.014	.011	.009	.008	.006	.005	.004
1.25	--	--	--	--	--	--	--	--	.002	.002	.001	.001	.000
1.30	.008	.006	.004	.003	.002	.001	.001	.000	.000	.000	.000	.000	.000
1.40	.001	.000	.000	.000	.000	.000	.000	.000	.000	.000	.000	.000	.000

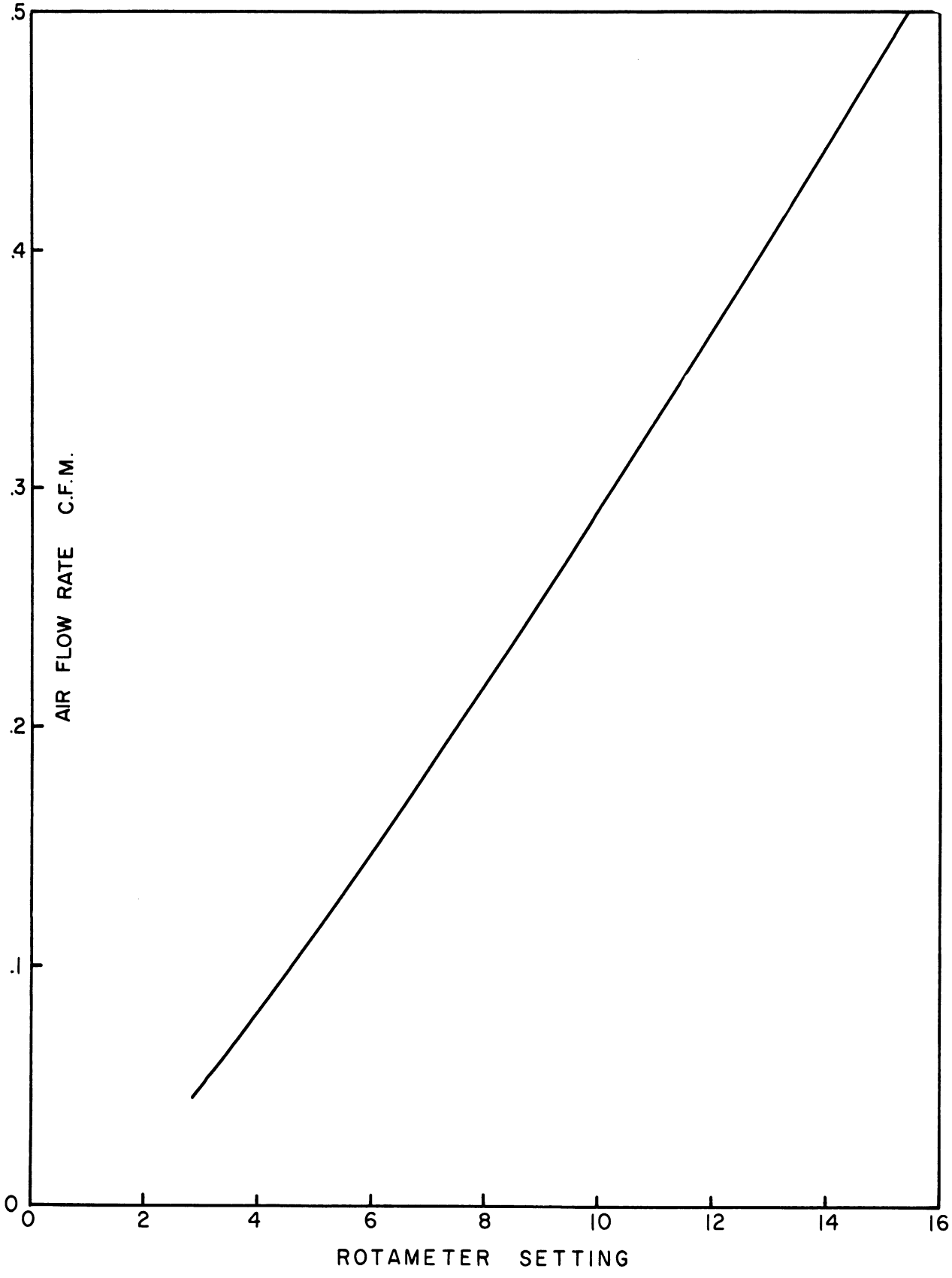

Figure 54. Rotameter No. 1 Tube No. 2F-1/4-16-5/70
Calibration for Air at 60°F and 14.7 Psia.

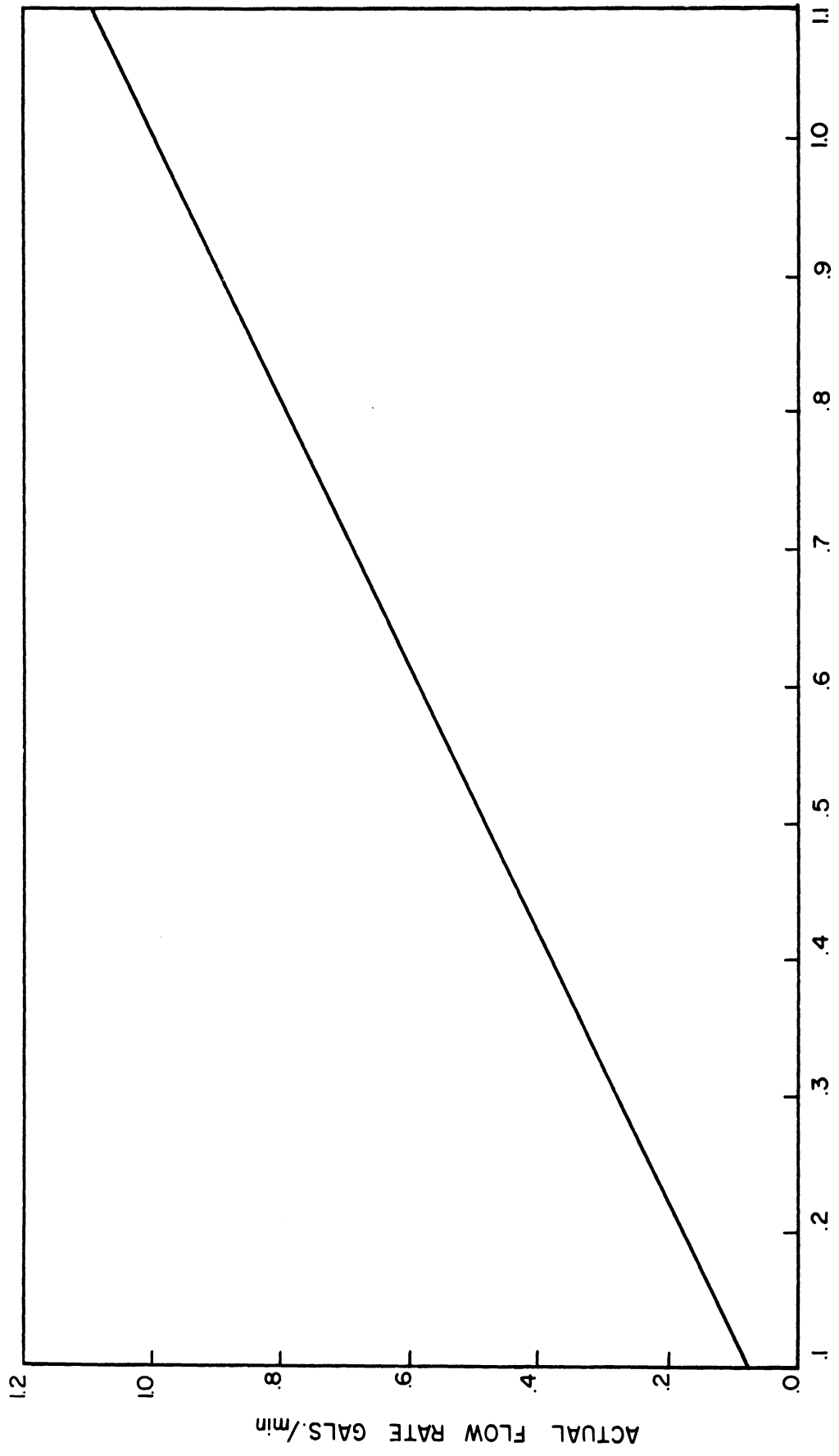

Figure 55. Rotameter No. 2 Tube No. B4-27-10/70-G Calibration for Water at 64.4°F.

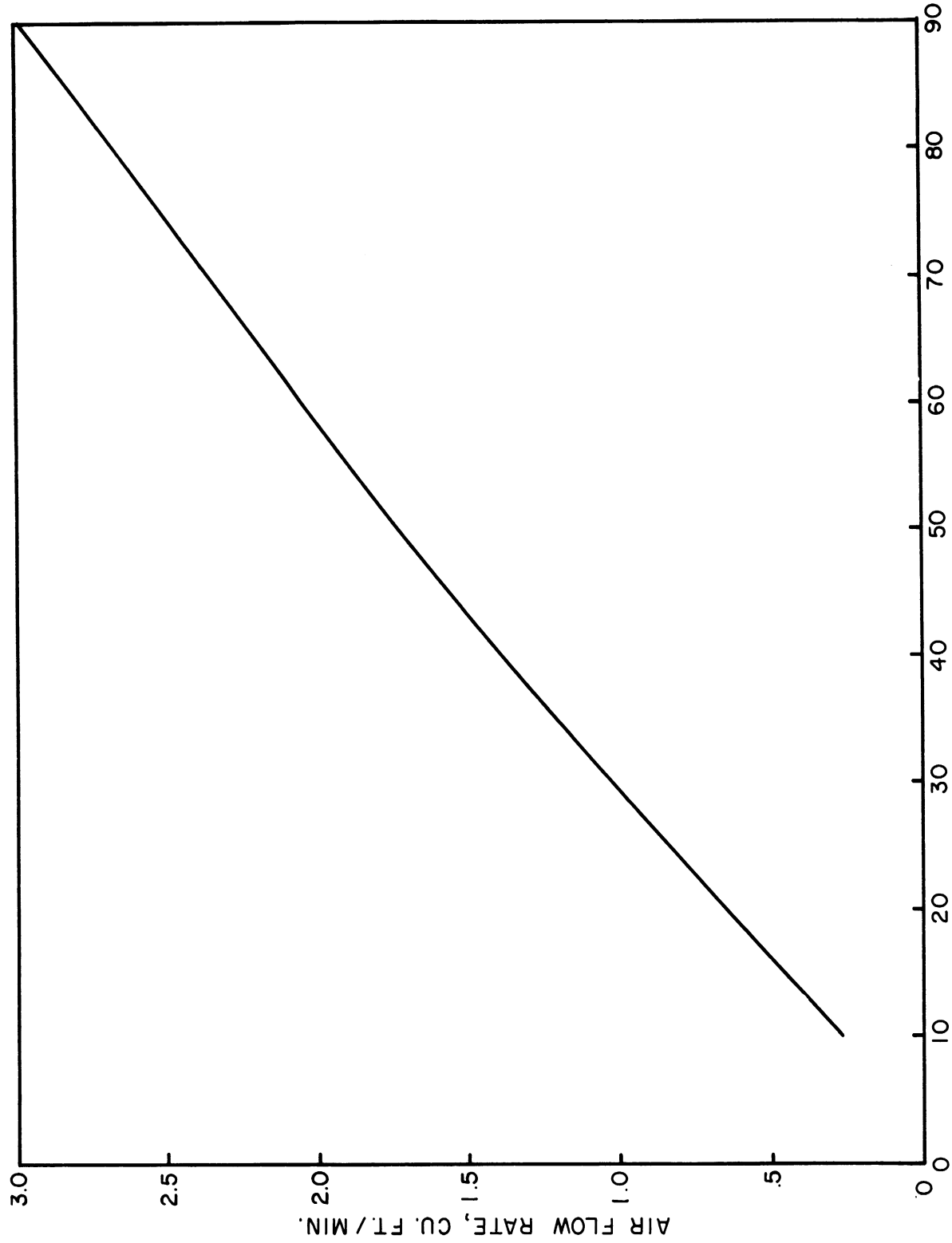

Figure 56. Rotameter No. 3 Tube No. B4-27-10/27 Calibration for Air at 60°F and 14.7 Psia.

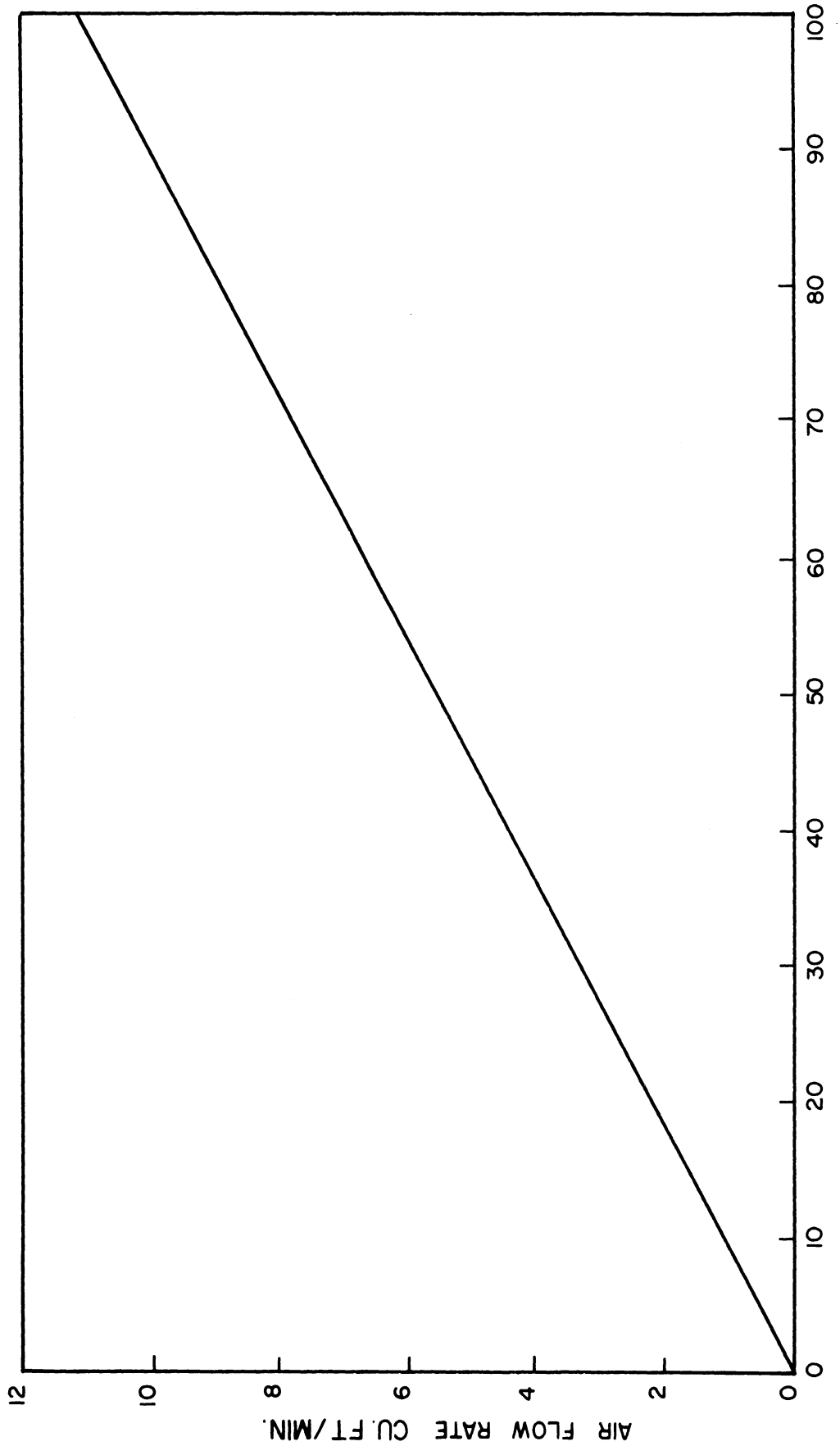

Figure 57. Rotameter No. 4 Tube No. B5-27-10/77 Calibration for Air at 60°F and 14.7 Psia.

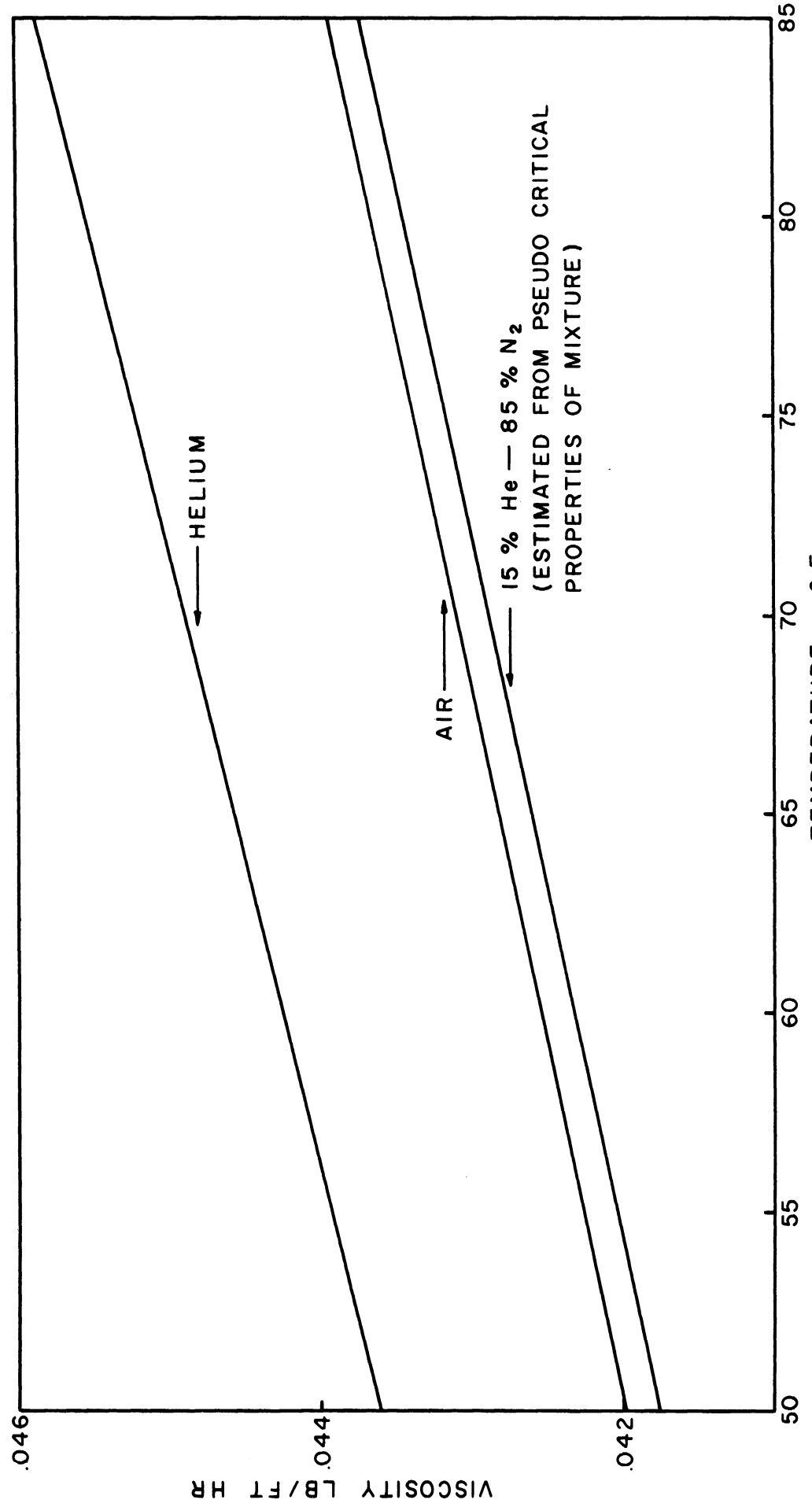

Figure 58. Viscosity of Gases.

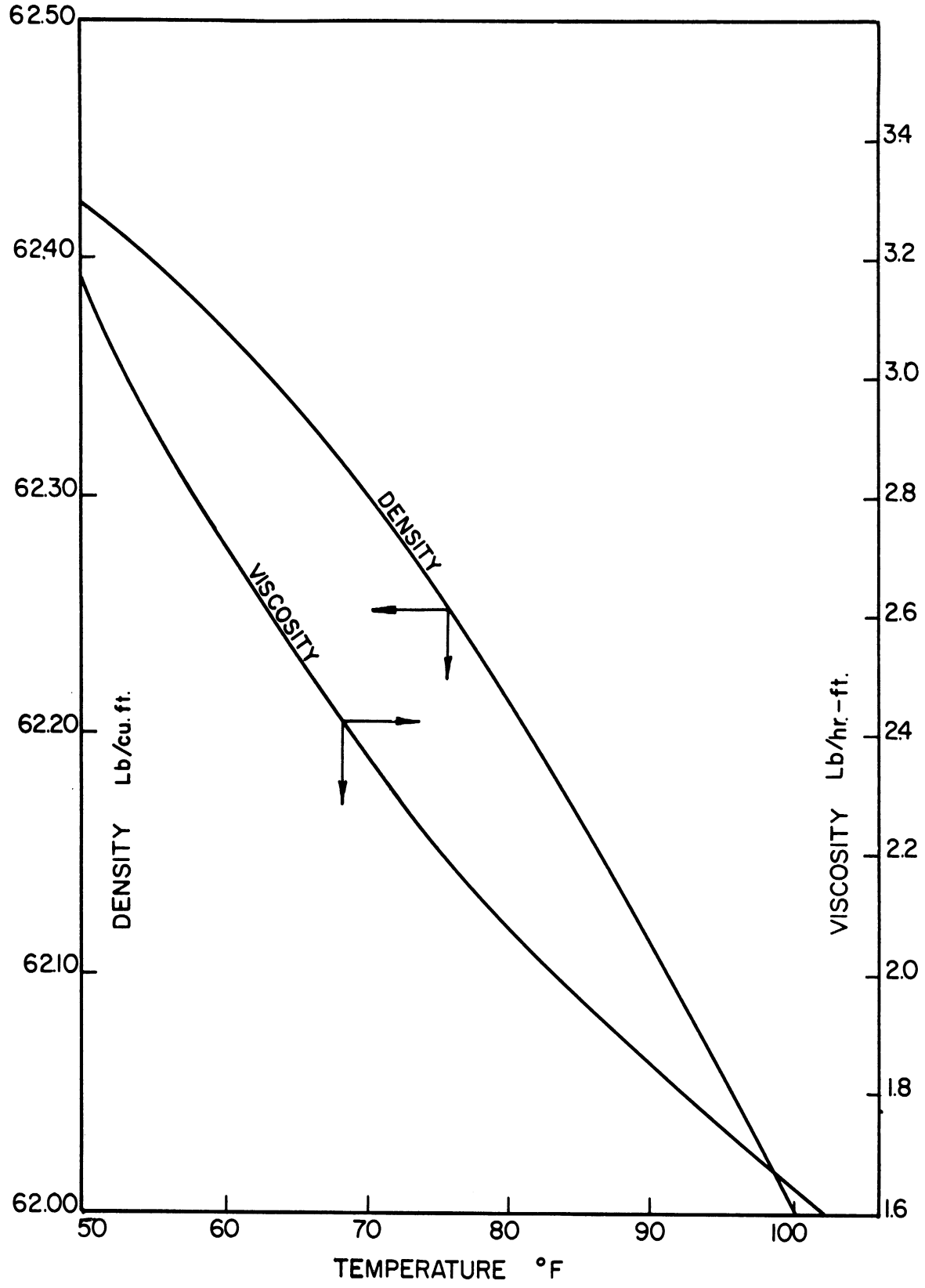

Figure 59. Properties of Water.

NOMENCLATURE

A = cross sectional area of empty column, sq. ft.

a = total surface area of bed, sq. ft./cu. ft.

a_w = total surface area of irrigated bed, sq. ft./cu. ft.

c = tracer concentration in effluent at time t, moles/unit vol.

c_o = tracer concentration in entering stream, moles/unit vol.

$\bar{c}(s)$ = Laplace transform of c

D = effective diffusivity, sq. ft./sec.

D_L = effective diffusivity in the direction parallel to flow in the packed bed, sq. ft./sec.

D'_L = effective diffusivity in the direction parallel to flow in the foresection, sq. ft./sec.

D''_L = effective diffusivity in the direction parallel to flow in the aftersection, sq. ft./sec.

D_r = effective diffusivity in the direction normal to flow, sq. ft./sec.

d = nominal diameter of packing element, ft.

d_m = hydraulic mean diameter, $\frac{\epsilon}{a}$, ft.

d_p = diameter of sphere having equal volume as packing element, ft.

d_t = diameter of packed column, ft.

$E(t)$ = distribution of residence-times function, seconds^{-1}

= $\frac{d\, c/c_o}{dt}$ for a step input

= $\frac{vc}{Q}$ for an impulse input

NOMENCLATURE (Cont'd)

$\text{erf}(\lambda) = \frac{2}{\sqrt{\pi}} \int_0^{\lambda} e^{-\lambda^2} d\lambda$

$\text{erfc}(\lambda) = \frac{2}{\sqrt{\pi}} \int_{\lambda}^{\infty} e^{-\lambda^2} d\lambda$

$f\{s\}$ = Laplace transform of any function

$f^{-1}\{s\}$ = inverse Laplace transform of any function

$f'\{s\}$ = derivative of Laplace transform with respect to the argument

G = superficial mass flow rate of gas, lb./hr., sq. ft.

H = height of a perfectly mixed stage L/n, ft.

H_w = height of a perfectly mixed stage for irrigated bed, ft.

$\bar{i}$ = unit vector in the x direction

$\bar{j}$ = unit vector in y direction

$\bar{k}$ = unit vector in z direction

L = height of packed bed, ft.

M = coefficient for porosity correlation, dimensionless

m = total number of perfectly mixed cells in packed bed

N = coefficient for mixing correlation for irrigated packing, dimensionless

n = number of perfectly mixed cells in series in longitudinal direction

$\bar{n}$ = apparent number of perfectly mixed stages in series or inverse of the variance

Pe_L = longitudinal Peclet number, du/D_L, dimensionless

NOMENCLATURE (Cont'd)

Pe'_L = modified longitudinal Peclet number, $\frac{d_p u}{D_L}$, dimensionless

Pe''_L = modified longitudinal Peclet number, $\frac{d_m u}{D_L}$, dimensionless

Pe_r = radial Peclet number, $\frac{du}{D_r}$, dimensionless

Pe_w = longitudinal Peclet number for irrigated packing, $\frac{2d}{H_w}$, dimensionless

Pe''_w = modified longitudinal Peclet number for irrigated packing, $\frac{2d_m}{H_w}$, dimensionless

Pe_{w_0} = coefficient for mixing correlation for irrigated packing, dimensionless

Q = quantity of tracer material injected, moles

r = mass transfer rate, moles/sec., sq. ft.

Re_G = Reynolds number for gas, $\frac{Gd}{\mu_G}$, dimensionless

Re_w = Reynolds number for liquid, $\frac{Wd}{\mu_w}$, dimensionless

S = specific surface of the material, sq. ft./cu. ft.

s = argument of the Laplace transform

t = time measured from introduction of signal, sec.

u = average superficial velocity through interstices, ft./sec.

U = dimensionless group $\frac{uL}{2D_L}$ used in solution "C" of diffusion equation

V' = volume of a perfectly mixed stage, cu. ft.

NOMENCLATURE (Cont'd)

V = volume of empty column, cu. ft.

v = volumetric flow rate through column, cu. ft./sec.

v' = volumetric flow rate through a perfectly mixed stage, cu. ft./sec.

W = superficial mass flow rate of liquid, lb./hr., sq. ft.

x = distance along coordinate axis parallel to flow, ft.

y = distance along coordinate axis normal to x and z, ft.

z = distance along coordinate axis normal to x and y, ft.

α = variable defined in Appendix I

α' = variable defined in Appendix I

β = variable defined in Appendix I

γ = variable defined in Appendix I

Δt = finite increment of time, sec.

ϵ = porosity of dry bed; volume fraction of empty column

ϵ_w = porosity of wet bed; volume fraction of empty column

ϵ_{w_o} = coefficient for porosity correlation, dimensionless

θ = mean residence-time; $\frac{\epsilon V}{v}$ or $\frac{L}{u}$, sec.

θ' = mean residence-time for a single perfectly mixed cell; $\frac{V'}{v'}$, sec.

λ = variable used for a generic designation of the argument of the error function or as dummy variable of integration

μ_G = viscosity of the gas, lb./ft., hr.

μ_w = viscosity of the liquid, lb./ft., hr.

NOMENCLATURE (Cont'd)

μ_n = eigenvalues of solution "C" of diffusion equation

ν = skewness of the dimensionless time distribution function about $t = \theta$; dimensionless

π = 3.1416 radians

ρ_G = density of gas; lb./cu. ft.

ρ_w = density of liquid; lb./cu. ft.

σ^2 = variance of the dimensionless time distribution function, dimensionless

τ = dummy variable of integration expressing time

φ = arbitrary function of s

χ = arbitrary function of s

Ψ = time distribution function for element of surface, seconds^{-1}

ψ = fractional rate of surface renewal, seconds^{-1}

Subscripts D, E, P and w for the quantities n, V, θ and σ refer to portion of packed bed above liquid distributor, empty section below packed bed, total packed bed and irrigated portion of packed bed respectively

Subscripts 1, 2, i and n for quantities V', θ' refer to mixed stages number 1, 2, i and n respectively. These subscripts may also refer to several mixers of types 1, 2, i and n when used for quantities V, θ and n.

BIBLIOGRAPHY

1. Aris, R., Amundson, N. R., A.I. Ch. E. Journal 3 280 (1957)

2. Baron, Thomas, Chem. Eng. Progress 48 118 (1952)

3. Bernard, R. A., Wilhelm, R. H., Chem. Eng. Prog. 46 233 (1950)

4. Chandrasekhar, S., Rev. of Modern Physics 15 1 (1943)

5. Chu, J. C., Kalil, J. and Welteworth, W. A., Chem. Eng. Progress 49 141 (1953)

6. Churchill, R. V., "Modern Operational Math. In Engineering", pp. 117, McGraw Hill Book Co., New York 1944

7. Churchill, S. W., Abbrecht, P. H., Chu, Chiao-Min, Ind. Eng. Chem. 49 1007 (1957)

8. Cohen, W. C., and Johnson, E. F., Ind. Eng. Chem. 48 1031 (1956)

9. Colpitts, G. P., Ph.D. Thesis in Progress, University of Michigan

10. Cramér, H. "The Elements of Probability Theory", John Wiley and Son, New York (1955)

11. Danckwerts, P. V., A.I. Ch. E. Journal 1 456 (1955)

12. Danckwerts, P. V., Appl. Sci. Research A3 279 (1953)

13. Danckwerts, P. V., Chem. Eng. Sci. 2 1 (1953)

14. Danckwerts, P. V., Ind. Eng. Chem., 43 1460 (1951)

15. Danckwerts, P. V., Jenkins, J. W., and Place, G., Chem. Eng. Sci. 3 26 (1954)

16. Deisler, P. F., McHenry, K. W., and Wilhelm, R. H., Anal. Chem. 27 1366 (1955)

17. Deisler, P. F., and Wilhelm, R. H., Ind. Eng. Chem. 45 1219 (1953)

18. Ebach, E. A., Ph.D. Thesis, University of Michigan, May, 1957

19. Elgin, J. C., and Weiss, F. B., Ind. Eng. Chem. 31 435 (1939)

20. Evans, G. C., and Gerald, C. F., Chem. Eng. Progress 49 135 (1953)

BIBLIOGRAPHY (CONT'D)

21. Feller, Wm., "Probability Theory and its Applications", Volume 1, John Wiley and Sons, Inc., New York (1950)

22. Fellinger, L., ScD. Thesis, Mass. Inst. Technology (1941)

23. Fowler, F. C., and Brown, G.G., Trans. Am. Inst. Chem. Engrs. 39 491 (1943)

24. Fry, T. C., "Probability and Its Engineering Uses", D. Van Nostrand Co., Inc., New York (1928)

25. Gamson, B. W., Chem. Eng. Progress, 47 19 (1951)

26. Gardner, G. C., Chem. Eng. Science 5 101 (1956)

27. Gilliland, E. R., and Mason, E. A., Ind. Eng. Chem. 41 1191 (1949)

28. Gilliland, E. R., and Mason, E. A., Ind. Eng. Chem. 44 218 (1952)

29. Grimley, S. S., Trans. Inst. Chem. Engrs. (London) 23 228-35 (1945)

30. Handlos, A. E., Kunstman R. W., Schisler, D. O., Ind. Eng. Chem. 49 25 (1957)

31. Hanratty, T. J., A.I.Ch.E. Journal 2 359 (1956)

32. Higbie, R., Trans. Am. Inst. Chem. Engrs. 31 365 (1935)

33. Hughes, R. R., Ind. Eng. Chem. 49 947 (1957)

34. Jesser, B. W., and Elgin, J. C., Trans. Am. Inst. Chem. Engrs. 34 277 (1943)

35. Kaplan, W., **Operational Mathematics for System Analysis, Notes for** Math. 148 Univ. of Michigan (1956)

36. Keyes, J. J., Jr., A.I.Ch.E. Journal 1 305 (1955)

37. Kozeny, J., Ber. Wien. Akad., 136A 271 (1927)

38. Kramers, H. and Alberda, G., Chem. Eng. Sci. 2 173 (1953)

39. Lapidus, Leon, Ind. Eng. Chem. 49 1000 (1957)

40. Lapidus, L., and Amundson, N., J. of Phys. Chem. 56 984 (1952)

BIBLIOGRAPHY (CONT'D)

41. Leva, M., "Tower Packings and Packed Tower Design" U. S. Stoneware Co., Akron, Ohio (1953)

42. Levenspiel, O., and Smith, W. K., Chem. Eng. Sci. 6 227 (1957)

43. Lobo, W. E., Friend, L., Hashmall, F., and Zenz, F., Trans. Am. Inst. Chem. Eng. 41 693 (1945)

44. Mach, E., Dechema Monograph 6 38 (1933); Z. Ver. Deut. Ing. Forsh. 375, (1935)

45. Mayo, F., Hunter, T. G., and Nash, A. W., J. Soc. Chem. Ind. (London) 44 375T (1935)

46. McCune, L. K., and Wilhelm, R. H., Ind. Eng. Chem. 41 1124 (1949)

47. McHenry, K. W., Jr., Wilhelm, R. H., A.I.Ch.E. Journal 3 83 (1957)

48. McMullin, R. B., and Weber, M., Jr., Trans. Am. Inst. Chem. Engrs 31 409 (1934-35)

49. Ranz, W. E., Chem. Eng. Progress 48 247 (1952)

50. Sarchet, B. R., Trans. Am. Inst. Chem. Engrs. 38 283 (1942)

51. Sherwood, T. K., and Pigford, R. L., Absorption and Extraction, McGraw-Hill Book Co., Inc., New York, 1952

52. Sherwood, T. K., Shipley, G. H., and Holloway, F. A. L., Ind. Eng. Chem. 30 765 (1938)

53. Shulman, H. L., Ullrich, C. F., Proulx, A. Z., and Zimmerman, J. O., A.I.Ch.E. Journal 1 253 (1955)

54. Shulman, H. L., Ullrich, C. F., and Wells, N., A.I.Ch.E. Journal 1 247 (1955)

55. Singer, E., D. B. Todd, Guin, V. P., Ind. Eng. Chem. 49 11 (1957)

56. Singer, E., Wilhelm, R. H., Chem. Eng. Progress 48 247 (1952)

57. Tillson, P., SM Thesis MIT (1939)

58. Uchida, S., and Fujita, S., Soc. Chem. Ind. (Japan) 39 432 (1936); 40 238 (1937)

BIBLIOGRAPHY (CONT'D)

59. Wehner, J. F., and Wilhelm, R H., Chem. Eng. Sci. 6 89 (1956)

60. White, R. R., and Othmer, D. F., Trans. Am. Inst. Chem. Engrs. 38 1067 (1942)

61. Whitman, W. G., Chem. and Met. Eng. 29 147 (1923)

62. Whitt, F. R., Brit. Chem. Eng. 1 437 (1957)

63. Wylie, C. R., Jr. "Advanced Engineering Math" McGraw-Hill Book Co. (1951)

64. Yagi, S., Miyauchi, T., Chem. Eng. (Japan) 17 382 (1953)